A DETERMINISTIC MODEL FOR LAKE CLARITY; APPLICATION TO MANAGEMENT OF LAKE TAHOE, (CALIFORNIA-NEVADA), USA

Joaquim PÉREZ LOSADA

Universitat de Girona

A Deterministic Model for Lake Clarity;
Application to Management of Lake Tahoe,
(California-Nevada), USA

Joaquim Pérez Losada
Girona, July 2001

Professor **Samuel Geoffrey Schladow** of the Department of Civil and Environmental Engineering at the University of California, Davis, and Professor **Elena Roget Armengol**, of the Department of Physics at the University of Girona,

CERTIFIED that the Doctoral dissertation presented with the title "*A Deterministic Model for Lake Clarity; Application to Management of Lake Tahoe, (California-Nevada), USA*", was completed under our supervision by **Joaquim Perez Losada**.

Girona, July 2, 2001

Signed: Samuel Geoffrey Schladow   Signed: Elena Roget Armengol

El professor **Samuel Geoffrey Schladow**, del Departament d'Enginyeria Civil i Mediambiental de la Universitat de Califòrnia, Davis, i la professora **Elena Roget Armengol**, del Departament de Física de la Universitat de Girona,

CERTIFICA que la tesi doctoral que aquí es presenta sota el títol de *"A Deterministic Model for Lake Clarity; Application to Management of Lake Tahoe, (California-Nevada), USA"*, ha estat realitzada sota la nostra direcció per en **Joaquim Pérez Losada**.

Girona, 2 de juliol de 2001

Signat: Samuel Geoffrey Schladow   Signat: Elena Roget Armengol

Acknowledgements

Table of Contents

Chapter 1: Introduction

This dissertation has as its goal the quantitative evaluation of the application of coupled hydrodynamic, ecological and clarity models, to address the deterministic prediction of water clarity in lakes and reservoirs. Prediction of water clarity is somewhat unique, insofar as it represents the integrated and coupled effects of a broad range of individual water quality components. These include the biological components such as phytoplankton, together with the associated cycles of nutrients that are needed to sustain their populations, and abiotic components such as suspended particles that may be introduced by streams, atmospheric deposition or sediment resuspension. Changes in clarity induced by either component will feed back on the phytoplankton dynamics, as incident light also affects biological growth. Thus ability to successfully model changes in clarity will by necessity have to achieve the correct modeling of these other water quality parameters. Water clarity is also unique in that it may be one of the earliest and most easily detected warnings of the acceleration of the process of eutrophication in a water body. Long before changes in nutrient levels are at readily detectable levels, clarity may start to be impacted. This is indeed the situation in Lake Tahoe, the lake modeled in this dissertation. Thus, an ability to model this phenomenon will have great potential for studying systems in which impacts of anthropogenic activities are at the very early stages, and are therefore most easily addressed.

Rather than attempt the construction of a totally new model, at the outset it was decided to use an existing, freely available model. The water quality model used is the Dynamic Lake Model - Water Quality, here after referred to as DLM-WQ. The model was enhanced to represent processes that were not included in the original model (both physical and biological). This choice was constrained to a modeling approach that lent itself to the use of the final product as a management tool. Thus model run-time was a crucial issue, a factor that virtually constrained the modeling to be one-dimensional (preserving the vertical direction) in approach. This imposed criterion

thus provides a further goal for the dissertation. Namely, to address the question of whether the deterministic prediction of lake clarity can be achieved with the simplifying assumption of one-dimensionality, in a lake that is clearly three dimensional in nature.

Data from Lake Tahoe - required for model initialization, forcing, calibration and validation - was collated and a semi-automated calibration procedure was developed and used to calibrate the biological and chemical components of the model. The calibrated model was successfully validated using data from a different time period, and has been used to test hypotheses about the decline of the water quality under given environmental conditions.

1.1 Research Objectives

Four specific objectives have driven this research effort toward achieving the broader goals described above. The first objective was the implementation of new water quality and optical sub-models into DLM-WQ. The water quality components reflect biochemical processes such as nutrient uptake and cycling, algae growth and zooplankton dynamics, and dissolved oxygen cycling. The optical component derives Secchi depth and other optical parameters from absorption and scattering characteristics based on dissolved and particulate matter predictions from the other model components. The previous phytoplankton sub-model needed improvement to represent conditions important for phytoplankton adapted to the specific characteristics of the ultra-oligotrophic ecosystem found in Lake Tahoe. The role of atmospheric nutrient deposition was taken into account. Assumptions about both the form and rates for the mathematical relationships among the variables were applied and their impact on the simulations analyzed. Ground water contribution to the water and nutrient budgets was also modeled. The sensitivity to variable environmental conditions of this oligotrophic system required taking into account a more accurate model for the light attenuation coefficient of water. In doing so, the extinction coefficient, which is strongly dependent on the particle and chlorophyll concentration and size distributions, could be accurately estimated from the output of the DLM-WQ.

2

The second objective was to provide a calibration strategy based on a Genetic Algorithm technique. The mechanisms relating the different variables are represented by one or several empirical functions determined from experimental results. The value of those function coefficients representing poorly known processes (i.e., without references or difficult to analyze experimentally), had to be numerically estimated during the calibration of the model. The calibration consists in finding, for the set of coefficients, a combination of values that allow, for each variable, a simulation that best fits the observations. During the development procedure, an impressive number of simulations had to be done until an acceptable description was achieved. The combination of the automated procedure along with user interpretation has provided a way to reduce the time spent in the calibration, as well as giving an objective criterion to evaluate the goodness of the found (set) of solutions.

The third objective was to successfully validate the model. Due to the inherent complexity of biological systems, an exact agreement between simulation and observations is not expected. The limited number of measurements that are available give a highly discretized image of the ecosystem, subject to very strong spatial-temporal fluctuations while the model simulates the evolution of average variables under highly idealized conditions. Also, conditions at Lake Tahoe are such that many parameters are close to the limits of resolution, and thus measurement uncertainty is large. Rather than aiming for an exact coincidence between experimental data and simulations, the model task is focused on reproducing the seasonal pattern and the proper trend of changes in the phytoplankton population, estimated as Chlorophyll a, and the nutrient concentrations, Secchi disk and other selected variables.

The fourth objective was to describe, through simulation studies, the effects of different management and physical scenarios on the lake water quality and on the clarity. This task was not intended to be an exhaustive study of the various management options. Rather, it is to be viewed more as a demonstration exercise of the suitability and potential of the present modeling approach to realize the management goals of resource managers in the Tahoe Basin and other similar systems.

1.2 Site Description

Lake Tahoe (California-Nevada) is a deep ultra-oligotrophic, sub-alpine lake. It is 35 km long north to south by 19 km wide east to west with an average surface elevation of 1,898 m above mean sea level. The bathymetry of the lake is shown in **Fig. 1.1**. With a maximum depth of 499 m (Gardner et al., 1998) and an average depth of 301 m, it is the second deepest lake in the United States and the eleventh deepest in the world. Despite its relatively high altitude and latitude (39.6 deg N), the surface does not freeze in winter. The lake has a surface area of 501 km^2 (within a watershed of only 800 km^2), and a mean residence time of about 700 years. High water clarity allows phytoplankton growth down to 120 m (Holm-Hansen et al., 1976). Over the past decades, Lake Tahoe has experienced the commencement of the early stages of eutrophication. Time series analysis of measured Secchi depth has shown a gradual decline in clarity, at a rate of approximately 0.3 m/yr., although the record exhibits strong variability at the seasonal, inter-annual, and decadal scales (Jassby et al., 1999). Changed nutrient inputs has also been hypothesized to drive the change from nitrogen (N) limitation of phytoplankton growth to either phosphorus (P) limitation or N:P co-limitation (Goldman, 1988). The introduction of allochthonous species as shrimp *Mysis relicta* and kokanee salmon *Oncorhyncus nerka* has induced changes in both the phytoplankton and zooplankton communities (Goldman, 1974; Richards et al., 1975; Rybock, 1978; Goldman, 1981).
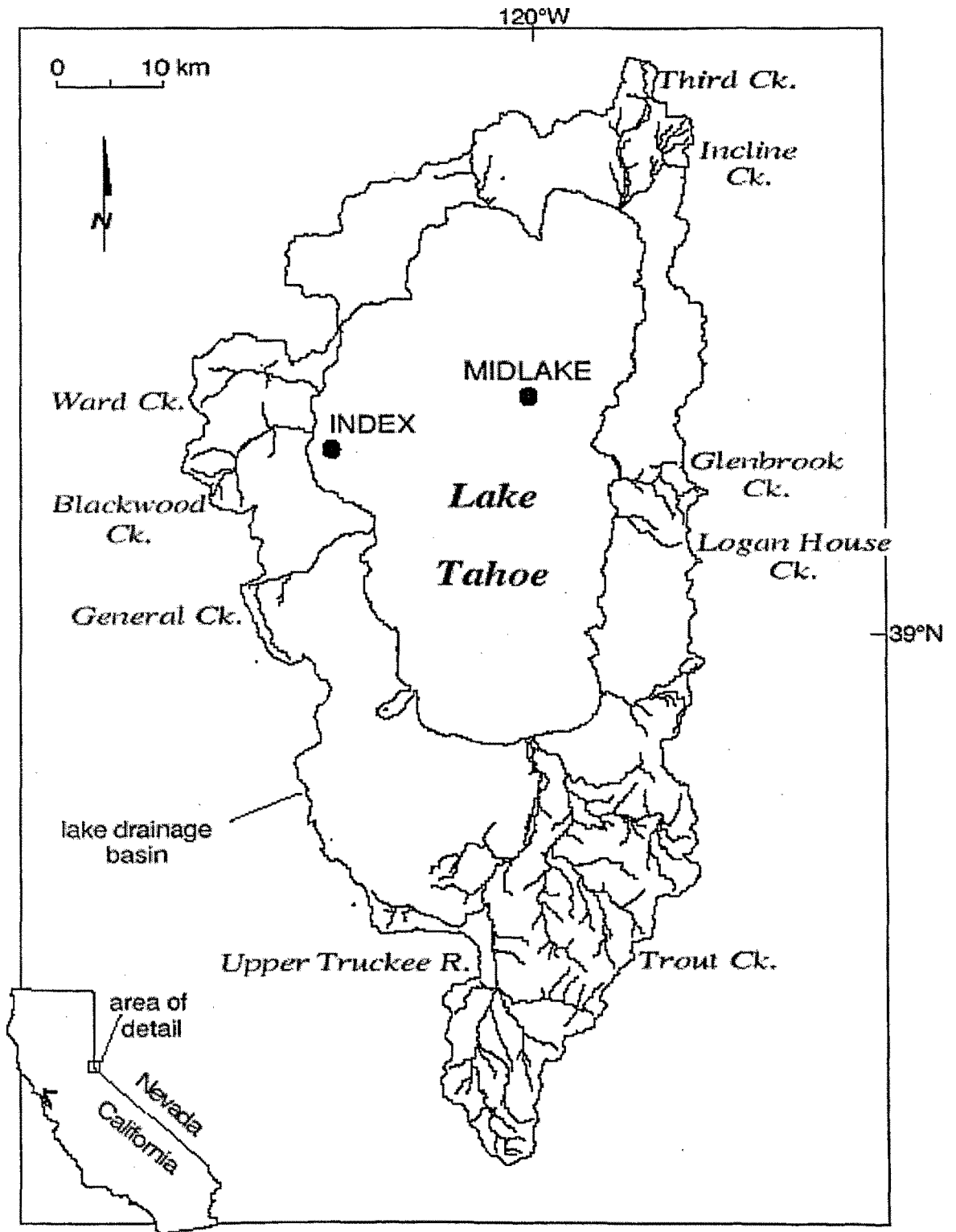
Figure 1.1 Lake Tahoe map. Dots indicate the position of the two stations.

1.3 Organization of Dissertation

The remainder of this dissertation has been laid out in 8 chapters. The structure has been chosen to guide the reader step by step through the modeling approach, from the statement of the problem, the methodology developed and the assumed hypothesis, and the model outputs with a discussion, to conclude with a discussion of the model limitation and proposed future research.

Chapter 2 offers an overview of the state-of-the-art of water surface modeling of hydrodynamics and Water Quality (WQ). Some basic concepts about model calibration is introduced. The linking problems between hydrodynamics and WQ have been highlighted.

Chapter 3 provides a detailed description of the model DLM-WQ. Hydrodynamic sub-model had been improved in the thermodynamics algorithm and adapted to the specific characteristics of Lake Tahoe (for example, depth and number of stream inputs, groundwater flow). Several water quality sub-models were developed to represent conditions important for phytoplankton more accurately and an optical model was implemented.

Chapter 4 describes the origin and availability of the needed data used in the modeling exercise. Two sets of independent data were used for calibration and validation purposes. The impact of the quality of data on the simulations is discussed in terms of spatial and temporal resolution.

Chapter 5 presents and discusses the water balance, nutrient balance and sensitivity analysis of the spatial and temporal grid for the simulated periods. Assessing the internal coherence of the model is a necessary pre-requisite.

Chapter 6 is devoted to a detailed sensitivity analysis over the hydrological and WQ sub-components of the model, along with an estimation of the output sensitivity to the uncertainty of the input data.

6

Chapter 7 provides a detailed explanation of the calibration method. A basic introduction to Genetic Algorithm theory is included; a more detailed discussion on the specific algorithm developed, and its applicability to the DLM-WQ model is also given. The results of the model's calibration and its validation applied to Lake Tahoe are presented. Possible causes of disagreement between simulations and measured variables are discussed.

In **Chapter 8** the calibrated model was used to test several hypotheses on possible management scenarios and physical scenarios. Qualitative predictions based on simulated conditions are presented and discussed giving some qualitative criteria to quantify the uncertainty of the predictions.

Chapter 9 summarizes the lessons learned from the application of the model to Lake Tahoe. In addition, some alternative options of model's development are discussed and future research areas are pointed out.

Chapter 2: Review

In this section, brief summaries of the hydrodynamic models and water quality models are given. Another part is devoted to the link between clarity and water quality, and finally there is a brief review of Lake Tahoe and its ecosystem.

2.1 Lake Hydrodynamic and Water Quality Models

The spectrum of models that have evolved over the last 30 to 40 years to address lake hydrodynamic and water quality issues is broad, and still evolving. This section is intended to briefly review the range of models that do exist, mainly for the purpose of placing into context the modeling approach that has been adopted in this work. It is therefore not intended to be exhaustive, but rather illustrative. It is also not intended to provide the rationale for the present modeling approach.

The environmental systems of the type considered in this thesis are far too complex to be modeled in someway other that highly approximately (Beck, 1983). The level of approximation is determined by taking into account the objectives of the model, and the test of their usefulness is of utmost importance. It must be recognized therefore, that a model —which is a deliberate simplification of the infinitely more complex real world - does not need to fit all the data to be useful (Klepper, 1997).

Models can be distinguished by a variety of classification criteria (Reckhow and Chapra, 1983). Models can be based on relationships between measured data (*empirical models*) rather than derived from an understanding of all the processes (*mechanistic models*). A model can be *static* (time-independent), or *dynamic* (time-dependent). A model may try to describe the functioning of a system (*simulation* model) or be designed to find a solution that that fits a set of criteria (*optimization*

model). Models have also been divided between *scientific* and *management* models (Jorgensen, 1994), although this distinction is somewhat arbitrary as scientific models are increasingly being used as input to management decisions. If a model incorporates uncertainty and random measurement errors in its input parameters, it is said to be a *stochastic* model. However if the model uses expected values for all parameters and variables and yields predictions that are also expected values, it is classified as a *deterministic* model. In reference to the space-dependence of the model's parameters, the models can be classified as *lumped parameter* models if they are zero dimensional in space (an assumption of uniform conditions throughout the system) while in a *distributed parameter* model the parameters are considered to vary in one or more spatial dimensions.

Modeling of eutrophication has been a topic of growing interest. Eutrophication, while being a natural process, is considered to be undesirable when its rate of development is greatly accelerated due to anthropogenic causes. In general, eutrophication can be understood as being an increase in the rate of primary production, stimulated by an increase in the supply of one or more nutrients. As a result of this process, the parameters that describe the water quality degrade (for example, lower concentrations of dissolved oxygen, loss of transparency, benthic release of metals and toxic substances). An impressive number of models for quality management purposes have been developed and tested with different degree of success, ranging from simple empirical, input-output models to very sophisticated ones based on neural networks and Geographical Information Systems (GIS). Comprehensive reviews can be found in Jorgensen et al. (1986), Jorgensen et al. (1996), Straskraba and Gnauck (1985), and Straskraba (1994). Further, the *Register of Ecological Models (REM)* is a meta-database for existing mathematical models in ecology. Models can be registered and technical as well as scientific documentation can be accessed (http://www.wiz.uni-kassel.de/ecobas.html).

The earliest water quality models consisted of steady state, input-output models. A variety of relatively simple empirical models have been developed since the mid-1960's to predict eutrophication on the basis of the phosphorous (P) loading concept (Vollenweider, 1968) (*see reviews by Mueller, 1982, and Ahlgren et al., 1988*). The P-loading concept assumes that algal growth is limited by the availability of

phosphorus in the water and that increased P, often derived from sewage discharges and from runoff into lakes and streams, has caused water quality degradation - but the sources are controllable. Typically, these models are used to relate the loading rates for P into the lake to summer concentrations of phosphorus in the lake water. Then, other empirical relationships are used that link P to various measures of water quality, such as clarity (Secchi depth), algae (chlorophyll concentration) and oxygen depletion in bottom waters.

A second water quality modeling approach, often referred to as ecological water modeling, provided a more complex description of the biological, chemical and physical processes that the affect biomass of phytoplankton (DiToro et al., 1971; Scavia, 1980; Jorgensen, 1983, Matsuoka et al., 1986). Several models have been developed following this approach. Examples include AQUASYM (Reichert, 1994), GIRL (Kmet and Straskraba, 1989) and MONOD (Karagounis et al., 1993). In ecological water quality models, the physical processes of transport and mixing within the water body have generally been oversimplified, with the assumption of continuously stirred or two or three compartment vertical systems being common (Hamilton and Schladow, 1997).

A third approach has been the extension of hydrodynamic models to include water quality components of variable resolution (from simple input-output models to 3-D models). A common approach for the hydrodynamics has been to use a one-dimensional (1-D) model. The assumption of purely vertical variability is based on the fact that density stratification enhances the horizontal mixing, occurring on time scales much shorter than vertical transport. Horizontal exchanges generated by weak temperature gradients communicate over several kilometers on time scales of less than a day, suggesting that the one-dimensional model is suitable for simulations over daily time scales (Orlob, 1983).

Even with the assumption of one-dimensionality, the vertical density structure is the result of a complex interaction of a number of partially understood processes (Patterson et al., 1984). Many of the early hydrodynamic models (Orlob and Selna, 1970, Markofsky and Harleman, 1973, for example) relied on a calibrated diffusion model to represent these processes. However, this approach has severe limitations in

representing profiles outside the range over which the model is calibrated, and is thus unsuitable as a basis for water quality models, is not transferable to other lakes and gives little insight into the dynamics of the lake and the interactions between the various processes.

Another family of models are termed process based models (Stefan and Ford, 1975; Imberger et al., 1978; Bloss and Harleman, 1980; Gaillard, 1981). These models present a description of the mixing and transport processes associated with inflow, outflow, diffusion and mixed layer dynamics. All of them have been coupled with ecological models, giving fairly complete water quality models (Riley and Stefan, 1988; USCE, 1986; Hamilton and Schladow, 1997; Salençon and Thébault, 1996). In an intermediate step towards fully spatial segmentation, CE-QUAL-W2 is a laterally-averaged, two-dimensional hydrodynamic and water quality model that has been extensively used in reservoirs, particularly by the US Army Corp of Engineers (Cole and Buchak, 1995). The time required to run a full 3-D model and number of calibration parameters are reasons favoring a 2-D model. Recently, development of parallel computing techniques as well as the continued improvement of processor speed has allowed the coupling of fully 3-D hydrodynamic models with 1-D spatial resolution ecological model. Examples of that coupling are 3-D hydrodynamic code ELCOM coupled with CAEDYM for simulation of biological and chemical processes (http://www.cwr.uwa.edu.au/~ttfadmin/index.html). However, the time required to run such a models on a long-term simulation simulations (especially in deep lakes where more spatial discrimination is needed) is still prohibitive for most applications.

Some models have been set up to specifically model the processes of primary production in oligotrophic waters, as typically found in oceanic waters. Varela et al. (1992) coupled an upper ocean model to a nutrient/phytoplankton model to describe the formation and maintenance of the Deep Chlorophyll Maximum (DCM). Unlike the case of Lake Tahoe, which has displayed co-limitation by nitrogen and phosphorus, the ocean waters considered here are solely nitrogen limited. Varela et al. (1994) discussed the influence of several physical and biological factors on the depth and magnitude of the DCM. Doney et al. (1996) presented a 1-D hydrodynamic model coupled with a biological model to simulate subtropical oceanic waters. Gecek and Legovic (2001) improved the original model developed by Varela et al. (1992)

refining the nutrient limitation formulation and proposing an alternative formulation of the zooplankton grazing. They found that grazing processes were important in the correct modeling of that system.

Perkins and Effler (1996) analyzed measurements of light penetration, turbidity, Chlorophyll and suspensoids to depict seasonal dynamics and long-term trends in these optical characteristics for Lake Onondaga, USA. Effler and Perkins (1996) applied a deterministic optics model for predicting measures of light penetration to Lake Onondaga. Research specifically dealing with lake management and restoration of water clarity has been conducted by Effler et al. (1998) on the Cannonsville Reservoir, USA. Effler et al. (1998) measured apparent optical properties, lake chemistry, and individual particle analysis. The BHMIE algorithm (Bohren and Huffman, 1983) and Tyler's (1968) equation of Secchi Depth were used together to determine the spatial gradients of apparent optical properties and the development of management strategies to improve the optical aesthetics of the reservoir. The authors concluded that the optical water quality could be significantly improved through reduction of external nutrient loading as well as erosion control. However, they suggested the benefits of reducing phytoplankton would be masked in major draw down years due to the resuspension of inorganic particles (Effler et al., 1992).

Fields of future research in water quality modeling are in application of goals functions to account for adaptation and structural changes of the high flexibility of the ecosystems. Neural networks, which are composed of simple elements operating in parallel, can be trained to solve eutrophication management problems (Scardi, 1996; Yabunaka et al., 1997; Karul et al., 1998). GIS based systems are another way of future development. An example is the package BASINS that integrates a geographic information system (GIS), watershed data, and environmental assessment and modeling tools (http://www.epa.gov/OST/BASINS/basinsv2.htm).

In summary, it can be said that predictive models, if they are to be used in practice, must be simple. It is possible that more than one approach is feasible to treat a specific problem. For example, an empirical-statistical approach can be complementary to dynamic models (Hakanson and Peters, 1995). However, a compromise must be achieved among the quality of the output and the complexity of

13

the model (Jorgensen, 1993). Different needs and quantities and qualities of data will determine the complexity of the model (Jorgensen and Gromiec, 1996), so it is important to specify the scope of the model exercise and the availability of data (present and future) in order to keep the balance between complexity and practicality. The mechanistic approach of water quality sub-model of lakes and reservoirs has been recognized as a powerful tool for lake management and scientific applications (Chapra, 1997). Acceptable results with such models can be obtained as long as the main driving forces are correctly described (Hamilton and Schladow, 1997).

As alluded to in **Chapter 1**, the modeling approach adopted in this thesis was dictated by self-imposed constraints related to the utility of the model. In terms of the preceding review, this model may be viewed as being a one-dimensional (therefore partially lumped), dynamic, process based, deterministic hydrodynamic simulation model. It is linked to an ecological (water quality) model, with additional enhancements to link the usual water quality parameters to descriptions of lake clarity. Though by no means a stochastic model, by incorporating elements of the measurement and parameter uncertainty into a quantitative sensitivity analysis, some of the features of a stochastic approach have been gained. While clearly in the class of scientific models, the intended use of the model results is to guide management.

2.2 Water Quality and Lake Clarity

Water clarity is closely related to water quality, and provides a basis upon which to judge the actual state of safety of water (Smith et al., 1995a; 1995b). The depth of light penetration in water influences visual aesthetics and, in addition to nutrients and temperature, regulates the growth of phytoplankton (Effler et al., 1998). Water clarity also affects the depth over which solar radiation heats the water (Mazumder and Taylor, 1994). Thus water clarity is a vital determinant of water quality, it is affected by water quality, and in turn water quality affects the clarity.

The clarity of water is a function of how efficiently light is transmitted - (Davies-Colley et al., 1993). The behavior of light is determined by the optical properties of

14

the medium, and the optical properties, in turn, depend upon the constituent composition of the medium (Davies-Colley et al., 1993). The bulk optical properties of water are divided into two classes. Inherent optical properties (IOPs) depend only upon the water composition, and are independent of the ambient light field (Preisendorfer, 1961). IOPs include the absorption coefficient, the scattering coefficient, the volume scattering function, and the beam attenuation coefficient. Apparent optical properties (AOPs) describe the optical behavior of water bodies in a particular light field (Preisendorfer, 1961), and include the irradiance reflectance, the average cosines, the diffuse attenuation coefficients, and the Secchi depth (Mobley, 1994). The Secchi depth, the maximum visual range in the water of a white (or black and white) disc viewed vertically (Preisendorfer, 1986; Davies-Colley and Vant, 1988) is the most familiar of the AOPs. Davies-Colley (1988) develops theory of using black disc to measure the beam attenuation of the light in streams and lakes. Effler (1988) reviewed the optical principles that govern the Secchi disc transparency and turbidity as a common measures of clarity, and demonstrated that these measurements differ fundamentally in their sensitivity to light attenuating processes, and that they cannot be uniquely specified by each other.

Natural waters contain a heterogeneous mixture of dissolved and particulate matter, which are both optically significant and highly variable in type and concentration (Mobley, 1994). These can be divided up into water molecules, dissolved organic substances (gelbstoff or yellow substances), biological organic matter, and inorganic particles (tripton) (Kirk, 1994). Microorganisms and detritus in the size range of 0.1 μm to tens of micrometers strongly influence light scattering in the open ocean (Kirk, 1994).

2.3 Lake Tahoe

This section is intended to briefly summarize what is presently understood about Lake Tahoe, in particular those aspects that have a bearing on the modeling of water quality. Much of the data described is not used directly as input data to the model. However, it did provide a basis for many of the assumptions required for some model parameters. It also provides a basis for a "reality check" when considering the model results in **Chapter 8**. Clearly, if the model results are to simulate real conditions, they will need to conform to the present understanding of the lake's physical, chemical and biological features. If model results differ, they could offer insight into how the field data may be re-evaluated.

2.3.1 Lake Characteristics

Most of the land in the Tahoe basin is mountainous, occupied by a mixed conifer forest, with interspersed brush-lands and meadows. Soils are derived primarily from granitic and andesitic rocks, glacial moraines, and glacial outwash deposits. The watershed is dissected by 63 tributaries and 44 intervening areas draining directly into the lake. The Upper Truckee River has the greatest load of suspended sediment and nutrients, because this watershed is the largest basin (146.7 km^2) and contributes the most flow at nearly 25% of the total stream discharge (Marjanovic, 1989). Over 90% of precipitation in the lake watershed occurs as snow at the higher elevations; at lake level, both rain and snow fall in significant amounts. The greatest transport of sediment and some associated nutrients occurs during high flows caused by storms and snowmelt (Hatch et al., 2001). Watershed on the western side of the basin (California) of the lake have higher loads of sediment and nutrients than the sites on the eastern side (Nevada) primarily because the east-west rain-shadow results in more precipitation on the west side and because the east-sdie watersheds are typically smaller. Outflow of Lake Tahoe into the Truckee River is regulated by a dam at Tahoe City (California). The combination of great depth (±500 m), small ratio of watershed to lake area (1.6:1), and granitic geology of the basin has produced a lake of extremely low fertility and high transparency (Jassby et al., 1994). **Table 2.1** gives the main features of the lake.

Table2.1 Lake Tahoe data (from USGS and Tahoe Research Group).

CHARACTERISTIC	VALUE
Watershed area	41,340 ha
Volume at full capacity	$62 \times 10^9 \, l$
Surface area at full capacity	$501 \, Km^2$
Maximum water depth	505 m
Depth of euphotic zone	~120 m
Average inflow rate	$\sim 440 \times 10^6 \, m^3$ year
Residence time	650 years (but variable)
Inflow	63 creeks and rivers. Upper Truckee River, Blackwood Creek, Trout Creek, General Creek, Ward Creek (main streams)
Outflow	Upper Truckee River
Sedimentation rate	$\sim 1 \, cm \, yr^{-1}$
Water temperature variation	$\sim 12 \, ^\circ C$ (top to bottom)
Nutrient limitation	Nitrogen and Phosphorus Co-limitation, shifting to consistently Phosphorus limitation

2.3.2 Nutrient Dynamics

Lake Tahoe is characterized by a high degree of environmental variability, which is reflected in the annual resource availability. Lake Tahoe does not mix to the bottom 500 m) every year, and therefore the amount of nutrient enrichment varies from one year to the next (Goldman et al., 1989; Goldman and Jassby, 1990). The pool of nutrients in the lake itself may be responsible for a large portion of the annual production (Goldman et al., 1989; Jassby et al., 1995). Indeed, the depth of mixing explains a large portion of the interannual variation in the phytoplankton primary productivity record (Jassby et al. 1992). Five major categories of nutrient loading to Lake Tahoe have been identified: direct atmospheric deposition (including wet and dry fallout), stream discharge, overland runoff that drains directly to lake, groundwater and shoreline erosion. The magnitude of the nutrient loading from specific sources is still being studied (J. Reuter, pers. comm.). Estimates based on annually averages of time series records for Total Phosphorus (TP), Dissolved Phosphorous (DP), and Total Nitrogen (TN) loading are given in **Table 2.2** (from Reuter et al., 2000). The major losses include settling of material from the water column to the bottom and discharge to the Truckee River, the sole tributary outflow.

Table 2.2 Budget of total nitrogen, total phosphorus and dissolved phosphorus inputs to Lake Tahoe during the period 1980-1993. Data are presented as metric tons (MT) per year. Percentages are fractions of each nutrient group.

	Total N	Total P	Dissolved P
Atmospheric deposition	234 (56%)	12 (26%)	5.5 (32%)
Stream loading	82 (20%)	13 (28%)	2.5 (15%)
Direct runoff	42 (10%)	16 (35%)	5.0 (29%)
Groundwater	60 (14%)	4 (11%)	4 (24%)
Shoreline erosion	<1 (<1%)	<1 (1%)	No Data
Total	**418**	**45**	**17.0**

The causes of the accelerated eutrophication in Lake Tahoe are attributable to increased nutrient loading, particularly of nitrogen and phosphorus, coupled with the lake's long retention time and efficient recycling of nutrients (Goldman, 1988, Goldman et al., 1989). As a consequence of on-going atmospheric loads of nitrogen, lake phytoplankton shifted from primarily N-limitation to a condition of P and N+P-limitation (Goldman et al., 1993). Research is conducted to quantify the relative contribution of dry and wet deposition of atmospheric nitrogen (Tarnay et al., 2001). Recent measurements of atmospheric deposition suggest a spatial and temporal gradient of deposition across the lake (Liu et al., 2001). Control of phosphorus originating in the watershed became a dominant feature of watershed management, (Jassby et al., 1995, 2001; Reuter et al., 2000). The losses of nutrients from the system are mostly due to sedimentation (Heyvaert, 1998). The remaining nutrient losses are through the Truckee river discharge (Marjanovic, 1989).

By definition, Total Nitrogen (TN) and Total Phosphorous (TP) contain both Dissolved (<0.45 μm) and Particulate (>0.45 μm) forms. Estimated Nitrogen pools in Lake Tahoe by Marjanovic (1989) indicate that Particulate Nitrogen (PartN) comprises nearly 15% of TN. The majority (85%) of TN occurs in the dissolved form either as Dissolved Organic Nitrogen (DON) or Dissolved Inorganic Nitrogen (DIN). DIN consists of nitrate and ammonium and accounts for approximately 25% of TN. DON constitutes the largest Nitrogen fraction at 60%. Particulate Phosphorous (PartP) was approximately 10% of TP; the remainder (majority) of the lake's P is in the dissolved form. Total Acid-Hydrolyzable Phosphorous (THP) represents that Phosphorous converted to orthophosphate (Ortho-P) following a relatively mild acid

digestion during chemical analysis, and it could be understood as a measure of the potentially bioavailable P. Dissolved-P in streams at Lake Tahoe was found to be related to biologically available P (Hatch et al., 1999). The liberation of orthophosphate by hydrolysis of the DOP may also be partially bioavailable to Lake Tahoe algae in the euphotic zone (Holm-Hansen et al., 1976). Phosphorus associated with particles larger than 63 µm may require biological mineralization to become bioavailable, which occurs on the time scale of years (Hatch, 1997).

Average lake NO3 concentrations in the euphotic zone are strongly affected by spring mixing depth (Goldman et al., 1988). De-nitrification processes are not important since oxygen concentrations are close to saturation at all times (Goldman, 1974; Jassby et al., 1995). Nitrate depletion in the epilimnion occurs primarily during early stratification (Paerl et al., 1975). Total phosphate and soluble reactive phosphate did not show such clear trends (Carney, 1987). Total suspended particulate matter, both organic and inorganic, does reach a maximum at intermediate depths in Lake Tahoe (Jassby et al,. 1999). Mineralization is not totally complete in top 200 m (Heyvaert, 1998). The concentration of silicate-silicon range between 4-8 ppm (Goldman, 1974), an order of magnitude higher than levels found in silica limited lakes (Margalef, 1977).

2.3.3 Phytoplankton Dynamics

A large number of phytoplankton species are present in Lake Tahoe. These phytoplankton communities display both spatial and temporal patterns (Abbot at al., 1982). In Lake Tahoe the strong resource gradient is due to both the exponential extinction of light (Carney, 1987) and the gradual increase of nutrients with depth (Holm-Hansen et al., 1976). While the lake has quite homogeneous distributions of phytoplankton in a horizontal direction (Richards et al., 1975; Loeb and Eloranta, 1984), the deep light penetration and great clarity are responsible for the vertical separation of phytoplankton communities (Lopez, 1978). Phytoplankton growth in Lake Tahoe seems to be nutrient limited in approximately the top 40 m of the lake and light limited in the remainder of the productive zone.

There is strong periodicity within the algal groups on an annual basis. Diatoms dominate the phytoplankton during periods of peak biomass (April-June), although their relative contribution to the total biomass has decreased in the last decade (Byron and Elorante, 1984). *Chysophytes* are better competitors than diatoms under low phosphorus concentrations (Sandgren, 1988) and replace the diatoms linked to low concentrations of both nitrogen and phosphorus. *Cryptophytes* reach peak biomass and species richness during winter months dominating throughout the water column. During periods of thermal stratification, these genera are found below the thermocline (Hunter at al., 1990). Green algae have never been important in the Lake Tahoe phytoplankton and have shown no major changes over the years (Hunter at al., 1990). The contribution of dinoflagelates and blue-green algae to the total annual biomass appear to be negligible. Goldman (1988) has shown that algal growth rates have increased over the past few decades. Added to the productivity increase, the structure of the phytoplankton community has continually changed, shifting from diatom dominance to a shared dominance among diatoms, *chrysophytes* and *cryptophytes*. Evidence suggests that the high N:P ratio in Lake Tahoe are responsible for changes in the phytoplankton community structure (Hunter et al., 1990). Field experiments conducted by Carney et al. (1988) have shown that inter-specific resource-based competition might cause the seasonal succession and spatial segregation of dominant phytoplankton species of diatoms in Lake Tahoe during the high productivity period. Inter-specific differences in loss rates (natural death, sedimentation, and grazing) can be as important as differential growth in controlling seasonal succession of species. During spring and summer resources limited growth for all species of diatoms analyzed, while sinking and death were the major loss processes, and grazing was not important.

The lake possesses a seasonal Deep Chlorophyll Maximum (DCM) at 60-120 m (Kiefer et al., 1972). The formation and maintenance of the DCM depends on sufficient radiation penetrating below the pycnocline that provides some protection from surface-driven turbulent mixing (Abbott et al., 1984). There is also evidence supporting the notion that the Tahoe DCM is regulated by light and nitrate fluxes, depending on physical conditions (Coon, 1978; Coon, 1987). Abbot at al. (1984) have hypothesized that there are two types of DCM in Lake Tahoe: a spring DCM near the assimilation number maximum, dominated by nutrient availability, and a deeper

20

summer DCM, below the assimilation number maximum and dominated by light availability. The nutrient-dominated DCM is a high-growth regime, resulting from a moderate nutrient-light environment (growth rates are high and losses are relatively high). The light-dominated DCM is a low-loss rate regime resulting from a high-nutrient, low-light environment (growth and loss rates are low). Thus, changes in vertical mixing as they affect diffusion, nitrate supply rates, and changes in light availability at the DCM are the essential processes in the formation of the DCM. Thermal stratification usually peaks in August, and the thermocline begins to deepen in September. As it penetrates to the 60-120 m region around December, it encounters the DCM. The subsequent upward vertical mixing of phytoplankton from this maximum can contribute, in some years, to a phytoplankton increase in surface waters. Further erosion of the thermocline below the DCM then gradually dilutes phytoplankton concentration in the upper layer.

The magnitude and longevity of the annual biomass peaks are related to the depth of mixing (Goldman et al., 1989). The extent of mixing during the autumn-winter period has a profound effect on interannual variability of primary production because of variable upwelling (transport of nutrient-rich aphotic waters to the surface during winter mixing) of nutrients from the depths (Goldman et al., 1989; Goldman et al., 1990; Goldman and Jassby, 1990). Upwelled nutrients are far in excess of nutrients from runoff. Vincent (1978) has suggested the role of dormant and viable algal cells during mixing events. Phytoplankton cells below the productive zone may remain viable for prolonged periods. Resting cyst survivorship characteristics are adequate to provide a seed source for populations that reappear annually (Sandgren, 1988).

2.3.4 Zooplankton Dynamics

Lake Tahoe supports zooplankton populations of low density and diversity (Goldman, 1981). The community structure was first examined by Richerson (1969). Typically, copepods (*Diaptomus tyrrelli, Epischura nevadensis*) are abundant in Tahoe in spring and summer with cladocerans (*Bosmina longirostris, Daphnia rosea, Daphnia pulicaria*) and rotifers (*Kellicottia longispina*) dominating in the fall and winter. The introduction in the 1970s of opossum shrimp, *Mysis relicta*, and planktivorous kokanee salmon (*Oncorhyncus nerka*), and the cladoceran disappearance occurred at

the time of algal species changes and shifts in the timing of peak primary production (Morgan et al., 1978; Goldman et al., 1979). These species introductions significantly altered the zooplankton community in Lake Tahoe (Goldman, 1974). The introduction of exotic species (*Mysis relicta*) appears to be responsible of the disappearance of cladocerans (two species of *Daphnia* and *Bosmina longirostris*) (Richards et al., 1975). Except for brief reappearances of *Bosmina*, the remaining two species of calanoid copepods and one dominant rotifer species now constitute the major species in the macro zooplankton assemblage (Goldman, 1981; Byron et al., 1984; Byron and Goldman, 1986; Richards et al., 1991). Further effects on the phytoplankton, however, probably did not occur (Elser and Goldman, 1991).

It must be highlighted that *Mysis relicta* may affect the net annual internal nutrient loading of the photic zone through its effect upon the nutrient losses to the sediment (Rybock, 1979). *Mysis relicta* and zooplankton may act as nutrient pumps, transporting phosphorous and nitrogen through the water column (Morgan, 1979; Van Tassell at al., 2000). On a daily basis, *Mysis* migrate over 200 m as they go from the hypolimnion into the upper mixed layer where zooplankton prey occurs (Morgan, 1980; Rybock, 1979). Its vertical movement follows a complicated pattern. The depth and clarity of the Lake Tahoe water regulates the movement of the *Mysis*. The thermocline becomes an effective predation barrier to adult *Mysis* at lake surface temperatures above 15°C (Richards et al., 1991). *Mysis* are never found at the surface in mid-summer when the temperature is above 10° C at night but they are at the surface in the winter when it is colder. Mostly, they are below 150-200 m in the daytime and they are rarely picked any up in the routine top 0-150 m zooplankton tows at the Index Station (Bob Richards, per. comm.).

The copepods also appear to migrate at least more than 10 m since none are usually found in the top 10m during the day (Burgi et al., 1993). They also segregate by sex, with males being nearer the surface. Another factor is that the copepods do segregate by life stage with naupli and copepidites usually being found deeper in the water column. Little is known about their vertical movements. It is presumed that Daphnia and Bosmina probably do the same things, perhaps with a less pronounced vertical movement (Bob Richards, per. comm.). They tend to remain deeper in the photic zone when they appear in any numbers in the fall and are most concentrated at about 60-

22

100 m where the deep chlorophyll maximum is. It should also be remembered that these cladocerans might be somewhat limited in their vertical movements by predation from the *Mysis* passing through the cladoceran layers on their way to the surface to feed on copepods.

2.3.5 Light and Extinction Coefficient

Over the last thirty years, large declines in clarity have occurred in Lake Tahoe. Long-term monitoring of lake chemistry and biology since the early 1960's has revealed algal production is increasing at a rate greater than five percent per year, and water clarity, as measured by the Secchi depth, is decreasing at a rate of approximately 0.25 meters (m) per year (Jassby et al., 1999). Since 1968, the average annual Secchi depth has decreased from approximately 31.2 m in 1968 to 20.5 m in 2001 (Tahoe Research Group, unpublished data). The long-term data record suggests that if the current trend continues, Lake Tahoe will only boast of "ordinary" water clarity by 2030 (Reuter et al., 1998). The euphotic zone in Lake Tahoe extends well below the 1% light level (that level is commonly defined for the compensation depth), typically to below 100m for the phytoplankton (Holm-Hansen et al., 1976; Abbot at al., 1984). The long time series of records of Secchi disc registered for Lake Tahoe (see **Fig. 2.1**) exhibits strong variability at the seasonal, interannual, and decadal scales. The long-term (decadal-scale) change in Secchi depth appears to be due to an accumulation of materials in the lake (Jassby et al., 1999). Although both phytoplankton-derived materials and mineral suspensoid could be responsible for the loss of clarity, a significant role for mineral suspensoids seems likely (Jassby et al., 1999). The interannual scale exhibits two modes of variability, one weaker local minimum during the weakly stratified autumn-winter period, and another with a strong Secchi depth minimum during the more stratified spring-summer period. The extent of mixing during the first period has the effect of dilution of light-attenuating particles as mixing arrives at the DCM. The first mode is a probably result of variable depth mixing. Deeper mixing dilutes phytoplankton and other light-attenuating particles in a maximum below the summer mixed layer (Jassby at al., 1999). The second mode results from year-to-year changes in spring runoff. Linear regression analysis showed that the interannual variability in discharge seems to cause interannual variability in clarity at this time (Jassby et al., 1999).

LAKE TAHOE
Annual Average Secchi Depth ± 1 s.d.

r = 0.91
n = 32
p < .001

TAHOE RESEARCH GROUP
U.C. DAVIS
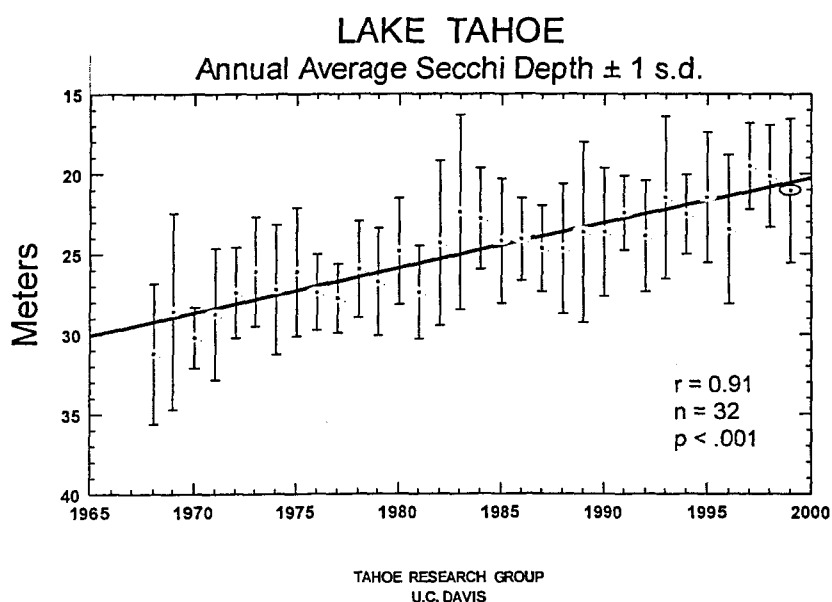
Figure 2.1 Annual average Secchi Depth. Dots indicates annual mean. Bars indicate one standard deviation about the mean. Provided by TRG, UC-Davis.

Considering the physical characteristics of the mineral component (i.e. very small size), an accumulation of mineral suspensoids seems plausible. According to Jassby et al., (1999), with Lake Tahoe's average depth of 313 m, particles settling at a rate less than 10^{-5} ms^{-1} (315 myr^{-1}) could easily remain suspended in the water column through the annual mixing or through other forms of vertical exchange. This would include all clay particles (less than 2 μm) and a large fraction of the silt particles (2-50 μm). The majority of particles in Lake Tahoe are smaller than 2 μm in diameter, with an average depth weighted concentration of about 11,600 particlesml^{-1} (Coker, 2000). These settling calculations are based upon the assumption of spherical particles and a specific gravity of 2.65 for particles. Clay particles, which are known to be plate-like in structure, would tend to settle even more slowly than the above estimates. Therefore, mineral particles in the size range of 0.5-2 μm, which have the highest scattering efficiency, would tend to be retained in the water column of Lake. Although mineral particles of this size range can settle faster through flocculation with algae, detritus, and bacterial polyelectrolytes, this is expected to be minimal in an ultra-oligotrophic lake such as Lake Tahoe with low particle concentrations and low ionic strength. Organic particles are expected to settle slowly as well, however, they are subject to zooplankton grazing, packaging in fecal pellets, and decomposition (Jassby et al., 1999).

24

Chapter 3: Model Description

The version of the DLM-WQ that has been developed as part of this research is based on the DLM-WQ program described by McCord and Schladow (1998). The program comprises a sub-model for the hydrodynamics coupled with a water quality model. As a key part of the present work, a light clarity model has been coupled to DLM-WQ. The parameterizations included in this clarity model were developed by Theodore J. Swift, as part of his Doctoral research program at the University of California, Davis.

In contrast with the biological sub-model, the physical sub-model does not require calibration. This is because the descriptions of the physical processes are better understood and hence parameterized (Schladow and Hamilton, 1997). The hydrodynamic component of the DLM-WQ program is based on the Dynamic Reservoir Simulation Model (DYRESM). DYRESM was originally developed as a one-dimensional simulation model of the vertical distribution of temperature and salinity in small to medium lakes and reservoirs (Imberger et al., 1978). Further research has been done to improve the original model (Imberger and Patterson, 1981; Ivey and Patterson, 1984; Patterson et al., 1984; Hocking et al., 1988; Imberger and Patterson, 1990). The equations that characterize the physical processes of the model have been clearly elucidated by Imberger and Patterson (1990), and will not be repeated in what follows.

For reference, **Fig. 3.1** presents the overall flow chart for DLM-WQ. It will serve as a partial road map for the discussions below.
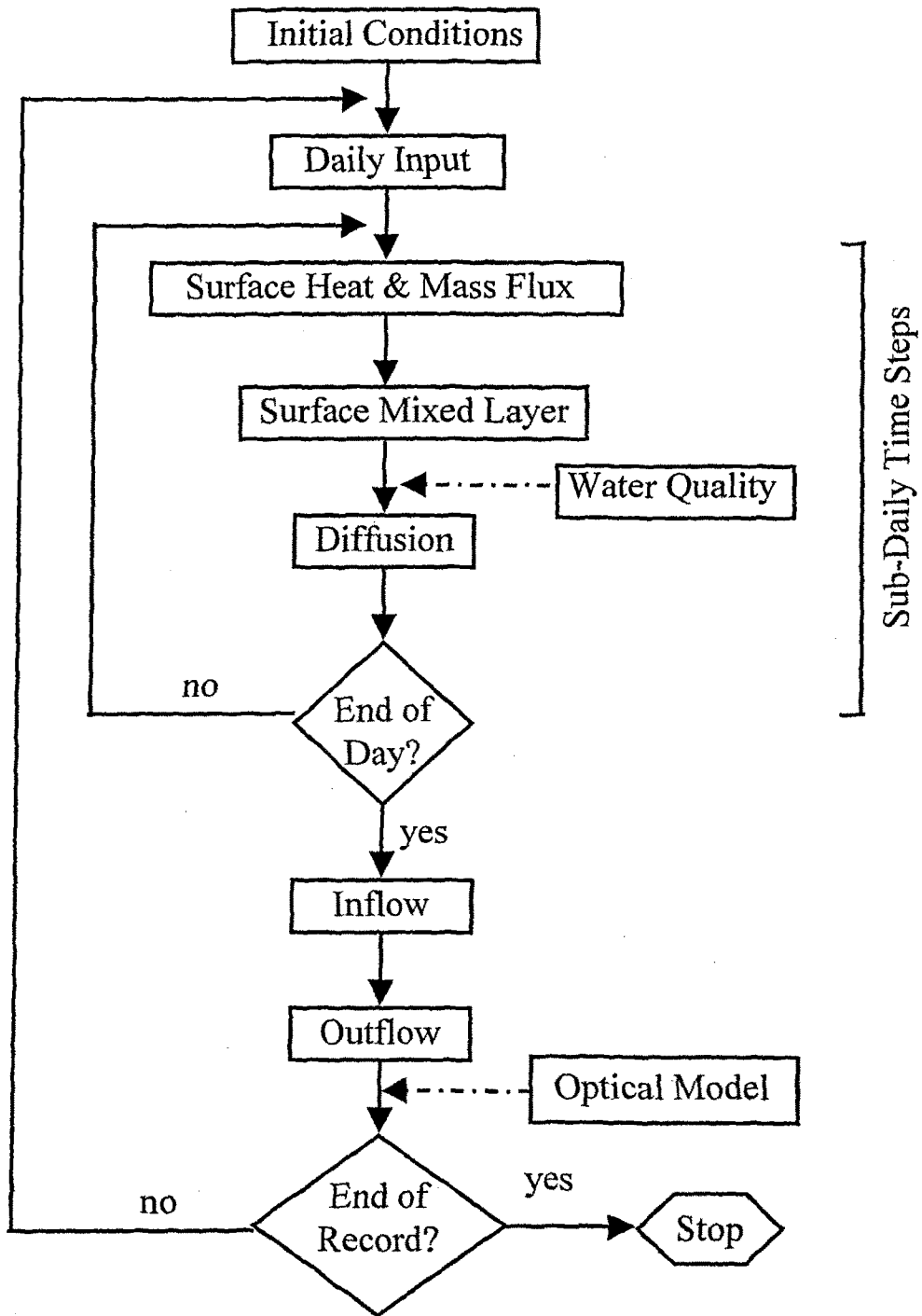
Figure 3.1 Flow chart indicating the order and time step of modeled processes in DLM-WQ.

3.1. Physical Sub-Model

The model is a one-dimensional, process-based, deterministic lake simulation model. Thus, the first-order balances of mass, momentum and energy are controlled only by the vertical variations in each property. The individual processes that contribute to transport and mixing are parameterized and coupled sequentially to predict the vertical density stratification of the lake as a function of time. The model is based on a Lagrangian layer scheme in which the lake is modeled by a series of horizontal layers of uniform properties. The layer positions change in response to inflow and outflow, and layer thickness changes as the layers are moved vertically to accommodate volume changes.

Necessary daily meteorological data for DLM-WQ include total solar radiation, average air temperature, average vapor pressure, average wind speed, and total rainfall. Daily total inflow volumes and average daily concentrations of temperature and salinity along with water quality parameters must be given with the inflow data. Daily total outflow volumes from specified heights above the lake bottom must also be given. Lake bathymetry is input as a table of height from the lake bottom versus the surface area, and cumulative volume. Initial conditions in the form of vertical profiles for temperature and salinity along with all water quality parameters in the water column must also be provided. Physical constants, although no longer calibrated, are given in a separate input file. See **Chapter 4** for a more detailed description of the input data and file formats.

3.1.1 One Dimensionality Assumption

Vertical stratification in a lake results when the vertical stable density gradients cannot be overcome by mixing forces. In most systems, solar (short wave) radiation heats the water near the surface, causing it to expand and thereby to decrease its density. Density can be also affected by inputs of dissolved and suspended solids from inflows and from re-suspension from the bottom. Under stratified conditions, the water column is divided into regions called the epilimnion (surface layer), metalimnion (region of highest gradient) and hypolimnion (the deeper, more

quiescent region). Seasonal trends in heat and mixing energy allow for a classification of lakes as ranging from holomictic (often completely mixed) to meromictic (never completely mixed) (Horne and Goldman, 1994).

The validity of the 1-D hypothesis should be assessed based on the available data on bathymetry, stratification, wind forcing, as well as the inflow and outflow of water. Rotational effects, inflow, outflow and the action of the wind on the surface can modify the structure sufficiently that the 1-D hypothesis is no longer valid or at least introduces error. Inflow and outflow effects are negligible for Lake Tahoe. Thus, rotation and wind are the only effects must be considered while interpreting the model results.

Rotational effects, as described by Hutter (1984; 1986) and Stocker and Hutter (1986), are important in larger lakes like one of the investigated in this work. The Coriolis force can lead to some deformations of the surface as well as of the thermocline. These include Kelvin waves and Poincare waves. Recognizing that the external (surface) modes have time scales that are too short for rotational effects to be an influence, we need only consider the internal modes. The length scale of these internal deformation modes is given by the Rossby radius of internal deformation R_I. This scale is defined by equating the speed of internal gravity waves $(g'h)^{(1/2)}$ (Fischer et al., 1979) with the propagation speed of inertial waves due to terrestrial rotation fR_I, such that

$$R_I = \frac{\sqrt{g'h}}{f} \qquad (3.1)$$

where g' is the reduced gravity and h is the depth of an equivalent two-layer thermal structure, and f is the Coriolis parameter defined as $f = 2\,\Omega\,sin\Phi$, where Ω is the angular velocity of the earth (in radians), and Φ is the latitude of the lake. R_I indicates the distance to which the Coriolis force balances the pressure gradient created by an inclined interface. In comparing R_I and the smallest characteristic dimension of the lake (in general the width B), the Rossby number R is obtained:

$$R = \frac{R_I}{B}$$

(3.2)

If the ratio R is large, the Coriolis forces are small compared with the pressure forces, the interface remains horizontal, and the mixed layer retains its 1-D character. Thus $R > 1$ is the criterion for the absence of rotational effects.

The Lake Number, L_N, characterizes the response of an arbitrarily stratified water column to a surface wind. L_N is defined as (Imberger and Patterson, 1990):

$$L_N = \frac{(1 - z_m / Z)gS}{\rho_h u_*^2 A_z^{3/2}(1 - z_* / Z)}$$

(3.3)

where g is the gravitational constant, z_m is the height to the center of the metalimnion, ρ_h is the water density in the hypolimnion, u_* is the shear velocity, A_z is the area at the lake surface, and S is the lake stability defined as:

$$S = \int_0^z (z - z_*)\rho_z A_z dz$$

(3.4)

The total water depth is Z, A_z is the water surface area at height z, z_* is the height from the bottom to the center of volume of the lake and ρ_z is water density at height z. If $L_N \gg 1$, then the restoring force is greater than the disturbing forces and mixing below the thermocline will be minimal. If $L_N \ll 1$, the disturbing forces dominate and significant deflections of the isopycnals may occur. A one-dimensional representation of a lake requires large values of L_N.

New routines have been added to DLM-WQ to calculate the Rossby number and the Lake number. Thus an estimation of the validity of the 1-D assumption can be given when interpreting the simulations. The routine for Rossby number calculation was provided by Francisco Rueda of UC Davis. **Figures 3.2** plot the estimated *Lake number* based on the measured wind speed and simulated temperature profiles for 1992 and 1999. Though values of the Lake Number vary (1999 is generally lower), during thermally stratified periods the Lake Number is always much greater than 1. Thus from the viewpoint of wind mixing, the one-dimensional assumption is valid.

During winter, when the lake undergoes deep mixing, the Lake Number falls to of order 1. Measurements have also confirmed this (Thompson, 2000). This is not considered to be a problem, as the net effect of mixing is accomplished by the one-dimensional representation, and lake clarity is not critical during deep mixing.

Figure 3.3 shows the calculated *Internal Rossby Number* for 1992 and 1999. As before, the values are larger during the strongly stratified period, although they are only of order unity. Outside of the strongly stratified periods, the Rossby Number is less than 1, indicating that rotation does play a role. However, these effects will not invalidate the predicted thermal structure using the 1-D assumption as will be considered in the following Chapters.

3.1.2 Thermodynamics

The surface heat exchange is modeled as the sum of six heat fluxes:

$$S = K \cdot (1 - A_s) + L_{in} - L_{out} - H_E - H_C + H_F \tag{3.5}$$

The first three terms on the right-hand side of the equation represent the radiation balance of the lake surface: $K(1-A_s)$ represents the short-wave radiation absorbed by the lake surface with A_s the short-wave reflectivity, L_{in} represents the long-wave radiation absorbed by the lake surface and L_{out} represents the long-wave radiation emitted by the lake surface. The fourth and fifth terms, the non-radiative terms, represent heat exchange at the air-water surface by processes of evaporation/condensation and convection/conduction, respectively. The last term is the heat exchange due to inflows and outflows.

The daily-integrated short wave radiation is input to the model. A value of 0.03 has been assumed for the short wave reflectivity (Henderson-Sellers, 1986). The incident long wave radiation is also input to the model. The daily-integrated values for both must be supplied at to the model. Long wave emission is calculated by the model. To calculate the long wave radiation emitted by at the air-water interface, it is assumed that the water surface acts as a grey body with an emissivity of 0.97, such that (Henderson-Sellers, 1986):
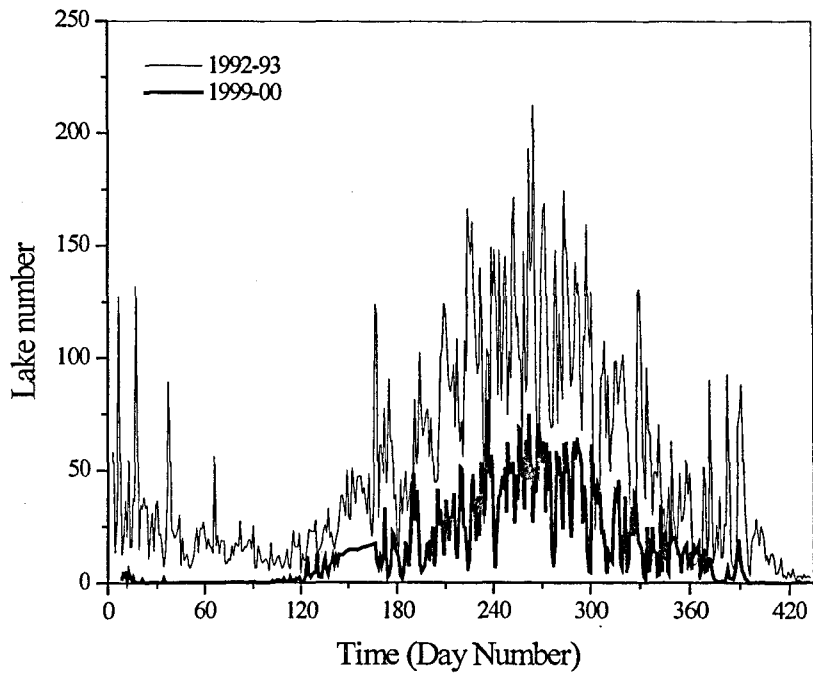
Figure 3.2 Calculated Lake number for 1992 and 1999.
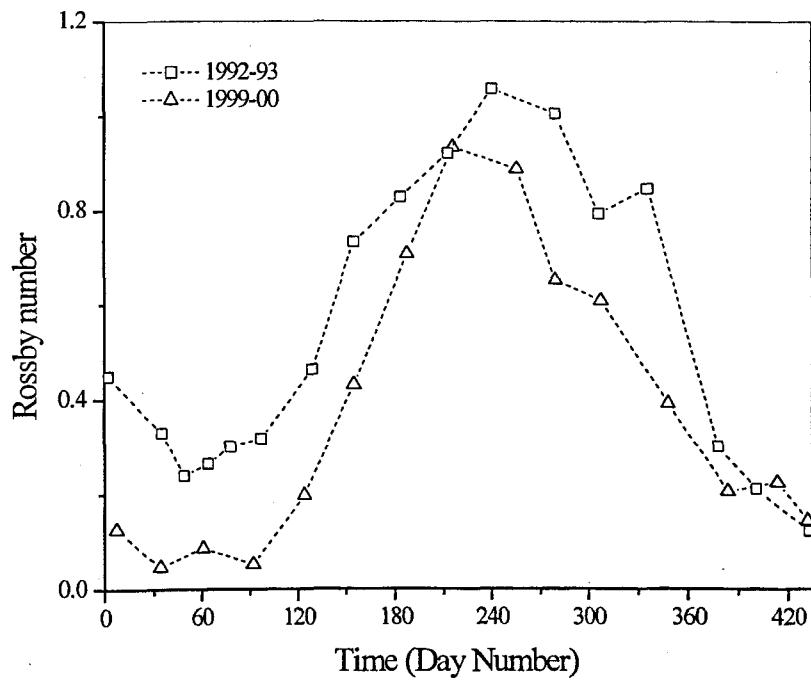
Figure 3.3 Calculated Rossby numbers for 1992 and 1999. Measured temperature data were used.

$$L_{out} = -0.97 \cdot \sigma \cdot T_w{}^4 \qquad\qquad (3.6)$$

where σ is the Stefan-Boltzmann constant (56.7×10^{-9} Wm^{-2} K^{-4}), and $T_w(K)$ is the water surface temperature (in degrees Kelvin) calculated by the model.

The heat exchange at the water surface of the lake occurring as the result of the processes of evaporation/condensation and convection/conduction is described by:

$$H_E + H_C = -f(u) \cdot \left[(e_w - e_a) + 0.63 \cdot (T_w - T_a) \right] \qquad\qquad (3.7)$$

where f(u) is set as a constant value (TVA, 1972) and $(e_w\text{-}e_a)$ is the difference between the water vapor pressure of the air over the lake (e_w) and the saturation water pressure at the temperature of the lake surface (e_a), T_w is the water surface temperature and T_a is the air temperature (in degrees Celsius).

The heat loss or gain by the inflows and outflows is calculated by readjusting the temperature of each layer affected by entrainment during the insertion and withdrawal algorithms. The bottom boundary is considered adiabatic for temperature. The flux of heat from the rest of the sediment area is not considered.

The heat budget algorithm has been improved in several ways. Solar (short wave) radiation, which is an input in the form of a daily total, is varied sinusoidally during sunlight hours. The model's internal clock, which is controlled in the heat budget subroutine, was changed from starting at noon to starting at midnight, thereby avoiding the splitting of daily input between parts of two days. The previous practice amounted to using a 2-day running mean for all meteorological parameters, which diminished the strength of large meteorological changes on the heat; mass and momentum transfer during the day. The sub-daily time step interval may be selected by the user. The model uses a partial time step to coincide with the exact times of sunrise and sunset (also calculated). A user-selected time of day for model output purposes allows for a better comparison between simulated and measured profiles.

3.1.3 Mixed Layer Dynamics

The mixing algorithm implemented in DLM-WQ is based on a *Turbulent Kinetic Energy (TKE)* budget similar to the mixing algorithm of DYRESM that is well described in the literature [see for example, Sherman et al., 1978; Imberger and Patterson, 1981; Imberger and Patterson, 1990]. The mixed layer dynamics are modeled in four distinct sections: deepening by convective overturn, deepening by stirring, deepening by shear production which includes continual readjustment of the shear velocity, and mixing of the pycnocline by Kelvin-Helmholtz billows. The mixed layer algorithm acts on the density profile generated by the heat transport routine. Surface heat exchanges and penetrative heating from radiation modify the density profile, potentially producing an unstable density profile at the water surface. This potentially unstable density profile is stored in the density vector until the mixing routine is called. The algorithm proceeds by first computing available energy for mixing the layers from top to bottom produced by convective overturn and wind stirring, and then calculating the energy produced by shear and billowing. The time step for each of the processes can be set by the user in the range 15 min to 12h, or be fixed automatically by the model itself, by limiting the maximum rate of change in temperature or momentum at the top layer.

3.1.4 Hypolimnetic Processes

Turbulent transport in the hypolimnion is modeled as a diffusion-like process, with eddy diffusivity relating the dissipation of turbulent kinetic energy and to the local density gradient (Imberger, 1982; Imberger and Patterson, 1981; Spigel and Imberger, 1980; Spigel et al., 1986).

3.1.5 Inflows and Outflows

Inflow and outflow are modeled as the expansion and depletion of layers directly affected by the inflow and outflow. In the case of inflow, the mechanisms of plunging underflow and entrainment are also modeled. The inflow process is divided into three parts. As the stream enters the reservoir it pushes the stagnant reservoir water ahead of itself until buoyancy forces dominate, then either flows over water surface or plunges beneath the surface, depending on the relative density. Once submerged, the stream will flow down the river valley and entrain lake water. Outflows are modeled

as either point or line sinks, as specified by the user, following the equations for the vertical velocity developed by Hocking et al. (1988). Inflows and outflows are characterized by a daily time step. Inflows and outflows may change the depth and thickness of layers but not their density (Imberger et al., 1976). Coriolis effects on the inflows and outflows are not considered although Lake Tahoe inflow and outflow do not modify the thermal structure.

The routines that perform the inflow and insertion processes have been adapted to the conditions at Lake Tahoe. The maximum number of inflowing streams has been increased up to 21. The rationale behind this choice is described in **Section 4.2**. In actuality, Lake Tahoe has 63 inflowing streams. The maximum number of model layers has been increased to 500.

3.1.6 Ground Water

The magnitude of the contribution of the ground water to the water and nutrient budget of Lake Tahoe is poorly known. Here it has been assumed that the groundwater flux can be approximated as a constant fraction of the mean daily stream inflow. The rationale is described in **Section 5.1.1**. It must be noted that with such an approach, seasonal changes could not be elucidated. The resulting flow is distributed equally between all the model layers. The temperature and salinity of the groundwater were assumed to be the same as the temperature and salinity of the layer in which the groundwater is being inserted. Water quality variables were different in the groundwater. These differences are described in **Section 4.3**.

3.2 Water Quality Sub-Model

The water quality sub-model comprises descriptions for phytoplankton, nutrients and particles. Modeling of chemical and biological components is done in conjunction with modeling of temperature and salinity, and uses the same sub-daily time-step. A fixed stoichiometry approach in which the nutrient composition of the algae is assumed to remain constant was implemented. Under this assumption, the nutrient uptake rates are proportional to the algal growth rate multiplied by the corresponding nutrient fractions of the algal cells. Nutrient excretion is modeled as the product of the

respiration mass flux and the nutrient stoichiometry of the organisms. The main features of the implemented water quality sub-model will be discussed in the following sections. The equations describing the biological and chemical dynamics are well established (see for example Bowie et al., 1985; Chapra, 1997; Ferris and Christian, 1991; Jorgensen and Gromiec, 1989; Lehman et al., 1975). Therefore the bulk of the equations will be presented without further citation.

3.2.1 Phytoplankton

The basic kinetic interactions for phytoplankton biomass are formulated in terms of the concentration of Chlorophyll a (hereafter referred to as Chla) per unit volume. Although Chla concentrations can be simulated for up to two functional algal groups (in this version of DLM-WQ), only one lumped phytoplankton species with bulk-averaged properties has been modeled for Lake Tahoe. The reason for this is that there were insufficient data on species-specific chlorophyll distribution.

The effect of biologically mediated processes (e.g. without considering the sedimentation loss term) on the dynamics of a phytoplankton group in layer i over the time step may be expressed as:

$$\frac{\partial Chla_i}{\partial t} = G_{max} \cdot \vartheta^{T-20} \cdot Chla_i \cdot Min\{f(I_i), f(P_i), f(N_i)\} - (k_r + k_m) \cdot \vartheta^{T-20} \cdot Chla_i$$
$$- k_z \cdot f(Z)$$

(3.8)

where $Chla_i$ is the concentration of the considered phytoplankton group as Chl a in layer i, G_{max} stands for the maximum rate growth of phytoplankton, θ the non-dimensional temperature multiplier for growth, respiration and death of phytoplankton, k_m is the rate coefficient for temperature dependent mortality rate, k_r is the rate coefficient for respiration, and k_z is the rate coefficient for zooplankton grazing.

As can be seen in Eqn 3.8, limitation of phytoplankton growth rate by environmental factors is modeled by multiplying the maximum potential phytoplankton growth rate by a temperature adjustment factor and a growth-limiting fraction with a value between zero and one. This fraction is the minimum value determined from equations

for limitation by light ($f(I_i)$), phosphorus ($f(N_i)$), and nitrogen ($f(P_i)$). Growth reduction of phytoplankton due to light is computed by the Steele equation (Jassby and Platt, 1976):

$$f(I_i) = \frac{I}{I_{sat}} \cdot EXP\left(1 - \left(\frac{I}{I_{sat}}\right)\right)$$

(3.9)

where I is the ambient light intensity and I_{sat} is the saturation light intensity. This form for the light response function assumes that the phytoplankton respond to changing light conditions instantaneously and with no light history effect. The effect on phytoplankton growth limitation by nitrogen or phosphorus is based on Michaelis-Menten kinetics and assumes that the growth rates are determined by the external concentrations of available nutrients. In this approach, it is assumed that the nutrient composition of the algae cells remains constant:

$$f(N_i) = \frac{(NO3 + NH4)}{k_{(NO3+NH4)} + (NO3 + NH4)}$$

(3.10)

$$f(P_i) = \frac{SRP}{k_{SRP} + SRP}$$

(3.11)

where $NO3_i$, $NH4_i$ and SRP_i are respectively the nitrate, ammonia nitrogen and the bio-available phosphorus concentrations in layer I, and k_{SRP} and $k_{(NO3+NH4)}$ are the half saturation constants.

Loss of phytoplankton biomass through respiration and mortality is considered after the appropriate growth increment has been applied to the chlorophyll concentration. Grazing by zooplankton and Mysis are modeled by applying a built-in forcing function that simulates the seasonal and diurnal population of these grazers (zooplankton and Mysis biomass is not explicitly modeled). This is described in **Section 3.2.7**. The nutrient compositions of zooplankton are assumed to be the same as for algae. The mortality and respiration rates are modeled as first order, temperature-dependent losses.

Phytoplankton settling is computed from input settling rates. Actual algae settling rates may change as a function of available light, light history and internal nutrient

stores (Smayda, 1974), but are assumed constant here. There is also no effect of nutrient limitation on buoyancy regulation in the model. Phytoplankton re-suspension is handled in a relatively simple manner. Whenever the chlorophyll concentration falls below a minimum value of 0.19 μg l^{-1} a fraction of the settled phytoplankton is re-suspended to keep the minimum concentration level above that threshold. This concentration is on the order of minimum chlorophyll levels observed in the hypolimnion of Lake Tahoe (Vincent, 1978).

3.2.2 Nutrients

Nutrients that are modeled are different species of Phosphorus and Nitrogen. The analytical determination of the chemical species does not match what is biologically available. This is specifically true for the case of the Phosphorous (Thébault, 1995). Segmentation can differentiate between dissolved and particulate fractions, that both could be either inorganic and organic. In turn, particulate material divided between living and non-living associated phosphorous. The kinetic segmentation scheme proposed is based on available measurements and follows a mechanistic basis, taking into account the numerical definition of the state variables.

The Phosphorus pool is partitioned between available (soluble) phosphorus SRP, a non-bioavailable phosphorus termed Refractive Phosphorus (RP), a non-living particulate organic fraction Particulate Organic Phosphorus, (POP), and a particulate living fraction, Phytoplankton Phosphorus (PhytoP). Thus Phosphorus variables explicitly modeled are SRP, RP, POP and potentially two PhytoP groups. **Figure 3.4** shows the modeled linkages between the various phosphorus pools. Total Phosphorous (TP) is simply obtained by addition of the individual groups:

$$TP = SRP + RP + POP + PhytoP \qquad (3.12)$$

Available measured fractions are Total Hydrolizable Phosphorous (THP), Dissolved Phosphorous (DP), and Particulate Phosphorous (PartP). The definition of these species are based on the analytical method employed. They are not additive (i.e. Total Phosphorous can not be expressed as their sum). The nutrient data are inferred as follows. Measured THP is assumed to be representative of the immediately biologically available Phosphorous, or

$$SRP = THP \qquad (3.13)$$

RP is obtained from the equation:

$$RP = DP - THP \qquad (3.14)$$

PartP is assumed to be mainly of organic origin (Jassby, per. comm.). The constant stoichiometric ratio P vs. chlorophyll is applied to split the PartP fraction into POP and PhytoP:

$$PhytoP = a_p \cdot Chla \qquad (3.15)$$

$$POP = PartP - PhytoP \qquad (3.16)$$

The model includes five nitrogen components: particulate organic nitrogen (PON), phytoplankton nitrogen (PN), dissolved organic nitrogen (DON), nitrate nitrogen (which includes nitrite nitrogen) (NO3), and ammonia nitrogen (NH4). Measured species are TKN, NH4, and NO3. **Figure 3.5** shows the modeled linkages between the various nitrogen pools. The relationships between the modeled and measured magnitudes are:

$$ON = TKN - NH4 \qquad (3.17)$$

$$PhytoN = a_n \cdot Chla \qquad (3.18)$$

$$PON = 0.166 \cdot ON - PhytoN \qquad (3.19)$$

$$DON = 0.834 \cdot ON \qquad (3.20)$$

The factors 0.166 and 0.834 are annually mean averaged fractions from Marjanovic (1989). A sensitivity analysis between the maximum and minimum values must be performed to check its impact on the predicted nutrient concentration. The modeled species are summarized in **Table 3.1**.
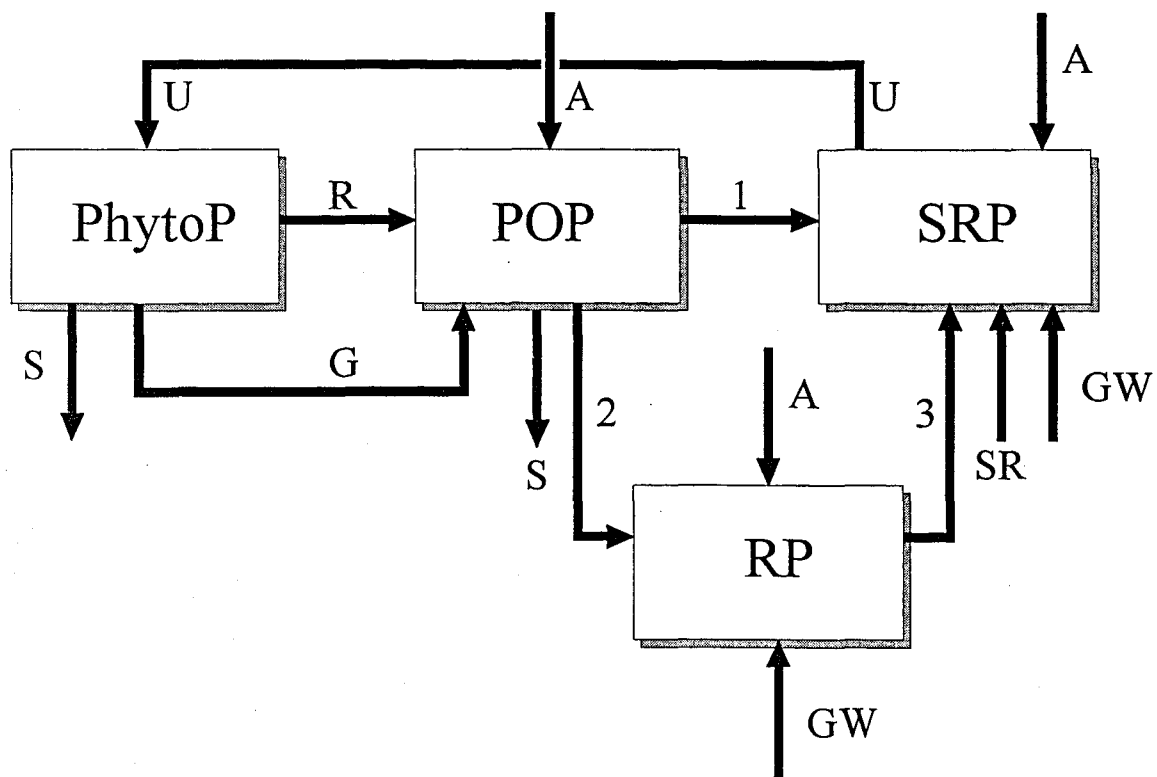
Figure 3.4 Linkages between the various phosphorus pools in DLM-WQ (except stream and outflow). They include Uptake (U), Respiration and Mortality (R), Grazing (G), Release from the sediments (SR), Atmospheric Deposition (A), Ground Water (GW), Settling (S), Organic Decay to THP from POP (1), Organic decay to RP from POP (2), Alliberation from RP (3).
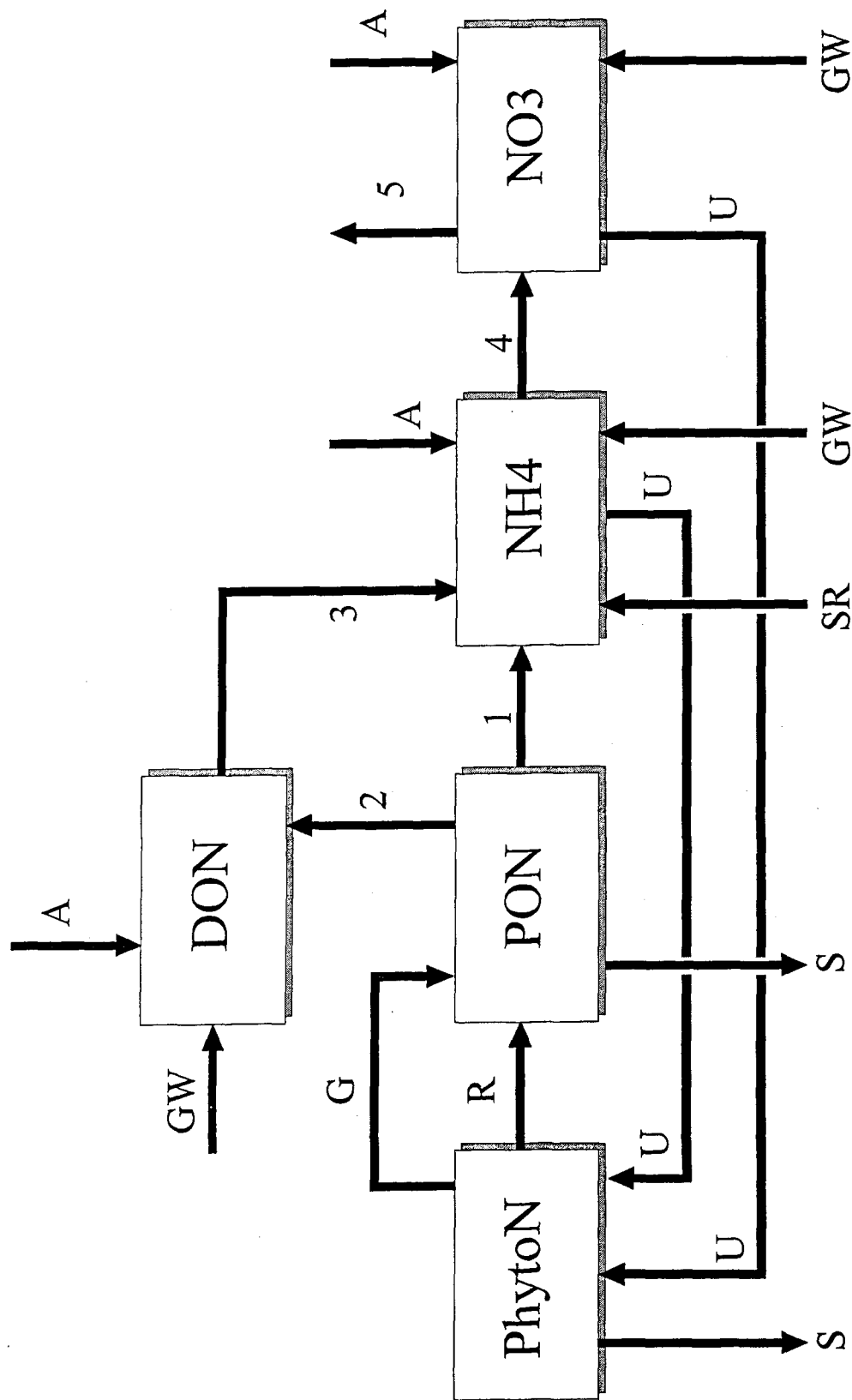
Figure 3.5 Linkages between the various phosphorus pools in DLM-WQ (except stream and outflow). They include Uptake (U), Respiration and Mortality (R), Grazing (G), Release from the sediments (SR), Atmospheric Deposition (A), Ground Water (GW), Settling (S), Ammonification from PON (1), Organic decay from PON (2), Ammonification from DON (3), Nitrification under oxygenated conditions (4), De-nitrification under anoxic conditions (5).

40

Table 3.1 Water quality state variables with their units.

#	Name	Symbol	Units
1	Temperature	T	C
2	Salinity	Sal	$mg\ l^{-1}$
3	Chlorophyll 1	Chla1	$\mu g\ l^{-1}$
4	Chlorophyll 2	Chla2	$\mu g\ l^{-1}$
5	Dissolved Oxygen	DO	$mg\ l^{-1}$
6	Biological Oxygen Demand	BOD	$mg\ l^{-1}$
7	Total Hydrolizable Phosphorus	THP	$\mu g\ l^{-1}$
8	Internal Phytoplankton Phosphorous 1	PhytoP1	$\mu g\ l^{-1}$
9	Internal Phytoplankton Phosphorous 2	PhytoP2	$\mu g\ l^{-1}$
10	Particulate Organic Phosphorus	POP	$\mu g\ l^{-1}$
11	Refractive Phosphorus	RP	$\mu g\ l^{-1}$
12	Nitrate	NO3	$\mu g\ l^{-1}$
13	Ammonia	NH4	$\mu g\ l^{-1}$
14	Internal Phytoplankton Nitrogen 1	PhytoN1	$\mu g\ l^{-1}$
15	Internal Phytoplankton Nitrogen 2	PhytoN2	$\mu g\ l^{-1}$
16	Particulate Organic Nitrogen	PON	$\mu g\ l^{-1}$
17	Dissolved Organic Nitrogen	DON	$\mu g\ l^{-1}$
18	Silica	Si	$\mu g\ l^{-1}$
19	Particle 1	Part1	$\#\ m^{-3}$
20	Particle 2	Part2	$\#\ m^{-3}$
21	Particle 3	Part3	$\#\ m^{-3}$
22	Particle 4	Part4	$\#\ m^{-3}$
23	Particle 5	Part5	$\#\ m^{-3}$
24	Particle 6	Part6	$\#\ m^{-3}$
25	Particle 7	Part7	$\#\ m^{-3}$

The equations for the effect of biological processes on concentrations of the modeled nutrients in layer i are:

$$\frac{\partial SRP_i}{\partial t} = k_{p1} \cdot \vartheta_o^{T-20} \cdot POP_i + k_{p3} \cdot \vartheta_o^{T-20} \cdot RP_i + S_p \cdot \vartheta_s^{T-20} \cdot \frac{AS_i}{V_i} \cdot \Delta time$$
$$- a_p \cdot G$$

$$(3.21)$$

$$\frac{\partial POP_i}{\partial t} = a_p \cdot k_z \cdot (Z) + a_P \cdot (R+M) - k_{p1} \cdot \vartheta_o^{T-20} \cdot POP_i - k_{p2} \cdot \vartheta_o^{T-20} \cdot POP_i$$

$$(3.22)$$

$$\frac{\partial RP_i}{\partial t} = k_{p2} \cdot \vartheta_o^{T-20} \cdot POP_i - k_{p3} \cdot \vartheta_o^{T-20} \cdot RP_i$$

$$(3.23)$$

$$\frac{\partial NH4_i}{\partial t} = k_{n1} \cdot \vartheta_o^{T-20} \cdot PON_i + S_N \cdot \vartheta_S^{T-20} \cdot \frac{AS_i}{V_i} + k_{n3} \cdot \vartheta_o^{T-20} \cdot DON_i$$

$$- k_{n4} \cdot \vartheta_{NO}^{T-20} \cdot NH4_i \cdot \frac{DO_i}{K_{ON} + DO_i} - a_n \cdot G \cdot f_{NH4}$$

$$(3.24)$$

$$\frac{\partial NO3_i}{\partial t} = k_{n4} \cdot \vartheta_{NO}^{T-20} \cdot NH4_i \cdot \frac{DO_i}{K_{ON} + DO_i} - k_{n5} \cdot \vartheta_{NO}^{T-20} \cdot NO3_i \cdot \frac{DO_i}{K_{ON} + DO_i}$$

$$- a_n \cdot G \cdot (1 - f_{NH4})$$

$$(3.25)$$

$$\frac{\partial PON_i}{\partial t} = a_n \cdot (R + M) + a_n \cdot k_z \cdot (Z) - k_{n1} \cdot \vartheta_o^{T-20} \cdot PON_i - k_{n2} \cdot \vartheta_o^{T-20} \cdot PON_i$$

$$(3.26)$$

$$\frac{\partial DON_i}{\partial t} = +k_{n2} \cdot \vartheta_{NO}^{T-20} \cdot PON_i - k_{n3} \cdot \vartheta_o^{T-20} \cdot DON_i$$

$$(3.27)$$

where, k_{n1}, k_{n2}, k_{n3}, k_{n4}, k_{n1}, k_{p1}, k_{p2}, k_{p3} are the rates for the nutrient reactions, θ_O and θ_{NO} are the non-dimensional temperature multipliers, S_p is the sediment release rate of THP, S_N is the sediment release rate of nitrogen as ammonia, θ_S is the non-dimensional temperature multiplier for sediment nutrient release, AS_i is the area of sediments in contact with layer i, V_i is the volume of water in layer i, DO_i is the dissolved concentration of oxygen in layer i, f_{NH4} is the coefficient for preferential uptake of ammonia, K_{ON} is the half saturation constant for the effect of oxygen on the rate of nitrification, K_{NH} is the half saturation constant for effect of oxygen concentration on de-nitrification. The coefficient for preferential uptake is defined as (Bowie et al., 1985)

$$f_{NH4} = \left(\frac{NH4}{NH4 + k_{NH4}}\right) \cdot \left(\frac{NO3}{NO3 + k_{NH4}}\right) + \left(\frac{NH4}{NH4 + NO3}\right) \cdot \left(\frac{k_{NH4}}{NO3 + k_{NH4}}\right)$$

$$(3.28)$$

where k_{NH4} is the half saturation constant.

Excluding settling, phytoplankton nutrient dynamics are represented by the equations:

42

$$\frac{\partial PhytoP_i}{\partial t} = a_p \cdot G_{max} \cdot \vartheta^{T-20} \cdot Chla_i \cdot Min\{f(I_i), f(P_i), f(N_i)\}$$

$$- a_p \cdot (k_r + k_m) \cdot \vartheta^{T-20} \cdot Chla_i - k_z \cdot f(Z)$$

(3.29)

$$\frac{\partial PhytoN_i}{\partial t} = a_n \cdot G_{max} \cdot \vartheta^{T-20} \cdot Chla_i \cdot Min\{f(I_i), f(P_i), f(N_i)\}$$

$$- a_n \cdot (k_r + k_m) \cdot \vartheta^{T-20} \cdot Chla_i - k_z \cdot f(Z)$$

(3.30)

where $PhytoP_i$, is the phytoplankton phosphorus concentration in layer i, $PhytoN_i$ is the phytoplankton nitrogen concentration in layer i, a_p is the constant ratio of Phosphorus to Chlorophyll, a_n is the Nitrogen to Chlorophyll ratio, k_z is the rate for zooplankton grazing, with the remaining terms as described above.

Loss terms applied to phytoplankton dynamics also apply to the phytoplankton nutrients. The loss of phytoplankton nutrients through settling is treated with the same velocity as those for the corresponding algal group. SRP, NO3, and NH4 are decreased by phytoplankton uptake, with an additional term for ammonia and nitrate to distinguish preferential nitrogen uptake. Phytoplankton respiration, mortality, and breakdown of organic matter and release from the sediment/water interface increase NH4 and SRP concentrations. Nitrate concentrations are increased by nitrification under well-oxygenated conditions, but when the oxygen concentration declines below 0.5 mg/l, de-nitrification becomes the dominant process. To date, oxygen concentrations as low as this have not been observed or simulated at lake Tahoe.

3.2.3 Particles

The settling of inorganic and organic particulate matter and BOD, POP and PON is included in the model. The algorithm for particle settling is described in Casamitjana and Schladow (1993b). As available data of inorganic particles are measured in units of particle number per cubic meter (# m^{-3}, the code has been modified to directly handle the number of particles, rather than mass concentration. The same change has been made in the stream inflow inputs. Inorganic particles are represented in 7 size ranges. A hyperbolic diameter distribution from 0.5 to 5 µm for the 7 ranges has been assumed. The 8 values that constitute the bounds of each size range are 0.5, 1.08,

1.69, 2.32, 2.97, 3.64, 4.31 and 5.00 μm. The specific gravity of particles is assumed to be that for quartz, i.e. 2.6. The settling velocity of each inorganic particle class is calculated from Stokes' law. As there is a monotonic decrease in lake area with depth, particles can intercept the sediment throughout the water column. The fraction of particles that settle to the sediment from each model layer is in proportion to the difference in surface area of each layer. Once the inorganic particles have settled, they cannot be resuspended. The effect of coagulation was neglected by setting to zero the coagulation parameter in the particle model. Insufficient is known about this process in Lake Tahoe.

The particulate nutrient fractions (POP and PON) along with BOD (included but set to zero for Lake Tahoe) and phytoplankton (Chla) are modeled in a different way. The settling velocity for these state variables must be provided as input parameters, along with transfer functions to relate mass concentration to particle concentration. Usually, Chla, PON and POP are expressed in units of mass concentration, but need to be equated with particle concentration to calculate the settling. After settling and resuspension, they must be reconverted back into mass concentration units. For Chla, biomass measurements, derived from vertical plankton tows in the top 100 m of Lake Tahoe, were correlated with integrated Chlorophyll concentration over a similar depth (from discrete measurements at 0, 10, 50 and 100 m). For 1999 this produced a linear fit with $R^2 = 0.710$. Phytoplankton cell counts for 1987 (D. Hunter, unpubl. data) were also correlated with biomass concentration, yielding an $R^2 = 0.727$. If it is assumed that these correlations are preserved from year to year, then a transfer factor is obtained by combining the two correlations, thereby yielding particle number in terms of chlorophyll concentration. This factor was assumed to be constant throughout the year, although it is likely that in reality it changes seasonally.

POP and PON (detritus or non-living organic nutrients) were assumed to be spherical particles with a mean diameter of 5 μm. A transfer coefficient was derived by dividing the mass concentration of POP and PON (see **Section 3.2.2**) by the mass of one particle (the product of the particle volume and its density, assumed to be 1030 kgm^{-3}). The number of particles typically obtained in this manner was consistent with those measured by Coker (2000) for Lake Tahoe.

44

Given the expected high uncertainty associated with these factors, and as the concentration of living and non living particles present in the water column have a profound impact on the Secchi depth, these factors have been included in a sensitivity analysis (see **Chapter 6**).

3.2.4 Oxygen

The dissolved oxygen concentration is the result of contributions from surface aeration, advection by inflows and outflows, phytoplankton photosynthesis and respiration, biochemical and sediment oxygen demand, and nitrification. Surface aeration can act as either a source or a sink of oxygen depending on the temperature and oxygen concentration of the surface water. This only impacts the top model layer. The equation for the effect of phytoplankton photosynthesis and respiration on the dissolved oxygen concentration is similar to that for changes in Chla, except for the inclusion of a stoichiometric conversion factor. The effect of nitrification on dissolved oxygen is handled similarly, with the equation being identical to that for the effect of nitrification on the nitrate concentration and a stoichiometric factor to convert nitrate produced to oxygen consumed in the process. Oxygen demand of the sediments is assumed to be zero. Biochemical oxygen demand is modeled for each layer using an oxygen demand equivalent corresponding to the detrital mass. It is replenished through phytoplankton mortality and by assigning an appropriate stoichiometric factor.

3.2.5 Sediment

The sediment layer is not explicitly modeled. However, the model was improved to take into account the release of nutrients from either the bottom and the sides of the lake by treating the nutrient release from the sediment as a zero-order process. The time, area and volumetric effects are lumped into a single factor. The time lag for lateral dispersion is assumed inconsequential. Release rates (r_T) of SRP, and NH4 from the sediment bed of these elements in the water column are modeled temperature-dependent. The equation takes the form:

$$r_T = r_{SRP}\theta^{(T-20)} \cdot F \qquad (3.31)$$

$$r_T = r_{NH4} \theta^{(T-20)} \cdot F \qquad\qquad (3.32)$$

where r_{SRP} and r_{NH4} are the rate constants of bioavailable phosphorous and ammonia at 20 °C respectively, θ is an sediment release temperature multiplier and F is the lumped factor. Sediment release rates are highly site-specific, and in absence of experimental confirmation, must be determined by model calibration.

3.2.6 Atmospheric Deposition

Atmospheric deposition was introduced in the model as a source of nutrients. Particles enter the surface of the lake by settling (dry deposition) or by being transported with precipitation (wet deposition). A constant daily flux, for either wet deposition or dry deposition, was estimated for each nutrient fraction, based on the mean of measurements for years 1989 to 1992 (Jassby et al., 1994). Wet deposition rates apply for days with precipitation. Otherwise dry deposition rates apply. Atmospheric deposition is handled at the end of each day by the model. The measured variables for atmospheric deposition were fluxes of SRP, TP, NO3, and NH4. In order to translate the measured magnitudes to the modeled ones, the following assumptions have been made:

$$SRP = SRP \qquad\qquad (3.33)$$

$$PhytoP = 0 \qquad\qquad (3.34)$$

$$RP = 0.5 \cdot (TP - SRP) \qquad\qquad (3.35)$$

$$POP = 0.5 \cdot (TP - SRP) \qquad\qquad (3.36)$$

$$NH4 = NH4 \qquad\qquad (3.37)$$

$$NO3 = NO3 \qquad\qquad (3.38)$$

$$PhytoN = 0 \qquad\qquad (3.39)$$

$$DON = TN - (NH4 + NO3) \qquad\qquad (3.40)$$

$$PON = 0 \qquad\qquad (3.41)$$

46

The factor 0.5 in Eqn (3.35) and Eqn (3.36) is a first estimate that should be substantiated with further experimental results.

3.2.7 Zooplankton and Mysis

As depicted in **Chapter 2**, the behavior of zooplankton and Mysis is very complex and it is difficult to incorporate taxa-specific behavior into a single "zooplankton" term (where in what follows the term zooplankton should also be taken to include Mysis). It has been shown that *Mysis relicta* and zooplankton may act as nutrient pumps, transporting phosphorous and nitrogen through the water column (see **Section 2.3.4**). Thus, it has been assumed that it is important to also include vertical migration behavior. This task is complicated by the fact that in this model zooplankton concentration is not an explicit state variable, but rather it is a forcing function. That is to say, the effect of zooplankton on phytoplankton (and hence nutrients) is prescribed.

The zooplankton grazing rate (0.05 day^{-1}) is a constant loss term in the phytoplankton growth equation (Eqn 3.8). The nutrient equivalent of this loss is a source term in the POP and PON equations (Eqn 3.22 and 3.26). As both these terms are first order representations (dependent only on chlorophyll concentration), the grazing loss and the associated nutrient release will be proportional to the vertical distribution of chlorophyll. In reality, vertical migration of zooplankton (typically residing in the upper water column by night and in the lower water column by day) changes this.

In the model the effect of vertical migration has been taken into account by spatially and temporally varying the excretion term as follows. During night conditions in the upper 150 m of the water column, only a fraction of the grazed nutrients are released via excretion immediately. The remainder is released during day conditions in the lower part of the water column only (between 150 and 500 m). Excretion of grazing products from the lower water column is not affected by this. Thus the net effect is simply to transfer excretion products (nutrients) vertically downward.

3.3 Optical Sub-Model

The optical sub-model seeks to provide a mechanistic link between predicted concentrations of dissolved and particulate matter in the lake, and water clarity as measured with a Secchi disk or other instrument. The optical model calculates the scattering and absorption characteristics of the water and its constituents (particulate organic, particulate inorganic, and dissolved matter) based on particle size distributions, composition, and concentration, and then calculates the Secchi depth from the inherent optical properties. Inorganic particles have been discretized within 7 size ranges, organic particles (i.e., phytoplankton) are parameterized as chlorophyll-a concentration, and Colored Dissolved Organic Matter (CDOM) and pure water appear as constants. Early measurements determined that absorption by CDOM in Lake Tahoe, while measurable, was a minor attenuant relative to the particulate species (T. Swift, pers. comm.). Values for pure water were taken from the literature (Buitveld et al., 1994).

3.3.1 Absorption

Particulate absorption coefficients were derived from laboratory measurements of filtrates on GF/F glass fiber filters (e.g., Mitchell, 1990). For the present, we assume that inorganic matter does not absorb significantly. The absorption coefficient is depicted as:

$$a(PAR, Chla) = a_{water} + a_{gelb} + a^*_{Chla} \cdot [Chla] \tag{3.42}$$

where a_{water} is the absorption by pure water 0.050 m^{-1}, a_{gelb} is absorption by gelbstoff (yellow matter) and is assumed to be constant in Lake Tahoe with a value of 0.0119 m^{-1}, a^*_{Chla} is a chlorophyll-specific absorption, set to 0.024 m^2 mg^{-1}, and Chla is the concentration of chlorophyll. The values for these coefficients are from a combination literature values and research (T. J. Swift, pers. comm.). The terms *PAR* and Chla in parentheses indicate a functional dependence on the particle distribution and chlorophyll concentration respectively.

48

3.3.2 Scattering and Particles

Mie light scattering theory, applicable to particles larger than the wavelength of light (approximately 0.5 μm), is used to calculate scattering by inorganic particles, given their size and refractive index. These calculations indicate that it is the smallest size classes, from approximately 0.5 to 5 μm, which contribute most of the light scattering (van de Hulst, 1981; Davies-Colley et al., 1993). It is the combination of the individual particle's scattering efficiency and the large population of small particles that makes them particularly important. The scattering efficiency of each size range of particle is integrated across the visible spectrum and reduced to a single scattering coefficient for that size range (see **Table 3.2**). The coefficients are multiplied by the number of particles in each size class and summed to arrive at total particulate scattering. Inorganic particles are assumed to have a refractive index close to that of quartz (n = 1.15). Scattering by organic algal particles is represented by a specific-scattering coefficient multiplied by the chlorophyll concentration. Thus the scattering coefficient is expressed as:

$$b(PAR, Chla) = b_{water} + b^*_{Chla} \cdot [Chla] + b_{sed} \qquad (3.43)$$

where b_{water} is the pure water contribution, assumed constant at 0.0019 m^{-1}, b^*_{Chla} is chlorophyll-specific scattering, set constant to 0.20 m^{-2} mg^{-1}, and b_{sed} is the total scattering due to particles in the model's size ranges.

Table 3.2 Scattering coefficients (Swift, pers. comm.).

Particle Class	Diameter (μm)	Scatter Coef. (m^{-1})/particle)
1	0.500 -1.077	1.172E-05
2	1.078 -1.687	1.189E-04
3	1.688 -2.321	3.885E-04
4	2.322 -2.971	7.336E-04
5	2.972 - 3.636	1.072E-03
6	3.637 -4.312	1.453E-03
7	4.313 - 5.000	1.940E-03

3.3.3 Link to Secchi Depth

Tyler (1968) and Priesendorfer (1986) derived the relationship between Secchi depth, the human eye's ability to detect contrast, and the optical properties of the water of the form:

$$SecchiDepth = \frac{\gamma}{(c + K_d)} \qquad (3.44)$$

Here, c is the beam attenuation, the sum of absorption and scattering, $[\,m^{-1}]$:

$$c = a(PAR, Chla) + b(PAR, Chla) \qquad (3.45)$$

K_d stands for the downwelling irradiance attenuation (also called the extinction coefficient), due to scattering, absorption, and the strength and direction of the sunlight illuminating the disk, $[m^{-1}]$:

$$K_d = a(PAR, Chla) \cdot \left[\frac{\left(1 + (0.425 \cdot \mu_o - 0.19) \cdot \frac{b(PAR, Chla)}{a(PAR, Chla)} \right)^{1/2}}{\mu_o} \right] \qquad (3.46)$$

where μ_o is the average cosine of the refracted solar angle,

$$\mu_0 = \cos\left[\arcsin\left(\frac{\sin(\varphi)}{1.34} \right) \right] \qquad (3.47)$$

where φ is the solar zenith angle. μ_o varies from 0.72 to 0.97 from winter to summer. A mean value of 0.9 has been assumed, as SD is weakly dependent on μ_o. K_d and c are weighted by the eye's photopic response; γ is quasi-constant; represents eye's ability to distinguish contrast. γ is known to vary somewhat from water body to water body, but usually has a value of ~8.9 (Davies-Colley et al., 1993).

An iterative procedure was implemented to integrate the Tyler equation. The surface waters (down to and including the Secchi depth) are usually almost homogenous from wind mixing, and the mixed layer is deeper than the Secchi depth. Starting from the top, the mean depth averaged values of absorption and scattering for the top layer is calculated and a Secchi depth calculated. If the predicted Secchi depth exceeds the

50

depth to the bottom of this layer, the process is repeated using the averaged properties of the two top layers. When the actual distance to the bottom of the last layer included exceeds the calculated Secchi depth, the process is stopped and the calculated Secchi depth is utilized. Although simple, this iterative procedure gives enough resolution to resolve trends of spatial variability within the minimum and maximum layers thickness criteria.

3.4 Model Assumptions and Forcing Parameters

The model requires a set of input data. In deriving the causal relationships among the state variables of the model, some assumptions have been made. These reflect the best available knowledge at the present time, but need further research to be fully supported. Many of these parameters are related to the input fluxes to the lake, although strictly speaking, some of the listed parameters are an integral part of the model itself. The forcing parameters have been categorized into 4 classes: atmospheric deposition rates, stream inflows, ground water, and initial conditions (see **Table 3.3**). Within atmospheric deposition were included the parameterized nutrient fluxes, for both dry and wet deposition. Those related to stream inflows include the assumptions about overall nutrient fluxes, nutrient partitioning between species, the temperature and the factor to parameterize the stream run-off contribution to the water budget. These assumptions are needed to convert measured chemical species into suitable water quality state variables, to estimate the contribution of run-off in the water balance from the available (up to date) water data. The ground water parameters are used to describe the amount of flow and nutrients coming into the lake. as explained **Chapter 4**. The initial conditions include the parameters used to derive the initial profiles (of the nutrient variables, the assumed fraction of inorganic to organic particulate matter) as well as parameters describing the dynamics of zooplankton and the range of particulate matter.

Table 3.3 Model forcing model parameters.

#	Description	Value	Units	Ref.
Atmospheric Deposition Nutrient Rates				
1	DON_DRY	686.56	$\mu g\ m^{-2}\ d^{-1}$	1
2	NH4_DRY	109.2	$\mu g\ m^{-2}\ d^{-1}$	1
3	NO3_DRY	266	$\mu g\ m^{-2}\ d^{-1}$	1
4	SRP_DRY	12.08	$\mu g\ m^{-2}\ d^{-1}$	2
5	POP_DRY	16.57	$\mu g\ m^{-2}\ d^{-1}$	2
6	RP_DRY	16.57	$\mu g\ m^{-2}\ d^{-1}$	2
7	DON_WET	648.2	$\mu g\ m^{-2}\ d^{-1}$	1
8	NH4_WET	224	$\mu g\ m^{-2}\ d^{-1}$	1
9	NO3_WET	103.6	$\mu g\ m^{-2}\ d^{-1}$	1
10	SRP_WET	28.80	$\mu g\ m^{-2}\ d^{-1}$	2
11	POP_WET	7.59	$\mu g\ m^{-2}\ d^{-1}$	2
12	RP_WET	7.59	$\mu g\ m^{-2}\ d^{-1}$	2
Streams inflows				
1	PON, DON stream nutrient fractions:	0.50 (f1)	n. d.	2
	ON = f1*DON + f2*PON	0.50 (f2)	n. d.	2
2	POP, DOP Stream fractions	0.7(f1)	n. d.	2
	PP = f1*RP + f2*POP	0.3(f2)		
3	Gaussian temperature distribution for streams	1-20	Deg. C	3
4	Estimated direct runoff flow factor: Factor x Stream flow	0.117	n. d.	4
5	Nutrient Load Factor [Nutrient]= f3*[Nutrient]	1	n. d.	5
Ground water				
1	Ground Budget	592 (1999)	$10^6\ x\ m^3$	4
		164 (1992)	$10^6\ x\ m^3$	4
2	Estimated ground water flow factor: Factor x Stream flow	0.114	n. d.	6
3	Ground total Nitrogen conc.	1000	Kg year^{-1}	6
4	Ground total Phosphorus conc.	74	Kg year^{-1}	6
5	Fraction of SRP	0.58	n. d.	6
6	Fraction of RP	0.42	n. d.	6
7	Fraction of NO3	0.85	n. d.	6
8	Fraction of NH4	0.05	n. d.	6
9	Fraction of DON	0.10	n. d.	6

Table 3.3 Continued.

	Initial conditions			
	Nutrient profiles factors:			
1	DON = f1 x ON	0.834 (f1)	n. d.	4
	PON = f2 x ON-PhytoN	0.166 (f2)	n. d.	4
2	Particle profiles fraction Inorganic/Organic	0.3/0.7	n. d.	2, 7
3	Fraction of P and N excreted from zooplankton that goes onto POP and PON in the daily vertical migration	0.5/0.5	n. d.	8
4	Amplitude of diel vertical migration of Mysis	150	m	8
5	Diameter minimum of the range of particle size distribution in a Log scale	0.5	μm	7
6	Diameter maximum of the range of particle size distribution in Log scale	5	μm	7

1) Jassby et al. (1994), 2) Reuter (pers. comm.), 3) Fitted from TRG data, 4) Marjanovic (1989), 5) Schladow (pers. comm.), 6) Thodal (1997), 7) Swift (pers. comm.), 8) Jassby (pers. comm.)

Chapter 4: Data Description (1992 and 1999)

DLM-WQ requires input data for the boundary conditions, for the initial conditions, for the forcing and to specify certain parameter values. The input files contain information of daily meteorology, daily inflow and withdrawal discharge, daily tributary water quality, lake and river channel bathymetry, physical model parameters, water quality boundary conditions and water quality parameters.

As described in **Chapter 3**, the ecological sub-model requires calibration. The sensitivity analysis, calibration and validation study was performed with two sets of independent data. The sensitivity analysis and calibration of the WQ sub-model has been performed over year 1999-2000, while independent data for the year 1992 was used to validate (verify) the calibrated model. The rationale behind this choice was the fact that the quality of the calibration relies to a great extent on the quality of the input data. As the water temperature, water quality data and meteorological data for the period 1999-2000 are of better quality (both in time and space resolution), this period was used for calibration. The data for 1992, though not as intensive as that for 1999-2000, still provided one of the most complete data sets available for Lake Tahoe.

By contrast, the water balance and its sensitivity analysis was performed for the year 1992 (see **Chapter 5**), because the complete set of data for year 1999 was not available at the time when the study was executed. Although both periods comprise nearly the same number of days, the periods represent years of very distinct meteorological conditions.

Data files containing more data are available on internet at http://www.engr.ucdavis.edu/~edllab/.

4.1 Meteorological Data

Required meteorological data on a daily basis include solar short wave radiation (SW), air temperature (T_a), incoming long wave radiation (LW) or a surrogate such as fraction of cloud cover, relative humidity (RH), rain, and wind speed (Wind). The source of the raw meteorological data used for 1992 was 9 a.m. and 3 p.m. measurements from the South Lake Tahoe Airport (Schladow, pers. comm.). This site is approximately 5 km from the lake. Radiation data were from Reno, approximately 50 km east of Lake Tahoe. Data of 1999 and 2000 were collected at the UC Davis meteorological station at the US Coast Guard pier near Tahoe City (see **Fig 4.1**). All parameters were measured at 10 second intervals and 10 minute averaged data were recorded. The recorded data were then further averaged or integrated as necessary. Precipitation data were not available for Julian days 1999340 to 1999365. Gaps were filled with daily mean between closest available daily values. Any induced error by this assumption for precipitation will be negligible. All variables have been daily averaged, except precipitation, and SW and incident LW, where integrated values have been calculated as required by the model format input. Data were processed and filtered to detect unrealistic or badly formatted values, and then, filtered data were checked by visual inspection of the time series plots.

Figure 4.2 shows the plots of the time series of the meteorological variables for the two periods under study. **Table 4.1** shows the mean values for variables of the baseline meteorological file. Although the inter-annual variability may explain much of the variability present, some observed trends might give us some idea about qualitative uncertainty associated with the measurements. The comparison shows divergences in both temporal pattern and magnitude of the wind speed, SW values and estimated RH. Looking at **Fig. 4.2** and at **Table 4.1** it can be seen that the SW registered at second period is systematically greater than SW for first period. This persistent offset suggests an instrument induced variability. Minor changes are found in air temperature and incoming LW. The recorded wind speed of the first period is systematically lower than that measured in the second period. Wind data measurements during the period under study seem to be affected by either a shielding effect in the anemometer, the effect of a site far removed from the lake, or an artifact

56

of the 9 a.m. 3 p.m. measurement. In order to correct this effect, various mathematical relationships were investigated. An annual averaged factor of 5.5 times was applied at the original wind speed data. Differences in precipitation between 1992 and 1999 may well be accounted by the fact that 1992 was a drought year, whereas 1999 was an El Nino year.
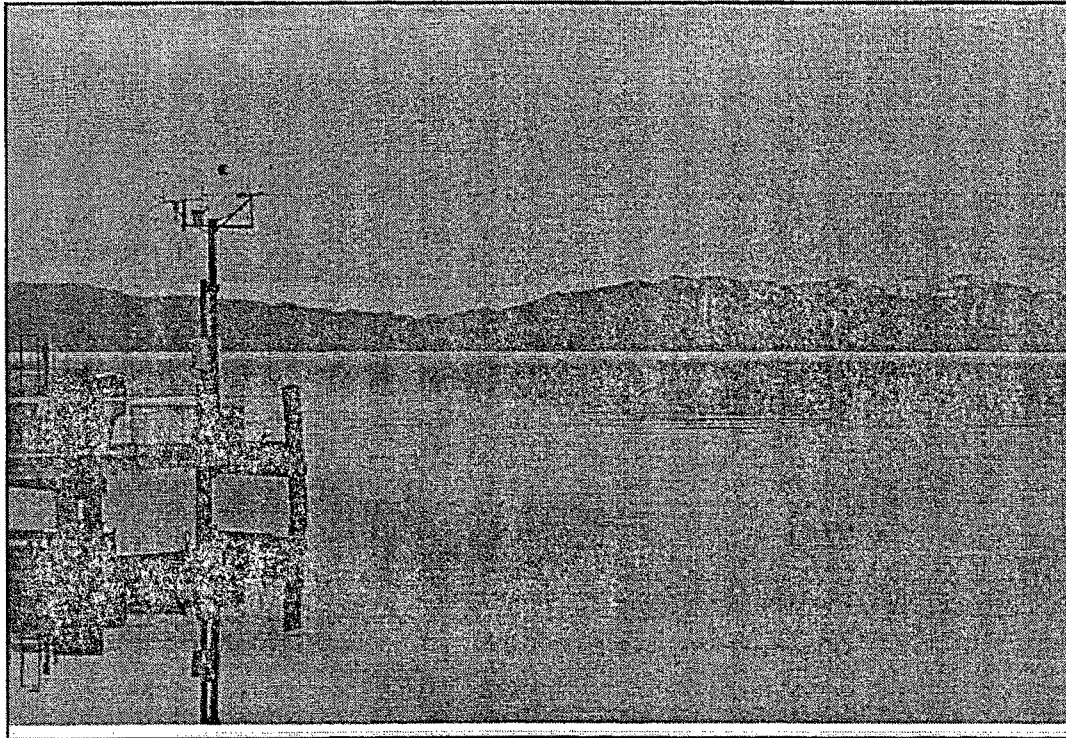

Figure 4.1 UC Davis meteorological station at the US Coast Guard pier near Tahoe City. Photo by Kelley Thompson.

Table 4.1 Mean and standard deviation of each meteorological variable for 1992 and 1999.

Variable	1992 Mean	1992 SD	1999 Mean	1999 SD	Units
SW	16005	8158	17361	9071	$kJm^{-2}day$
LW	23298	4210	23203	5029	$kJm^{-2}day$
T_{air}	6.40	7.13	5.44	5.87	C
RH	0.67	1.72	0.66	0.15	Frac.
Wind	1.53	0.69	3.08	1.51	ms^{-1}
Precip.	1.77	6.49	0.90	3.25	mm
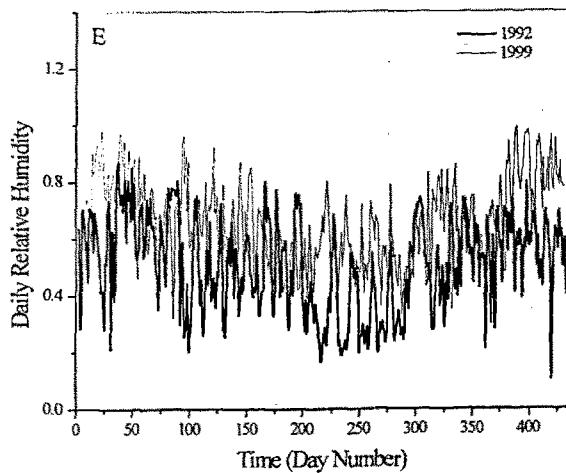
Figure 4.2 Time series of the daily values of the meteorological variables for the two periods under study. A) Short wave radiation, B) Incident long wave, C) Air temperature, D) Wind speed, and E) Relative humidity.

58

4.2 Stream Data

The daily flow volumes and physical, chemical and biological characteristics of all of the inflows that are entering the lake must be supplied to the model. DLM-WQ allows specifying the number of stream inputs flowing into the lake. The daily value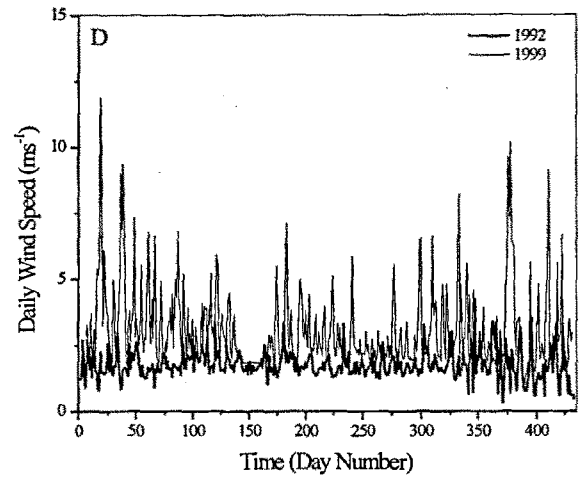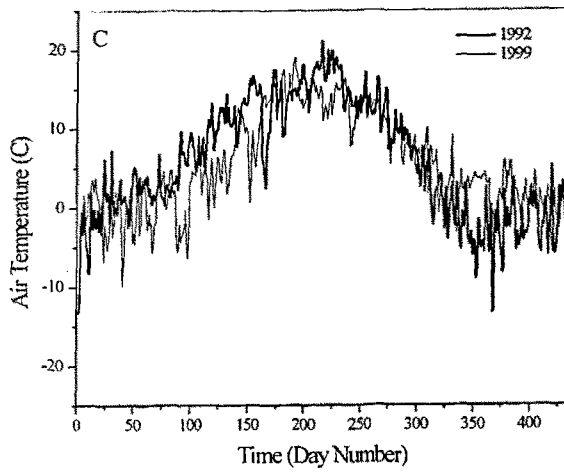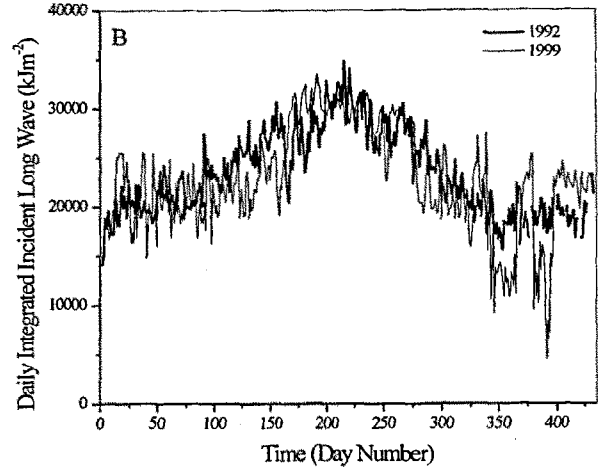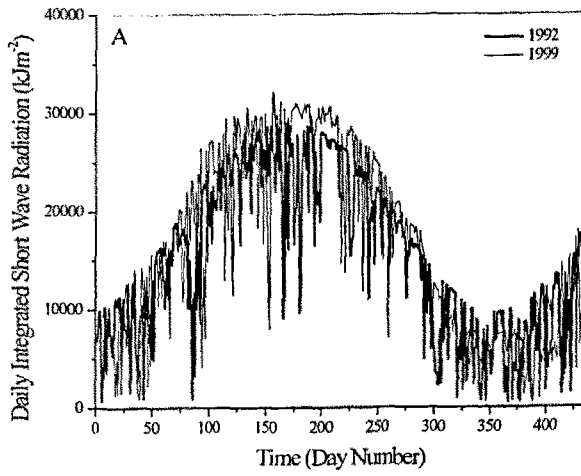 of the following model variables need to be provided: Flow Volume, Temperature, and concentrations of Salinity, Chlorophyll a (Chla), Dissolved Oxygen (DO), Biological Oxygen Demand (BOD), Available Phosphorous (SRP), Internal Phytoplankton Phosphorous (PhytoP), Particulate Organic Phosphorous (POP), Refractive Phosphorous (RP), Nitrate (NO3), Ammonia (NH4), Internal Phytoplankton Nitrogen (PhytoN), Particulate Organic Nitrogen (PON), Dissolved Organic Nitrogen (DON), and concentrations of 7 classes of particles.

Of the 63 streams flowing into Lake Tahoe, 10 have been regularly monitored. They are estimated to account for up to 40% of the total stream input. Tributary monitoring includes field measurement of stream flows, temperature, pH, dissolved oxygen, and specific conductance; and laboratory measurement of major nutrients: dissolved Nitrate and Nitrite, Dissolved Ammonia, Total Ammonia and Organic Nitrogen, Total Hydrolizable Phosphorous (THP), Total Phosphorus (TP), and suspended sediment. Daily flow data for 5 streams are available at the USGS web site: Upper Truckee River, Blackwood Creek, General Creek, Trout Creek, and Ward Creek (see **Fig. 4.3**). Daily data of Trout ends at 09/30/1992. Flow data for the remaining 5 streams (Edgewood Creek, Incline Creek, Third Creek, Logan House Creek, Glenbrook Creek) and the missing data for Trout stream have been estimated based on the monthly averaged data provided by the TRG. For 1999, flow data for the 10-gauged streams was available until 09/30/1999. Replicate values of the year 1992 were used to fill the remainder days of year 1999, as no other data were available when this analysis was performed. **Figure 4.4** displays the daily flow of Upper Truckee River for year 1992 and year 1999. For its application to Lake Tahoe, the model was configured with 21 stream inputs. Ten of the streams corresponded to the ten gauged streams described above. A further ten fictitious streams replicated these gauged inputs, to account for the remainder 53 streams flowing into the Lake Tahoe.

As nothing was known of their characteristics (other than the approximate sum of their contributions) it was not considered meaningful to explicitly attempt to model each of them. One additional fictitious stream was also included to account for direct runoff. Its value was set at 11.7% of stream input, as estimated by Marjanovic (1989).
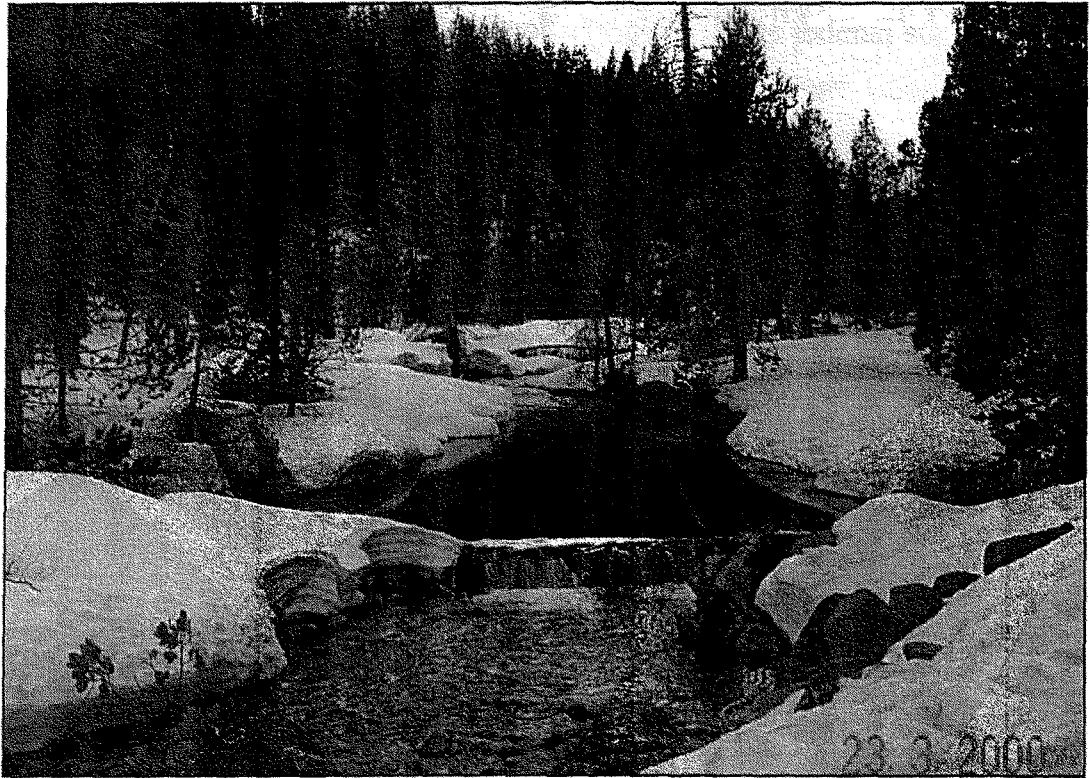
Figure 4.3 Ward Creek. Photo by Geoffrey Schladow.

The assumptions described in **Chapter 3** were applied to convert the measured variables into the WQ state variables of the model. The assumed values of stream temperature were derived through a correlation with a Gaussian temperature distribution for the annual temperature variation (see **Fig. 4.5**). This was applied uniformly to all the streams for both years. Algae concentrations in the streams were set to zero with the assumption of negligible transport, as well as internal nutrients. Silica (not modeled) was set to zero. DO was set to 10 mgl^{-1}. BOD was set to 0 mgl^{-1}. Salinity was set to 100 mgl^{-1}. Daily values of nutrients were assumed to be equal to the corresponding monthly average stream nutrient concentration. **Figure 4.6** displays the THP, NO3, NH4 for years 1992 and 1999.

Figure 4.4 Upper Truckee River daily stream flow A) 1992 and B) 1999.
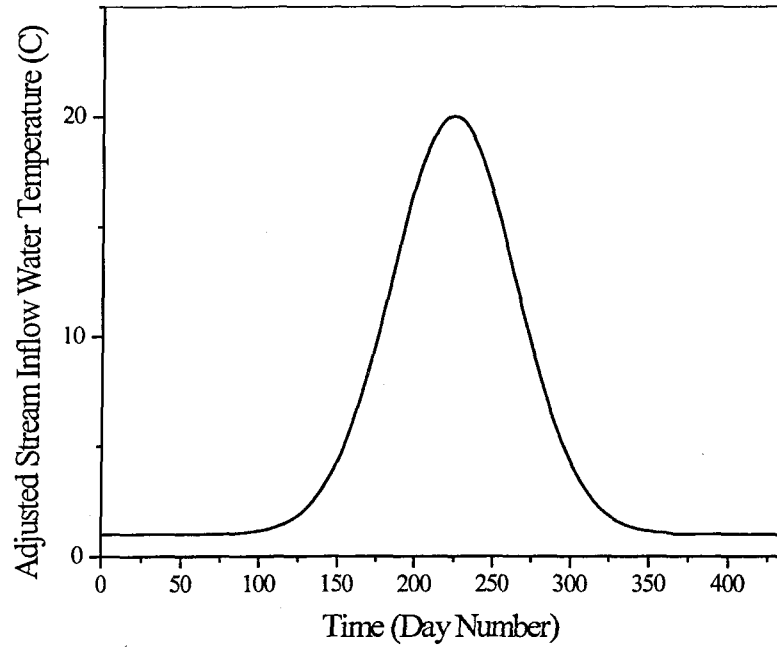
Figure 4.5 Gaussian fit of stream inflow temperature applied for both years 1992 and 1999.

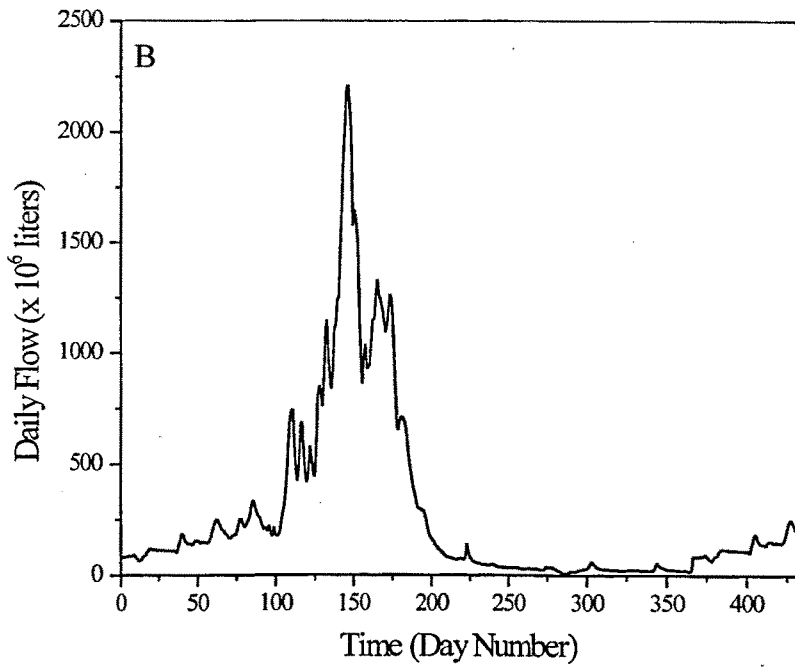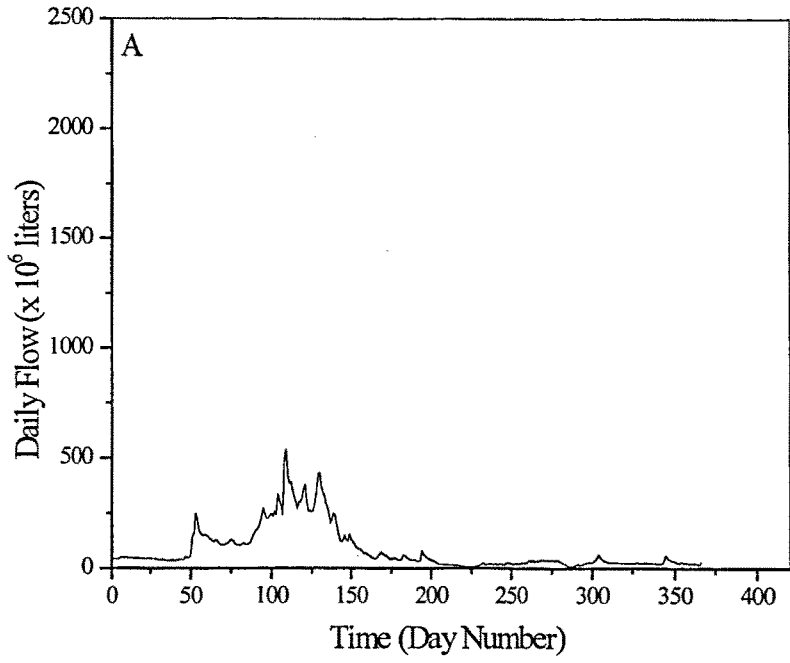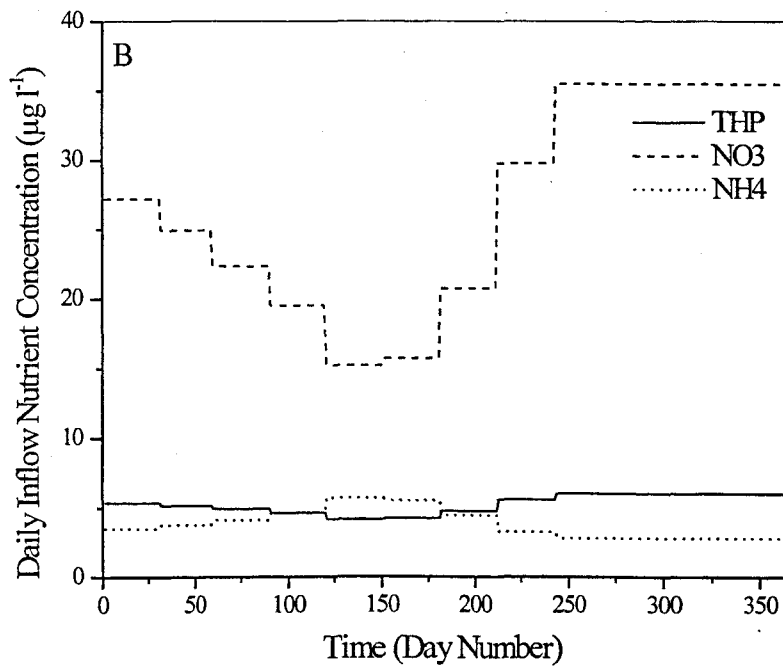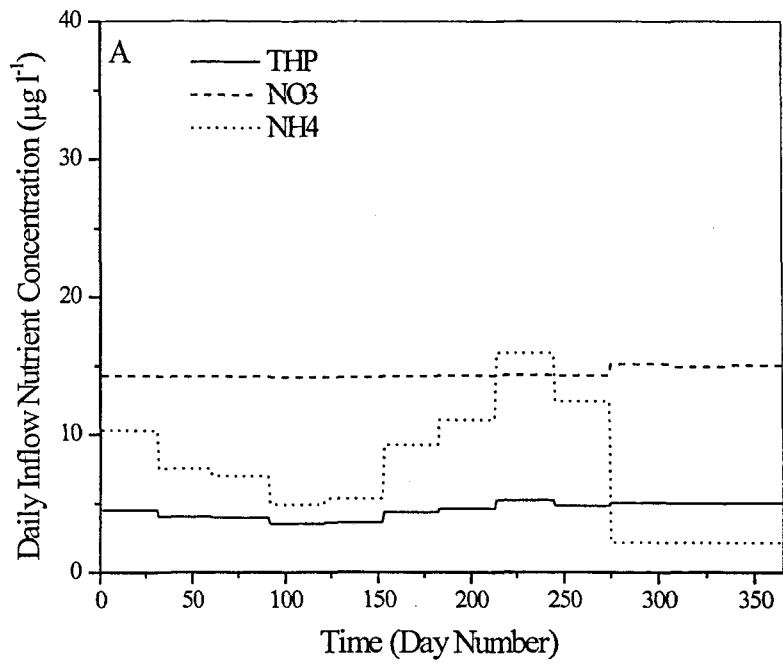**Figure 4.6** Daily stream nutrient concentrations for A) 1992 and B) 1999. Estimates from monthly averaged values.

Particle concentration (particles ml^{-1}) was set to a constant value derived from the expression of Coker (2000):

$$[Particle]_i = 19553 \cdot \Delta D_i \cdot Dia_i^{-2.85} \qquad (4.1)$$

where Dia_i is the diameter (μm) of the ith particle and ΔD_i stands for the bin width of the ith particle class (μm). The model requires daily flow gauging data at the points of outflow. The model was set with only one stream outflow for Upper Truckee River. Lake outflow is regulated by a 17-gate concrete dam at Tahoe City (see **Fig 4.7**). Water quality state variables are not needed for the outflow as the model calculates these. The stream outflow data were generated from USGS outflow data after appropriate conversion of units. Note that the reported data of the USGS for year 1992 were not measured but estimated. The available records for year 1999 end at 09/30/1999. The remainder days of the second period were filled with the last recorded stream outflow.
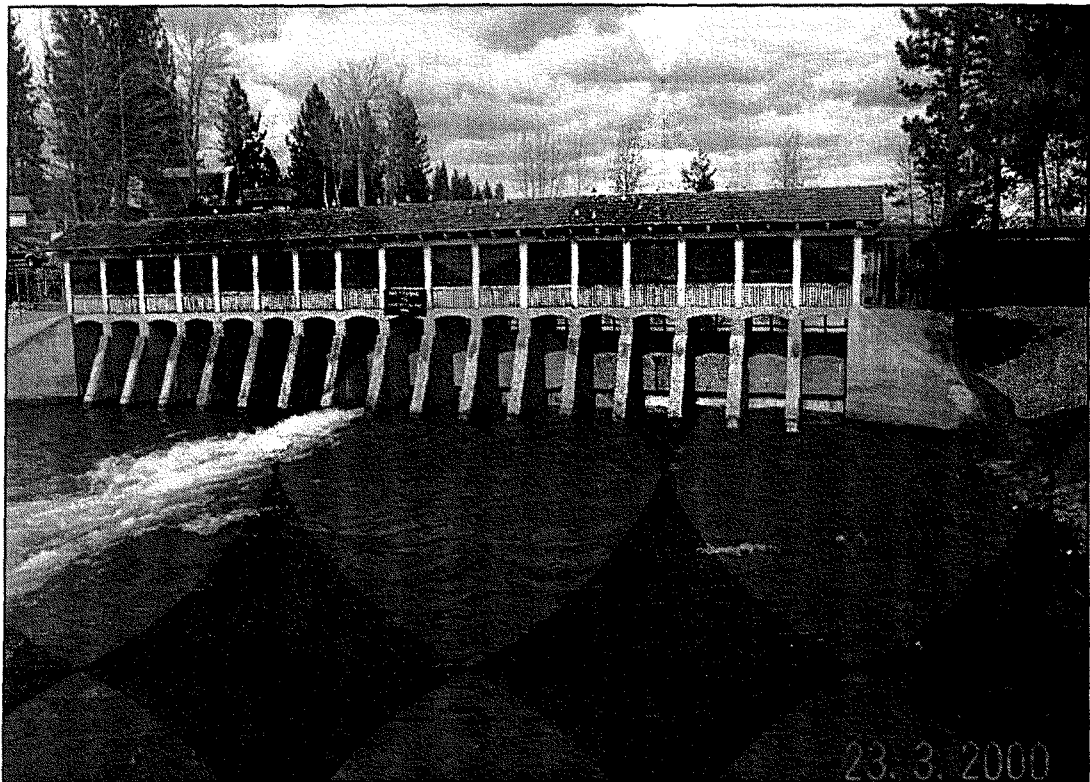
Figure 4.7 Concrete dam at Tahoe City to regulate outflow to Lower Truckee River. Photo by Geoffrey Schladow.

4.3 Ground Water Data

The ground water net inflow has been estimated using the relative contribution of sources and sinks to the water budged of Lake Tahoe (Thodal, 1997). The ground water was calculated to be 11.4% of the annual stream + direct runoff inflow. A positive value indicates an input to the lake. Dissolved forms of nutrients are assumed to be the main contributions of the ground water to the nutrient budget. Thodal (1997) estimated the mean concentration of total Nitrogen 1.0 mgl^{-1}, and of total Phosphorus 0.074 mgl^{-1}. NO3 (included nitrite) is the predominant form (85%), followed by dissolved organic nitrogen DON (10%) and ammonia NH4 (5%). Speciation of phosphorus concentrations is more balanced; orthophosphate form (assumed to go to the SRP pool) (55%) compared with the organic form (42%), that are assumed to be simulated RP. The assumed magnitude, the spatial distribution, the net contribution to the water budget (whether is input or output), nutrient budget fractions and its seasonal behavior must be confirmed by further investigations. For the purposes of adding the groundwater to the lake, it was assumed to be uniformly distributed all over the computational layers.

4.4 Atmospheric Nutrient Loading Data

Although recent measurements of atmospheric deposition suggest a spatial and temporal gradient of deposition across the lake (see **Section 2.3.2**), nutrient concentrations were estimated from Jassby et al. (1994) and assumed values from near Ward Creek as being representative for the lake. The reason for this choice was because of the longer record of data was more representative of the average conditions found across the lake. The measured magnitudes are fluxes of SRP (measured), TP, NO3, and NH4. The fluxes of the state variables NH4, NO3, and SRP (state variable) fluxes estimated based on the averaged ratios shown in **Table 4.2** of the available measurements that extended from years 1983 to 1992. Conversion factors between measured and water quality state variables were applied (see **Chapter 3**).

Table 4.2 Estimated atmospheric deposition rates (μmol m^{-2} day^{-1}). From Jassby et al. 1994.

	NO3	NH4	SRP
Wet	19 ± 2	16 ± 2	0.39 ± 0.10
Dry	7.4 ± 1.4	7.8 ± 0.9	0.93 ± 0.02

4.5 Lake Data

The initial conditions data provide the model with the starting conditions of the lake and include profiles of water quality variables, temperature and salinity. Data were collected at two lake stations - the Midlake station in the deeper part of the lake (460 m), and the Index station on the western shelf (150 m). A comparison of the data from the Index and Midlake Stations revealed that the water quality variables experience the same patterns of variation but with a time lag in the response against perturbations (Jassby et al. 1999). Assuming horizontal homogeneity, water samples collected from the Midlake station were used as representative of the average conditions of the lake. Data at the Midlake station were collected at approximately 20 day intervals throughout the year.

The profiles of the following model variables need to be provided: Temperature, Salinity, Chlorophyll a (Chla), Dissolved Oxygen (DO), Biological Oxygen Demand (BOD), Available Phosphorous (SRP), Internal Phytoplankton Phosphorous (PhytoP), Particulate Organic Phosphorous (POP), Refractive Phosphorous (RP), Nitrate (NO3), Ammonia (NH4), Internal Phytoplankton Nitrogen (PhytoN), Particulate Organic Nitrogen (PON), Dissolved Organic Nitrogen (DON), and concentrations of 7 classes of particles.

Available measured fractions of the Phosphorous pool are THP, DP, and PartP. Measured Nitrogen species are Total Kjeldahl Nitrogen (TKN), NH4, and NO3. Water samples were collected from the main water body from the surface to 100 m depth for the chlorophyll and down to 450 m depth for the nutrients at depths of 0, 10, 50, 100, 150, 200, 250, 300, 350, 400 and 450 m. The initial profile will need to be specified at the deepest point in the lake. The deepest measured value was considered to extend to the deepest point in the lake. Nutrients, oxygen and chlorophyll were

computed from linear interpolation fits to the measured profile data. Salinity was assumed constant through the water column at a value of 100 μgl^{-1}. At this concentration salinity has no impact on the density of water, and its inclusion is purely for reasons of model consistency. Chlorophyll concentration was linearly interpolated from the deepest measured value (100 m) to the bottom, assuming its value of 0.2 μgl^{-1}. This value is in general agreement with values reported by Vincent (1978). A constant internal Nitrogen and internal Phosphorus to Chlorophyll ratios were assumed to derive the PhytoN and PhytoP. Analyses of PartP for year 1999 were not available, and data of year 1992 were used instead.

Measured particle distributions were used for 1999, while particle data for 1992 were based on the annually averaged correlation derived for the whole water column by Coker (2000):

$$[Particle]_i = 0.30 \cdot 2210 \cdot \Delta D_i \cdot Dia_i^{-3.1} \qquad (4.2)$$

where Dia_i is the diameter (μm) of the ith particle and ΔD_i stands for the bin width of the ith particle class (μm). The factor 0.3 has been included to indicate that about 30% of the measured particles have been determined to be inorganic (Swift, pers. comm.). The importance of the particle concentration and its definition in the Water Clarity Model demands a more detailed explanation of how this factor was obtained. The original x-ray diffraction analyses of Coker used two large categories. Particles that had x-ray spectra with no elemental peaks, other than pure Si (synonymous with diatoms), were classified as organic particles. (This assumes that the particles are composed of elements lighter than sodium, such as carbon, nitrogen, and oxygen). Inorganic particles included any particle with spectra associated with heavy elements (a total of about 18 elements). Fragments of diatom frustules were counted with the inorganic group, whereas whole diatom frustules were counted with the organic group. Swift reanalyzed the same samples plus some additional samples, classifying the particles into Terrestrial (24.0%), Organic (68.0%), Artifact (2.2%), Salts (1.7%), uncertain (4.0%), where these numbers are expressed as percent of total particle composition. The category of "Organic" includes organic particles as defined in Coker (2000) and particles from diatom fragments. "Terrestrial" label includes particles containing Al, Ti, Fe, K, or Ca complexes together with Si. "Artifacts" were particles

suspected of being from the sampling equipment: Cu-Zn (bronze), Fe-Zn (galvanized steel), Sn, or pure Al. "Salts" are cases where only the ionic salt elements appeared (Na, K, Ca) with Cl. "Uncertain" included some particles, many of which contained Cobalt.

These water quality data are probably a poor spatial estimate of vertical change in the lake, however, they are the only available data. The data have historically been limited by the cost and time of taking more frequent samples. Aside from the analytical costs, the great depth of Lake Tahoe means that deep samples require a long time on station, and the spatial frequency typical of shallow lakes has not been possible. In addition, the questions being considered at Lake Tahoe have evolved, and the provision of data for numerical modeling has only recently become an issue. **Figure 4.8** illustrates the inherent shortcomings of the present data set. This figure shows a continuous profile of chlorophyll-a, as measured by a chlorophyll fluorometer on a Seabird SBE-25 CTD (Schladow, unpubl. data). These data are from the Midlake station on April 29, 2000. The hollow circled show the locations of the regular measurement depths at the Midlake station and the lines joining them indicate the interpolation that is used. It is clear that many important details are missing or would be misrepresented by the present sampling protocol. These include the magnitude and depth of the DCM, as well as the concentration of chlorophyll below 100 m. As no continuous measurements exist for nutrient concentration, it is not possible to produce such a figure for nutrients.
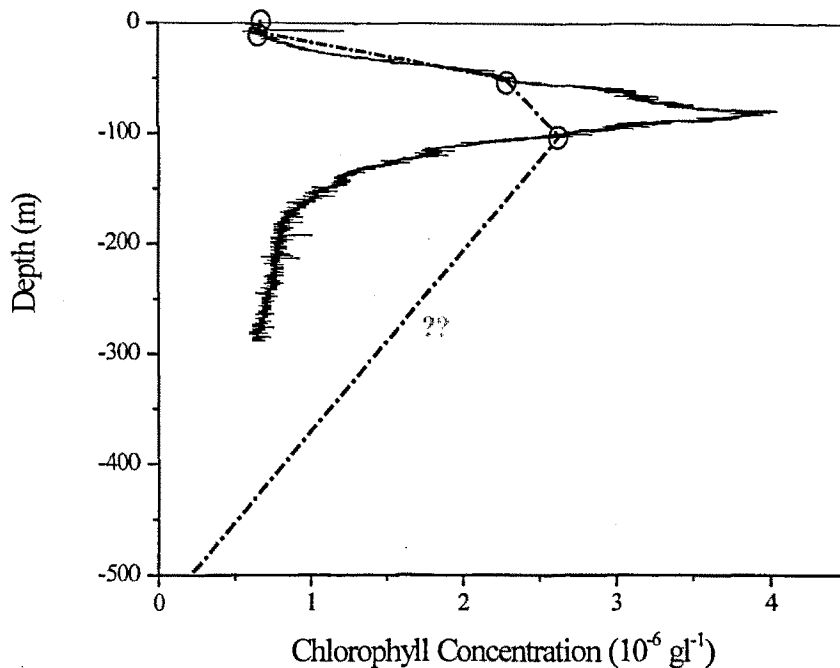
Figure 4.8 Continuous profile of Chla, measured by a chlorophyll fluorometer on a Seabird SBE-25 CTD. Circles indicate depths at which routine samples are taken. Chain dotted line indicates assumption made between routine measured values. Bottom value assumed to be $0.19\mu gl^{-1}$.

High resolution temperature profiles, from the surface down to about 200 m with about 10 cm vertical spatial resolution collected with a Richard Brancker Research (RBR) profiler were only available for 1999. Supplementary temperature profiles collected at the MLTP station with a cable bulb thermometer from surface down to 450 m depth were available for the year 1992 and year 1999. The resolution in depth ranges between 10 m at the surface to about 50 m at the bottom lake. **Figure 4.9** plots the profiles of the measured points of DP, PartP, THP, NO3, NH4, and temperature for the starting day January 7th 1999.

Figure 4.9 Measured profiles for January 7th 1999. A) DP, B) PartP, C) THP, D) NO3, E) NH4 and F) Temperature (many points have been removed for clarity).
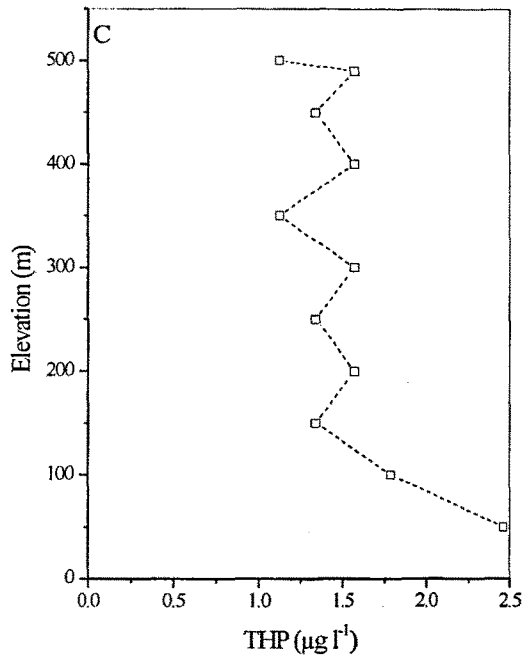
Figure 4.9 Continued.

4.6 Bathymetric Data

A capacity table (surface area and cumulative volume as functions of elevation) of the lake must be supplied. This information was obtained from Gardner, et al. (1998). The measurement method was not able to measure where water depth was less than meter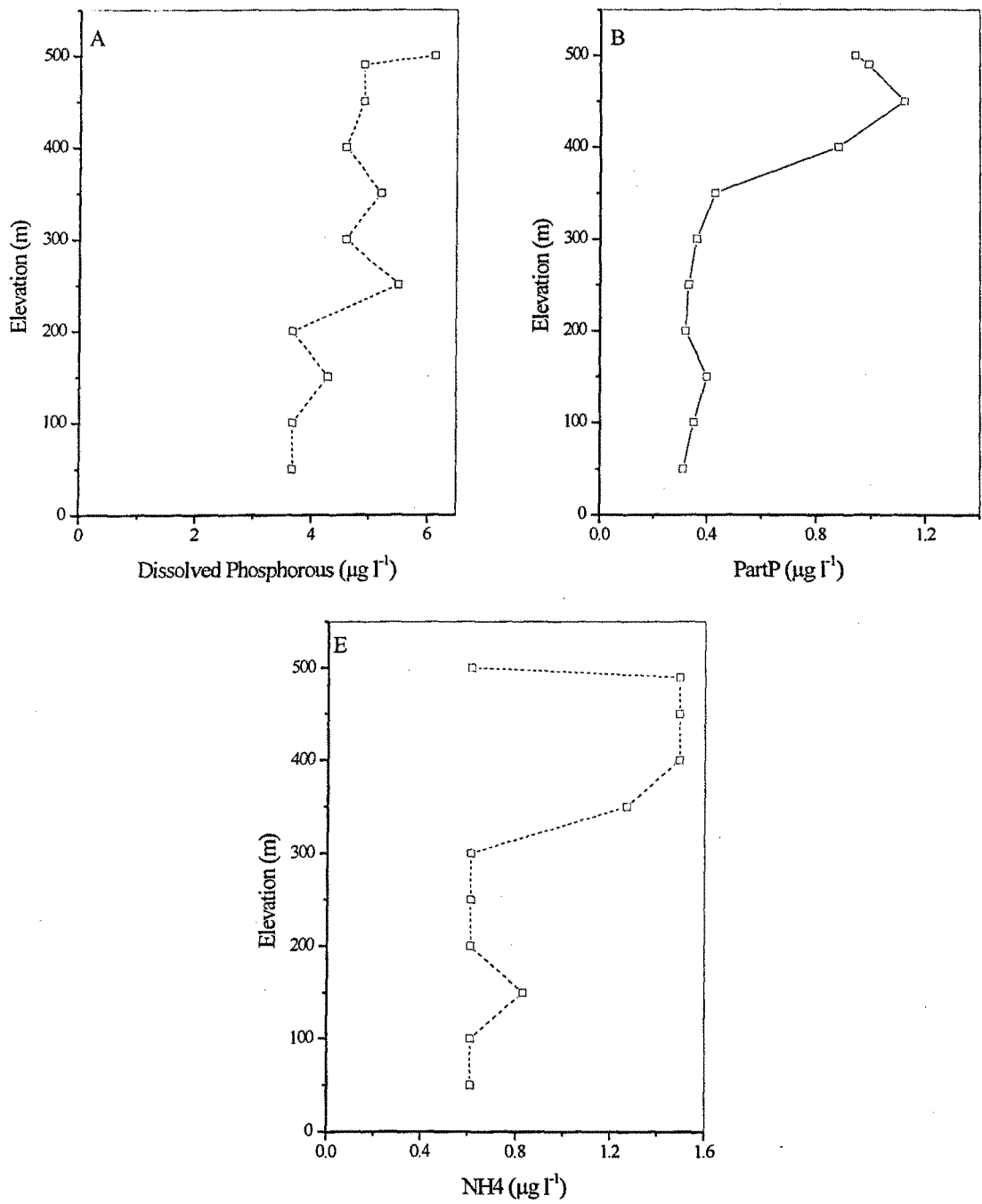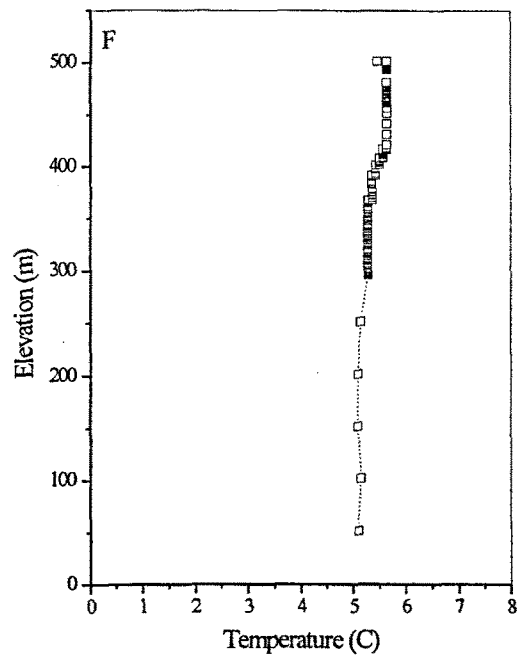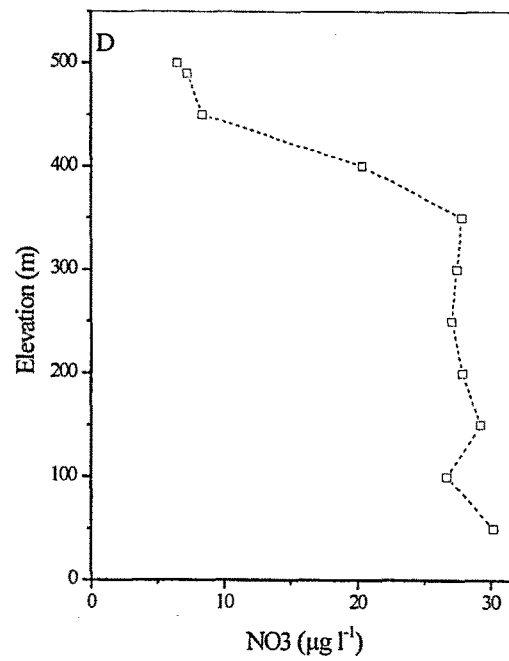s. Thus, linear extrapolation of the data was necessary to obtain near-surface values. **Figure 4.10** plots the derived capacity table.

4.7 Physical Parameters Data

The model must be provided with information about the physical and morphometric characteristics of the tributaries watersheds, and the mixing parameters required for the hydrological sub-model. For the mixing efficiency parameters, the values reported by Schladow & Hamilton (1997) were used (**Table 4.3**). Where $CK*ETA^3$, represents the coefficient measuring the stirring efficiency of the wind, CK is the coefficient that measures the efficiency of the convective overturn, CS is the coefficient that stands for the shear production for entrainment, and CT coefficient represents the temporal unsteady effects due to changes in surface wind stress or surface cooling. **Table 4.4** summarizes the physical and morphometric information derived from US Geological Survey data map scale 1:24,000. For Lake Tahoe, all elevations were set referenced to the USB of Reclamation Level (1895.85 m). The full supply elevation is the level of the spillway. The basin length at full supply is the length of the lake. As basin width, the width of the lake was considered appropriate.

Table 4.3 Mixing efficiency parameters. From Schladow & Hamilton (1997).

Parameter	Value
CK convective overturn	0.125
CT unsteady effects	0.51
AKH billowing	0.30
CS shear efficiency	0.20
ETA wind stirring	1.23
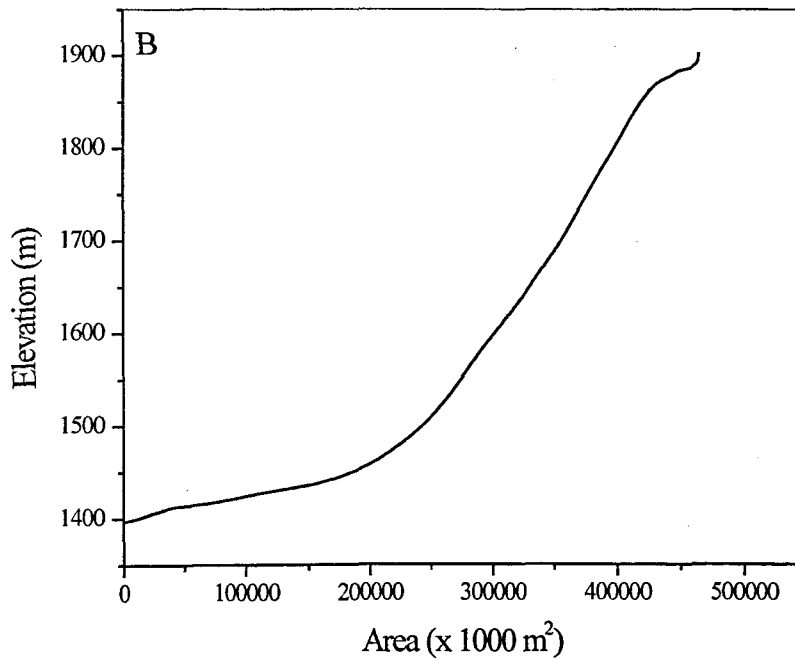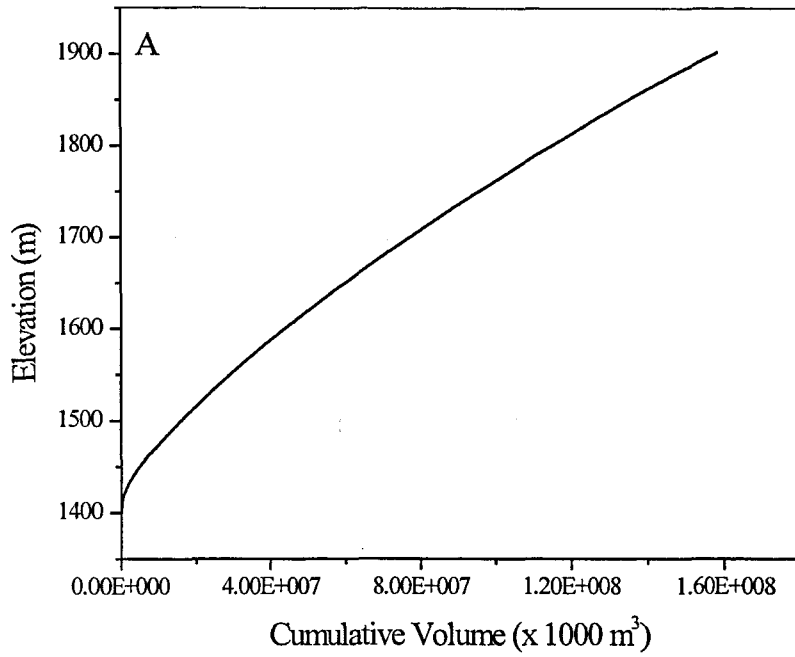
Figure 4.10 Capacity storage table: A) Cumulative volume, and B) area.

Table 4.4 Input physical and morphometric parameters for Lake Tahoe.

Parameter	Value
Base elevation (m)	1396.45
Crest elevation (m)	1898.73
Basin length at crest (m)	33714
Basin width at crest (m)	19048
Latitude in degrees	39.099
No. of outlets	1
Outlet elevations	1896.4
Basin length at outlets (m)	33714
Basin width at outlets (m)	19048
Stream half-angle (degrees)	0.75
Streambed slope (degrees)	0.5
Streambed drag coefficient	0.016

4.8 Conclusions

In many respects, the assembled data sets for Lake Tahoe are relatively complete. The temporal frequency of the lake data is reasonable, and good estimates of many meteorological parameters and stream inflow data exists. However, there are clearly major deficiencies, particularly in the vertical spatial resolution of the lake data and in the temporal frequency of water quality data for the inflows. The low resolution in time and space, limits the success of the calibration, as well as may bias the model's results. Lacking data were filled making some assumptions of the dynamics of the system. Inaccuracy in the nutrient determination is expected to account for much of the error associated with the simulations (Jorgensen, 1994). An estimation of the experimental error is difficult to assess.

Chapter 5: Model Prerequisites

Prior to any attempt to calibrate or use a model, certain internal checks should be undertaken (in addition to the usual testing and searching for bugs). The most important of these is to ensure conservation of mass, both for water and for the water quality constituents (such as nutrients). Any error here makes the model invalid and renders all further testing moot. Linked to this is the need to check for a correct water balance. This not only requires that the model conserve mass, but that the sum of all the sources and losses of water yields the correct water level (to within the expected measurement uncertainty).

In addition, it is advisable to examine the effects of the model discretization scheme. In many models, where the solution of a set of differential equations is undertaken using a finite element or finite difference scheme, there is in general an improvement in accuracy as the time step and spatial discretization are reduced (so long as stability criteria such as the Courant condition are not violated). This is primarily because the difference equations more closely approximate the underlying differential equations. However, in DLM-WQ and other similar models, the solution obtained is that of a set of algebraic parameterized equations. Inherent in these equations are assumptions related to both the spatial and temporal scale over which the parameterizations were developed. Thus it cannot be assumed that smaller is necessarily better, as the equations may not apply as well (or even be valid) for the smallest scales. Likewise overly large scales may also be poor choices. A thorough testing of a range of scales is required to be sure that the model is performing satisfactorily.

5.1 Water Balance

The magnitude of each component of the hydrologic balance for Lake Tahoe is not well known (Thodal, 1997). **Table 5.1** shows the mean annual absolute and relative contributions of the different sources and/or sinks of water to Lake Tahoe. These two sets of estimates are based on the results of Marjinovic (1989) and Thodal (1997). The percentages are relative to the total input and total output, respectively. **Table 5.1** also gives an estimate of the uncertainty of the sources and sinks[1]. These results illustrate the differences in the water budget that arise from using different methodologies and from considering different periods of time. Note in particular the difference in the estimated ground water contribution to the total input, as well as its related relative uncertainty.

In what follows, the components of the water balance for Lake Tahoe will be explored using the model. As will be seen, simply using the estimates of the components can lead to very significant errors in the predicted water level. While these errors may appear small for the 1-year considered, it must be borne in mind that an ultimate goal of the present dissertation is to provide a tool that can be used for conducting long-term simulations. Thus, slight errors in the water balance for 1 year could readily become huge errors for a 30-year simulation. While the model cannot correct the errors that lead to an incorrect water balance, it can readily be used to estimate the size of the errors in the input and/or output components that lead to these errors. As these same inputs and outputs also deliver nutrients to the system, this analysis provides some insight into the inherent uncertainty of a modeling approach. This analysis is first performed for the year 1992. The results are then compared with the water budget derived from 1999.

---

[1] As an example of uncertainty estimates, the inflow factor is obtained from the set relative uncertainty $\Delta I/I = -0.25$, thus $\Delta I = -0.25I$, and the modified value $I^* = I - 0.25I = 0.75I$

5.1.1. Model equations

The hydrologic mass-balance equation is expressed as:

$$S = P + I + G - O - E \tag{5.1}$$

where S is the change in storage in the lake, P is precipitation directly on the surface of the lake, I is the streamflow into the lake, G is the net ground water discharge into the lake, O is stream flow out of the lake, and E is evaporation from the surface of the lake. Diversions are not explicitly considered.

The effect of a change in storage on lake water level is evaluated by the model from the table of depth versus cumulative volume. The algorithm inputs the inflow, outflow and ground water contributions on a daily step. Evaporation is formulated in terms of bulk aerodynamic coefficients (TVA, 1972). Although evaporation and precipitation are calculated on a sub-daily time step, input data are provided on a daily basis. The groundwater contribution is based on the available annual estimates of sources and sinks to the water budget of Lake Tahoe estimated by Thodal (1997) from 70 years of data. The relative contribution of the annual estimate of the ground water represented 6.3% of the annual estimate of the total input (see **Table 5.1**), or 11.4% of the annual estimate of the combined stream and runoff inflow. Therefore in what follows it is assumed that the groundwater contribution is 11.4% of the combined stream and runoff inflow.

5.1.2 Analysis of water balance

The baseline simulation for the sensitivity experiments utilizes the data set described in **Chapter 4**. This corresponds to a period of 336 days starting at Julian 92003 (January 3) and ending at Julian day 92336 (December 1). Thus, almost one year is covered by the simulation period. The sub-daily time step was fixed at 180 minutes.

Table 5.2 lists the components of the hydrologic budget for 1992 for Lake Tahoe, the baseline case. The percentages refer to the total input and total output respectively. The stream inflow, runoff, precipitation, groundwater inflow and stream outflow are all data inputs to the model. The model calculates evaporation. This simulation of the baseline case predicts a net gain of water volume. By contrast, the measured lake

77

Table 5.1 Relative contribution of different sources and sinks to the annual water budget of Lake Tahoe based on compilations of historical data for years indicated. GW stands for ground water.

	Years	INPUTS				OUTPUTS		
		Stream $10^9 l$ (%)	Runoff $10^9 l$ (%)	Precip. $10^9 l$ (%)	GW $10^9 l$ (%)	Evaporation $10^9 l$ (%)	Outflow $10^9 l$ (%)	Diversion $10^9 l$ (%)
Marjanovic (1989)	1960-1989	468 (56.6)	54.7 (6.6)	299 (36.2)	4.81 (0.6)	508 (61.1)	315 (37.9)	9.01 (1.0)
Thodal (1997)	1901-1970	431.55 (54.7)		308.25 (39.1)	49.32 (6.3)	480.87 (65.8)	246.6 (33.7)	3.699 (0.5)
Relative uncertainty		(±30)		(±72)	(±250)	(±31)	(±15)	(±167)

Table 5.2 Components of the hydrologic budget for the baseline simulation year 1992 (from January 3 to December 1).

	INPUTS				OUTPUTS	
	Stream	Runoff	Precip.	GW	Evaporation	Outflow
10^9 liters	139	16	190	17	344	184
(%)	(39.3)	(4.5)	(52.4)	(4.8)	(99.9)	(0.05)

levels at the beginning and end of the simulation period indicates a loss of mass. Comparison of **Table 5.1** and **Table 5.2** highlights that the baseline year has a particularly low value for the stream outflow. Another feature of note is the relatively high rate of direct precipitation based input compared with stream flow. This can readily be accounted for by the very small size of the watershed compared to the lake. However, it does highlight how the Tahoe basin is distinct from most other watersheds, where direct precipitation is often negligible.

Table 5.3 summarizes the numerical experiments that were performed as part of this analysis. The columns are the 5 components considered in the water budget of the Lake Tahoe. Inflow (direct runoff and the 21 stream inflows), groundwater and the contribution of precipitation over the lake surface are considered inputs (positive). The stream outflow and the loss of water due to evaporation are the outputs of the system (negative). Rows correspond to the performed numerical experiment, with row A0 being the base case and rows A1 to A8 representing specific changes to the components of the budget. The symbol X indicates a contribution that was set to zero for this particular experiment while empty cells stands for values unaltered from the base case. Numerical factors indicate a multiplicative factor on the base case value.

Simulated water level as a function of time along with the measured water levels (shown as hollow squares and labeled M), are shown in **Fig. 5.1** to **Fig. 5.3**. Setting all the contributions of the water budget to zero while retaining all the internal mixing algorithms of DLM-WQ (Case A1) yields a horizontal line in **Fig. 5.1**. This indicates that the model conserves mass in the absence of external sources and sinks.

As already noted, the model over predicts the simulated water level (A0 compared to M in **Fig. 5.1**) but the time varying shape of the water level plot is similar in both cases. The mean difference is 0.180 m and the maximum difference of 0.364 m is found at the end of the simulation. The similarity in the shapes suggests that measurement error in one or more of the individual components may be what is causing the mismatch.

Table 5.3 Numerical experiments for 1992. Symbol X indicates an input that is set to zero. Other parameters were left unchanged. Numbers indicate a multiplicative factor on the base case value. GW stands for ground water.

	Inflow	GW	Outflow	Precip.	Evaporation
A0			BASELINE		
A1	X	X	X	X	X
A2	--	X		--	--
A3	--	--	X	--	--
A4	--	--	--	0.75	--
A5	--	--	--	0.5	--
A6	--	--	--	X	--
A7	X	--	--	--	--
A8	0.75	--	--	0.5	--
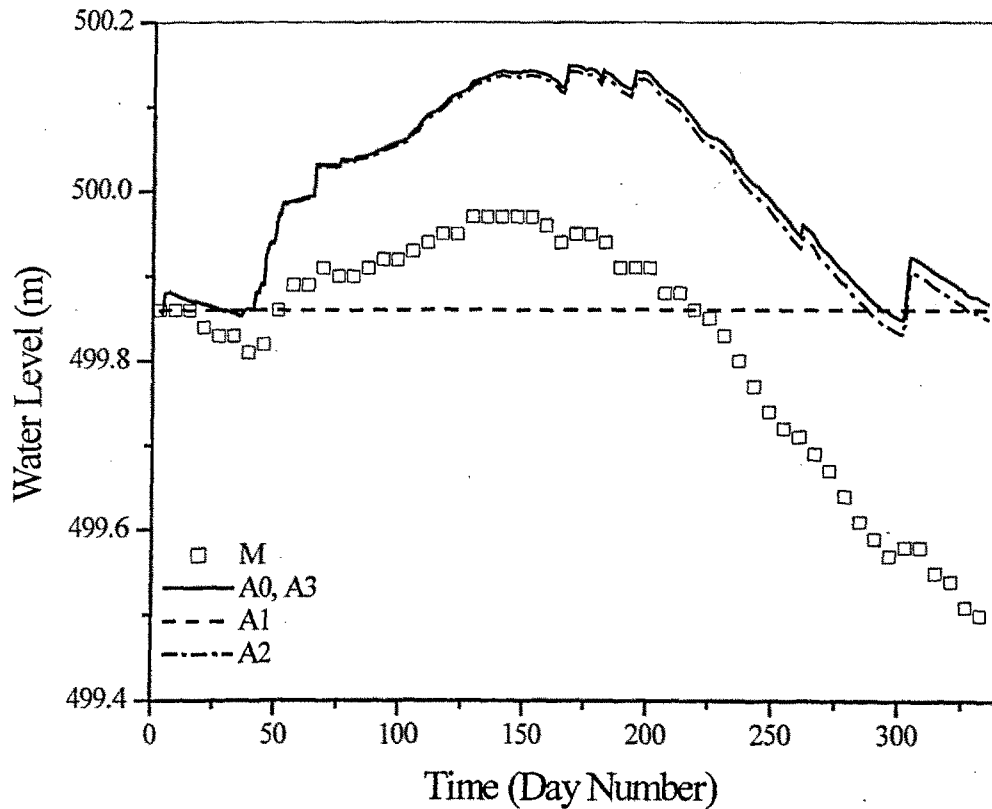
Figure 5.1 Simulated water level for 1992 under different assumptions. See **Table 5.3** for simulated conditions. The measured water level (M) is shown as hollow squares.
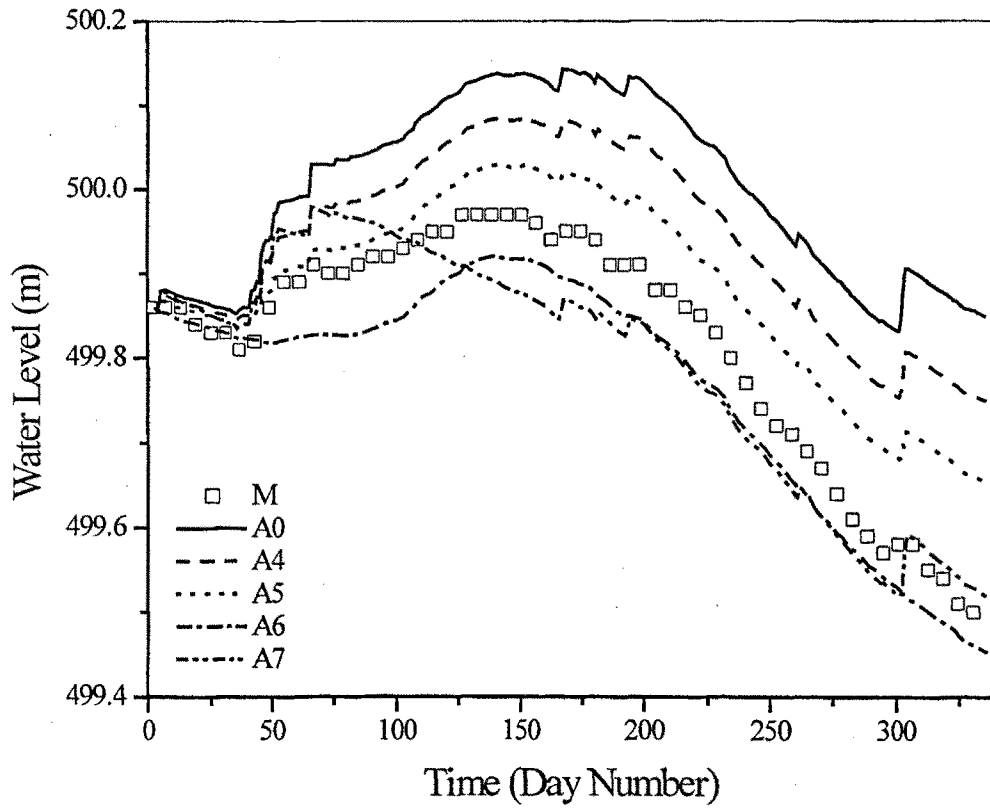
Figure 5.2 Simulated and measured water level for the Lake Tahoe. Labels correspond to the simulation experiments as referenced in **Table 5.3**.

Figure 5.3 Water level after applying a factor of 0.50 times the baseline value of daily precipitation and a factor of 0.75 times the baseline stream values.

Over the period considered, the effect of the outflow is negligible (curves A3 and A0 are coincident). As this was a drought year with greatly curtailed outflow at the end of a prolonged drought period, this is not surprising although it is not a usual condition. Consequently, evaporation is responsible for nearly all the decline in water level (**Table 5.2**). The simulated evaporative flux depends on the simulated surface water te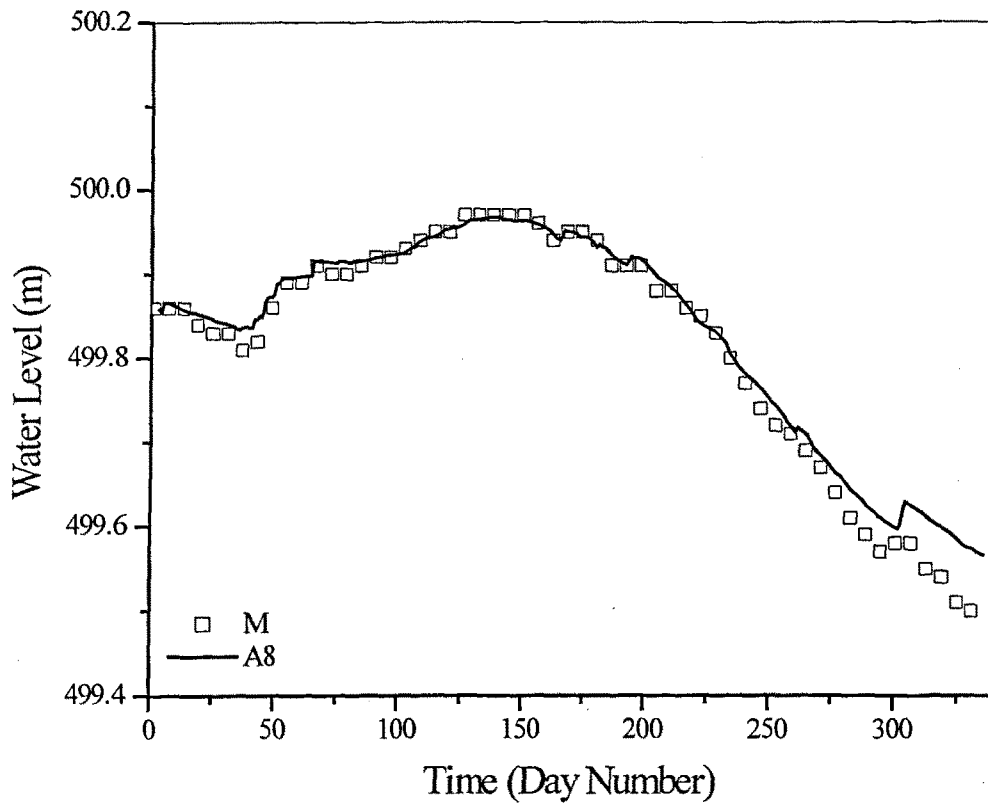mperature (itself a function of all the measured meteorological parameters) and the measured wind speed. As uncertainty of the measured wind field is high, this term is especially sensitive to both the quality of the meteorological data and a correct description of the evaporative fluxes in the modeled heat balance. The uncertainty range presented in **Table 5.1** is for measured values (for example from an evaporation pan) as presented by Thodal (1997), and is not applicable to the simulated evaporative flux. However, the uncertainty in the simulated value is unlikely to be much smaller.

The contribution of the ground water on the simulated water level can be seen by setting the groundwater contribution to zero (Case A2 compared to Case A0). Thus it can be clearly seen that groundwater flow, the component with the greatest uncertainty, is not accounting for much of the difference between the simulated amd measured water level. Note, if the assumed groundwater contribution had been based on the values suggested by Marjanovic (1989) there would have been no perceptible difference.

Although the total contribution to the input by direct precipitation is greater that the stream contribution (see Cases A6 and A7 on **Fig. 5.2**), the latter is distributed over a greater part of the year while precipitation is mainly concentrated in late autumn and winter. **Figure 5.5** and **Fig. 5.6** highlight the time lag between the peak stream inflow, corresponding to the melting of the snow pack, and the peak of precipitation, which occurs mainly as snow. In **Fig. 5.2** it is noteworthy that the increase in water level due to direct precipitation occurred during 10 days of February (from day 43 to day 53 on **Fig. 5.6**). Comparing Cases A6 and A7 on **Fig. 5.2**, it can be assumed that during those days direct precipitation is the larger contributor, and the subsequent over estimation of water level must be due in large part to an over estimation of the direct precipitation. The error due to this is propagated over the period of simulation (A1 compared to M from day 55 in **Fig. 5.2**). The idea that there may be high uncertainty

in the estimate of precipitation is not unusual. It is known, that at Tahoe there is a distinct decline in precipitation from west to east (TRPA, 1982; Marjanovic, 1989)

Cases A4 and A5 on **Fig. 5.2** show the result of applying reduction factors to direct precipitation. Although a better fit is obtained while the stream contribution is minor (between days 3 and 80), the error increases in the spring when the stream flow increases as a result of snowmelt. As during the late winter and early spring the evaporative losses are minor, and taking into account that the stream outflow is very low, and its estimated relative uncertainty is low, it may be concluded that the stream inflow is also overestimated. Assuming that the flow of the gauged set of streams was properly estimated, it could be inferred that the relative contribution to the total stream input of the un-gauged and the run off is overestimated.

Stream inflow (including direct runoff) and direct precipitation are the major inputs for year 1992 (**Table 5.2**). **Figure 5.3** shows the resulting simulated water level of numerical experiment A8, in which actual values of direct precipitation and stream inflow were multiplied by constant factors of 0.5 and 0.75 respectively. These values lay within the range of estimated uncertainties (**Table 5.1**). Making these assumptions, the measured level is quite well reproduced, with a mean error of 0.015 m and a maximum difference of 0.079 m.

Thus, through simple numerical experimentation it is possible to show that a correct water balance is attainable by adjusting the measured and estimated inputs by quantities that are within their inherent uncertainty range. For this particular year it is clear that the stream inflow and direct precipitation data are overestimated. The predicted water level is slightly sensitive to the modeled contribution of the ground water, although the effect is smaller than the uncertainty in the two other inputs.

5.1.3. Verification

Having established that a water balance can be readily achieved for one year by making acceptable changes to the inputs, it is instructive to consider a second year to verify the results. **Table 5.4** lists the components of the baseline case hydrologic budget for 1999 for Lake Tahoe. The figures are quite different from 1992, reflecting in large part the inter-annual variability. However, the different data sources could

84

also affect the difference. The main differences are in the water level fluctuation, stream input, stream outflow, and direct precipitation. For 1992 the measured water level change is a drop of approximately 0.5 m, while in 1999 it does not change overall. While stream outflow was almost negligible in 1992, its contribution for year 1999 is quite remarkable. The total input of the baseline case in 1992 is 3.73×10^5 ML day^{-1}, while the total input of the baseline case in 1999 is 7.39×10^5 ML day^{-1}, nearly a factor of two larger. The contribution of direct precipitation in 1992 is nearly three times larger than in 1999.

Table 5.5 lists the numerical experiments that were performed. The baseline case stands for actual data without modification. Figure legends are referred to the labels of the first column of **Table 5.5.**

Setting all the sources and sinks to zero again shows that the model conserves mass (Case B1). The simulated water level of the baseline case (B0) underestimates the measured water level, although the time varying pattern is again similar. The effect of ground water is highlighted in numerical experiment B2, where its contribution was set to zero. **Figures 5.5** and **Fig. 5.6** help in the interpretation. If it is assumed that the direct precipitation is under estimated (**Fig. 5.6**) then the stream outflow is over estimated (**Fig. 5.5**). Setting the direct precipitation contribution to zero (Case B3, **Fig. 5.4**) eliminates the peaks of days 43 and 50 (**Fig. 5.6**), while leaves unaffected the stream peak of early spring (Case B4) and **Fig. 5.5**. It seems that the direct precipitation during the peak of these days has been under estimated.

Experiment B5 on **Fig. 5.7** shows the simulated water level assuming that the measured direct precipitation has been under estimated by its maximum relative uncertainty of +70% (**Table 5.1**). The simulated peak is still above the measured water level peak. Stream outflow shows its greatest values over these days (**Fig. 5.5**). Experiment B6 on Fig. 9 keeps the assumption made in Case B5 while assumes that the overflow is over estimated by its maximum relative uncertainty (+15%, **Table 5.1**). The magnitude of the peak is correctly simulated by multiplying a factor of 2.75 times the measured precipitation values (B7). Cases B8 and B9 in **Fig. 5.8** are presented as examples of different possible combinations within the range of

Table 5.4 Components of the hydrologic budget for the baseline simulation year 1999 (day number 7 to day number 336).

	INFLOWS				OUTFLOWS	
	Stream flow	Run off	Precipitation	Ground water	Stream outflow	Evaporation
10^6 liters	520740	60927	141904	63033	419513	684608
%	66.20	7.74	18.04	8.01	38.00	63.00

Table 5.5 Numerical experiments for year 1999. Symbol X indicates an input that is set to zero. Other parameters were left unchanged. Numerical factors indicate a multiplicative factor on the base case value.

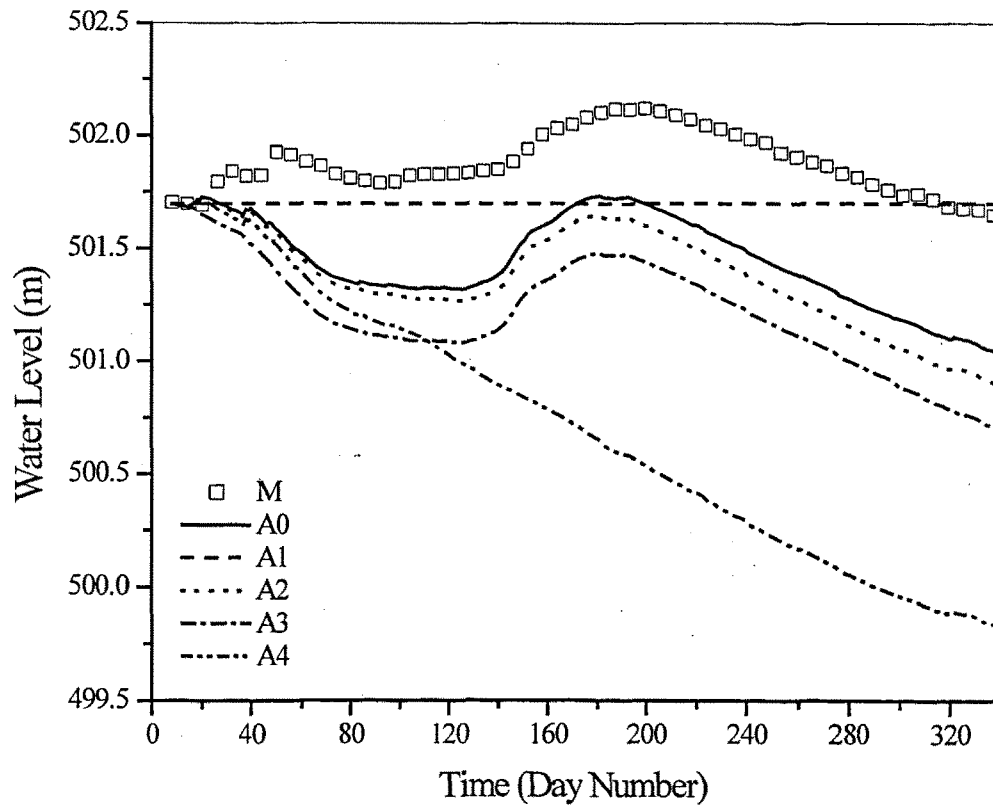|	Inflow	Ground Water	Outflow	Rain	Evaporation
A0			BASELINE		
A1	X	X	X	X	X
A2		X			
A3				X	
A4	X				
A5					1.70
A6			0.85		1.70
A7					2.75
A8			0.85		2.75
A9	0.85		0.85		2.75

86

Figure 5.4 Baseline water level (A0), predicted water levels by A1 through A4 numerical experiments, and the measured water level for 1999. Labels correspond to experiments referenced in **Table 5.5**.
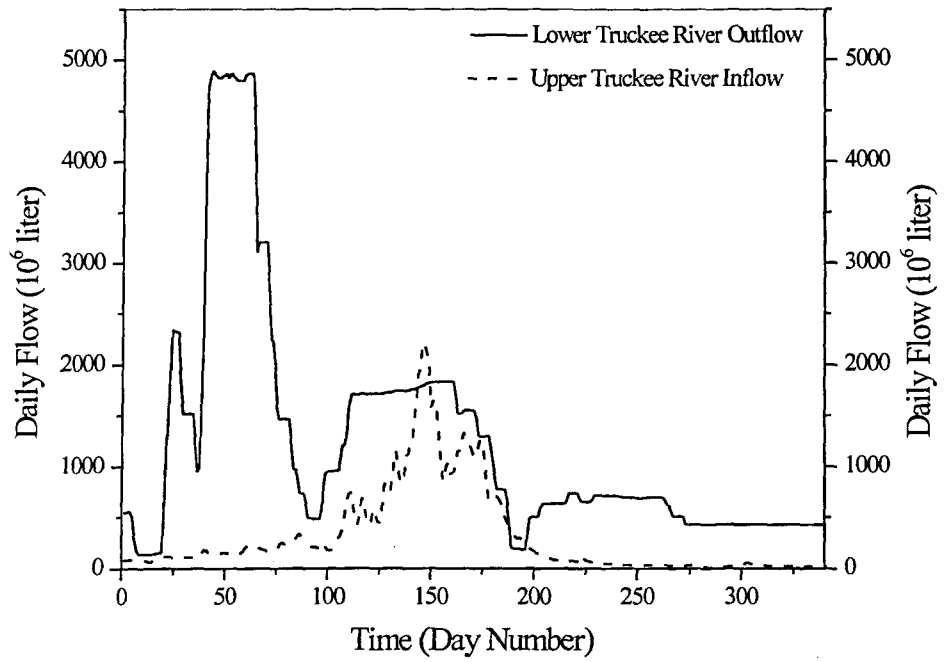
Figure 5.5 Measured Lower Truckee River outflow and Upper Truckee River inflow for 1999.
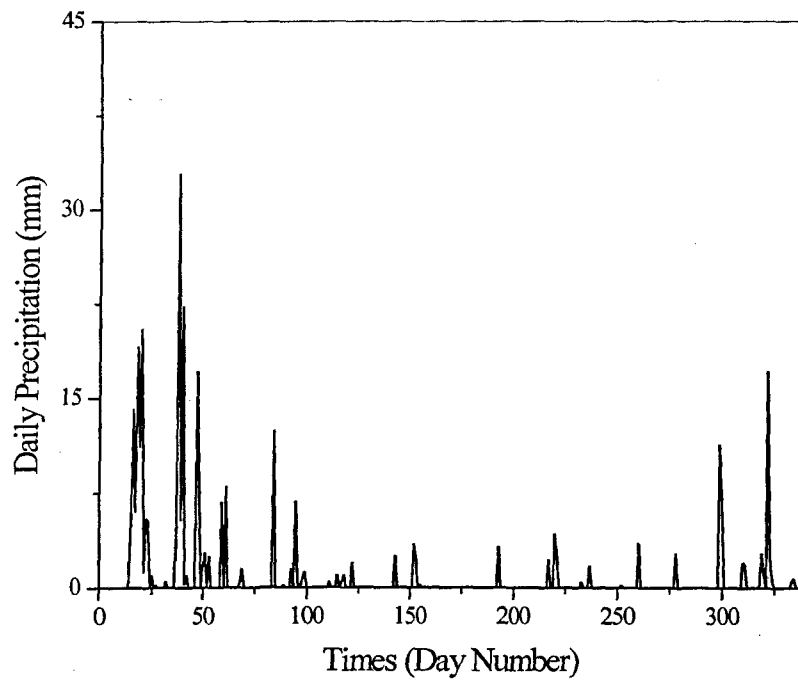

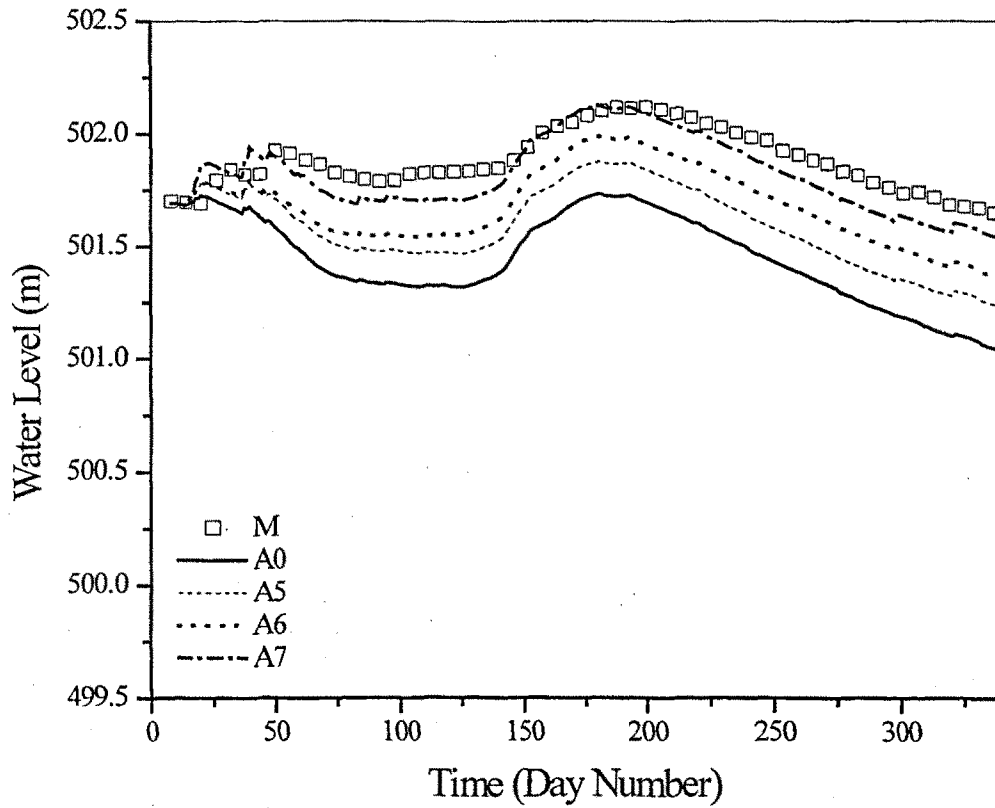**Figure 5.6** Measured precipitation for 1999.

88

Figure 5.7 Numerical experiments for the considered period of 1999. Labels correspond to the simulation experiments as references in **Table 5.5**.

uncertainty of the sources and sinks of the water budget that give quite good simulations. Note that after day 273, no inflow or outflow data were available.

Thus in contrast to 1992, the precipitation in 1999 needs to be increased in order to produce the right magnitude changes in water level. Certainly one contributing factor to this is the change in location of the source of meteorological data. However, it is also likely that the system is far more complex than can be appreciated with the limited data that are available. It may be argued that the applied factor of 2.75 to the precipitation falls beyond the maximum estimated relative uncertainty. By looking at **Fig. 5.7**, a time lag between the simulated and measured peaks is apparent. The peak in precipitation lags the measured water level peak in about 5 days. Possibly this reflects a lag in direct runoff or the time required by discharge of the ground water. The predicted water level does not lag the measured peak, as the 1-D model cannot take into account side effects, and the ground water in the model is related to the annual stream flow rather than the time variable precipitation over the watershed.

What is evident from this exercise, however, is that great care must be taken when synthetic, long-term data sets are produced from short records. Not achieving a water balance will lead to large accrued errors in not only the lake level but also the nutrients and sediment that is brought in by the components of the water budget. One cannot simply use measured data without checking that a water balance is achieved. Further, if perturbations on the few years of data that do exist are used to introduce "variability" to a synthetic long term data set, then it will be necessary to check each year to ensure that a realistic water balance is achieved through the application of appropriate factors on the sources and sinks of the water budget components.
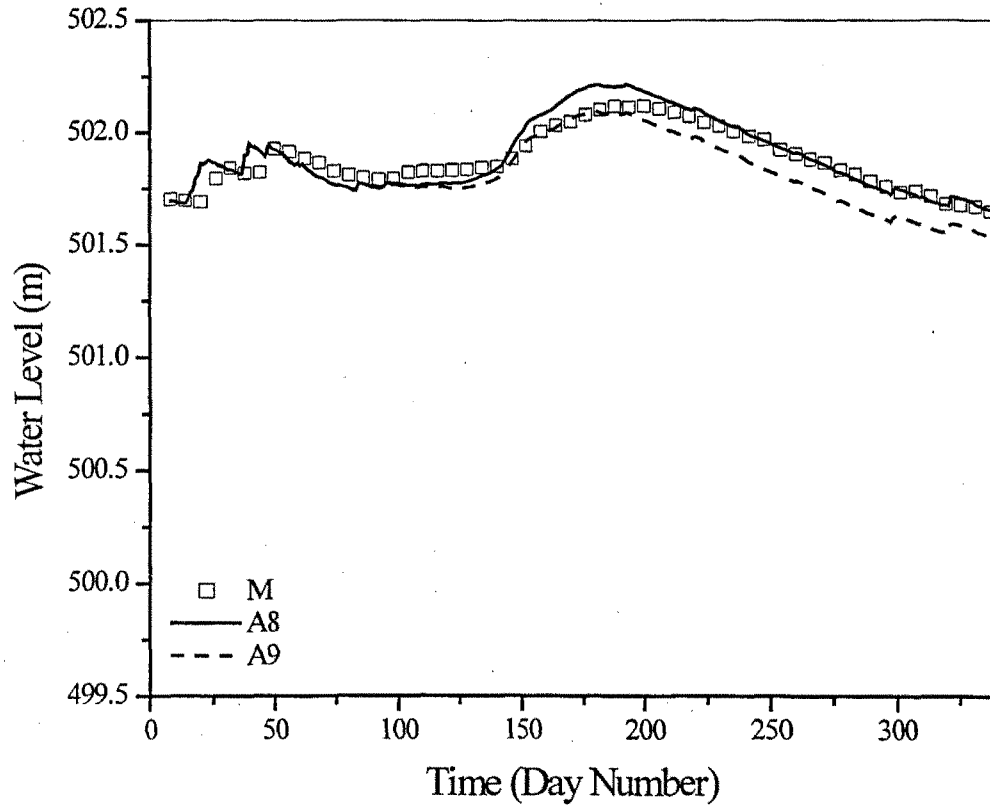
Figure 5.8 Some examples of possible fittings applying factors within the range of the estimated relative uncertainties.

5.2 Nutrient Balance

There is great uncertainty in each element of the Nutrient Budget of the Lake Tahoe. The modeling of the various components of the nutrient budget is described in **Section 3.2.2.** The sensitivity analysis of **Chapter 6** explores the impacts of these uncertainties. In this section the preliminary concept of checking the mass balance of the nutrients is considered. The nutrient mass-balance equation can be expressed as:

$$At + I + G + R - O - S - D - A = 0 \qquad (5.2)$$

where At is the nutrient input associated with atmospheric deposition, I is that due to insertion by inflows, G is that due to groundwater, R is for sediment nutrient released, O is for outflow, S is the loss of nutrients to the sediments, D is nutrient transformation due to denitrification (for the Lake Tahoe and the period simulated its contribution was found to be zero), and A is the mass of nutrients accumulated in the lake at each time step. The nutrient balance was performed on a daily basis. DLM-WQ uses artificial storage elements to temporarily "hold" the inflow water before it intrudes at its level of neutral buoyancy. Thus, the checking of the nutrient balance included a summation across all layers, across the artificial storage elements and included all the chemical and physical forms that nutrients are permitted to take in the model (including nutrients that are part of the algal biomass).

Figure 5.9 shows the variation of nutrient input, output and accumulation for the case of total Nitrogen (as N) for 1999. **Figure 5.10** shows the corresponding values for total Phosphorous. The inputs of nutrients are from stream inflows, ground water, atmospheric deposition and transfer across the sediment-water interface. Losses of nutrients are from stream outflow, particulate settling, and potentially (in the case of nitrogen) denitrification. Summing these components according to Eqn. 5.2. yields zero for each day simulated in both cases, confirming that the model does indeed conserve mass of N and P under all conditions.
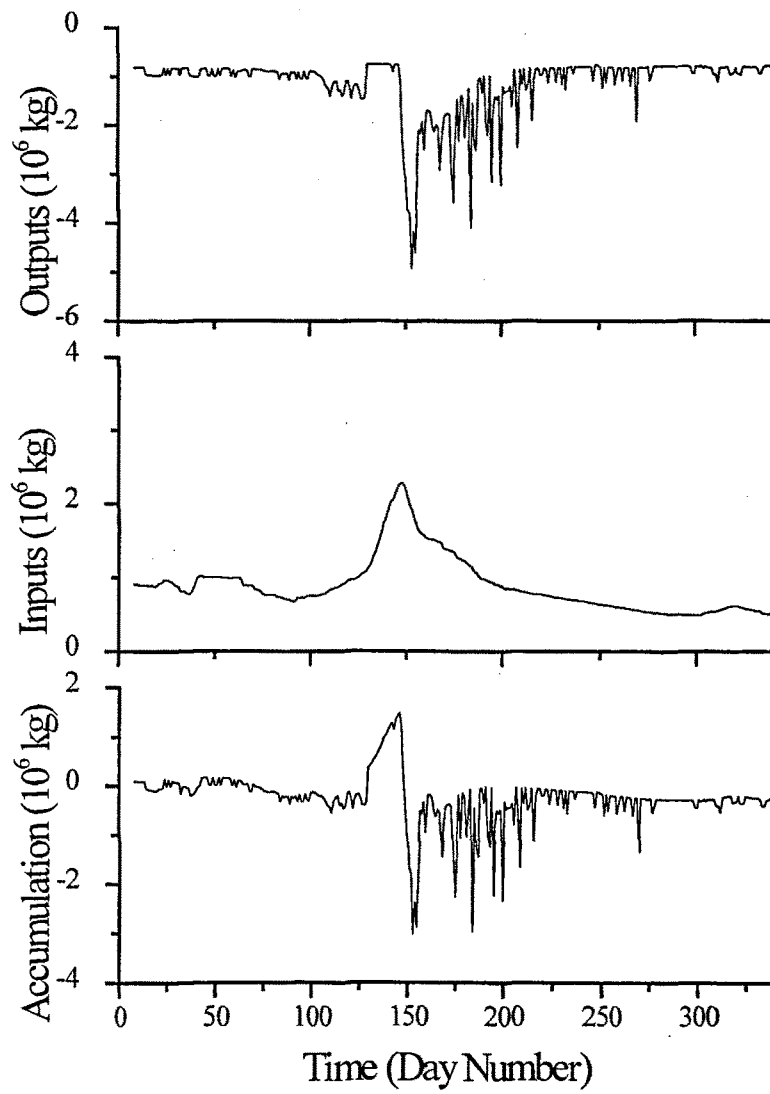
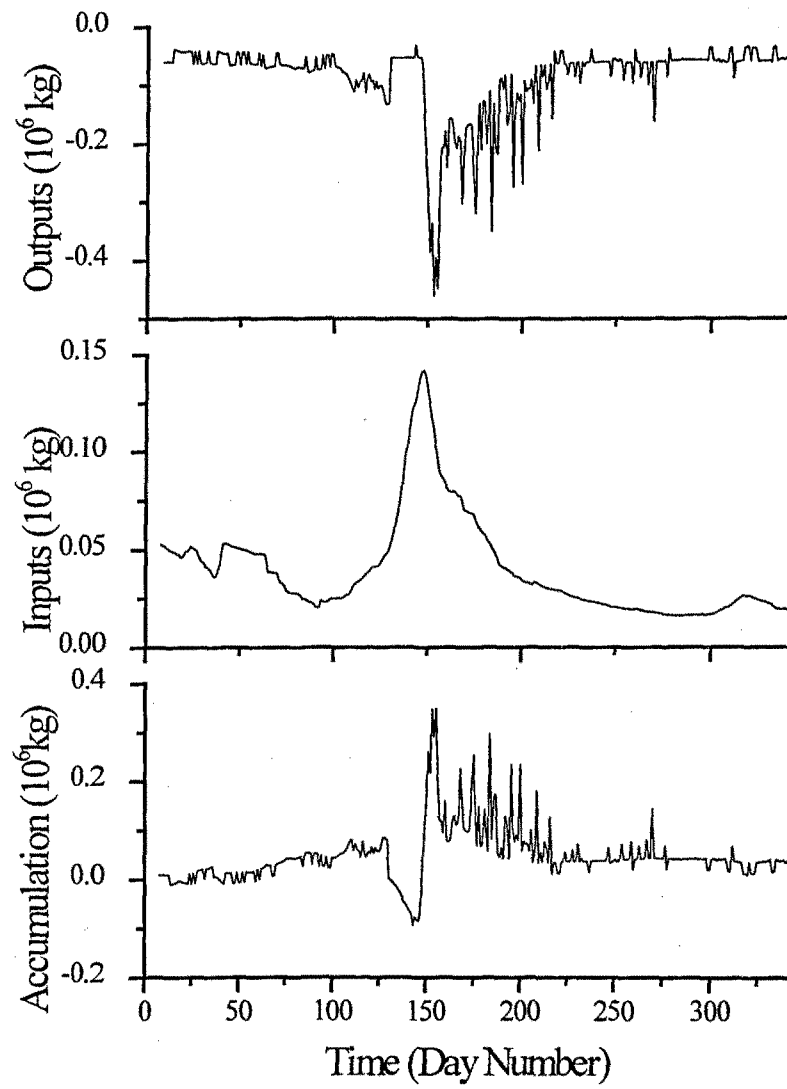**Figure 5.9** Nutrient balance for total Nitrogen as N for 1999.

Figure 5.10 Nutrient balance for total Phosphorous as P for 1999.

5.3 Spatial and Temporal Discretization

DLM is based on a Lagrangian layer structure, in which the lake is represented by a series of horizontal layers of uniform property but variable thickness. An algorithm maintains the thickness of each model layer between a maximum and minimum user prescribed value. It is desirable to use a combination of the space (i.e. layer thickness) scale and time step that will permit adequate accuracy and resolution whilst not unnecessarily extending the computational time required. This latter requirement is of particularly interest for the intended use of the model in long-term simulations.

A comparison of particular combinations of the maximum and minimum layer thickness has been made using the un-weighted Root Mean Squared (RMS) error, (Chapra, 1997):

$$Error(T) = \left[\frac{\sum_{i=1}^{n} (T_i^m - T_i^s)^2}{n} \right]^{\frac{1}{2}} \qquad (5.3)$$

where the superscripts m and s refer to measured and simulated values, and the subscript i refers to the value at layer i, where the layers are numbered from the bottom. The *RMS* error is evaluated by summing over the heights of the measured temperature data, using for T_i^s values of the simulated data interpolated onto these heights. The *RMS* error as calculated estimates the absolute fit of the predicted to the measured profile and can be interpreted as expected error (Patterson at al., 1984). The great depth of Lake Tahoe is such that significant errors in one part of the vertical profile may be masked by summing over all the layers. In this manner, the result is generally biased toward the fit in the hypolimnion. To avoid this bias, the position of the simulated thermocline was determined at each day and the water column was divided into areas above (epilimnetic) and below (hypolimnetic) the thermocline. The position of the thermocline below the surface was determined by calculating the first moment of the field density gradient profile:

$$h = H - \frac{\int_0^H z \cdot \left(\frac{d\rho}{dz}\right) \cdot dz}{\int_0^H \left(\frac{d\rho}{dz}\right) \cdot dz}$$

(5.4)

where z is the elevation, H is the total depth, and $\rho(z)$ is the density profile. The *RMS* error was then calculated for the whole water column, (global error), for the epilimnion (epilimnetic error), and the hypolimnion (hypolimetic error), separately.

The numerical experiments were performed for particular combinations of maximum and minimum layer sizes. For example, 3:1 indicates a maximum layer size of 3 m and a minimum layer size of 1 m. The combinations explored were 3:1, 5:1, 10:1, 9:3, 15:3, and 20:5 The time steps explored were 15, 60, 180, 360, 720, and 1440 min. The time steps were maintained constant during each run, except for the case of 1440 min, where the model automatically sets the time step at values between 15 minutes and 1440 minutes depending on the intensity of the forcing.

The error in temperature was the only parameter evaluated in this analysis. The reason for this is that temperature is the only parameter with sufficient vertical resolution (10 cm) to calculate a meaningful error. Only 1999 had these data available. It is therefore assumed that if a time step and spatial scale is satisfactory for purposes of simulating the temperature, then it should be suitable for the other variables modeled.

Figure 5.11 shows for one specific case, time plots of the global, epilimnetic and hypolimnetic error in degrees Celsius. It can be seen that global and epilimnetic errors follow the same pattern; the epilimnetic contribution has the greater weight on the global error, while the hypolimnetic contribution is negligible. The discrepancies are found in the top layers of the water column, while the deeper layers are not affected by the selected space and time step. The same trend has been found for the entire set of numerical experiments performed. Thus, in what follows, discussion will consider only the epilimnetic error.
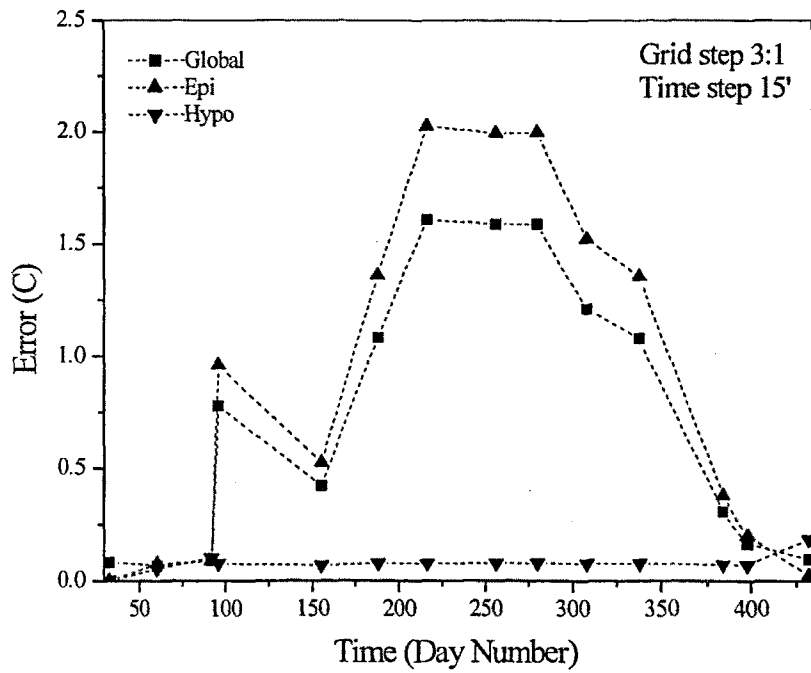
Figure 5.11 Global, epilimnetic and hypolimnetic errors for one specific case estimated as *RMS* temperature difference between measured and simulated temperature field.

Figure 5.12 shows the time plots resulting from varying time steps for the full set of spatial steps. Figure 5.13 shows plots at different fixed time steps for different spatial scales. It is clear that the simulated thermal structure is sensitive to both the time step and to the ratio and to the actual values of the minimum and maximum layer thickness. All the simulations follow the same seasonal trend. Starting from negligible errors during winter well mixing conditions, a sudden jump is found at day 96, followed by a sharp error drop. Looking at the measured temperature contours in **Fig. 5.14**, this rise and fall corresponds to the existence of a mass of cool water at the bottom of the Lake. Thompson (2000) has hypothesized that differential cooling between the shallow and deep parts of the lake, may be responsible of the displacement of cool water to the bottom of the lake. This two-dimensional mixing process is not parameterized in the model; it violates the assumption of one dimensionality on which the model is based. Thus it is not surprising that there is a difference ("error") between measured and simulated at this time. Following this, weak stratification of the top layers of the water column occurs, followed by its rapid destruction by a mixing event induced by wind as can be seen in **Fig. 5.15** The other large errors occur during the stratified period (late summer and beginning of autumn).

From **Fig. 5.12** it can be seen that higher errors occur for the shorter time steps (15' and 60'). Although the 20:5 grid step gives the lowest error during stratification period, the 3:1 and 5:1 grid steps are less sensitive to both the chosen time step. Keeping constant the minimum thickness and increasing the maximum thickness (3:1, 5:1, and 10:1) results in a greater sensitivity to the selected time step while the range of error remains the nearly the same. If the grid ratio is held constant, increasing the maximum layer thickness (3:1 to 9:3, and 5:1 to 15:3) results in increased sensitivity of the solution to the time step. **Figure 5.13** shows that, for any grid step, the global error is reduced at longer time steps. Again, 15' and 60' cases show a separate trend with a marked shaped bell seasonal pattern, which is less evident for the larger time step cases. A time step of 180 min is the shortest time step that reduces the very large errors in the stratified season. The 1440' (variable) and 720'(fixed) cases remain nearly within the same error bound, but 720' case is less sensitive to the grid step during stratified conditions.
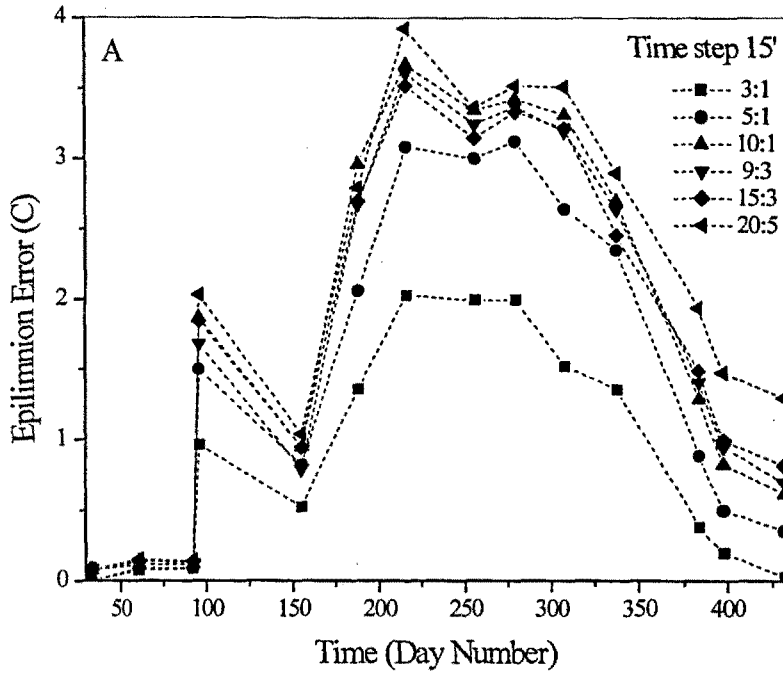
Figure 5.12 Plots of epilimnion error between the simulation and the measured temperature for different combinations of time step for the second period for 1999: A) time step 15 min, B) time step 60 min, C) time step ratio 180 min, D) time step ratio 360 min, E) time step ratio 720 min, and F) time step ratio 1440 min.

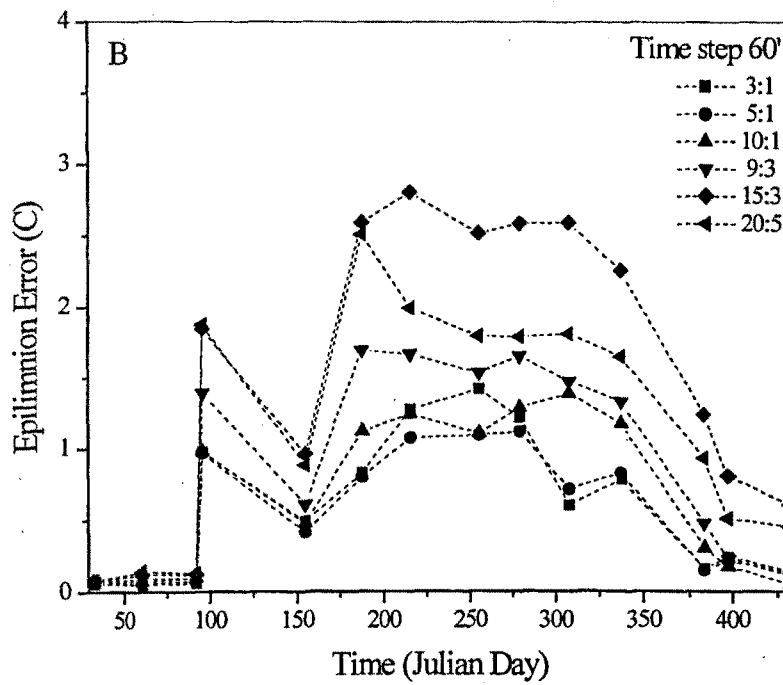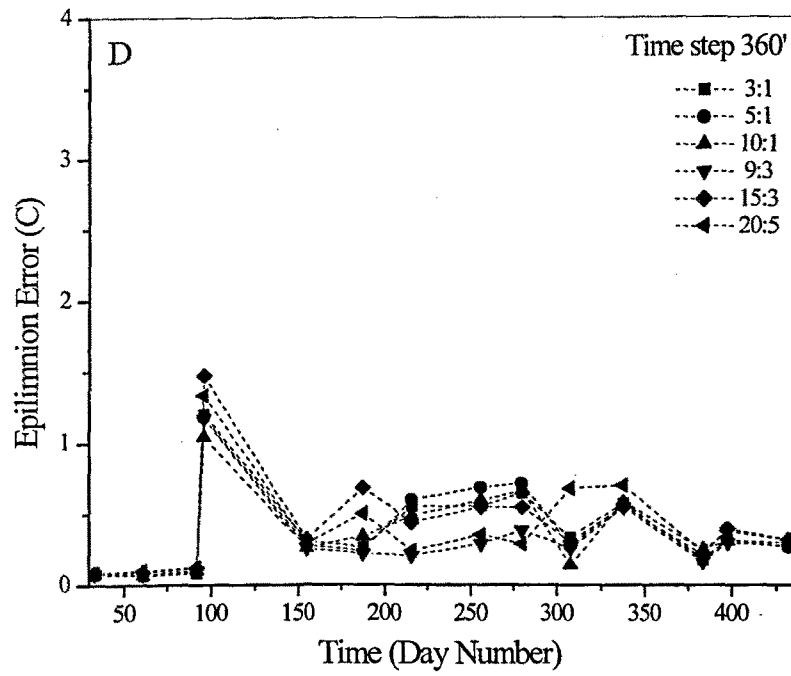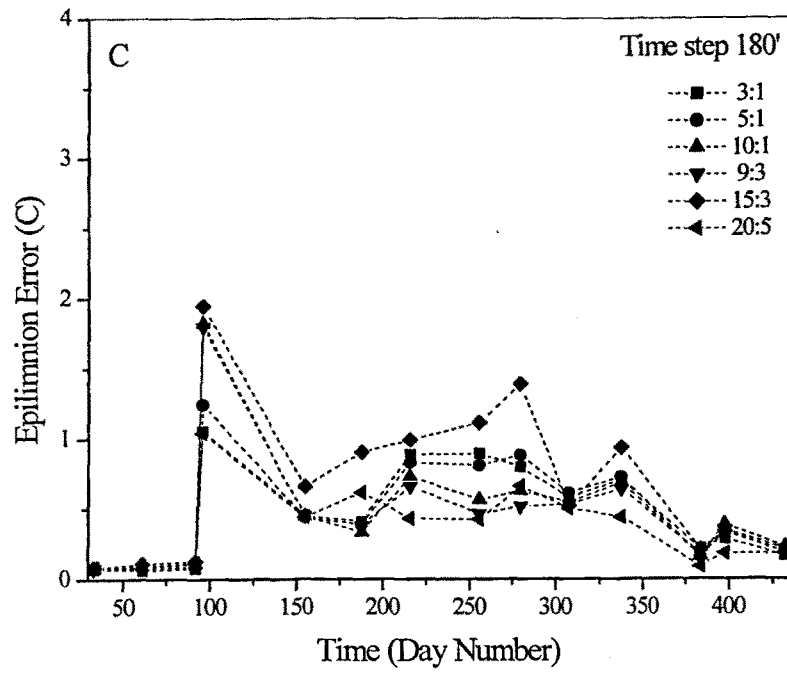**Figure 5.12** Continued.
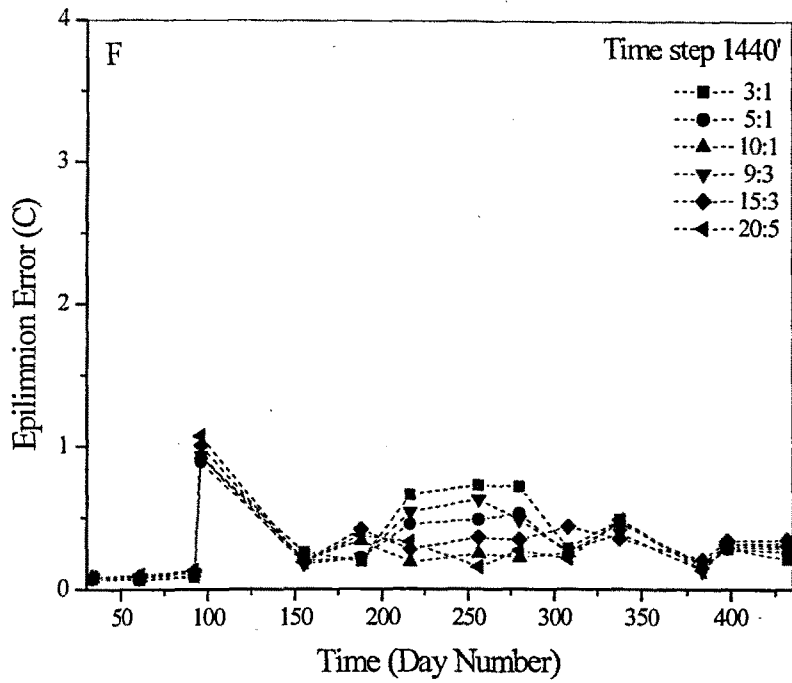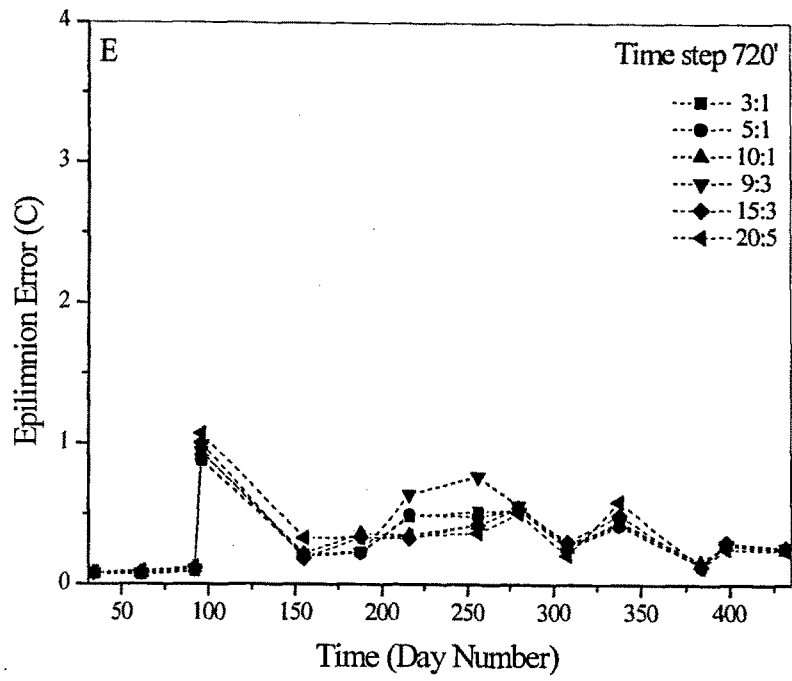
Figure 5.12 Continued.
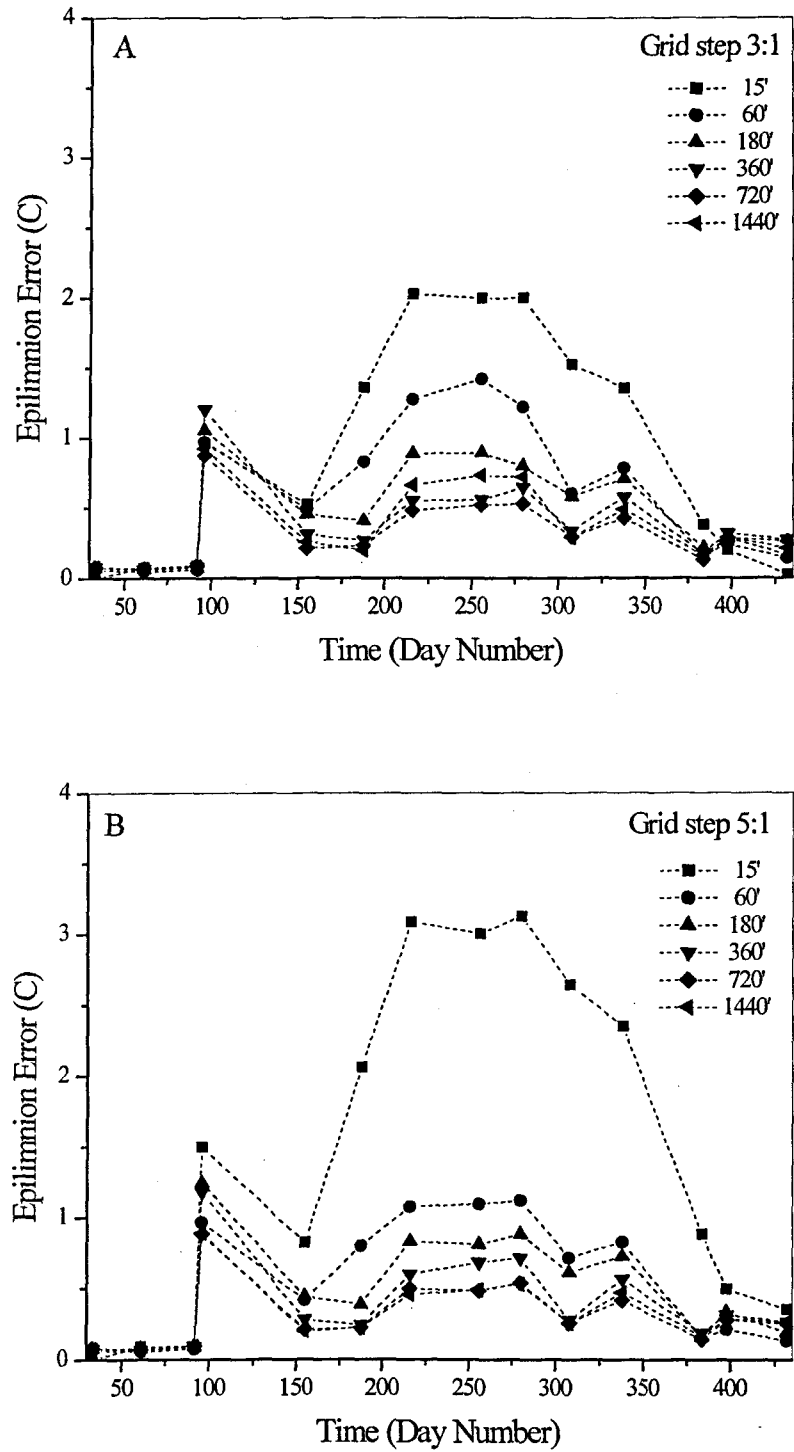
Figure 5.13 Plots of epilimnion error between the simulation and the measured temperature for different combinations of space step for 1999: A) grid step ratio 3:1, B) grid step ratio 5:1, C) grid step ratio 10:1, D) grid step ratio 9:3, E) grid step ratio 15:3, F) grid step ratio 20:5.

Figure 5.13 Continued.

Figure 5.13 Continued.
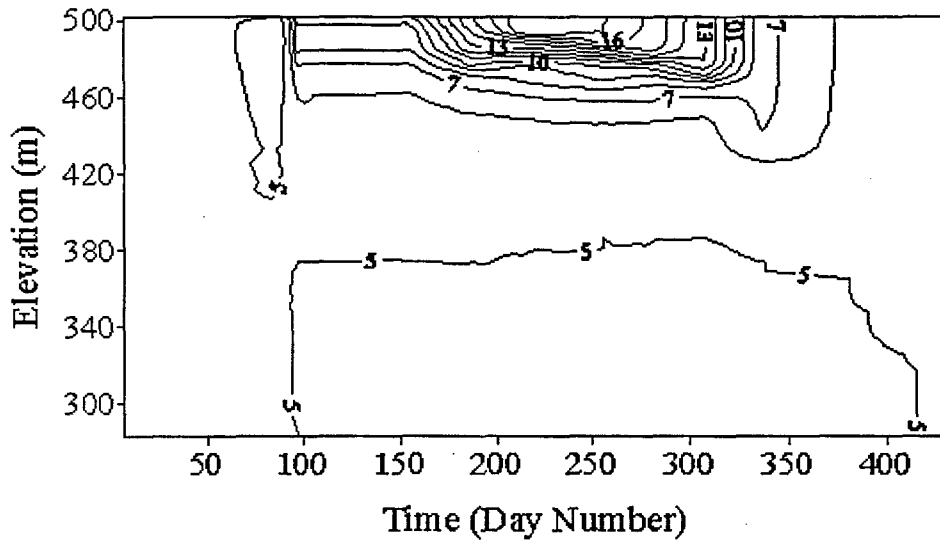
Figure 5.14 Temperature contour plot of measured RBR profiles, starting at 1999/01/07 (day number 7) and ending at 2000/03/07 (day number 432).
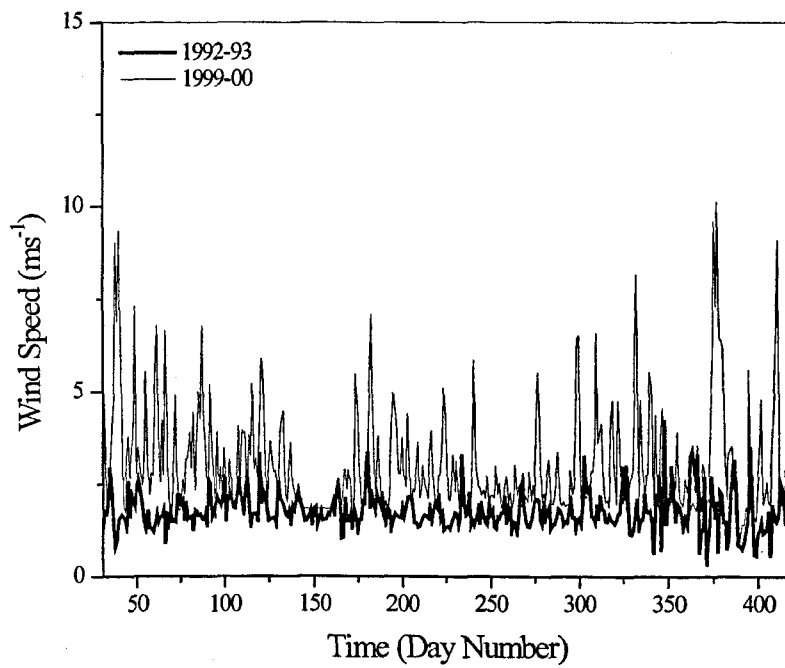
Figure 5.15 Time series of wind speed for the two periods under study.

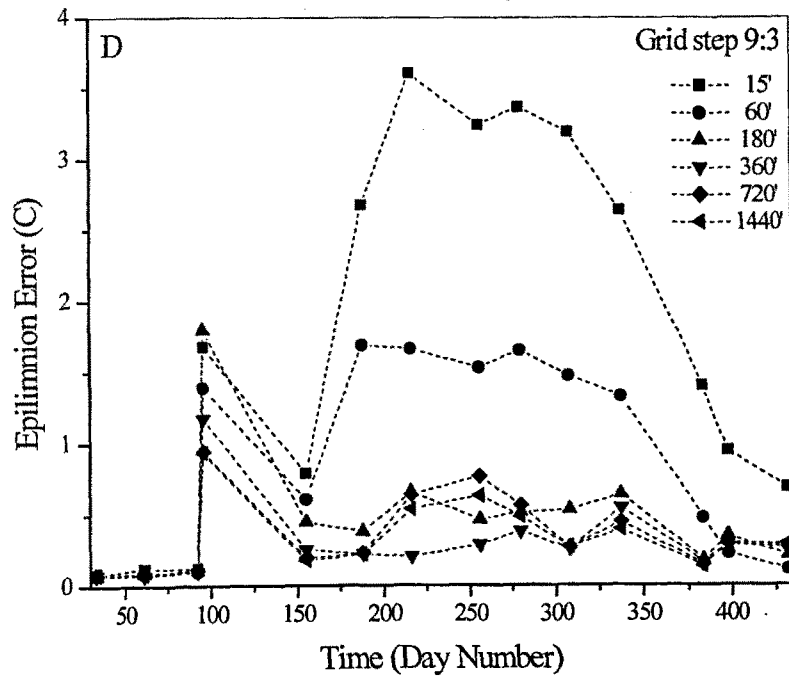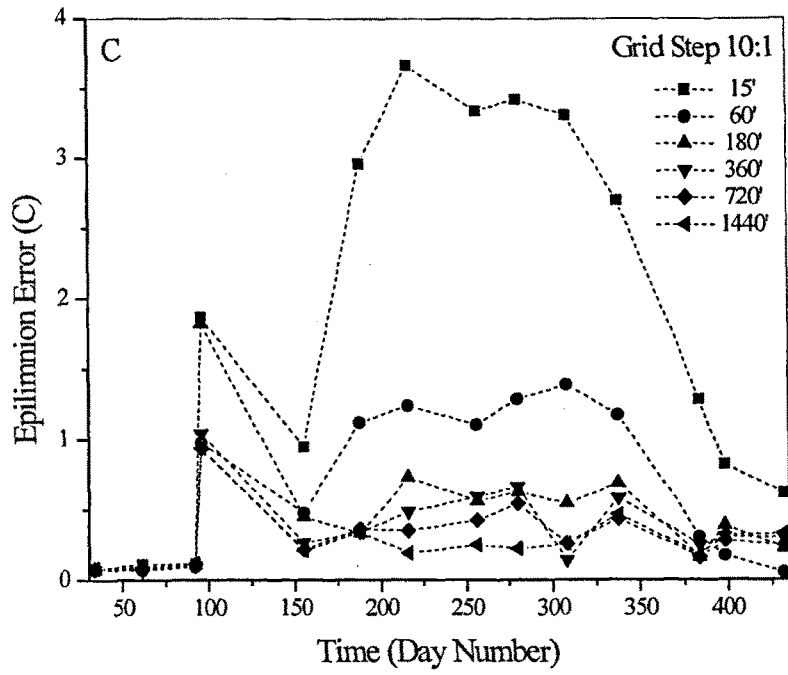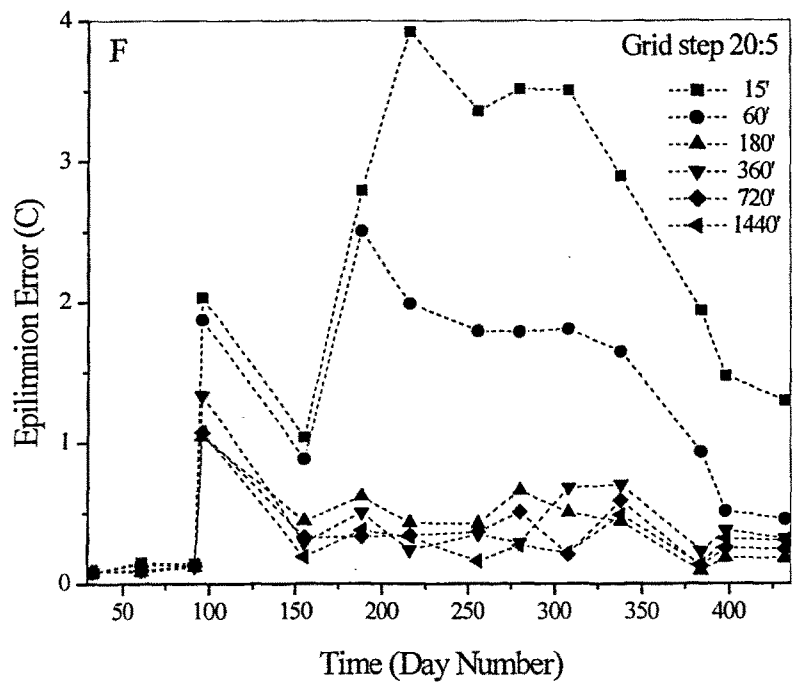It may seem contradictory that decreasing the time step results in increased errors. DLM parameterizes turbulent kinetic energy as a fixed proportion of the work done by wind and by heat loss accompanying cooling of the water surface. This assumption of fixed proportionality implies that mixed-layer turbulence adjusts rapidly to changing external inputs (Imberger, 1981). However, this assumption of quasi-equilibrium must not be valid for shorter time scales (minutes to hours) because of the time required for adjustment of mixer-layer turbulence to a change in response to the surface wind stress (Spigel et al., 1986). The turbulence parameterization used in this model neglects temporal changes in mixed-layer turbulence in mixed-layer turbulence and it seems to be suitable for long time step simulations.

A compromise in the selected space and time grid must be achieved to balance several opposing requirements. Reducing the time step is necessary for a proper description of algal growth by photosynthesis (Wallace et al., 1996). However, it has been shown that longer time steps result in smaller errors. The layer structure must represent the actual mixing space scale events. Thus, even though a combination of 20:5 noticeably speeds up the model run, and keeps the errors within a reasonable range, it seems to be unrealistic to describe the scale of the mixing events. Also, as the model is intended to predict Secchi depth changes, a minimum layer size that is much grater than 1 m would yield less resolution than is desirable.

In consideration of the above, a combination of 3:1 for the grid space and 180 minutes for time step was selected and is in what follows.

5.4 Conclusions

DLM-WQ has been checked to verify the mass balance over the scale of the performed simulations (~1 year). The model is able to correctly conserve mass and to represent the observed pattern of water level change under different input weather conditions. The quality of the input data determines the accuracy of the predicted water level. The main sources of error seems to come from: i) records of direct precipitation during short and strong events when precipitation seems not to be

correctly represented by a single measurement site, ii) estimates of the un-gauged streams as well as direct runoff, and iii) stream outflow over estimation especially at times of high flow. Though comparison data do not exist, the correctness of the evaporation formulae used in the model must be considered a potential source of error, especially as evaporation is such a large part of the water budget.

The simulated water budget is somewhat sensitive to the contribution of groundwater. Groundwater has been modeled in a very simple manner. Further improvements in representing groundwater may be worth considering in future developments. Although its contribution is within the range of the estimated uncertainty of the water budget, it seems that the inclusion of a term that takes into account the ground water may be interesting for long-term simulations.

The mass balance of the modeled nutrients was confirmed.

Space and time resolution was shown to greatly affect the simulation quality. The time and space grid should be selected according to physical and biological requirements. The water quality component restricts the selectable sub-daily time step. In order to properly describe the daily dynamics of light limitation, sub-daily time step should not be much greater than approximately 180 min.

Chapter 6: Model Evaluation and Sensitivity Analysis

The main objective of the present model is to predict water clarity on at least, a decadal scale. As the model will be used as a management tool, its sensitivity to uncertainty in model parameters and input data must be properly assessed.

There is uncertainty of the true values of the input data used in a model and therefore uncertainty is inherent in the predictions of the model. Sources of error are the estimation error of the initial conditions, driving variables for the system, and sampling errors in the field data that are compared with model results to assess performance (Loehle, 1997). Additionally, there are errors associated with the structure of the model and the parameter values used in the simulations. Using the model in a predictive fashion also requires that inputs for some future, unknown set of conditions can be provided. Thus, the model must be supplied with synthetic input data that have in some manner been generated from past conditions assumed to be representative of future conditions. However, future conditions and their associated uncertainties are difficult to estimate (Beck, 1987). It is likely that some input variables are going to contribute more to the variability of the model output than others.

In what follows, sensitivity of model formulation is evaluated by testing a limited set of alternative formulations of the hydrodynamic sub-model where such formulations could be reasonably applied. Many components of the hydrodynamic model have been tested before, through the application of DYRESM (see **Section 3.1.3**) and more recently DLM to a great variety of different lakes and reservoirs. Thompson (2000), for example, has applied DLM to Lake Tahoe (under winter deepening conditions only) and found that the mixed layer algorithms give good agreement when mixing occurs over almost the full depth of the lake. Two areas where the model formulation has been relatively untested are in its sensitivity to the drag coefficient formulation

and to light extinction variations. This latter area is of particular relevance to the present work, as one of its goals is to more rigorously predict changes in light extinction on a daily basis through the addition of an optical sub-model. Thus addressing the question of whether this will have a noticeable feedback effect on the thermal simulation is important at the outset.

Sensitivity to model parameters and input data is evaluated separately for the hydrodynamic and water quality sub-models through a perturbation analyses performed over a range of meteorological, hydrologic and limnological variables. The studies were performed for two sets of independent data corresponding to years 1992-1993 (hereafter 1992), and for years 1999-2000 (hereafter 1999). As the data for 1999 are of better quality, the sensitivity analysis has been performed for this period. The simulated period starts January 7, 1999, and ends March 3, 2000. Verification has been performed with the 1992 data, starting January 2, 1992 and ending March 2, 1993. Both simulation periods commence at a time when the lake was relatively weel-mixed. Therefore it was possible to check whether the model is able to properly predict the time, position, and intensity of the stratification. Although both periods comprise nearly the same number of days, the periods has been chosen to represent years of distinct meteorological conditions (see **Chapter 4** for more details).

Once the model has been set to a reasonable combination of parameters, the model has been employed to predict the impact on the hydrodynamics of the Lake of different hypothesized scenarios – crude approximations to potential future conditions.

6.1 Review of Methods

Sensitivity analyses have traditionally provided insight as to which model components play an important role in determining model output (Rose, 1983). Sensitivity may be dependent on input values, making it necessary to distinguish between, e.g., sensitivities at historical inputs (calibration) and future inputs (prediction). Sensitivity to input data can be measured in several ways (Hakanson and Peters, 1995; Klepper, 1997). The sensitivity S can be measured in terms of the magnitude of the deviation

110

ΔX of the state variable, X, with respect to the perturbation ΔP of the perturbed parameter P (Beck, 1983):

$$S = \frac{\left(\dfrac{\Delta X}{X}\right)}{\left(\dfrac{\Delta P}{P}\right)} \qquad (6.1)$$

The relative change to the parameter value is determined based on our knowledge of the certainty of the parameters, thus results are, in general, stated as the change in model predictions as a result of small errors in parameter values (Gardner et al., 1981). Another measure of the sensitivity can be give through a dimensionless coefficient of variation (Reckhow and Chapra, 1983).

Larger models commonly use a Multiplicative Sensitivity Analysis (Loehle, 1997) that consists in the variation of a large number of parameters simultaneously (Janse et al. 1998, Gardner et al. 1981). This is typically performed through a Monte Carlo (MC) analysis in which some or all of the parameter values are selected randomly from a limited range of values or selection of the parameter values from their error distribution appropriately an error analysis (Loehle, 1997). Gardner et al. (1981) contrasts the error analysis to a sensitivity analysis in considering each parameter as a random variable.

Additional approaches to sensitivity analysis exist, such as Generalized Sensitivity Analysis (Spear and Hornberger, 1980) and Fractional Factorial design for testing model sensitivity (Henderson-Sellers and Henderson-Sellers, 1996). One method of determining the sensitivity of parameters is by determining an acceptable threshold for values of state variables (Spear and Hornberger, 1980). Simulation runs are then separated into acceptable or unacceptable based on if all of the variables fall within the acceptable window.

6.2 Hydrodynamic (Thermal) Model Evaluation and Sensitivity Analysis

As a criterion for comparison, an estimation of the error of the simulation must be provided. This is done, for the model evaluation, by comparison with measured values of temperature, assuming that they are representative of the actual state of the lake. For the sensitivity analysis, the model output is compared with results from baseline case obtained with what can be considered to be a reasonable combination of parameters.

6.2.1 Model Evaluation

The evaluation of the model structure was limited to two of the most critical factors: i) alternatives drag aerodynamic coefficient parameterizations, and ii) time dependent functions of the light extinction coefficient. The un-weighted RMS error, as described in **Section 5.3**, is used to quantify differences between simulated result and the measurements. When comparing the simulated data with the measured temperature data, some features must be kept in mind. The hydrodynamic model outputs daily temperature at a fixed time, while measured data may have been collected at any time. Also, single point profiles may not be fully representative of whole lake conditions. It should also be noted that the contour plot of the measured temperature consists of only 15 measurements, which affects the interpolation of the temperature isopleths and, therefore, the comparison of measurements and simulations. Tests with changing model output time showed that the differences are minor, thus output was set at the end of each day (i.e. midnight). The resulting simulations have been compared with available measured profiles using the RBR temperature profiles (see **Chapter 4**).

A contour plot of the measured RBR data is shown in **Fig. 6.1 A**. Initially the water column is well-mixed, with differences of temperature of less that 0.1°C between the top and the bottom. Weak stratification, set up by the end of February (Julian day 70), is destroyed when a mass of cold water plunged to the bottom and mixed the whole water column (Thompson, 2000). Stratification begins at beginning of April (Julian day 90), coincident with a series of low wind days and an increase of the shortwave radiation arriving at the lake surface. The degree of stratification is maintained
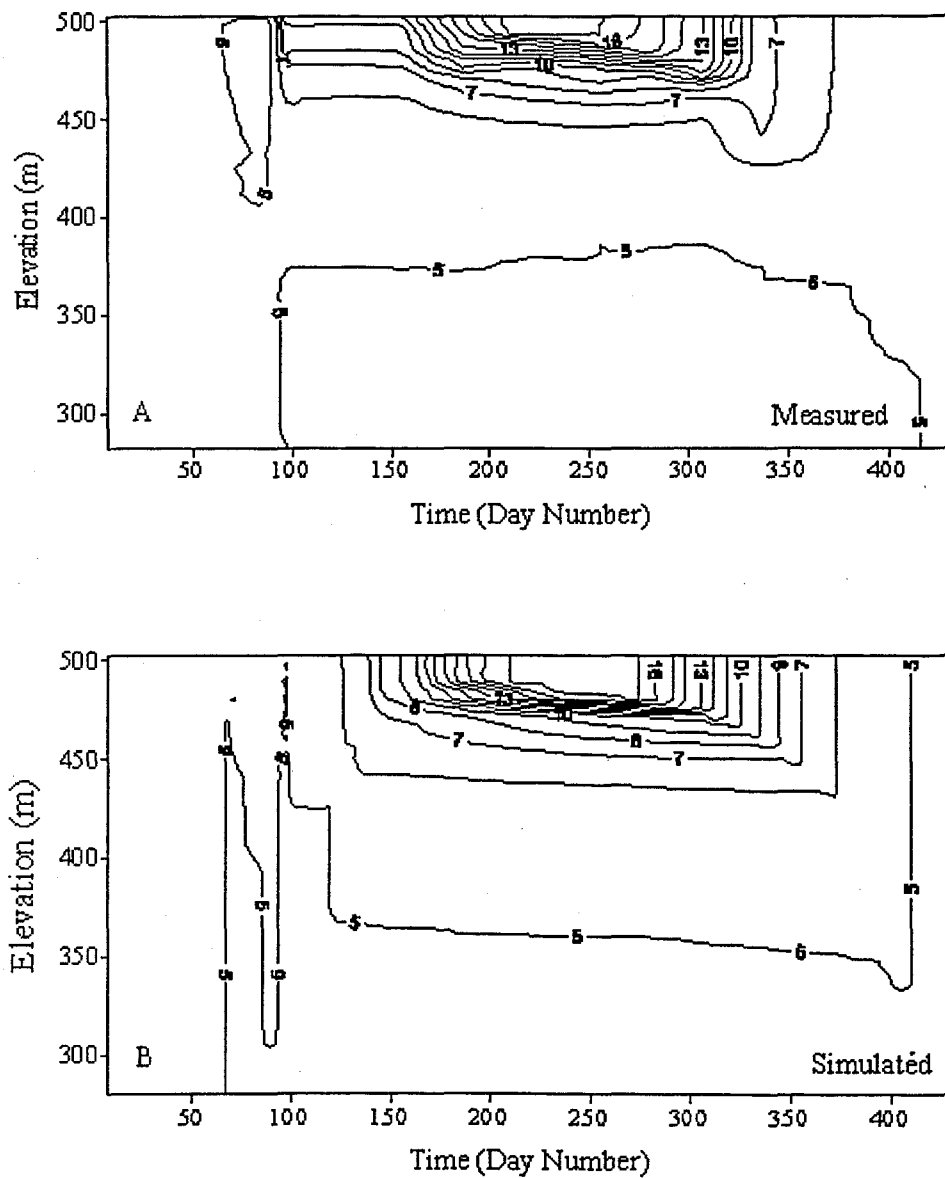
112

Figure 6.1 Temperature contour plot of: A) measured RBR profiles, starting at 7 January 1999 and ending at 7 March 2000 (Julian day 432), B) simulated starting with RBR profile as initial condition.

through the months of April to May, and thermocline started to deepen about Julian day 160 at a rate of 2 m per day up to 40 m depth, marked by a sharp gradient of temperature. The surface temperature reaches 18 C during August. The thermal stratification remains until the end of October (Julian day 300) at which time the thermocline is progressively eroded.

6.2.1.1 Drag coefficient formulation

Many empirical relationships have been proposed to relate the wind speed with the stress induced by the wind at the water surface; an analysis of their impact on a thermal simulation model of a lake can be found in Henderson-Sellers (1988). The original DLM-WQ uses a constant drag coefficient, C_D, set at a value of 1.3×10^{-3} (McCord and Schladow, 1998). For this test, the linear relationship of Smith and Banke between wind speed at 10 m high (U_{10}) and C_D (cited in Henderson-Sellers, 1989) has been used instead to quantify the sensitivity of the model temperature output to the drag coefficient formulation:

$$C_D = (0.63 + 0.066 \cdot U_{10}) \cdot 10^{-3} \qquad (6.2)$$

Figure 6.2 shows the epilimnion error, estimated as the RMS between the measured and simulated value, for the constant and linear drag aerodynamic formulations. It can be seen that the difference is minimal over the tested days. Temperature profiles (not shown) do not display any appreciable differences. Thus, the assumed constant value seems to be satisfactory.

6.2.1.2 Light extinction coefficient

The light extinction coefficient is where the linkage between the hydrodynamic and water quality models is most obvious. Light absorption corresponds to the absorption of heat, which is responsible for the thermal stratification. How important is the time scale over which variability in light absorption is incorporated in the model? For the following numerical experiment, the light extinction coefficient has been obtained from measured monthly Secchi depth (SD) from Lake Tahoe. These data were correlated with light extinction (Swift pers. comm.) and yielded the relationship:

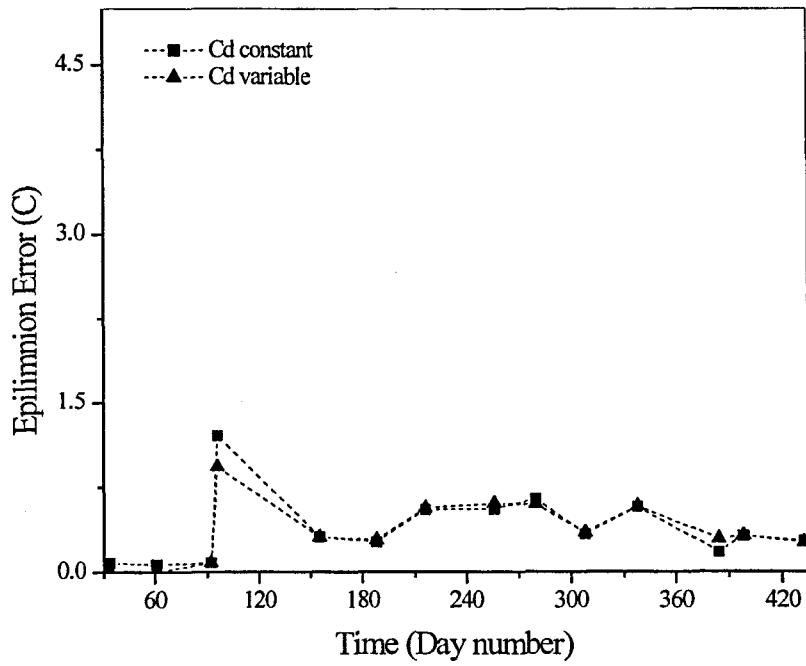$$\eta = \frac{1.87}{SD}, (m^{-1}) \qquad (6.3)$$

114

Figure 6.2 Epilimnion error for constant and linear drag aerodynamic formulations.
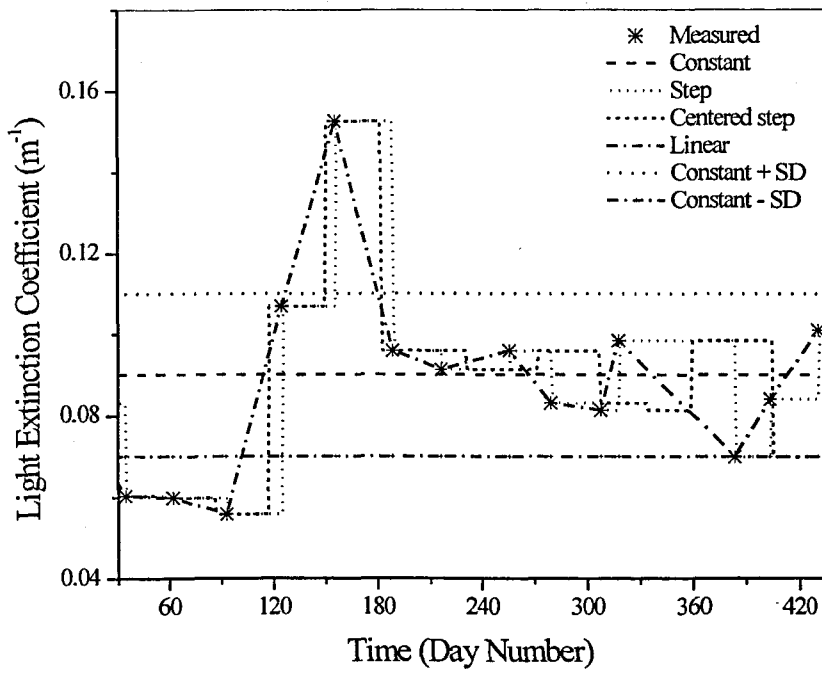

Figure 6.3 Measured and tested functions of the light extinction coefficient.

115

Two sets of experiments were run. In the first, a constant light extinction coefficient (0.09 m^{-1}, the mean for the year) was assumed for the simulation period. This was varied by ± one standard deviation (SD). In the second set of experiments, the monthly light extinction coefficients were used, but the method used to distribute these in time was varied (step, centered step and linear interpolation). **Figure 6.3** shows the time variation of the extinction coefficient for each of these cases. The epilimnion temperature error calculated as the RMS between the measured and simulated temperatures, has been used as a comparison criteria.

Figure 6.4.A shows the epilimnion error for the constant light extinction coefficient. **Figure 6.4.B** shows the epilimnion error as calculated by different time-dependent functions of η as well as the constant value of 0.09 m^{-1}. It can be seen that the model is sensitive to both the value and the temporal distribution of the light extinction coefficient, η. To visualize the effect of the modeled η in the simulated thermal structure, temperature profiles have been plotted in **Fig. 6.5.A and Fig. 6.5.B** for Julian day 216. The constant value + 1 SD gives higher temperatures on the top layers, with while the constant value – 1 SD gives lower surface temperatures. These results strongly suggest that in oligotrophic systems, such as Lake Tahoe, the formulation of the light extinction is critical. Even when using monthly data, as opposed to directly modeling the light extinction, it appears that the result changes depending on how the monthly data are applied. The effects are particularly important at the onset of stratification in the spring. Different values of light attenuation will yield different temperature, and hence, density stratification that will have varying degrees of resistance to mixing. This is what yields the different stepped structures seen.

6.2.2 Sensitivity Analysis

The numerical experiments in which the various model data are varied have been compared against a baseline simulation. This baseline is obtained running the model for 1999 with the best combination of time and step grid deduced in **Chapter 5** (a time step of 180 minutes, and a spatial resolution in the range of 1-3 m). A centered step time dependent light extinction coefficient, and a constant drag coefficient are also utilized. In the final model, the light extinction coefficient will be calculated as part of the model. However, the use of the measured extinction is satisfactory for the

116

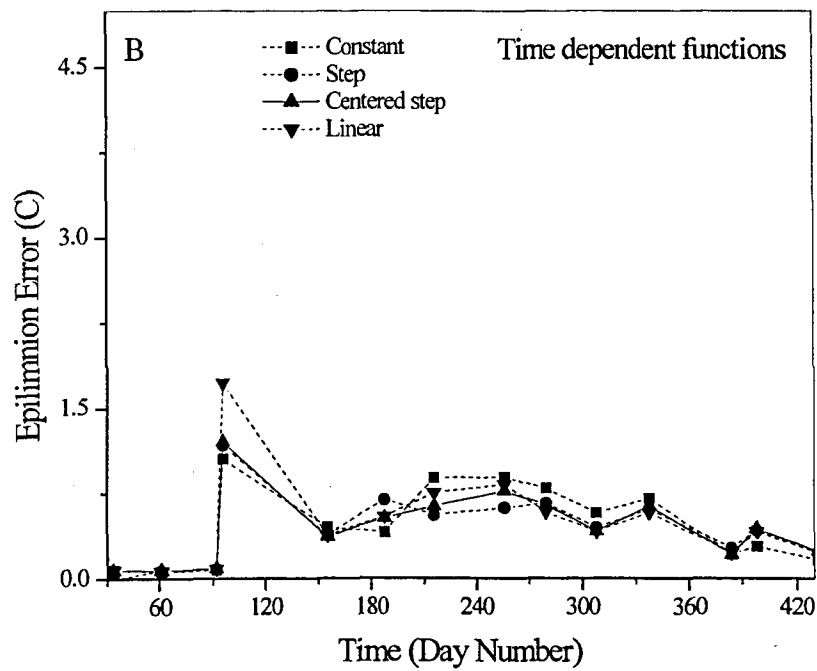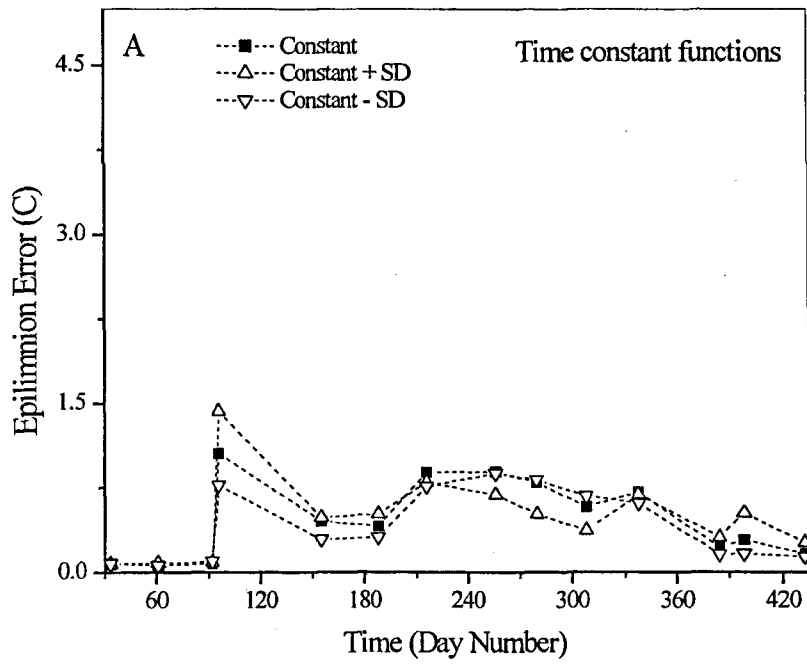**Figure 6.4** Epilimnion error for different light extinction coefficient temporal distribution: A) constant in time, and B) variable time function.
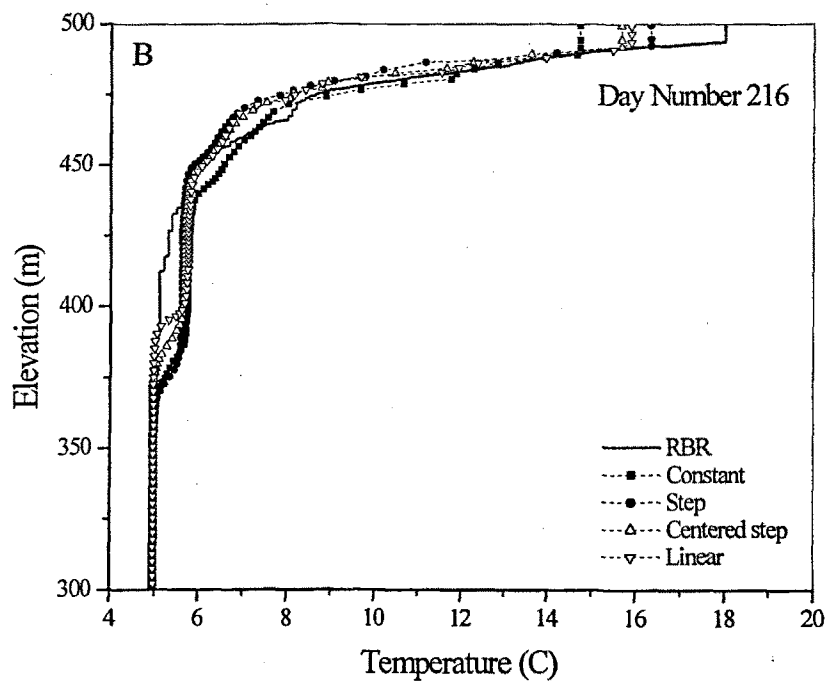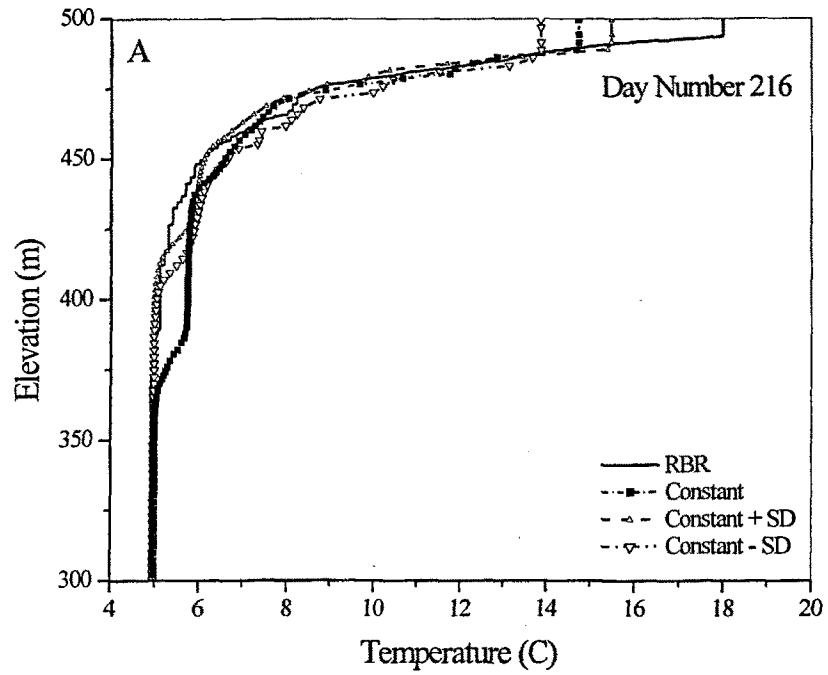
Figure 6.5 Top layer detail of the measured (RBR) and simulated temperature profiles using a) constant and b) time dependent temporal functional form for light extinction coefficient, η.
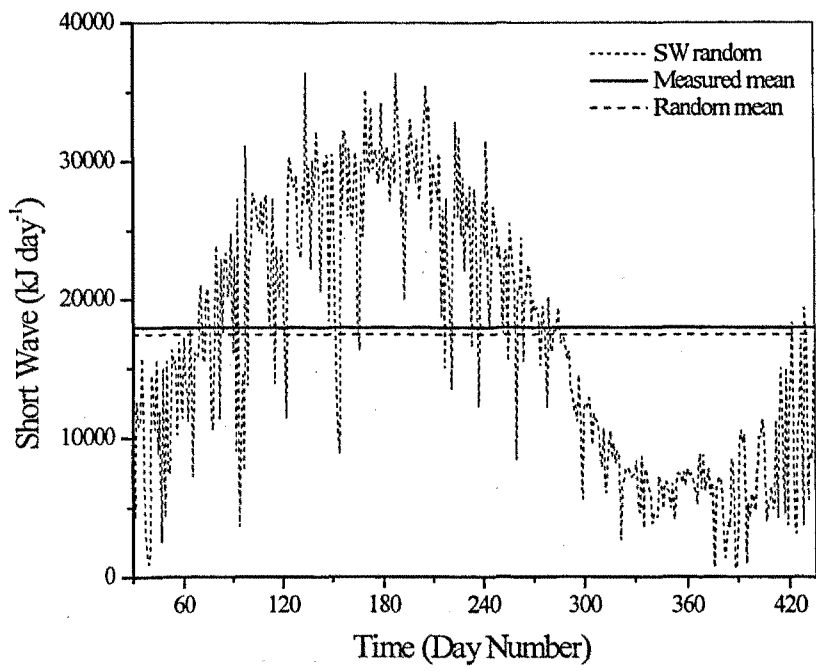
Figure 6.6. Randomly generated short wave distributions with the mean.

purposes of a sensitivity analysis. **Figure 6.1.B** shows the temperature contour plot of the baseline.

6.2.2.1 Meteorological input data

The goal was to analyze the impact on the predicted thermal structure of uncertainty in the meteorological input data. A one-at-a-time sensitivity analysis was performed. Such a procedure analyzes the response to variation of one input, while the other inputs are kept at nominal values.

In order to test for the effects of measurement uncertainty, but not skew the results, each meteorological input was varied without altering its mean. Table 6.1 shows the mean and the standard deviation of each meteorological variable of the original meteorological data file for 1992 and 1999. **Table 6.2** shows the relevant information of the synthetically generated meteorological files. It shows the set ranges of perturbation based on expected uncertainties in each meteorological variable. Each daily value of the baseline data set was multiplied by a randomly generated number within the set range, with the sign (±) also randomly assigned. The length of the simulated period is large enough that the positive and negative factors compensated and thus the mean of the distribution is maintained, as indicated by the % of variation. The greater variation of the pluviometry is explained because days of no rain are preserved and days with rain are augmented. Three different random data sets were generated for each variable. To avoid producing the identical data sets, a different seed number was used for each case. As an example, **Fig. 6.6** shows one of the randomly generated short wave distributions with the mean.

Although it is difficult to estimate the prior uncertainty of model data inputs, the selected ranges were chosen to reflect the uncertainty caused by both error of the measurement and spatial variability associated by using one single point measurement to be representative of the whole lake surface. The records of short wave radiation, SW, measured at the same period by both a Kipp-Zonen and a Licor radiometer at the UCD meteorological station show a discrepancy up to 10%. SW daily distribution must be bounded by the maximum attainable value outside the atmosphere (Duffie and Beckman, 1991) and the constraint to be a positive value. To avoid exceeding the maximum value, the minimum ratio between the maximum value and the actual value

120

Table 6.1 Mean and standard deviation of each meteorological variable of the original meteorological data file of 1992 and 1999.

Variable	1992		1999		
	Mean	SD	Mean	SD	Units
SW	16004	8158	17361	9071	$kJm^{-2}day$
LW	23297	4210	23202	5028	$kJm^{-2}day$
T_{air}	6.40	7.13	5.44	5.87	C
RH	67	17	66	15	%
Wind	1.53	0.69	3.08	1.51	ms^{-1}
Rain	1.77	6.49	0.90	3.25	mm

Table 6.2 Relevant information of the synthetically generated meteorological files. The mean of each perturbed distribution is kept almost identical to the initial condition.

#	Perturbed variable	Factor X	Mean	% variation of the mean	SD
1	SW	0.2	17439	0.45	9295
2	SW	0.2	17437	0.44	9297
3	SW	0.2	17443	0.47	9247
4	LW	0.2	23193	0.04	5403
5	LW	0.2	23400	0.85	5560
6	LW	0.2	23381	0.77	5475
7	Ta	0.4	5.45	0.18	6.12
8	Ta	0.4	5.55	2.02	6.45
9	Ta	0.4	5.52	1.47	6.39
10	RH	0.4	0.65	1.51	0.21
11	RH	0.4	0.66	0.00	0.19
12	RH	0.4	0.65	1.51	0.19
13	Wind	1.0	3.23	4.87	2.78
14	Wind	1.0	3.17	2.90	2.79
15	Wind	1.0	3.20	3.89	2.76
16	Rain	2.0	1.03	14.44	4.64
17	Rain	2.0	0.95	5.55	4.37
18	Rain	2.0	1.10	22.2	5.24

for each day was found (0.2), and then, the random variations restricted to this this interval. Incident long wave radiation, LW, air temperature, T_{air}, and relative humidity, RH, ranges were set at proposed literature values (Henderson-Sellers, 1988). Wind speed is known to show a high spatial variability (Henderson-Sellers, 1989) that has a large effect on the temperature predictions of water bodies (Imberger and Parker, 1985); hence a factor of two variation was allowed. As previously discussed, rain shows a maximum estimated uncertainty in measurements of about 72%, and there is registered a spatial variability between east and west shores of the Lake (Thodal, 1997). Thus, to ensure that the range was wide enough to account the reported variability, rain was allowed to vary up to 200%.

It may be argued that the results depend on the selected range of variability, and they are not the same for each variable, making the sensitivities not comparable. However, the selected ranges are based on the maximum reasonable, expected uncertainties. It is highly unrealistic to expect errors over 100% on properly measured SW, while this range of changes could easily be found in measured wind speeds at different points over the lake's surface.

To quantify the incidence of the perturbed variable, the RMS of the baseline case and each experiment has been calculated for a set of indicators, chosen to check the model's behavior in a wide sense. It has been demonstrated that the ecological behavior of the Lake Tahoe is sensitive to the depth of mixing attained at winter months (Jassby et al., 1999). Two measures of mixing depth are therefore included. The depth of mixing is the depth to the top of the thermocline (or more precisely the depth of the uniform temperature layer at the end of each model day). The depth of the thermocline was determined according to Eqn (5.4) as explained in **Section 5.3.** Both of these depths depend on the magnitude of the energy inputs to the lake. The individual turbulent kinetic energy inputs, described in **Chapter 3**, are also used as indicators, as are the thermodynamic fluxes that drive much of the mixing:

- total available kinetic energy (AKE)
- available kinetic energy for convective overturn, AKECO
- available energy produced for wind stirring, AKEWS,

- available kinetic energy produced by shear and billowing, AKETIL,
- the depth of mixing,
- the depth of the thermocline
- heat fluxes calculated by the model emitted long wave radiation, evaporation and conduction.

Figure 6.7 A-D shows the averaged RMS difference of each indicator for the 3 cases for each-perturbed variable. In **Fig. 6.7 A-D** it can be seen that, within the range of the tested meteorological variables, the model's behavior is particularly sensitive to the changes in the wind speed. The temperature of the surface is also affected by changes in the SW, LW, and T_{air} nearly at 50% of the wind effect, while the impact of the rain and RH variability are minor, although still noticeable. The thermocline depth is also greatly affected by the wind variability. This impact is particularly noticeable as the effect of the other potential variables is small. The depth of mixing and the depth of the thermocline show a similar pattern of sensitivity. However, the sensitivity of the thermocline depth is about twice that of the mixing depth for the wind variability. Of the calculated heat fluxes at the water surface, evaporative and conductive fluxes are most affected by the wind variability, while magnitude of the impact on the LW emitted is an order of magnitude less. As expected, LW emitted is affected for each variable. This is because the emitted LW is function of the calculated surface temperature, which in turn, has been shown to be sensitive to the all set of perturbed variables. The second and the third most influential variables are, by order, the RH and the T_{air}, almost by the same magnitude. While the T_{air} also affects the conductive flux, the RH primarily affects the evaporative flux. Precipitation variabilityhas negligible effect on the surface energy fluxes. The magnitude of the wind variability over the TAKE is 6 times all of the remainder variables. However, the greatest wind incidence is over the AKETIL, and the smallest on the AKECO. This fact is coherent with the shown incidence of the wind variability on the thermocline depth, as the AKETIL accounts for the energy produced by shear and billowing at the thermocline interface. AKETIL is also sensitive to a minor extend, to the remainder variables.
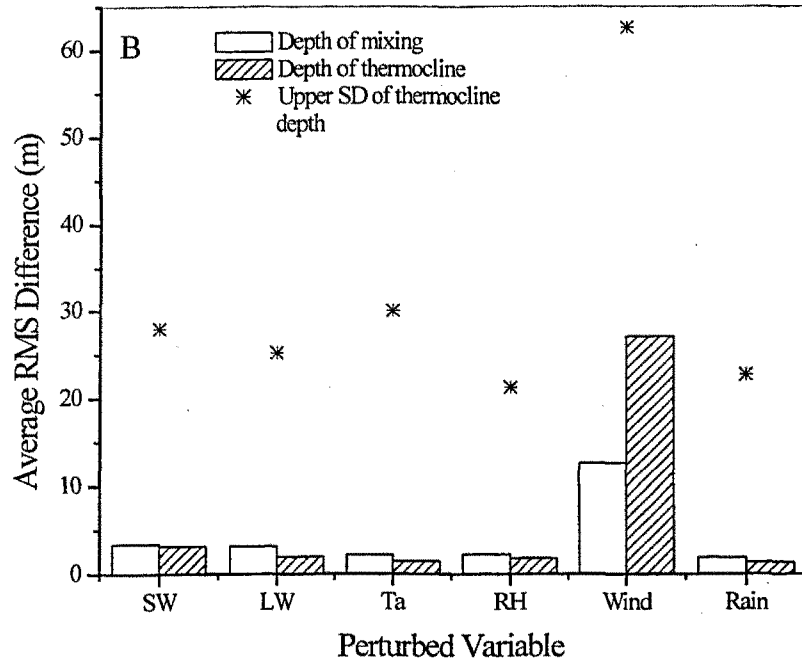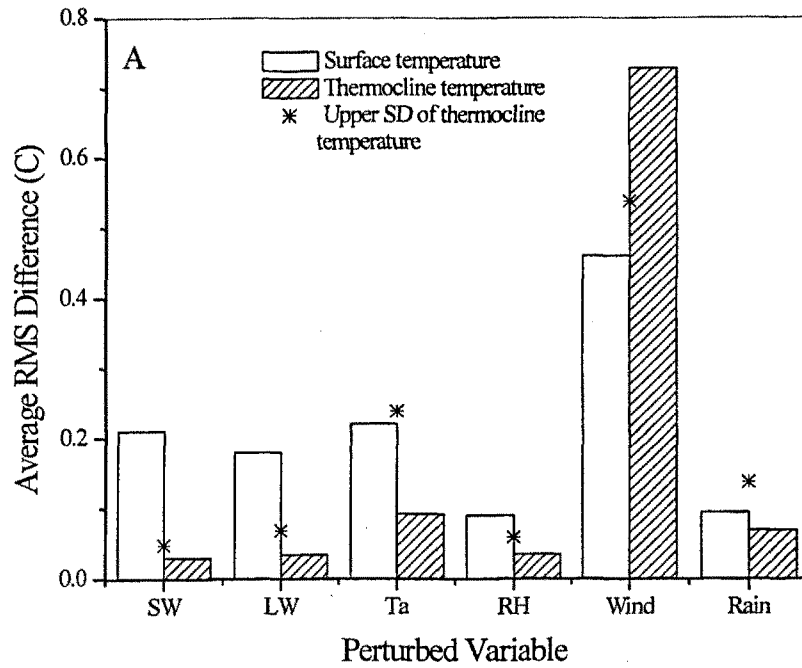
Figure 6.7 Plots of the sensitivity to the perturbed meteorological variables: A) temperature, B) depth, C) heat fluxes, and D) mixing energy terms.
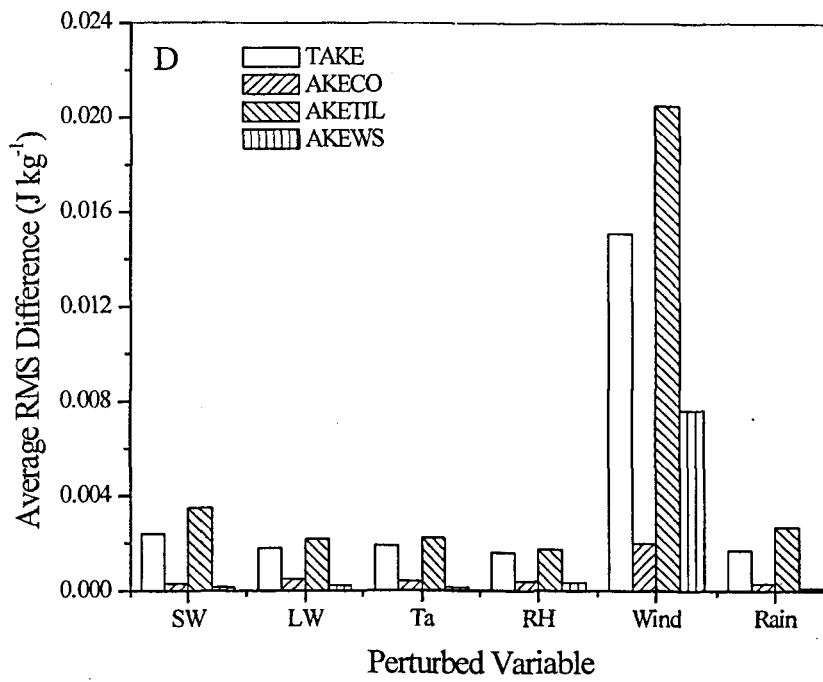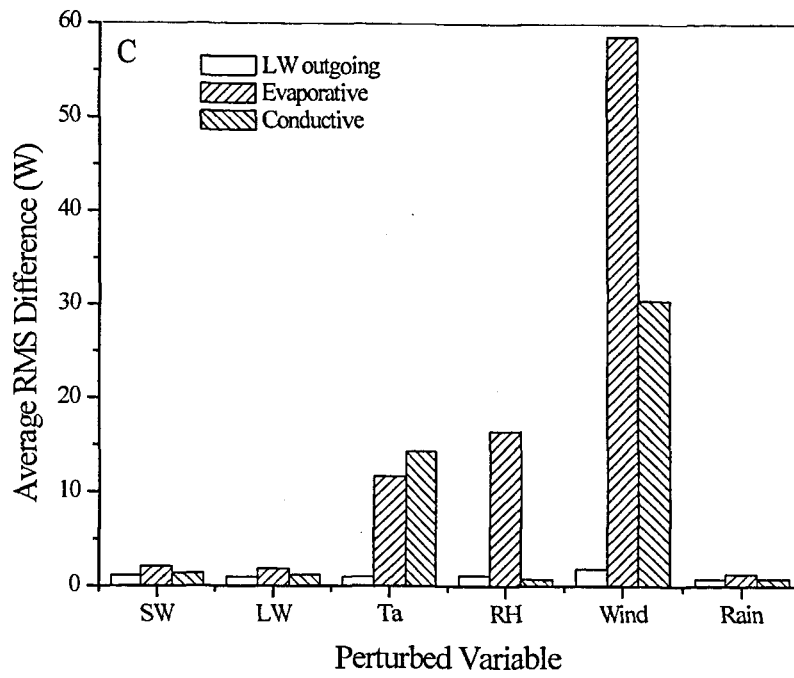
Figure 6.7 Continued.

6.2.2.2 Hydrology assumptions

Large uncertainty in the input and output contributions is known to exist in the water budget (see **Section 5.1.2.**). In order to quantify the incidence of inflow and outflow of water on the thermal stratification, the model was run setting to zero all the streams inflow, the outflow and ground water. The comparison between the simulated thermal structure and the baseline case (not shown) showed no perceptible difference in any of the sensitivity indicators. This is not surprisingly as expected by the large residence time of the lake of about 700 years (Marjanovic, 1989)

6.2.2.3 Validation and initial profile conditions

The spatial resolution of the temperature data varies from tens of meters for thermistor chains to centimeters for the RBR profiler data. Does coarse resolution of the initial and validation data affect the result of the simulations? -This analysis has been performed only for 1999, as no high-resolution data were available for 1992. The simulation starting with the initial RBR temperature profile of higher resolution was compared with the simulations produced with daily averaged data from a thermistor chain at the Midlake station (Schladow, unpublished data). As the lake was essentially homogeneous on the initial day, both model runs commenced with almost the same conditions.

Figure 6.8 shows the two recorded temperature profiles for each day on which both types of data were available. The difference in the spatial resolution and the recorded temperatures are apparent. For the temperature profiles of Day 7 (starting day for both simulations), the temperature differences are minor.

Looking at **Fig. 6.9** it can be seen that the uncertainty in the epilimnion is similar for either set of validation data. From **Fig. 6.10** it can be seen that the differences in the initial profiles of temperature have an impact on the predicted thermal structure even when they are minor. It is likely that this effect would be larger if the simulations commenced when the lake is stratified. However, even with these differences, the model is able to correctly predict the main trends of the thermal structure. This is due in part to the program automatically enhancing the resolution of the initial profile of each state variable by applying a 0th order linear interpolation. In time, the greater
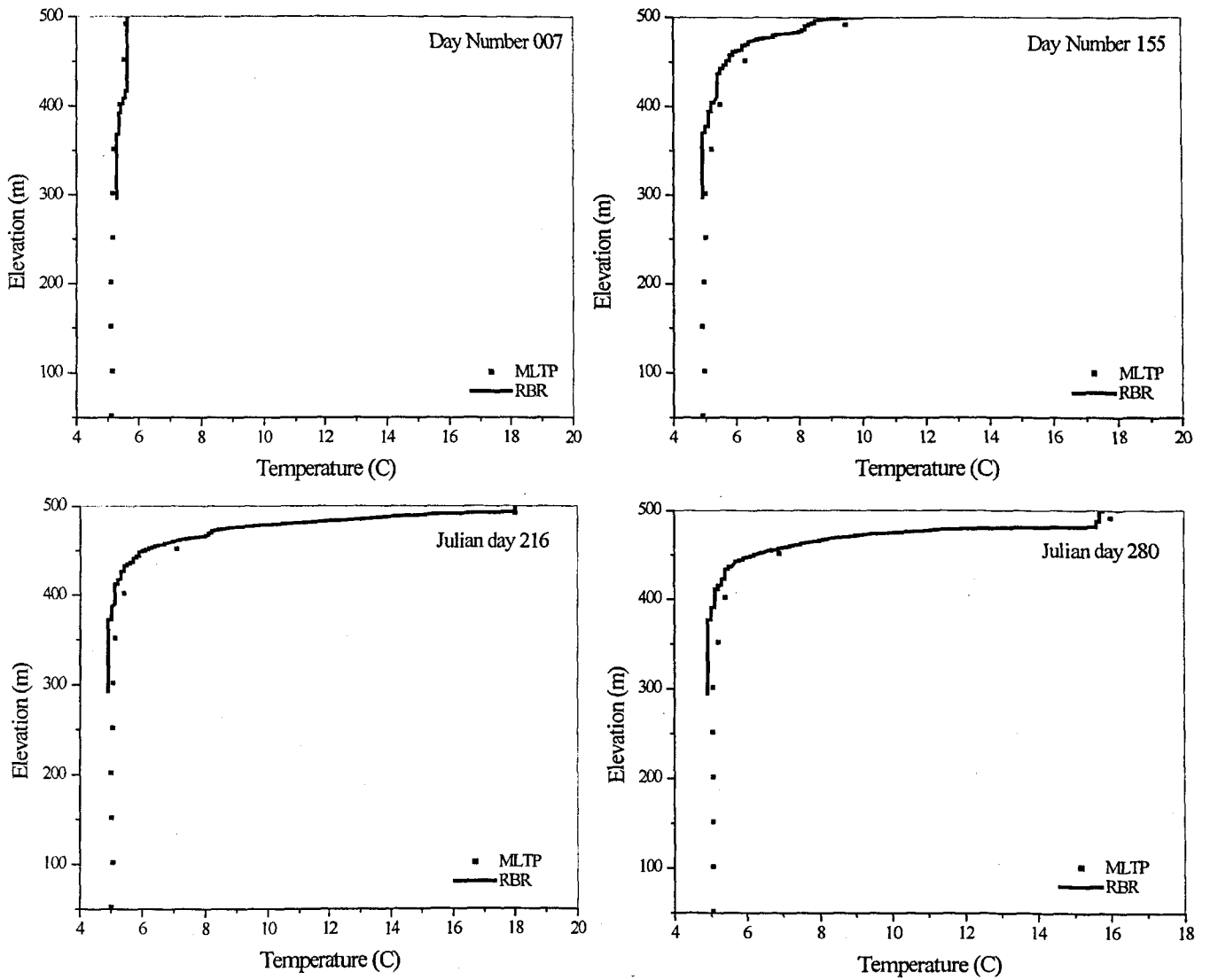
126

Figure 6.8 Measured temperature profiles from MLTP thermistor chain and from RBR profiler. Note the differences between temperature profiles for same days.
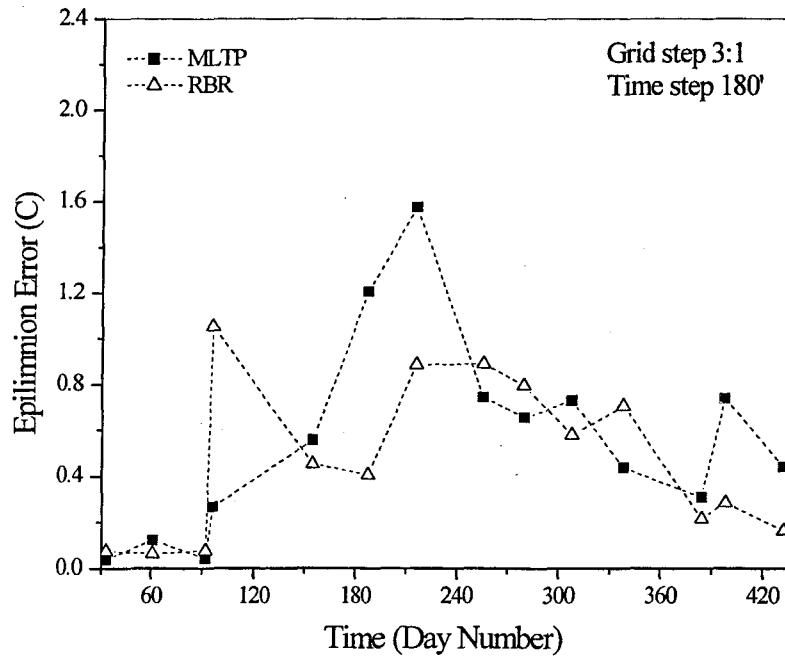
Figure 6.9 Epilimnion error from MLTP initial conditions provided by thermistor chain and RBR profiler.
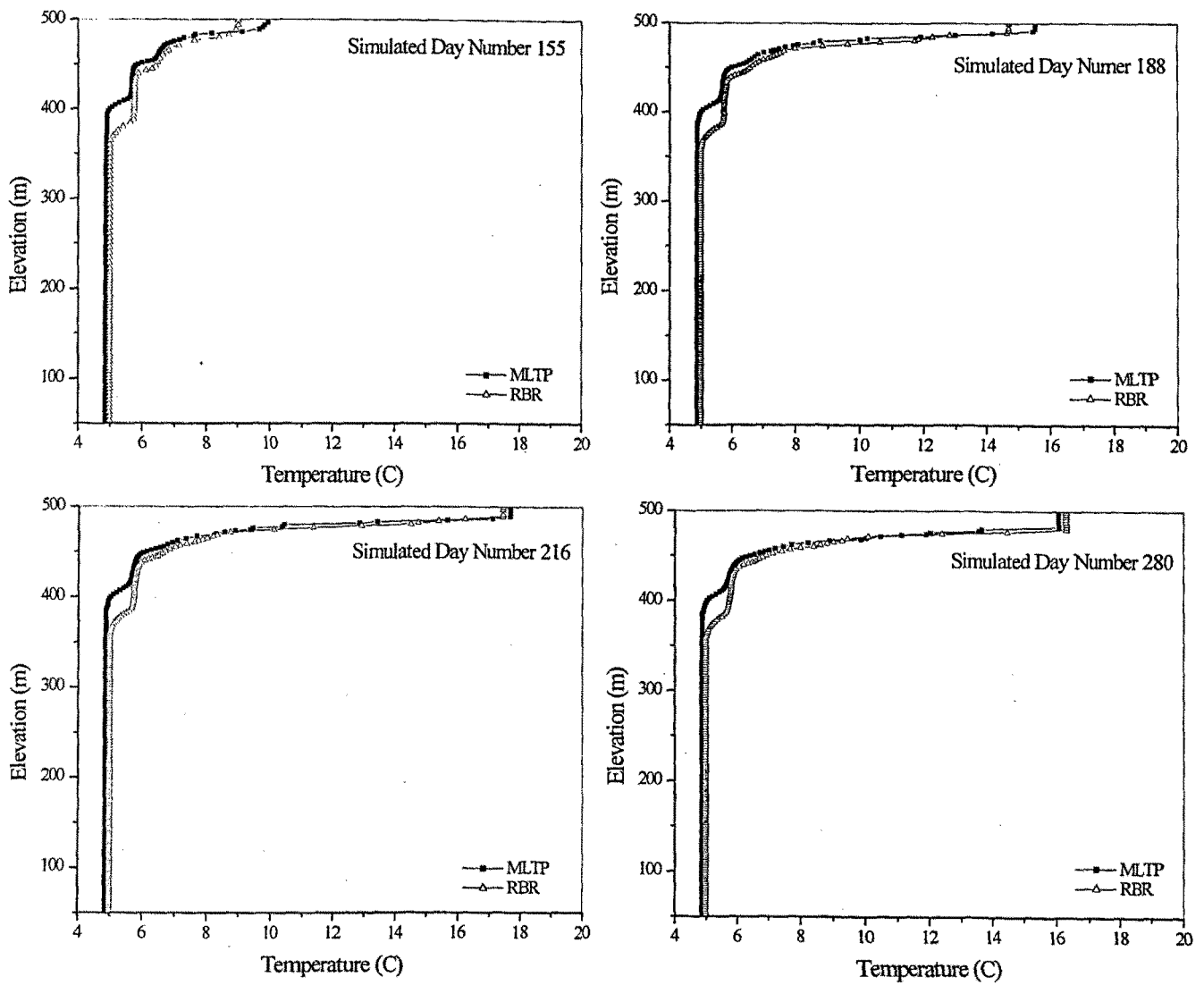
Figure 6.10 Comparison of sensitivity to the initial conditions.

difference between simulations is located at the beginning of the stratification period (between number day 92 and 155), while in space the variability is found at the top layers and between elevations 350 m and 400 m. It is interesting to note that once formed, the thermocline is well protected from the mixing processes and the error is more or less constant. Hypolimnetic temperature differences remain nearly constant over the simulated period. Deep hypolimnetic water is not affected; initial differences remain nearly constant over the simulated period.

6.2.3 Verification

Once the sensitivity of the model has been assessed, the model was run with the 1992 data, using the combination of parameters as discussed above. The light extinction coefficient was set to 0.08 m^{-1}, calculated as the mean averaged over the 14 available Secchi depth measurements. **Figure 6.11.A, B** shows the measured and simulated temperature contour plots. As discussed, compared to the 1999 input data, the uncertainty of available meteorological data for this period is greater; and the resolution of the initial profile is coarser. It can be seen that the model correctly simulates the mean features of the thermal development. Depth of the thermocline is at the right position, as well as the start of stratification. Gradient of temperature also is well simulated, and the deepening of the thermocline occurs at the correct time.

6.2.4 Thermal simulations of some selected scenarios

The model has been run to evaluate the impact on the simulated thermal structure of some hypothesized scenarios using data of the second period (1999-00). Rather that vary each variable within a range, two possible scenarios have been modeled involving the variation of several meteorological parameters at the same time:

Scenario A corresponds to a hypothesized "dry" year. Short wave radiation increases by 10%, air temperature increases by 2 C and precipitation and ambient humidity decrease by 30%.

Scenario B corresponds to a hypothesized "wet" year. Here the short wave radiation is reduced by 10%, the precipitation and relative humidity are increased by 30% and there is a decrease of 2C in the air temperature.

130
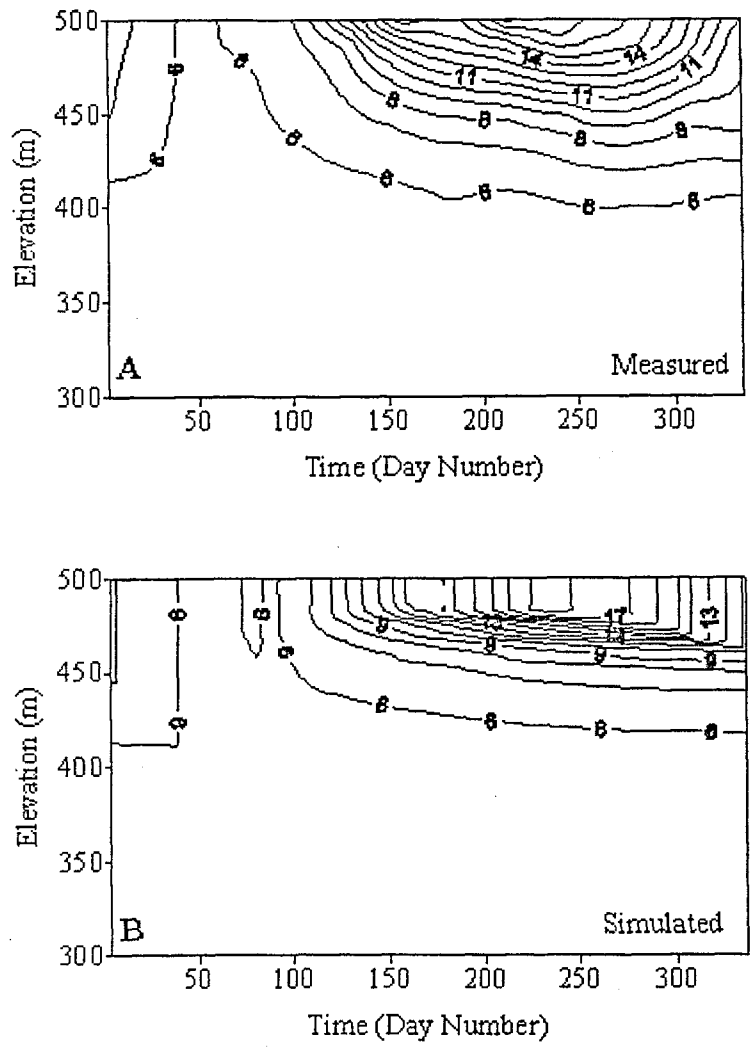
Figure 6.11 Temperature contour plots for 1992, A) measured and B) simulated. Starting day at 1992 January 3rd and last at day 1992 December 1st.

The selected ranges of variation may not be representative of extremely wet or dry years. However, the purpose of this numerical experiment was to check the response of the model's thermal predictions under a range of variability. As the simulations will be compared with the baseline case, it also can be interpreted as the sensitivity of the model to perturbations on the meteorological input data.

In **Fig. 6.12** the resulting temperature profiles has been plotted for the baseline case along with the two simulated cases. It can be seen that the imposed conditions result in a changes of surface temperature of ± 1C around the baseline temperature, warmer for the dry year and colder for the wet year. The variation around the baseline found in the top layers is preserved with depth, although the magnitude declines. The differences are minor during winter and early spring, divergences augment during late spring and summer to diminish with the end of the stratification. The depth of the mixer layer is also slightly deeper though Julian days 280 to 308 for the dry year; while the water column is almost isothermal by Julian day 384, some potential energy is still stored for the dry year case at the same day. For the three cases analyzed, the structure is nearly isothermal by Julian day 432, with the predicted final temperature of the dry year is slightly higher that of the cold year. However, is interesting to note that both the time of the onset of the stratification as well as the time of the erosion of the thermocline remains unaffected by the variability of the input. While some differences were found in the stratification, all simulations converge to the same final condition.
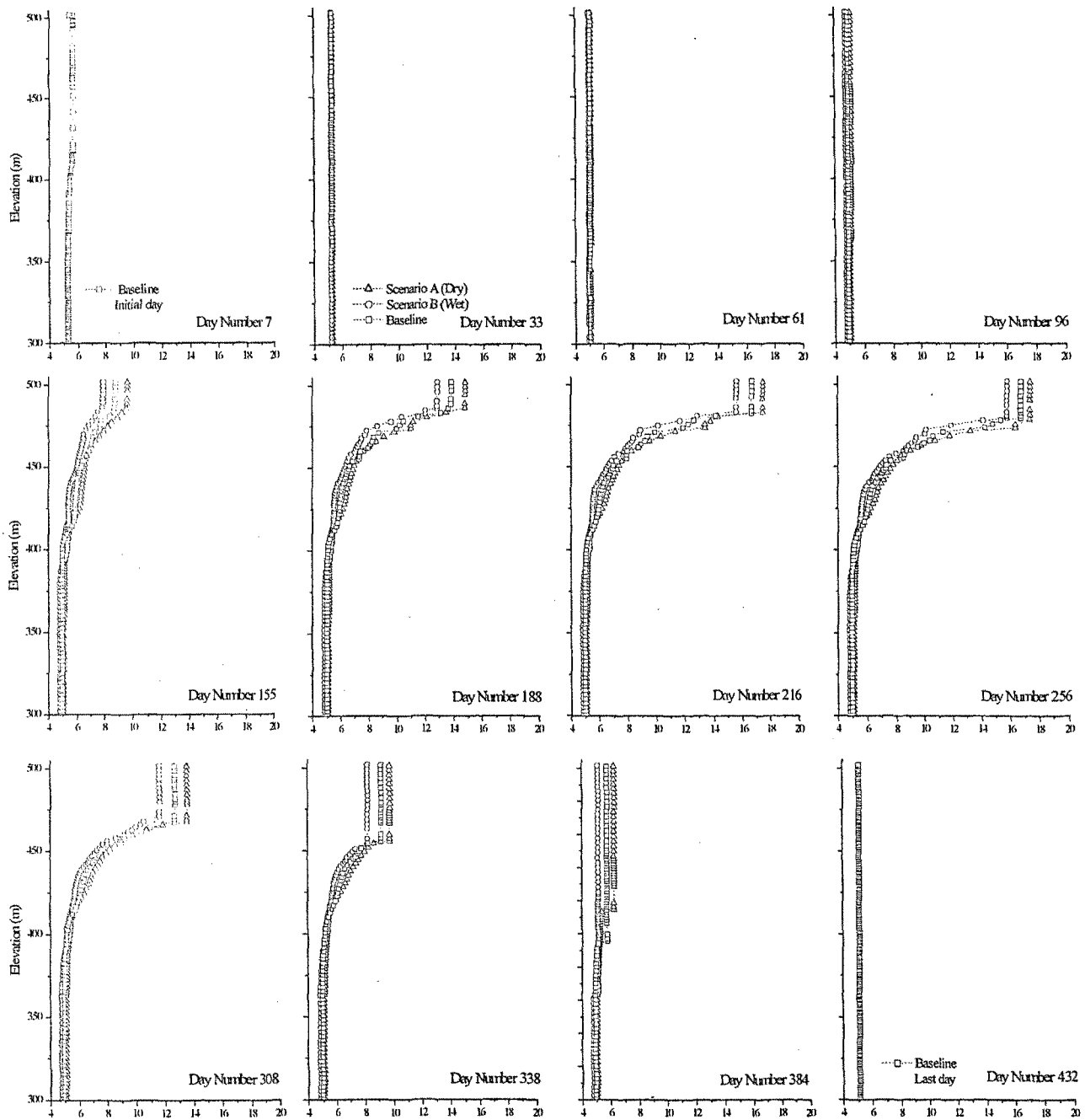
Figure 6.12 Temperature profiles of the hypothesized scenarios and the baseline case.

133

6.3 Water Quality Sub-Model Parameters Sensitivity Analysis

The sensitivity of model results to changed values of the calibration parameters was quantified with reference to a set of Water Quality state variables. The water quality state variables selected were Chla, SRP, POP, RP, PON, NH4, NO3, and DON. Only the results for Chla, NH4 and SRP are presented below. Plots for the other state variables are in **Appendix A**. The model sensitivity was performed following the procedure described in Schladow and Hamilton (1997). All but one of the adjustable parameters were fixed at the best estimate of the range given in **Table 6.3**. The model was then run twice for the calibration period, with the outstanding adjustable parameter set firstly to the minimum of its assigned range and secondly to the maximum of its assigned range. This process was repeated for each parameter in turn. The sensitivity analysis was performed over the year 1992 and the year 1999, using the pre-calibrated model's parameters for year 1999. In the figures presented below, only the 1999 results are shown. The 1992 results are included in **Appendix B**.

Three measures of sensitivity were used in interpreting the model output. These were designed to test for changes in mean concentration over the whole water column, changes in the vertical distribution, and changes in the temporal distribution of the selected WQ state variables.

6.3.1 Changes in Mean Concentration Distribution

To estimate changes in mean concentrations in the water column, the mean depth-averaged concentrations of the WQ state variables were calculated at every model time step (180 min.), and the maximum, minimum and mean values were recorded for each time step. From this set of values, the means of the maxima, minima, and the means were calculated and plotted. The results for 1999 are shown in the box plots of **Fig. 6.13** and in **Appendix A**. The histograms that display the greatest divergence (both high and low) indicate those parameters for which the state variable is most sensitive. For example, parameters for which Chla was highly sensitive (represented in the upper plots of **Fig. 6.13**) are those that directly alter growth rates, that is, the maximum growth ratio (1), maximum respiratory rate (2), the light saturation (4) and

Table 6.3 Model parameters implemented in the DLM-WQ. The ranges are estimates for composite phytoplankton ensembles. Asterisk (*) indicated that this parameter was not used by this version of the model. Value represents the selected value of each parameter in the sensitivity study.

#	Parameter	Symbol	Range Min/Max	Value	Units	Ref.
	Algae					
1	Maximum growth rate	G_{max}	1.0-2.5	1.2	d^{-1}	1
2	Maximum respiratory rate	k_r	0.05-0.20 (Including mortality)	0.15	d^{-1}	2
*	Maximum mortality rate	k_m	0.003-0.17	0.0	d^{-1}	3
3	Temperature multiplier for growth/respiration/death	θ	1.0-1.14	1.08	n. d.	4
4	Light saturation	I_s	50-500	75.0	$\mu E\,m^{-2}\,s^{-1}$	5
	Nutrient utilization					
5	Phosphorus to chlorophyll mass ratio	a_p	0.3-1.0	0.5	n. d.	6
6	Nitrogen to chlorophyll mass ratio	a_n	5.0-15.0	7.0	n. d.	6
	Settling					
7	Setting velocity for phytoplankton	v_s	0.1-1.0	0.5	$m\,d^{-1}$	7,8
8	Setting velocity for detritus POP & PON	v_{det}	0.1-2.0	0.2	$m\,d^{-1}$	9
9	Phytoplankton transfer function	T_{phy}	290000± 50%	290000	# (μgChla^{-1})	10
10	POP and PON transfer function	T_{part}	8100± 50%	8100	#(μgChla^{-1})	11
	Chemical reactions					
*	Biological oxygen demand of sub-euphotic sediments	k_{bio}	0.02-15.0	0.02	$mg\,m^{-2}\,d^{-1}$	12
*	Decomposition rate of BOD	k_{bod}	0.005-0.05	0.005	d^{-1}	12
*	Half saturation constant efficiency of DO on de-nitrification	k_{den}	0.01± 50%	0.01	$G\,m^{-3}$	13
11	PON ==> NH4	k_{n1}	0.001-0.1	0.01	d^{-1}	13
12	PON ==> DON	k_{n2}	0.02 ± 50%	0.02	d^{-1}	13
13	DON ==> NH4	k_{n3}	0.02 ± 50%	0.02	d^{-1}	13
14	NH4 ==> NO3	k_{n4}	0.10-0.20	0.15	d^{-1}	14
15	NO3 ==> N2	k_{n5}	0.1 ± 50%	0.10	d^{-1}	14
16	POP ==> SRP	k_{p1}	0.001-0.8	0.04	d^{-1}	14
17	POP ==> RP	k_{p2}	0.001-0.8	0.05	d^{-1}	14
18	RP ==> SRP	k_{p3}	0.01-0.100	0.02	d^{-1}	15
19	Half saturation constant for N nutrient limitation	$k_{(NO3+NH4)}$	3± 50%	3	$\mu g l^{-1}$	16
20	Half saturation constant for P nutrient limitation	k_{SRP}	1-5	1	$\mu g l^{-1}$	15

Table 6.3 Continued

21	Half saturation constant for Ammonia preferential uptake factor	k_{NH4}	20.0-120.0	25.0	$\mu g l^{-1}$	17
*	Half saturation constant for limitation of reactions by DO for nitrification	k_{nit}	0.5 or 2	2.0	$ml_{O2} l^{-1}$	12
*	Half saturation constant for limitation of reactions by DO for biochemical oxygen demand	k_{do}	0.5 ± 50%	0.5	$ml_{O2} l^{-1}$	12
*	Half saturation constant for limitation of reactions by DO for sediment processes	k_{sdo}	3.0 ± 50%	3.0	$ml_{O2} l^{-1}$	12
*	Density of BOD for settling	ρ_{BOD}	1040 ± 25%	1040	Kgm^{-3}	12
Nutrient temperature multipliers						
22	Nitrification	θ_{NO}	1.02-1.14	1.08	n. d.	18
23	Organic decomposition	θ_o	1.02-1.14	1.08	n. d.	18
24	Biological and chemical sediment oxygen demand	θ_{BOD}	1.02-1.14	1.08	n. d.	12
Sediment Fluxes						
25	Release rate of phosphorus SRP	r_{SRP}	0.0-0.05 0.005± 50%	0.0001	$\mu g\ m^{-2}\ d^{-1}$	12
26	Release rate of nitrogen NH4	r_{NH4}	0.0-0.05 0.05± 50%	0.0001	$\mu g\ m^{-2}\ d^{-1}$	12
27	Temperature multiplier for sediment nutrient release	θ_S	1.02-1.14	1.08	n. d.	12
Zooplankton parameters						
28	Zoo feeding rate on Chlorophyll	k_z	0.03± 50%	0.03	$\mu gChla\ l^{-1}$	11
Particles						
29	Density of 7 particle size groups	ρ	1040± 25%	1040	Kgm^{-3}	12

1) Bowie et al. (1985) Table 6-5, 2) Bowie et al. (1985) Table 6-18, 3) Bowie et al. (1985) Table 6-20, 4) Chapra (1997) Fig-2.11, 5) Chapra (1997), 6) Bowie et al. (1985) Table 6-4, 7) Marjanovic (1989) Table-16, pg. 326, 8) Jassby (per. com.), 9) Bowie et al. (1985) Table 6-19, 10) Hunter et al.(1990), 11) Hunter, per. Comm., 12) Schladow & Hamilton (1997), 13) Bowie et al. (1985) Table 5-3, 14) Bowie et al. (1985) Table 5-4, 15) Eppley et al. (1969), 16) Chapra (1997) Table 33.1, 17) Bowie et al. (1985) Table 5-5, 18) Chapra (1997) p 40.
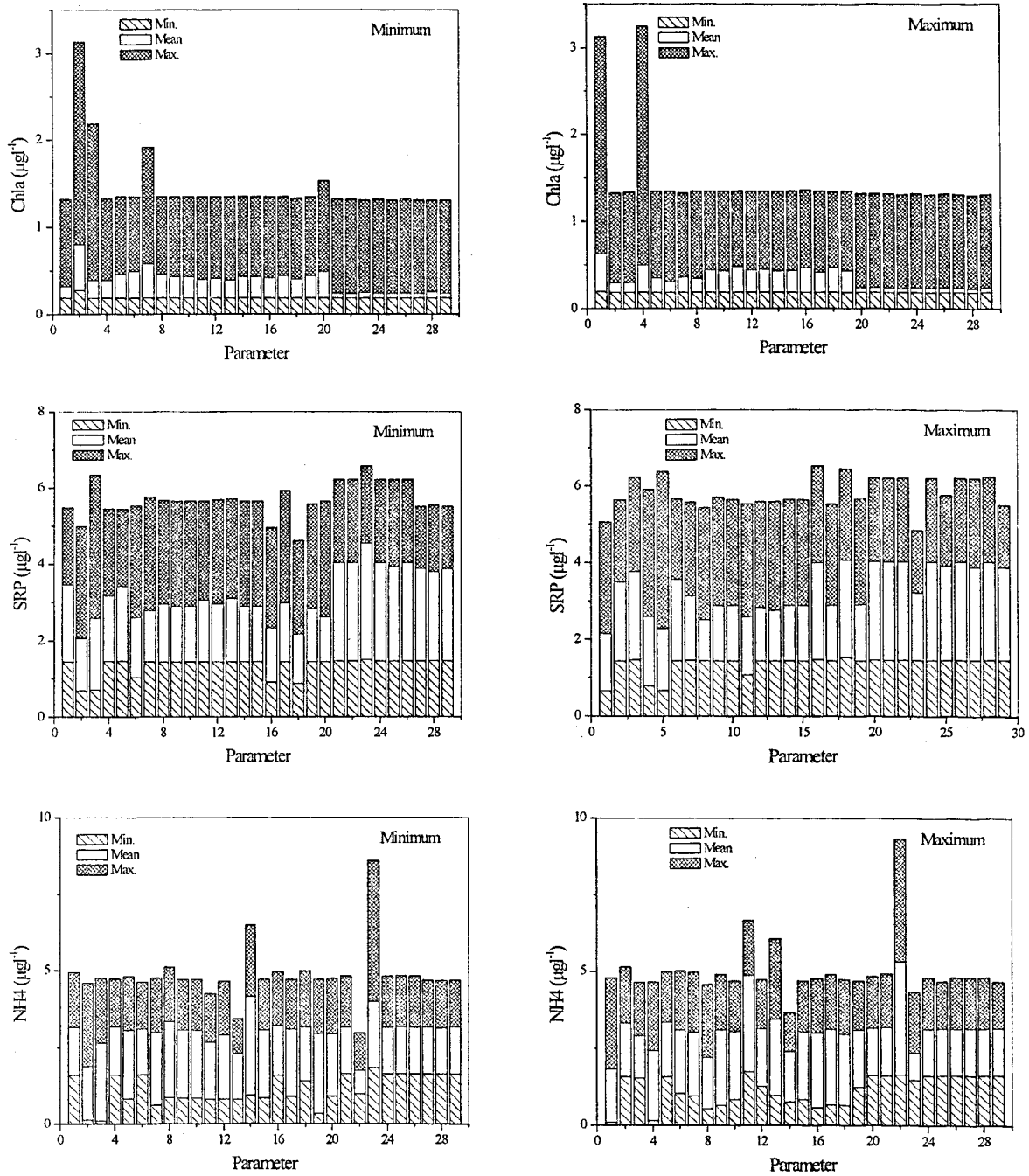
Figure 6.13 Minimum, maximum and mean differences between maximum and minimum value parameter of the depth-averaged daily concentrations of Chla, NH4 and SRP for 1999 (see **Appendix A** for the whole set of variables).

the setting velocity (7) or indirectly affect growth rates through their ability to take up or utilize phosphorus. This latter group includes the rate coefficient from POP to SRP (16) and the half saturation constant for P limitation (20).

6.3.2 Changes in Vertical Distribution

Changes in vertical distribution were measured by examining variations in the WQ state variables with depth. For each model timestep, the mean of the water quality variable and its standard deviation were calculated and the ratio of the standard deviation to the mean was calculated. The maximum value of this ratio was recorded and plotted, with each bar of the histograms being a different parameter. The minimum values are not plotted, as they were all zero corresponding to times when the water column was homogeneous, as seen in **Fig. 6.14** For example, the vertical Chla distribution is dominated by the temperature multiplier (3), widen the distribution with the upper values.

6.3.3 Changes in Temporal Distribution

Sensitivity of the temporal distribution of WQ state variables to changes in the various parameters was quantified from the distribution of the depth-averaged concentrations over the mixing depth and over the simulation period. The time since the start of the simulation when the center of this distribution (first moment) and one standard deviation on either side of this distribution (second moment) were attained was calculated and recorded. As seen in **Fig. 6.15** and in **Table 6.4**, only a few parameters have an effect on the temporal distribution of any of the control variables. For example, Chla distributions are affected by the phytoplankton setting velocity (7), with the value at the lower end of the range advancing the initiation of the spring bloom while the value at the upper end of the range delays the onset of the spring bloom by about 50 days.

138

Table 6.4 Sensitive model parameters with respect to mean concentration, vertical distribution and temporal distributions of the water quality control variables for year 1992 and year 1999, integrated over the mixing depth. Numbers are defined in Table 6.3.

WQ Estate Variable	Mean Concentration 1992	Mean Concentration 1999	Vertical Distribution 1992	Vertical Distribution 1999	Temporal Distribution 1992	Temporal Distribution 1999
Chla	2,4,7,16,20	1,2,4,7	1,2,3,4,6	3,25	7	1,2,3,4,7
NO3	1,2,3,4,11,23	1,2,3,11,20	4,6,12,19	1,2,3,4,5,11,20	1,2,7,20	1,2,4,11
NH4	1,2,3,4,13,22,23	2,11,13,8,22	3,4,12,19,22	1,2,3,11,19	23	2,8,13,23
DON	8,13,23	8,13,23	2,3,4,6,8,17,1 8,23,25,27,28	2,3,4,6,8,17,1 8,23,25,27,28	3,13,23	3,13,23
PON	1,3,7,8,11,12	1,3,7,8,11,20	11,23,28	2,3,23,25,27	None	2,8
SRP	1,2,3,4,5,6,7,16, 18,23	1,18,23	3,5,6,7,11,12, 13,16,17,18,2 3	5,11	2	6,16
POP	3,7,8,16,17,23	1,3,7,8,16,17,23	16,17	3,4,9,11,17,23 ,27	None	1,2,3,4
RP	3,17,18,23	3,16,17,18,23	12,23	2,3,4,17,18,23 25,27,28	16,17,18	3,16,17,18,23

139

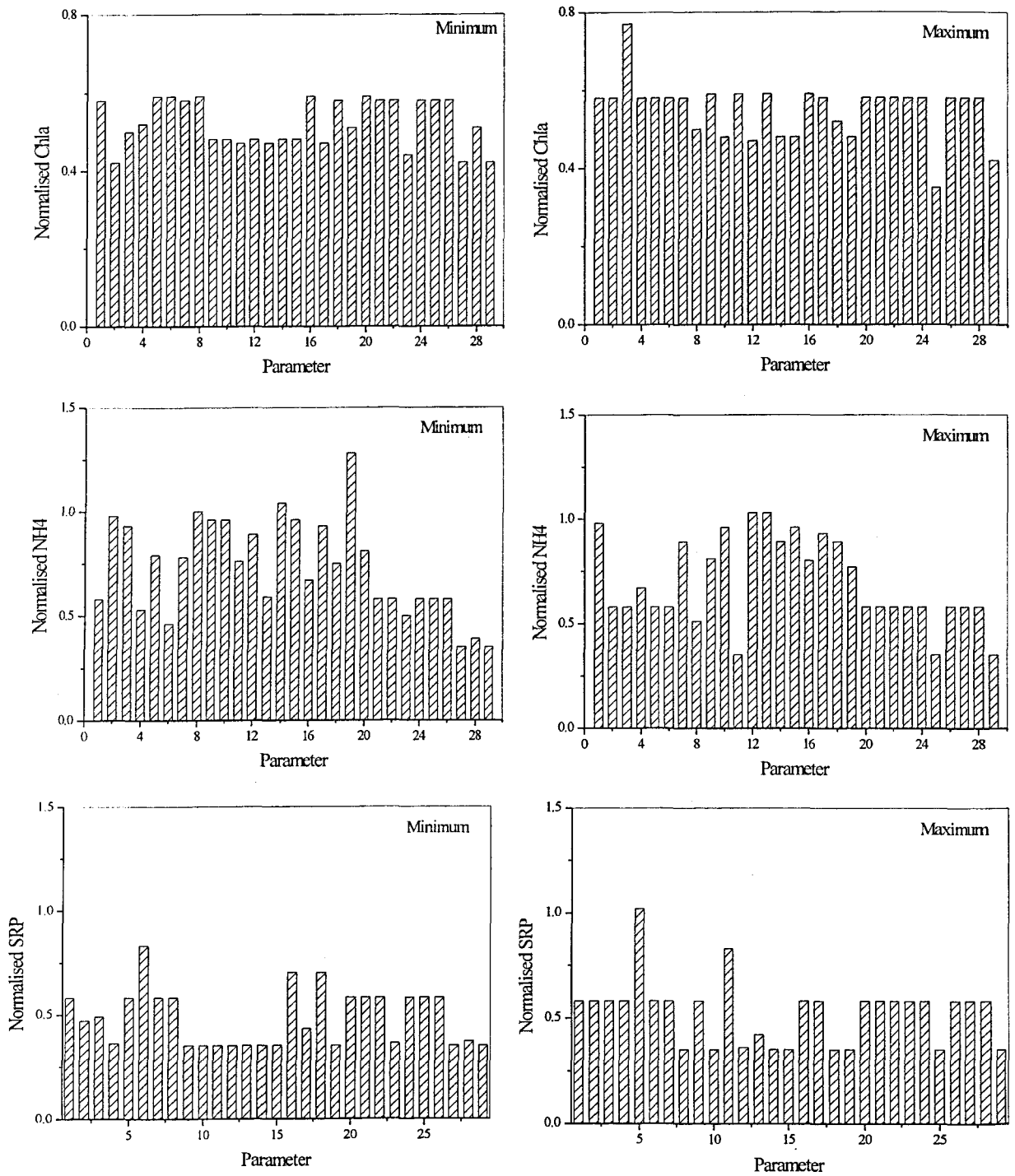**Figure 6.14** Maximum of the standard deviation normalized by the mean daily concentration over the water column for Chla, NH4 and SRP for 1999 (see **Appendix A** for the complete set of plots).
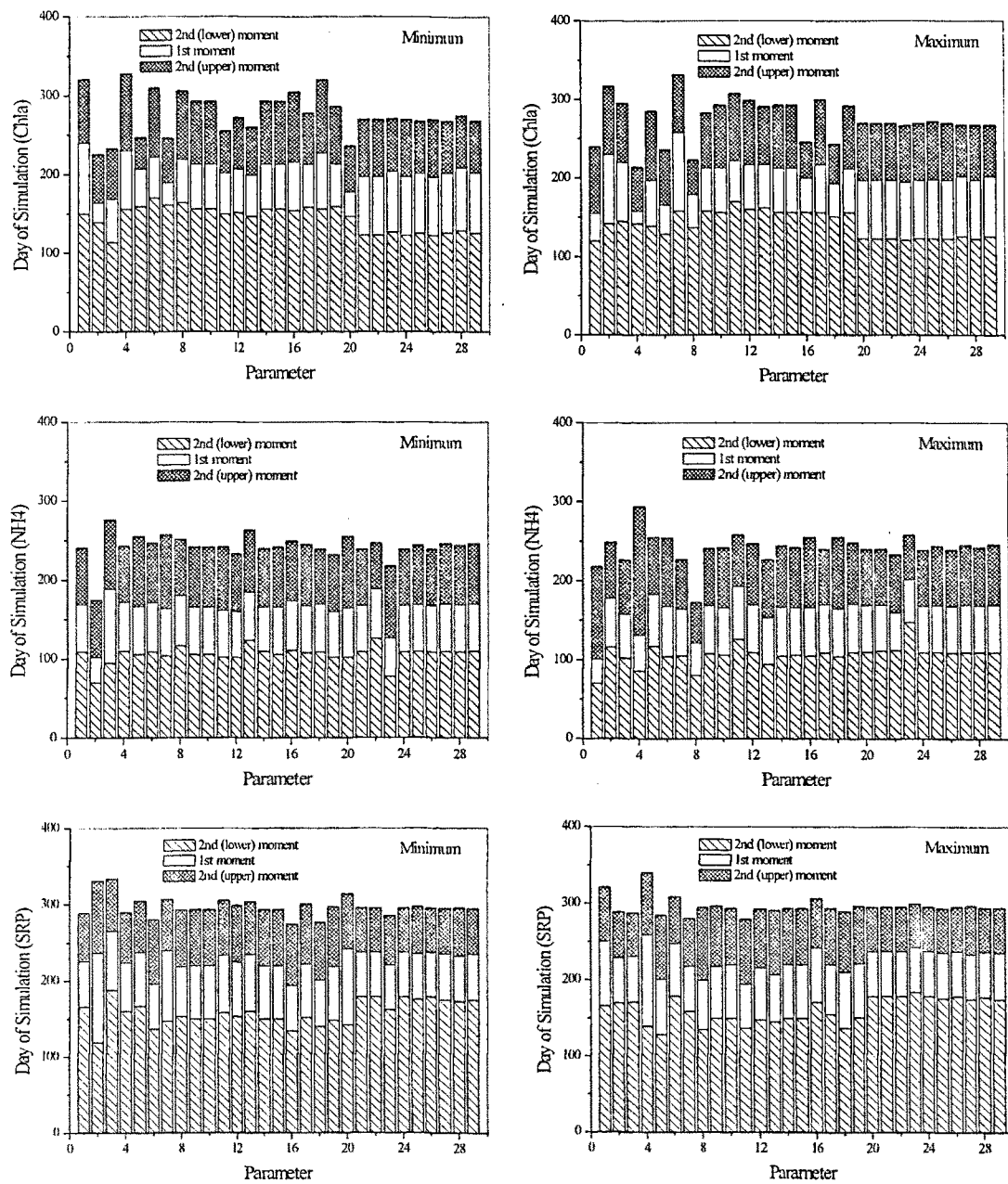
140

Figure 6.15 First moment (mean) and second moment (mean ± standard deviation) of the temporal distribution of daily, depth averaged Chla, NH4 and SRP concentrations for 1999. See **Appendix A** for the complete set of plots.

6.3.4 Summary of Sensitivity Analysis for Water Quality Sub-Model Parameters

The parameters to which the selected water quality state variables appeared to be most sensitive in both 1992 and 1999 are summarized in **Table 6.5**. **Figure 16 A-D** plots the frequency with which each parameter affects a water quality state variable in both 1992 and 1999. This way of displaying the sensitivity information, albeit prone to a degree of subjectivity, provides a clear picture of the impact of each parameter in the whole model formulation. Parameters that contribute for the 2 years with a frequency of more than 2 times are related to the phytoplankton dynamics (1,2,3,4,6,7): the maximum growth (G_{max}), the maximum respiratory rate (k_r), the temperature multiplier (θ), the light saturation (I_s), the Nitrogen to Chla mass ratio (a_n), and the setting velocity (v_s).

Within the range tested, the model is insensitive to the phytoplankton transfer function (9) and the POP and PON transfer function (10) transfer functions that determine the number of particles in the water column. The model is also insensitive to changes in the particle density ρ (10). As expected under well-oxygenated conditions, any change on the de-nitrification parameter k_{n5} (15) has no impact. Any change on the nitrification rate coefficient k_{n4} (14) yields no effect on any of the tested sensitivity measures. This may be due to the fact that available NH4 is either rapidly consumed or transformed into NO3. The anomalously high concentration of NO3 may indicate that the pre-calibrated selected rate is too high or that even if set to the correct range, a co-lateral effect is not detected. Sediment dynamics parameters r_{SRP}, r_{NH4}, θ_S, k_z (25,26,27,28) either weakly or negligibly contribute to the model sensitivity.

Clearly, the model is very sensitive to the temperature through the temperature multipliers for algae (3) and the nutrient cycles (24). The fact that the Chla and Nutrient (including particulate matter) are strongly dependent on the temperature highlights the need of an accurate thermal description of the lake, including the mixing processes. It also suggests that this effect may be peculiar to Alpine lakes where water temperatures are generally low. In the earlier use of this water quality

142

sub-model for a temperate reservoir (Hamilton and Schladow, 1997) the effect of temperature on water quality was minimal. This may also suggest that Alpine lakes may be highly sensitive to the effects of global climate change.

It is interesting to note that in all cases except for parameters T_{phy} (9) and k_{n2} (12) of the sensitive parameters, both 1992 and 1999 show a response. As these two years represent very different conditions, this concordance may reinforce the strength of conclusions.

Exploring only two values (the lower and upper) within the range of variation does not allow determining the local sensitivity of each parameter. A one at a time sensitivity procedure cannot evaluate the possible non-linear effects induced by simultaneous changes of several parameters. However, rather than quantifying the exact contribution of each parameter, the aim of the procedure was to determine qualitatively the relative contribution of each parameter spatially and temporally. As a result of the analysis, it is now possible to refine the focus of the calibration, reducing the number of parameters that need to be adjusted.

Table 6.5 Parameters to which the model is sensitive for 1992 and 1999.

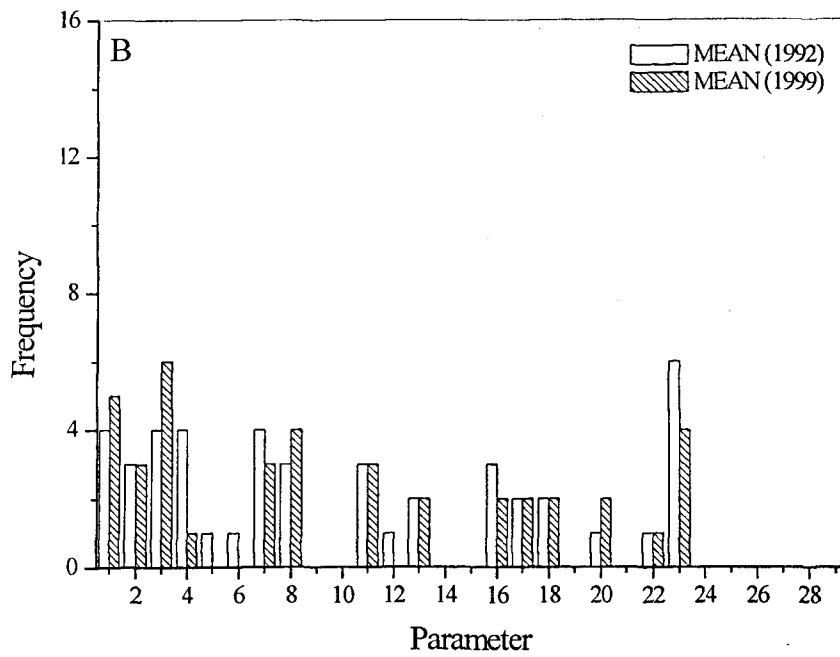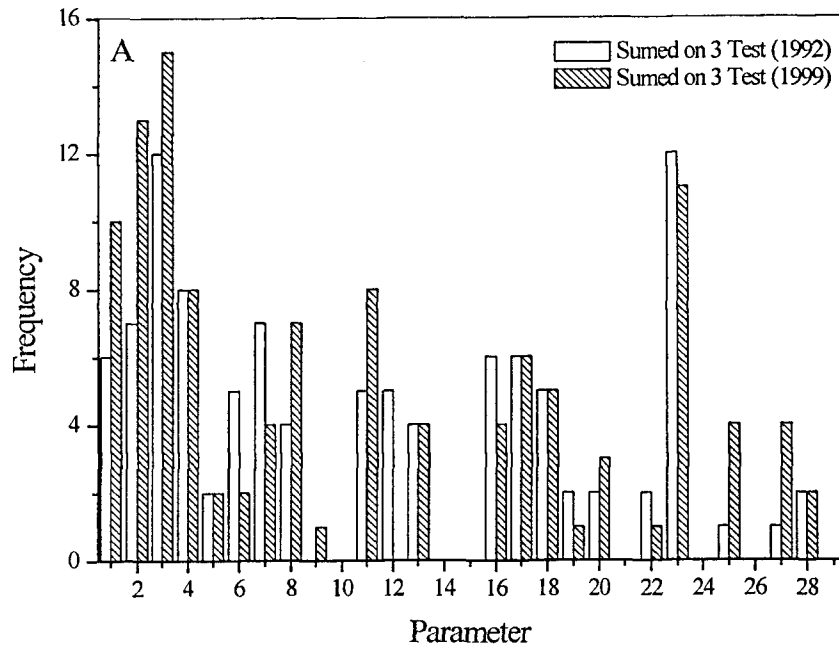| WQ State variable	Mean Concentration	Vertical Distribution	Temporal Distribution
Chla	2,4,7	3	7
NO3	1,2,3,11	4	2
NH4	2,13,22	3,19	23
DON	8,13,23	2,3,4,6,17,23,25,27,28	3,13,23
PON	1,3,7,8,11	23	None
SRP	1,18,23	5,11	None
POP	3,7,8,16,17,23	17	None
RP	3,17,18,23	23	16,17,18

Figure 6.16 Plot of the frequency of the most sensitive parameters for 1992 and 1999 to any of the control variables: A) the sum of all, B) mean, C) vertical, and D) time.
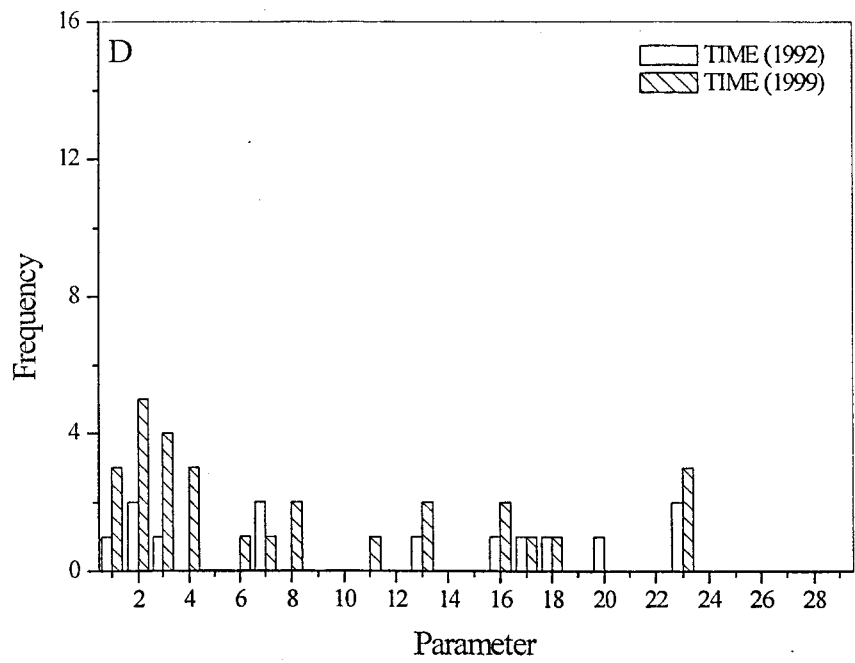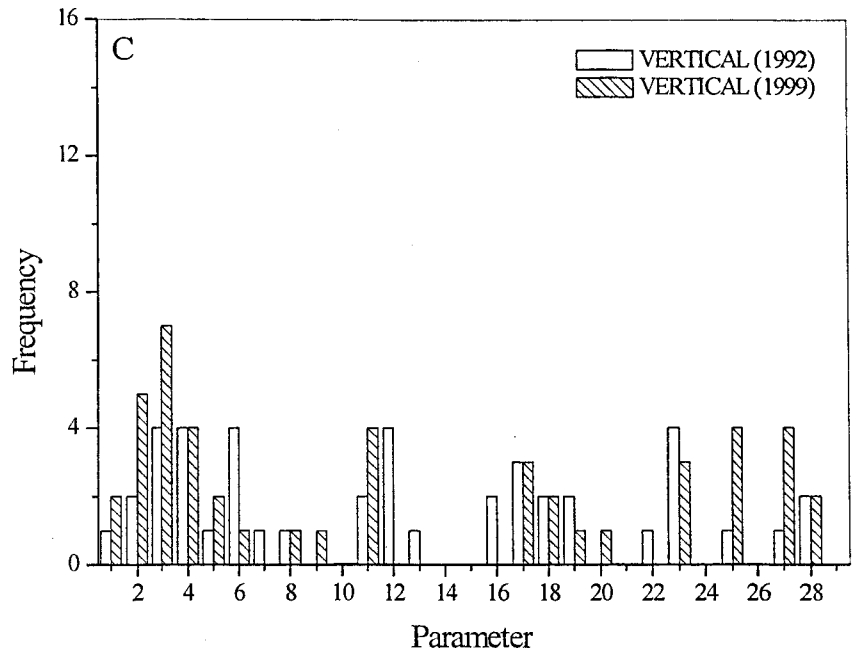
Figure 6.16 Continued.

145

6.4 Water Quality Sub-Model Forcing Parameters Sensitivity Analysis

These parameters include the assumptions made in defining the input fluxes to the model and the initial conditions. The sensitivity analysis of the model forcing parameters was performed with the same methodology used to test the sensitivity of the model parameters. Thus a one at a time methodology was used in that each parameter was set to its lowest and highest value, leaving unchanged the rest of parameters, and the statistical indicators of the selected WQ state variables defined in **Section 6.3** were calculated within the mixing depth. Taking the same approach permits the establishment of a common base for comparison. The chosen range of variation reflects the expected uncertainty of each parameter, with a higher variability indicating that the procedure for determining the values of the parameters is not well known (i. e. literature references of similar cases, preliminarily measurements, low confidence estimates). Through this sensitivity experiment, only Chla was used as a control variable because many of the parameters represent inputs of nutrients by different ways (air-water interface, ground water). The presented results are for 1999 only. Although 1992 is also sensitive to the imposed variations, it does not show such clear trends. **Table 6.6** shows the model forcing parameters and the selected ranges of variation.

6.4.1 Atmospheric

The variability of the tested parameters on the minimum and mean values of Chla concentration is negligible. The maximum is noticeably affected by P-species. Wet and dry deposition of RP set to the minimum (-50%) and SRP and POP set to the maximum (+50%) changed the maximum of the mean, depth-averaged concentrations of Chla in the mixing depth. **Figure 6.17 A, B** shows the changes in Chla concentration. The perturbation of the deposition rates of POP and SRP are correlated with changes in vertical distribution of Chla (see **Fig. 6.17 C, D**). The upper moment of the temporal distribution of Chla was slightly sensitive to changes in POP dry deposition rate, while the lower and mean were unaffected for all the parameters. **Figure 6.17 E, F** shows the changes in the temporal distribution of Chla. The

146

Table 6.6 Model forcing parameters and ranges for the sensitivity analysis.

#	Description	Value	Units	Ref.
	Atmospheric Deposition Nutrient Fluxes			
1	DON_DRY	686.56 ± 50%	$\mu g\ m^{-2}\ d^{-1}$	1
2	NH4_DRY	109.2 ± 50%	$\mu g\ m^{-2}\ d^{-1}$	1
3	NO3_DRY	266 ± 50%	$\mu g\ m^{-2}\ d^{-1}$	1
4	SRP_DRY	12.08 ± 50%	$\mu g\ m^{-2}\ d^{-1}$	2
5	POP_DRY	16.57 ± 50%	$\mu g\ m^{-2}\ d^{-1}$	2
6	RP_DRY	16.57 ± 50%	$\mu g\ m^{-2}\ d^{-1}$	2
7	DON_WET	648.2 ± 50%	$\mu g\ m^{-2}\ d^{-1}$	1
8	NH4_WET	224 ± 50%	$\mu g\ m^{-2}\ d^{-1}$	1
9	NO3_WET	103.6 ± 50%	$\mu g\ m^{-2}\ d^{-1}$	1
10	SRP_WET	28.80 ± 50%	$\mu g\ m^{-2}\ d^{-1}$	2
11	POP_WET	7.59 ± 50%	$\mu g\ m^{-2}\ d^{-1}$	2
12	RP_WET	7.59 ± 50%	$\mu g\ m^{-2}\ d^{-1}$	2
	Streams inflows			
1	PON, DON stream nutrient fractions: ON = f1*DON + f2*PON	0.50 (f1)	n. d.	2
		0.50 (f2) ± 75%	n. d.	2
2	POP, DOP Stream fractions PP = f1*RP + f2*POP	0.7(f1)	n. d.	2
		0.3(f2) ± 75%	n. d.	2
3	Gaussian temperature distribution for streams	Temp ± 50%	Deg. C	3
4	Estimated direct runoff flow factor: Factor x Stream flow	0.117 ± 75%	n. d.	4
5	Nutrient Load Factor [Nutrient]= f3*[Nutrient]	1 ± 50%	n. d.	5

Table 6.6 continued

Ground water				
1	Ground Budget	592 (1999)	10^6 x m^3	4
		164 (1992)	10^6 x m^3	4
		± 75%		
2	Estimated ground water flow factor: Factor x Stream flow	0.114 ± 75%	n. d.	6
3	Ground total Nitrogen concentration	1000 ± 50%	Kg/year	6
4	Ground total Phosphorus concentration	74 ± 50%	Kg/year	6
5	Fraction of SRP	0.58 ± 50%	n. d.	6
6	Fraction of RP	0.42 ± 50%	n. d.	6
7	Fraction of NO3	0.85 ± 50%	n. d.	6
8	Fraction of NH4	0.05 ± 50%	n. d.	6
9	Fraction of DON	0.10 ± 50%	n. d.	6
Initial conditions				
	Nutrient profiles factors:			
1	DON = f1 x ON	0.834 (f1)	n. d.	4
	PON = f2 x ON-PhyN	0.166 (f2) ± 50%	n. d.	4
2	Particle profiles fraction Inorganic/Organic	0.3/0.7 rule ± 50%	n. d.	2, 7
3	Fraction of P and N excreted from zooplankton that goes onto POP and PON in the daily vertical migration	0.5/0.5 ± 50%	n. d.	8
4	Amplitude of diel vertical migration of Mysis	150 ± 50%	m	8
5	Diameter minimum of the range of particle size distribution in a Log scale	0.5 ± 50%	µm	7
6	Diameter maximum of the range of particle size distribution in Log scale	5 ± 50%	µm	7

1) Jassby et al. (1994), 2) Reuter (pers. comm.), 3) Fitted from TRG data, 4) Marjanovic (1989), 5) Schladow (pers. comm.), 6) Thodal (1997), 7) Swift (pers. comm.), 8) Jassby (pers. comm.)
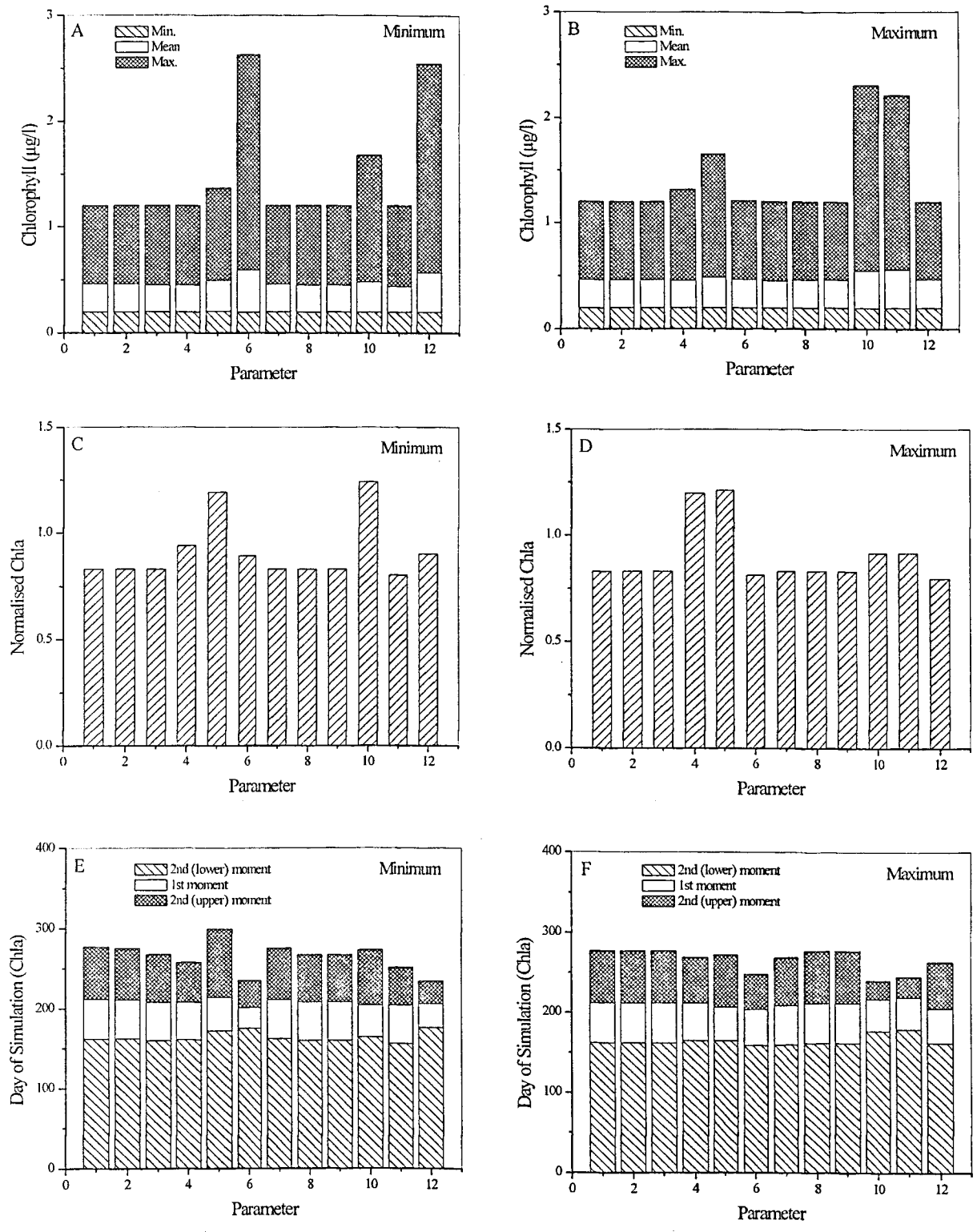
Figure 6.17 Variability in mean concentration (A, B), vertical (C, D), and temporal (E, F) distribution of Chlorophyll induced by atmospheric parameters, numbered according to **Table 6.6**.

evaluation of the sensitivity of the dry and wet deposition is also linked to the frequency of days with rain and this is linked to the meteorology.

6.4.2 Stream Flow

The maximum, mean averaged Chla concentration is clearly affected by both the lower and upper values of the stream run-off factor and the temperature of the streams. Direct run-off was modeled as an independent stream to the lake. Setting the run-off factor to its lower value results in an increase in the maximum value of the mean Chla due to less dilution. It is interesting to note that while the modeled thermal stratification is insensitive to the inflow temperature, the Chla distribution does respond; however, this sensitivity may be artificially induced by the way the streams are input to the lake (without any horizontal resolution) and may indicate that the 1-D assumptions may be not totally valid. Most of the tested parameters affect the vertical distribution of Chla (see **Fig 6.18 A, B**). The temporal distribution of Chla was insensitive to changes in any of the parameter (see **Fig. 6.18 C, D**), with only a slight effect of the runoff over the time of maximum occurrence (see **Fig. 6.18 E, F**).

6.4.3 Ground Water

The minimum and mean of the mean averaged Chla are not affected by any of the tested parameters (see **Fig, 6.19 A, B**); Total Nitrogen Mass, RP and SRP made changes on the maximum values of the depth mean Chla concentration. The vertical distribution of Chla is affected again by the P-species in their tested ranges (see **Fig. 6.19 C, D**). In reference to changes in time, setting P species (Total Phosphorous Mass, RP, and SRP) to their minimum values slightly advances (~25 days) the occurrence of the maximum values of Chla, while the opposite effect occurs when these parameters are set to their upper bounds (see **Fig. 6.19 E, F**). When discussing the presented results, this fact must be kept in hand, as the sensitivity could be a result of the model configuration not totally independent of the implemented formulation of the ground water to the nutrient budget that may be too simplistic.

6.4.4 Initial Conditions

Only the PON factor affects weakly the maximum mean concentration, in both tested values, while none of the parameters have any effect over the Chla distribution (see **Fig. 6.20 A, B**). The vertical and temporal distributions of Chla remain unchanged.

150

Figure 6.18 Variability in mean concentration (A, B), vertical (C, D), and temporal (E, F) distribution of Chla induced by stream flow, numbered according to **Table 6.6**.

Figure 6.19 Variability in mean concentration (A, B), vertical (C, D), and temporal (E, F) distribution of Chla induced by ground water, numbered according to **Table 6.6**.

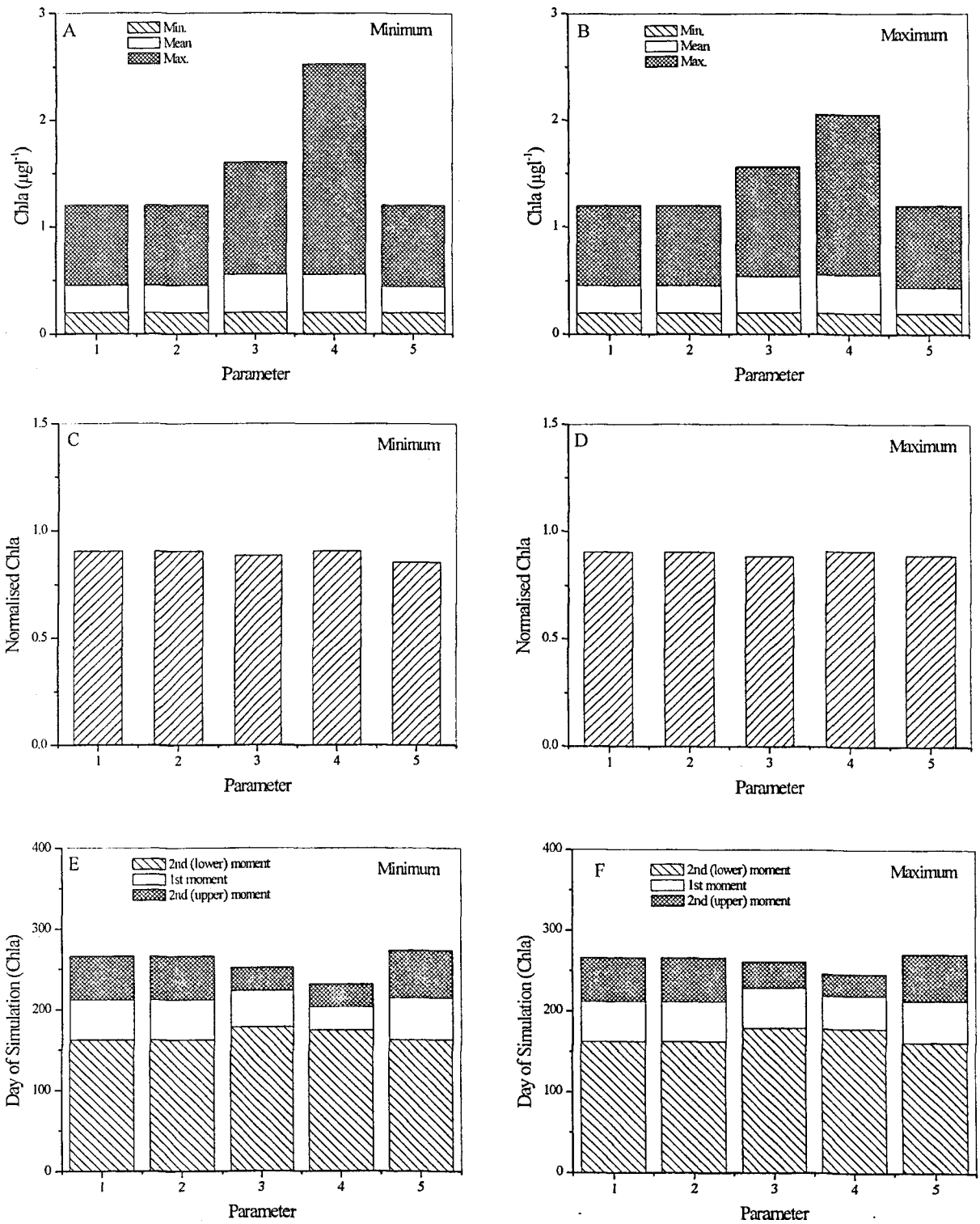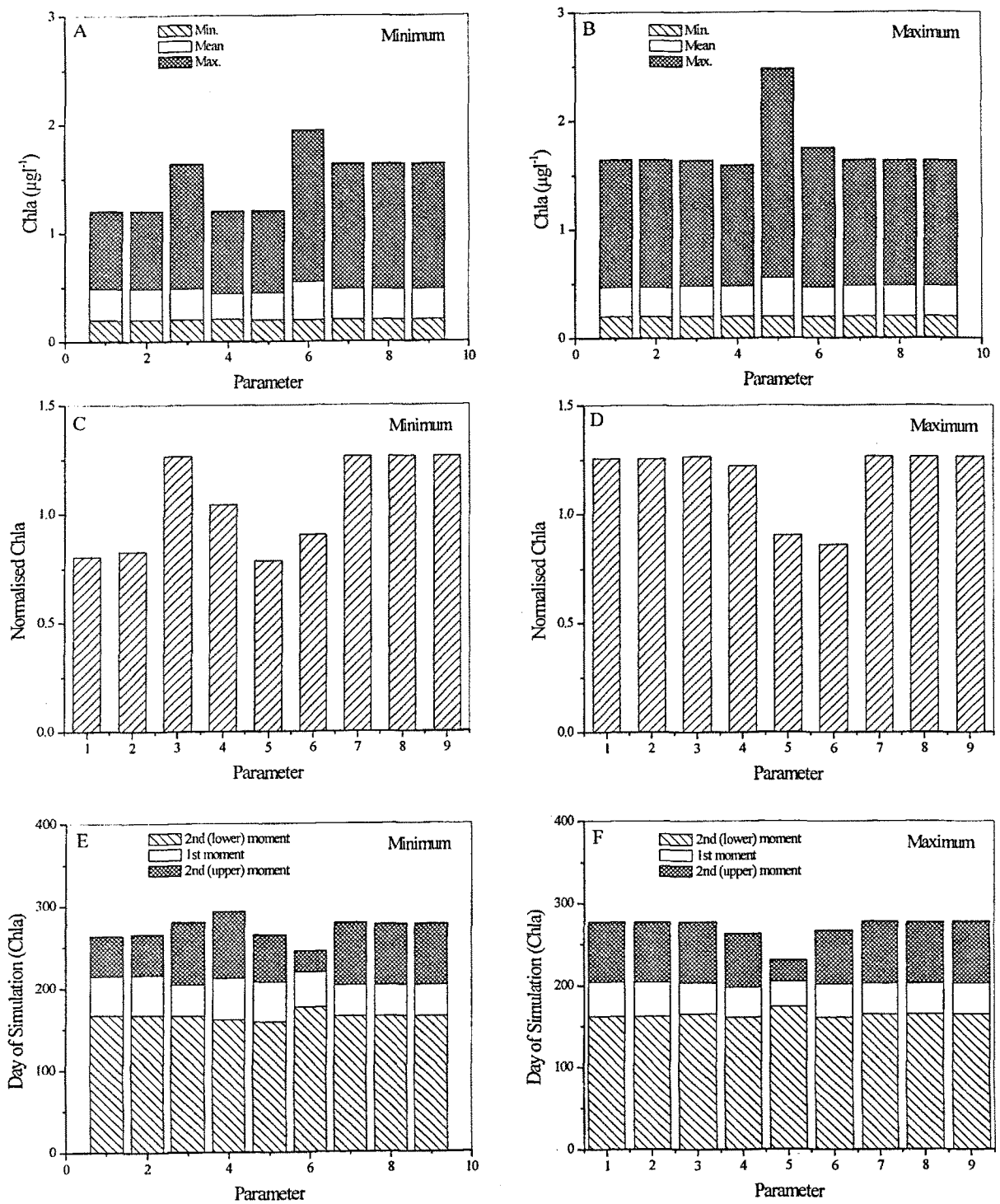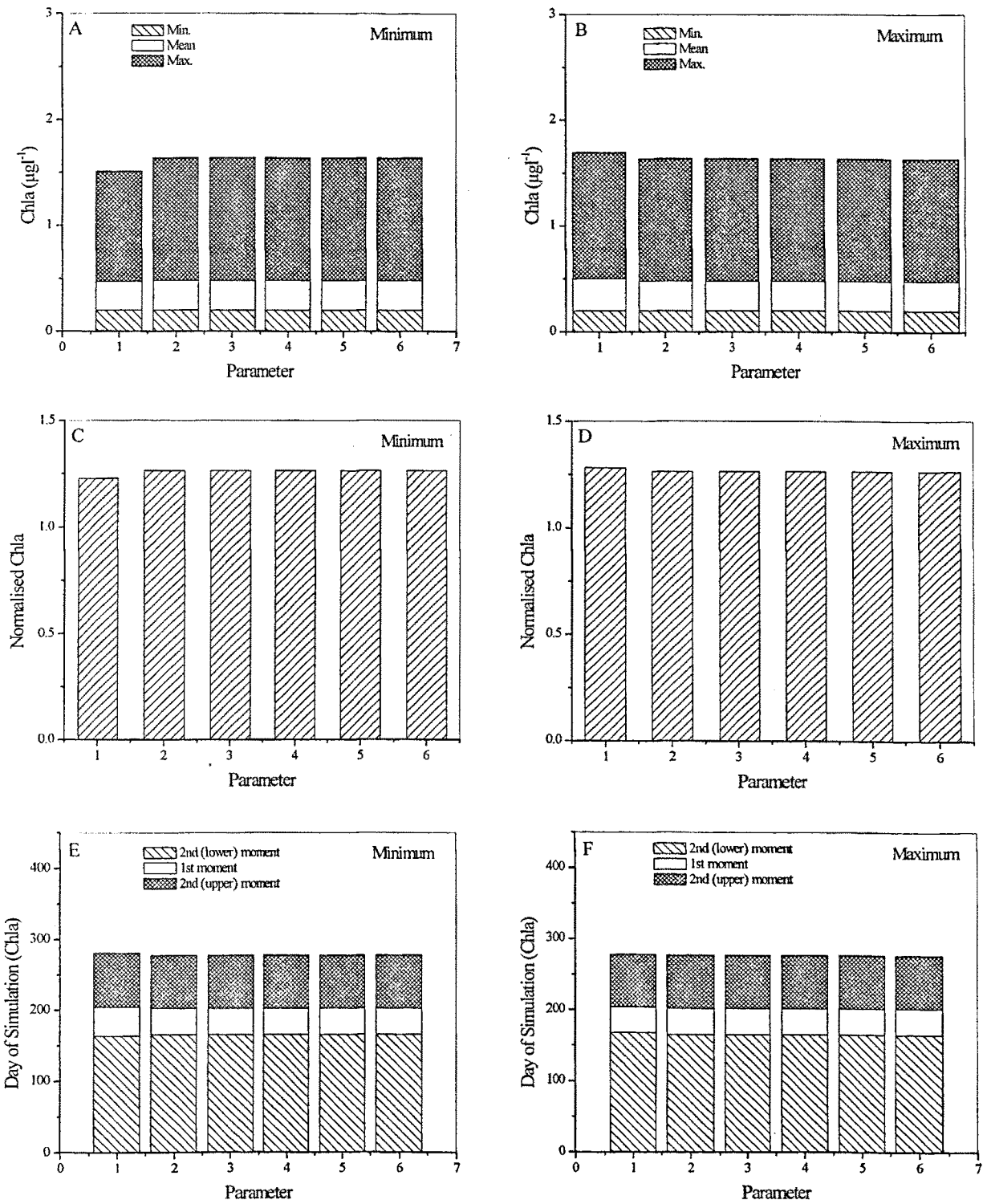**Figure 6.20** Variability in mean concentration (A, B), vertical (C, D), and temporal (E, F) distribution of Chla induced by initial conditions, numbered according to **Table 6.6**.

However, that Chla is not affected by changes in the assumed ratio of inorganic to organic particles is not indicative whether it has an effect on the predicted Secchi Depth by their scattering contribution.

6.5 Conclusions

Parameter sensitivity and the influence of input data uncertainty have been studied for DLM-WQ model of Lake Tahoe.

The conjunction of the TKE parameterization implemented in the DLM-WQ, with daily averaged meteorological data and bulk aerodynamic mass, momentum and heat coefficients seems to be adequate to predict both in time and space the development of the thermocline, the process of deepening at the adequate rate, and the ultimate destruction of the stratification in Lake Tahoe. Once the stratification is formed, the thermocline is well protected of mixing events, and the success of the simulation, in terms of location of the thermocline depends on the proper description during this critical days. If resources are limited, it seems that any field effort must be focused to characterize data at this particularly time of the year.

The model is not able to properly reproduce the thermal structure during periods where it is dominated by winter differential cooling, as this is a 2-D process. However, this occurs during very low stratification periods in the winter and tends to diminish as stratification begins. Except these particularly periods, the model predicts well the thermal structure during well-mixed conditions found in winter and late autumn. The match between the simulated and measured profiles decreases in summer and spring with stratified conditions. However, the error is limited to the top layers where actual conditions change diurnally.

Rotational effects, as indicated by the Rossby number less than 1, does not appear to invalidate the main hydrodynamic features predicted with the 1-D model.

The resolution of the initial conditions affects the calculation of the Potential Energy. However, the main hydrodynamic features are captured by the model's formulation, giving similar results whether resolution is employed. It could be concluded that sets of temperature data of low spatial resolution can be used to model years were there are available WQ information

Of the meteorological variables over the tested range, wind is the most critical variable. In the range of the performed experiments, the mixing depth and the thermocline depth show a high sensitivity to the wind speed.

Although the tested alternative formulations for aerodynamic drag coefficient have affected the thermal simulations, its effect is minor. From a thermal point of view, it seems reasonable to suggest concentrating research on wind field characterization whether than a more accurate description of the aerodynamic drag coefficient.

Under the ultra-oligotrophic conditions of Lake Tahoe, the simulated temperature is sensitive to the magnitude and the description (less) of the extinction coefficient. The tested modeled time dependent light extinction coefficient has a moderate effect on the thermal structure. Differences are more evident at the top layers, where simulated temperature may diverge by about $\pm$ 2C. There is a feed back between the extinction coefficient and the thermal structure. Results suggest a better description of the light extinction coefficient with a formulation splitting into abiotic and biotic terms.

Setting to zero the stream inflow and outflow results did not affect the thermal structure.

Chapter 7: Calibration and Validation

The water quality component of the DLM-WQ requires calibration because the rate and coupling parameters are site specific. Calibration is typically undertaken by varying the parameters until an acceptably good match between simulation and measurements is achieved. This is often done manually through simple trial-and-error. However, such a process is extremely tedious and time consuming, may be skewed by the necessarily limited choices made by the user, and the goodness of the match may be prone to subjectivity. In this section a different approach to calibration is described. A Genetic Algorithm (GA) has been adapted to perform the calibration. Using a potentially limitless array of parameter combinations, the GA has the ability to not only test the parameter combinations, but to selectively improve upon the combinations using objective assessment functions. In this Chapter we outline the basic idea behind GAs and their implementation with DLM-WQ. An example of the type of improvement in calibration made possible through using the GA is presented, and the results of model validation using a different data set are described.

7.1 Introduction

Mathematical models of aquatic ecosystems use a variety of formulations to describe the phytoplankton and nutrient dynamics, and to link them to the environmental conditions. The parameters are the coefficients in the mathematical representation of the processes. A parameter is understood as a model constituent whose value needs to be determined for each specific application of the model (Carstensen et al., 1997). The parameter values introduced in any model generally come from different sources. These can be classified as: i) parameters for which the measurement was taken, either on site, or during a specific experiment, and ii) parameters that come from the published literature (Salençon & Thébault, 1997). The quality of calibration is heavily dependent on the quality of data employed to obtain appropriate parameter values

(Jorgensen, 1981). Some parameters for a particular application may need to be estimated because measurements do not exist (Kleppler, 1997). In such case the literature provides ranges of values, often spanning orders of magnitude.

The aim of calibration (or parameter estimation) is to determine the set of parameters, which give the best agreement between simulated and observed data. The model calibration process may be affected by which formulation is used, as the model result may be influenced by the formulation (Klepper and Hendrix, 1994; Haney and Jackson, 1996). Thus, the correct development of a model requires both testing and calibrating a set of site specific parameters for the proposed mathematical relationship among the modeled variables (Salençon and Thebáult, 1997).

A measure of the relevance of a particular parameter is the response of the model to changes in its value. This is referred to as the parameter sensitivity. To reduce the number of parameters to calibrate, sensitivity analysis should be carried out prior to any calibration. A sensitivity analysis for DLM-WQ applied to Lake Tahoe was described in **Chapter 6**. In a time-dependent and multi-output model, like DLM-WQ, a single set of parameters is not possible (Klepper, 1997; Pacala et. al, 1996). Rather, the set of most sensitive parameters will vary depending on the particular output of the model considered. For example, if the primary concern were modeling benthic interactions as opposed to water clarity, then it is likely that the reduced parameter set from **Chapter 6** would be different.

After an acceptable calibration is attained, a validation test should be performed with a different (whenever possible) set of inputs and boundary conditions representing the state of the system (Rykiel, 1996). The validation should be performed over different years to cover the range of variability.

Current calibration efforts are often based on experience, by subjective variation of parameter values and qualitative comparison between model solutions and observations (Jorgensen, 1993). This technique thus implies a subjective, human intervention during model development and testing (Rechow & Chapra, 1983). However, this technique is extremely time consuming. Lake modelers face the prospect of running (and evaluating) the model thousands of times before an

acceptable solution is achieved. Usually, in manual calibration procedures, if the modeler judges a particular model variable of secondary interest, he would clearly give it a low weight in the calibration procedure. Weighing, whether explicit or simply in the mind of the modeler, is particularly important in calibration, as weights not only influence estimated parameter variance, but often the central value as well.

The use of automated calibration algorithms to obtain the set of parameters that best fit the objective function has been recognized as a valuable tool for modelers (Jorgensen, 1994). The systems modeled are usually non-linear thus the problem becomes one of optimization, response surface searching and iteration, because the usual equations have many solutions (Reckhow & Chapra, 1983). Various methods of parameter optimization for nonlinear eutrophication models have been developed (Keppler and Hendrix, 1994; Omlin, 2000). However, Salençon & Thébault (1997) have cited the difficulty of such automatic procedures, mainly because of the large number of parameters involved and the uncertainty associated with the input data.

Genetic Algorithms (GAs) are a class of evolutionary algorithms. They are based on the concept of the evolution of the best "fitted", i.e. adapted, individuals to the environmental conditions (Goldberg, 1989; Beasley et al. 1993a). This is done by the creation within the algorithm of a population of individuals represented as chromosome-type sequences, in essence a set of character strings analogous to the base-4 chromosomes in DNA. If this character string encodes the values for the different parameters to be optimized, then as the character string evolves different combinations of parameters are represented. Character strings that provide poor matches to the real conditions tend not to survive, overtaken instead by the more successful combinations. A complete database on GA techniques, developments and related publications can be found at http://www.aic.nrl.navy.mil/galist/dissert.html.

In this dissertation a GA-based methodology, comprising manual pre-calibration, parameter refinement through sensitivity analysis and the final fully automated GA calibration is presented. The GA code that was developed, was in large part based on that developed by Carroll (1996a).

7.2 Genetic Algorithm Technique

In the evolution of organisms, species adapt to their environment. Individuals and their characteristic genes evolve over many generations in the process of Darwinian selection and improve gradually in respect to certain criteria. Genetic Algorithms (GAs) are adaptive methods that try to imitate these. GAs are, according to Beasley et al. (1993a), a robust technique that have been successfully applied to various optimization or search problems, including problems with high complexity and non-linear behavior. Although this optimization method will always find reasonably good solutions (if the parameters are correctly set), it does not necessarily find the global optimum solution to a problem (Beasley et al, 1993a). However, given the inherent uncertainty present in hydrodynamic and water quality data, this is not considered to be a major shortcoming.

7.2.1 How Genetic Algorithms Work

The use of a genetic algorithm requires the addressing of seven fundamental issues (Holland, 1975): the genetic representation of the problem, the creation of the initial population of individuals, the definition of a suitable fitness (cost) function, the selection scheme of the parents, the genetic operators making up the reproduction function (recombination, mutation and replacement), the replacement of the old population by the new offspring, and the convergence criteria to stop the search process. A good synopsis of the basic principles can be found in Hüe (1997). The remainder of this section describes each of these issues separately, commenting on the specific application of each issue to the parameter calibration problem. **Figure 7.1** illustrates the sequence of the steps of the GA.

7.2.1.1 Genetic Representation

Typically, GAs work simultaneously with a set of possible solutions. This set is called a population and each encoded solution in it is referred to as an individual of the population. A generation is the population at a certain stage of the optimization process. A chromosome representation is needed to describe each individual in the population. The representation scheme determines how the problem is structured in the GA and determines the genetic operators that are used.
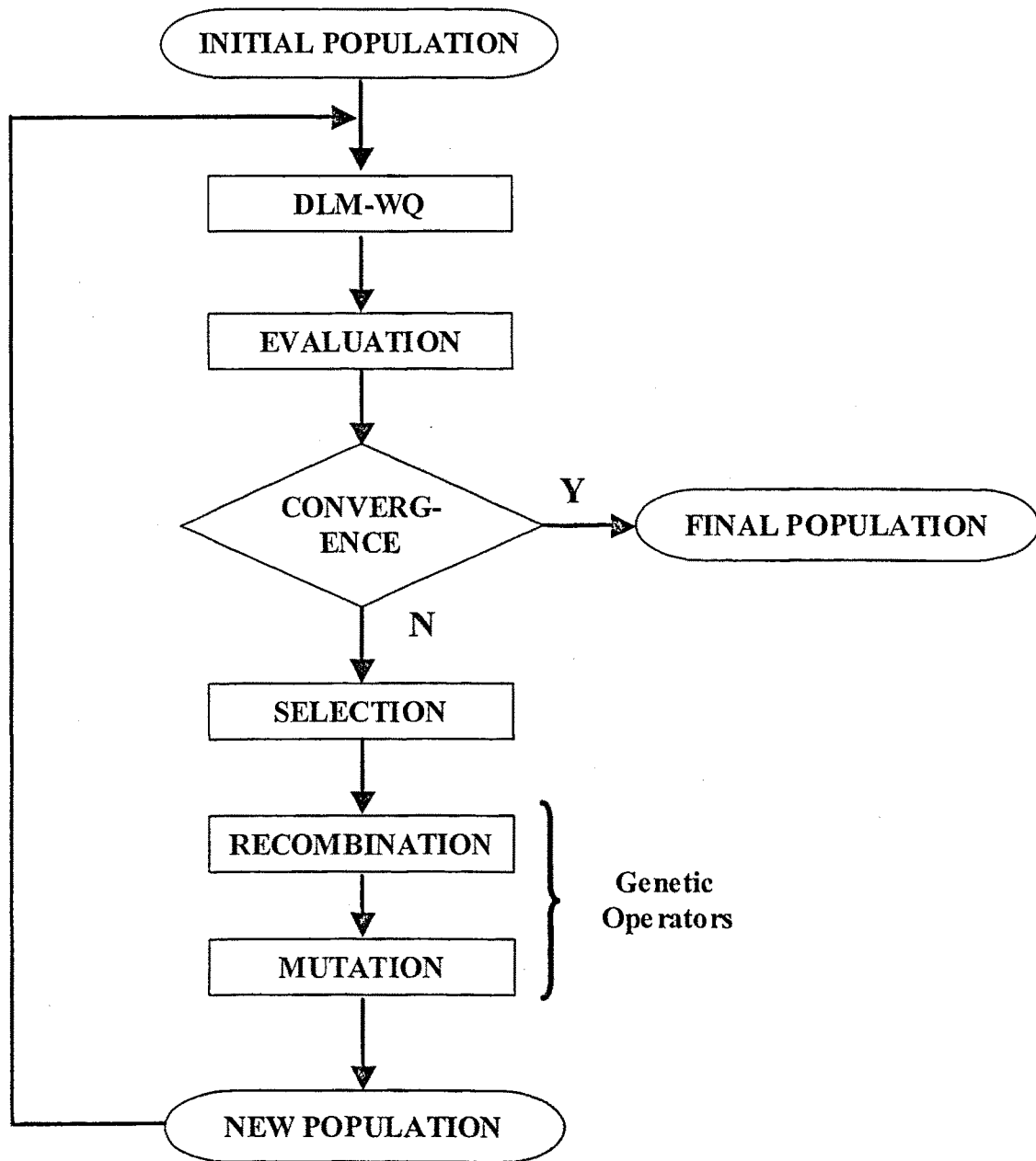
160

Figure 7.1 Flow chart showing the GA steps.

A prior requirement to the coding of a problem is a representation of potential solutions. This is achieved by finding a suitable representation for each of the parameters of the problem and joining them in a character string to form a code. The characters can be binary digits (0 and 1), floating-point numbers, integers, or symbols. An overview of possible parameter representations is given in Beasley et al. (1993b). The encoded parameters are called genes and the string of genes is referred to as a chromosome representing an individual, or one possible solution to the problem. In a deterministic model a unique set of parameters will always yield the same solution.

A binary codification varying in number of bits of resolution was used in the present work for the codification of the parameters. Binary codification is able to deal with a wide range of problems. Binary chromosomes are very simple to manipulate, although it has been shown that more natural representations are more efficient (Michalewicz, 1994). For each parameter, the user selects an integer number of possibilities (*nposib*). This should be a power of two, such that $nposib = 2^{ngene}$, where *ngene* is the number of genes (binary bits) of each individual (or parameter). A resolution measure of the calibration *(R)* can then be defined as:

$$R = \frac{(X_{max} - X_{min})}{nposib - 1} \qquad (7.1)$$

where X_{min} stands for the minimum value of the variable, and X_{max} is the maximum value of the variable. The range between the minimum and the maximum values (feasible region) is divided in 2^{ngene} different values following the expression:

$$X = X_{min} + \frac{n}{2^{ngene} - 1} \cdot (X_{max} - X_{min}) \qquad (7.2)$$

where *X* is the value of the parameter, n is an integer between 0 and $2^{ngene} - 1$. A higher resolution involves more simulations, slowing the process of convergence. A compromise between the resolution and the time consumed must be attained.

In the present application, each chromosome codes the parameters that were preselected to be optimized on the basis of the sensitivity analysis of **Chapter 6**. The resolution of parameter values depends on the range between the maximum and minimum values of the parameter and on the value of *ngene* selected to represent each

parameter. Usually, 32 possibilities (*ngene* = 5) were necessary to find stable solutions. However, where the range was large, 64 possibilities were used (*ngene* = 6).

7.2.1.2 Population

Two questions arise when facing the question of determining the population: i) how is the initial population generated, and ii) what is the appropriate population size (Goldberg, 1989). We discuss both items below.

i) The first generation should have a gene pool as large as possible in order to be able to explore the whole search space. The information contained in the initial population must be enough to produce all of the possible solutions. To achieve this, the GA can start with an initial solution randomly generated. However, if any information can be provided reflecting a previous knowledge of the system, the beginning population can be seeded with potentially good solutions, with the remainder of the population being randomly generated solutions. Thus, the mean fitness of the population is already high and it may help the genetic algorithm to find good solutions faster. In doing this, care must be taken to provide enough diversity. If the population lacks sufficient diversity, the algorithm will only explore a small part of the search space.

ii) The larger the population is, the easier it is to explore the search space. But the time required by a GA to converge also increases at a rate of order *(N log N)*, where N is the population size. The following crude population scaling law for binary coding was applied (Goldberg et al., 1992):

$$npopsiz = Order\left[\left(\frac{L}{K}\right) \times \left(2^{K}\right)\right] \tag{7.3}$$

where L stands for the number of bits of each chromosome (or in this case the number of parameters being calibrated), and K is the average number of bits per parameter (i.e the average of the values of *ngene* used for each parameter). **Figure 7.2** shows the population size as a function of the number of parameters and the number of possibilities (~ real resolution).
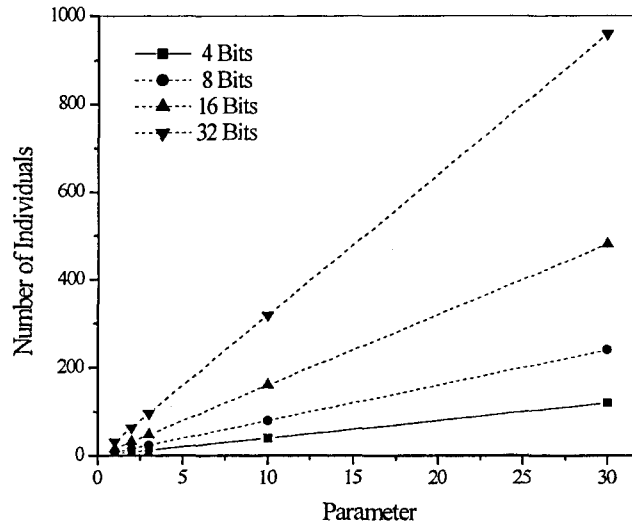
Figure7.2 Population size versus the number of parameters for 4, 8, 16, and 32 possibilities (resolution).

7.2.1.3 Evaluation Function

The evaluation function is called from the GA to determine the fitness of each solution string generated during the search. An evaluation function is unique to the optimization of the problem at hand; therefore, every time the GA is used for a different problem, an evaluation function must be developed to determine the fitness of the individuals. The fitness function can consider a single objective, or goal, or aggregate several criteria according to which the quality is determined. The fitness is a single numerical value and is used in the selection process to determine the probability of an individual to be represented in the next generation. Particular attention should be taken due to the fact that the selection is done according to the fitness of individuals. The fitness function should not only indicate how good the solution is, but also it should correspond to how close the chromosome is to the optimal one (Goldberg, 1989).

Definition of a feasible fitting for water quality is difficult to assess. The function adopted here uses Chla concentration, as it is a contributor to both the absorption and scattering of light in water. To test the robustness of the algorithm, two fitness functions were tested as a quantitative measure of the success of the simulation. The un-weighted Root Mean Squared (RMS) of the variable (Patterson et al. 1984) defined as:

164

$$Y = \sum_{j=1}^{d} \sum_{i=1}^{n} \left[\frac{\left(X^{s}_{i,j} - X^{m}_{i,j} \right)^2}{n} \right]^{1/2} \tag{7.4}$$

and the function criteria proposed by Jorgensen et al. (1986):

$$Y = \left[\frac{1}{n \cdot d} \cdot \sum_{j=1}^{d} \sum_{i=1}^{n} \left(\frac{\left(X^{s}_{i,j} - X^{m}_{i,j} \right)}{\overline{X}^{m}_{j}} \right)^2 \right]^{1/2} \tag{7.5}$$

where X^s stands for the simulated variable, X^m, is the measured variable at the same depth, $\overline{X}^m$ is the mean of the measured variable profile, and the index n represents the number of points, i, in a simulation profile. The spatial resolution of the measured profiles is much coarser than that of the simulation output. Therefore the functions were evaluated by first linearly interpolating the measured variable to the same locations as the simulated variables. Thus, any predicted structure on a scale less than the resolution of the field data will influence X^m, and register as an error in Y (Patterson et al., 1984). The index d represents the number of days on which there exists measured profile data to compare with the simulated output. The function is evaluated at the end of each of these days, j, and the total error is summed.

Although it must be recognized that they have different mathematical meaning, the value of Y estimates the absolute fitness of the predicted to the field profile and can be interpreted as the expected error of the simulation. Slightly different solutions could be attained with the two tested equations. Equation (7.5) is less sensitive to changes of the selected number of possibilities, while Eqn (7.4) is more affected by the range of possibilities tested. Solutions found using Eqn (7.4) also registered a greater sensitivity when the range of the parameters calibrated was wider. For the cases studied and the conditions presented, Eqn (7.5) seems to be more suitable than Eqn (7.4). By altering the weights water quality variables can be assigned different relative priorities. Giving high values of the weights to particular layers of the vertical profiles, Eqn (7.4) can also be spatially segregated. This was the technique applied at Lake Tahoe, where the calibration effort was focused on the layers above the mixing depth. This formulation also permits easy implementation of penalty functions, by assigning high values to the weighting functions if a certain imposed condition is

exceeded (for example, if the Chla concentration is greater that a user defined maximum level).

7.2.1.4 Selection

Selection is the process of choosing parents for the next generation out of he individuals of the previous generation. There are many ways to select individuals, but all of them randomly pick chromosomes out of the population according to the value they obtain for the evaluation or fitness function. The higher that value, the more chance an individual has to be selected. The selection pressure is defined as the degree to which the better individuals are favored. This selection pressure drives the GA to improve the population fitness over successive generations. The convergence rate of a GA is largely determined by the magnitude of the selection pressure (Goldberg, 1991). If the selection pressure is too low, the convergence rate will be slow. If the selection pressure is too high, premature convergence can occur (see **Section 7.2.1.7** below) (Goldberg, 1989).

There are two types of schemes for the selection process: i) proportionate selection and ii) ordinal-based selection (ranking methods).

i) Proportionate-based selection picks out individuals based upon their fitness values relative to the fitness of the other individuals in the population. Roulette wheel selection and its extensions are the most popular proportionate schemes. It simply assigns to each solution a sector of a roulette whose size (the angle it subtends) is proportional to the appropriate fitness measure (usually a scaled fitness of some sort), and then chooses a random position (and the solution to which that position was assigned).

ii) Ordinal-based selection schemes select individuals not upon their raw fitness, but upon their rank within the population. This requires that the selection pressure is independent of the fitness distribution of the population, and is solely based upon the relative ordering (ranking) of the population. It is also possible to use a scaling function to redistribute the fitness range of the population in order to adapt the selection pressure (Michalewicz, 1992).

166

The tournament and elitist schemes, both ordinal-based schemes, have been applied in this work. As with other ordinal-based selection, the evaluation function only maps solutions to a partially ordered set but does not assign probabilities. Tournament selection makes individuals compete directly. It works by randomly selecting two individuals and saving the better one for the new generation. This procedure is repeated until N individuals from the population of M individuals ($N < M$) have been selected. The elitist scheme is similar, but additionally requires that the best individual of the present generation is in the next generation.

7.2.1.5 Genetic operators

Genetic operators provide the basic search mechanism of the GAs. The operators are used to create new solutions based on existing solutions in the population. There are two basic types of operators: recombination and mutation. In the following, the basic ideas about the two genetic operators and their implementations used in this work will be discussed.

7.2.1.5.1 Recombination

Recombination is the process of taking two parent solutions and producing offspring from them. Several recombination operators have been proposed and used (Goldberg, 1989). Among them, uniform crossover has been shown to be an effective and robust process. In this scheme, each gene in the offspring is created by copying the corresponding gene from one or the other parent, chosen according to a random generated binary crossover mask of the same length as the chromosomes. If there is a 1 in the crossover mask, the gene is copied from the first parent. If there is a 0 in the mask, the gene is copied from the second parent. A new crossover mask is randomly generated for each pair of parents. Offspring therefore contain a mixture of genes from each parent. **Figure 7.3** depicts the procedure. The factor P_{cross} is the assigned probability of crossover occurring.
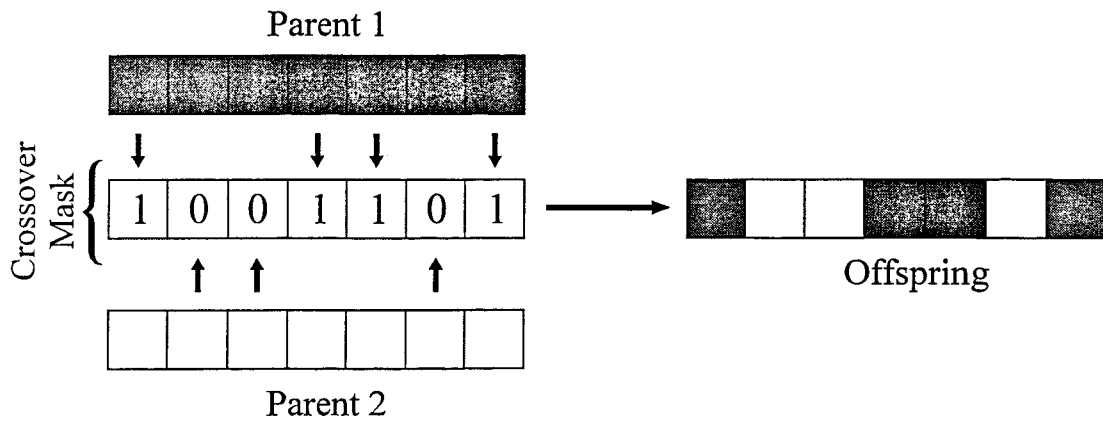
Figure 7.3 Scheme of chromosome recombination.

7.2.1.5.2 Mutation

Only mutation operators are able to maintain a realistic genetic diversity. To ensure that every potential solution has a non-zero probability of being found, the mutation operator creates individuals that contain new information besides the genes received from their parents. This is achieved by randomly selecting one bit in a chromosome and altering it (see **Fig. 7.4**). Jump and creep mutation operators were implemented. The factor *Pmutate* is the assigned probability of mutation occurring.

Chromosome before mutation   Chromosome after mutation

| 1 | 0 | 0 | 1 | 1 | 0 | 1 | → | 1 | 0 | 1 | 1 | 1 | 0 | 1 |

Figure 7.4 Scheme of mutation

7.2.1.6 Replacement

Once offspring are produced, a method must determine which of the current members of the population should be replaced by the new solutions. There are two kinds of methods for maintaining the population: generational updates, and steady state updates. The first scheme was implemented involving the substitution of all of the individuals of the old generation by the new generation, while retaining constant the number of individuals of the population.

168

7.2.1.7 Convergence

Convergence is understood as a loss of diversity in the population (most of the members of the population are similar or identical), due to the selection pressure (Goldberg, 1989). The GA moves from generation to generation selecting and reproducing parents until a termination criterion is met. Ideally this should be a near-optimal solution. One problem that may occur is premature convergence. The phenomenon of premature convergence means that some comparatively highly fit individuals, that may not be near-optimal, are represented strongly in the population. Thus, reduced diversity can cause the optimization to reach a stage where there is little chance of new solutions being created by the crossover operator (as the population is so genetically similar at an early stage). In such a case, the convergence criterion is met without reaching the best solution.

The most frequently used termination criterion was applied, namely: the number of generations was increased until the solution found was independent of the number of generations. Usually, for one or two parameters, stable populations were found after 40 generations, but as a more conservative criterion the algorithm was run up to 100 generations. Of course, as the number of parameters increases, the number of iterations required (and the CPU time consumed) is higher.

7.2.2 Model Implementation

The GA code and DLM-WQ were interfaced by a FORTRAN driver, which translates the individuals of the population into the parameters required by DLM-WQ and calculates the evaluation function.

Figure 7.2 shows the coupling between the GA and DLM-WQ. The population of individuals is constituted by the set of files *name.WAT*, which also contain the biological and chemical parameters needed to run DLM-WQ. Each element of the solution DLM-WQ is related to a specific element of the *name.WAT* file. The GA evaluates the fitness of each solution and creates a new population of *name.WAT* file. The process is repeated until the convergence criterion is reached. The modeler sets the parameters to be calibrated from the *name.WAT* file, and the number of possibilities of each parameter.

To visualize the procedure, suppose that the GA is set to calibrate three parameters of the *name.WAT* file, e.g. *G*, k_r, and I_s (the maximum algal growth rate, the maximum algal respiratory rate and the light saturation rate) of a phytoplankton group, with respective ranges of (in units of day^{-1}): 1.7-2.9, 0.03-0.2, 100-500. These parameters were chosen because of their very different ranges. Let us also set the number of possibilities (*nposibl*) to 4. Once having fixed the number of possibilities, the minimum number of bits necessary to code each parameter will be 2 ($2^2 = 4$). Thus, each parameter can have 4 possible values within its range. Setting the *nposibl* equal for the three parameters involves different resolution for each one. The real values for *G* are 1.7, 2.1, 2.5, and 2.9, expressed in binary form 00, 01, 10, 11. The values for k_r are 0.03 (00), 0.08 (01), 0.14 (10), and 0.2 (11), while the I_s values are 100 (00), 233 (01), 366 (10), and 500 (11).

A chromosome of the population will be formed by the junction (in order) of the three binary strings, e. g. the chromosome '110001' is decoded into the real values of G = 2.9, k_r = 0.03, and I_s = 233. It is also said that each chromosome of the population is composed of three genes. The remainder of the parameters of the *name.WAT* file will remain unchanged. Obviously, the resolution obtained by setting the number of possibilities to 4 is not fine enough to deal with the required resolution of the problem. The program randomly generates the first generation of parents from all of the possible combinations. If, for example, the initial population is set at 4 individuals, a possible first generation could be the set '000000', '110011', '000011', and '011101', here after referred to as chr1, chr2, chr3, and chr4 respectively. In this example, which has such a low population, there is a high probability that the searching procedure does not reach all of the space of the solutions. Once the first generation is created, the DLM-WQ is called and the simulation is performed using one individual (*name.WAT*) file each time. Following the present example, the DLM-WQ will be called four times for each generation. After the simulation is concluded, the predicted values are compared with the measured values of the control variables and the quality of the simulation is calculated according to the fitting criteria (e.g. the Eqn. 7.5). Each individual (*name.WAT* file) will have associated a fitting value (a real number). Let's associate the following fitness to each chromosome (in parenthesis): chr1(2.1), chr2(1.7), chr3(3.2), and chr4(3.5).

The next step is to proceed to the selection of the parents for the new generation. The tournament scheme implemented selects individuals for reproduction by picking two of them randomly and directly comparing their fitness. The better one is saved to procreate the new generation. The user must set the number of offspring per couple (*nchildr*), either 1 or 2. If the number of offspring is set at 1, the couple's selection is repeated as many times as the number of individuals of the population (each iteration involves two tournaments as is needed two individuals to form a couple). Thus, following our example, to form a couple two pair of mates will be randomly chosen, let's say chr1(2.1) and chr2(1.7), and chr1(2.1) and chr4(3.5). Their fitness will be compared and the winners (chr1 and chr4 in the example) will be selected. The procedure will be repeated 4 times, giving 4 different couples. The algorithm continues by applying the genetic operators of reproduction (uniform crossover and mutation successively) to the selected parents. Uniform crossover randomly generates a crossover mask of 0 and 1, from which the information of each gene is chosen from either parent. If for example, *nchildr* = 1 and if the uniform crossover operator applies the randomly generated mask '100' to the selected parents chr1 '000000' and chr4 '011101', it will yield the child '001101'. The mutation operator introduces variability into the pool of genes by assigning a probability to change the information coded in the genes of the individuals. The mutation is performed by randomly assigning a probability of mutation to each gene of an individual. If this random number is greater than a fixed value, then the gene is mutated (e.g. changing '0' to '1' and vice-versa). Then, the new individuals replace the old population, and the convergence criterion is checked. The procedure is repeated until the number of iterations equals the fixed maximum number of iterations or convergence occurs.

Table 7.1 shows the set values of the most relevant variables used by the GA. These variables control the GA evolution and have been set after comparative numerical experiments. Carroll's (1996b) recommendations were followed for the rest of the GA's controlling variables not shown in this table. Little difference on the time consumed by the entire process has been detected on the range tested for the probability of mutation and the probability of crossovers. The higher value of the probability of mutations slightly speeds the procedure. The mutation probability rate should be high enough to avoid premature convergence, but low enough to avoid a random walk search (Michalewicz, 1992). The maximum number of simulations and

171

the number of individuals of the solution's population have been set at the minimum number that produces stable solutions.

Table 7.1 The most important GA variables and their selected values.

Parameter	Symbol	Value
Number individuals population	Npopsiz	50
Number children per couple	Nchild	1
Probability of mutation	Pmutate	0.25-0.003
Maximum number of generation	Maxgen	100
Probability of crossover	Pcross	0.5
Number of possibilities	Nposibl	32

7.3 Calibration

The calibration included the following steps (Jorgensen et al., 1994):

- The range for each parameter was found from a literature survey.

- A rough calibration of the most sensitive parameters was carried out by a manual trial-and-error method (a process that took over two months).

- A sensitivity analysis was performed, which resulted in the reduction of the set of parameters that needed calibration from 29 to 7: 1,2,4,8,11,22,23, numbered according to Table 7.2.

- The automated calibration procedure (optimization of parameters) was run using the GA and the spatial and temporal errors of the simulated profiles were checked against the measured profiles of the control variables.

The calibration of Lake Tahoe focused on the upper part of the water column, and in particular above the depth of mixing. The mixing depth is highly variable and can change significantly in periods of less than one week (Abbot at al., 1984). This spatial segmentation focused the calibration effort on the most relevant zone, given that the immediate goal of the model was to predict surface water clarity. Although the dynamics of the nutrients and chlorophyll over the entire water column is of great

interest the sparse data below 100 m introduces considerable noise to the calibration procedure. In this manner it could be ignored.

Values of the calibrated parameters for Lake Tahoe are shown in **Table 7.2.** **Figure 7.5** shows the calibration results for Secchi depth and for Chlorophyll concentration (integrated above the Secchi depth). The measured values, the values obtained from the rough manual calibration, and the values resulting from the automated GA calibration are all shown. The main features of the clarity dynamics of Lake Tahoe are captured by the model – the deep mixing in the early part of the year (around day 30) that brings up clear, nutrient rich hypolimnetic water; the near-constant high clarity period that is followed by a sharp clarity decline due to algal growth (around day 90); the increase in clarity as algal concentration decreases and the mixed layer deepens; and the decrease in clarity as mixed layer deepening passes through the deep chlorophyll layer (around day 320).

For Secchi depth in **Fig. 7.5 A**, it is evident that the calibrated model does not reproduce the very largest Secchi depths in the early part of the year. As will be seen in the next Chapter, the greatest impact on Secchi depth is due to fine particles. A relatively small change in assumed particle concentration readily changes the Secchi depth. **Figure 7.5 A** demonstrates that the model parameters themselves are not capable of changing the result to obtain these high clarities, and for the parameter space considered this is the best match. What is highly encouraging, is that the temporal variation of the Secchi depth is very faithfully reproduced by the model, and that the GA calibration greatly improves this. For example, between days 60 and 90, the Secchi depth is relatively stable, but then sharply decreases. The timing of this sharp decline is much improved in the GA calibration. Also, events such as the decline in clarity around day 320 (as the mixing depth deepens through the deep chlorophyll maximum as described by Jassby et al. (1999)) is captured. The large Secchi depth in the measured data for day 384 (January 19, 2000) is in all likelihood an anomaly. A major upwelling occurred immediately prior to this date, the effects being felt at the Midlake station. This resulted in clear bottom water rising to the surface (Palmarsson et al., 2001), an effect that disappeared after a few days.

Table 7.2 Calibrated model parameters implemented in the DLM-WQ. Asterisk (*) indicated that this parameter was not used by this version of the model. Double asterisk (**) indicated that this parameter was fixed.

#	Parameter	Symbol	Value	Units	Ref.
	Algae				
1	Maximum growth rate	G_{max}	1.9	d^{-1}	1
2	Maximum respiratory rate	k_r	0.20	d^{-1}	2
*	Maximum mortality rate	k_m	0.0	d^{-1}	3
3	Temperature multiplier for growth/respiration/death	θ	1.08	n. d.	4
4	Light saturation	I_s	75.0	$\mu E\ m^{-2}\ s^{-1}$	5
	Nutrient utilization				
5	Phosphorus to chlorophyll mass ratio	a_p	0.5	n. d.	6
6	Nitrogen to chlorophyll mass ratio	a_n	7.0	n. d.	6
	Settling				
7	Setting velocity for phytoplankton	v_s	0.2	$m\ d^{-1}$	7,8
8	Setting velocity for detritus POP & PON	v_{det}	0.2	$m\ d^{-1}$	9
9	Phytoplankton transfer function	T_{phy}	290000	$\#\ (\mu gChla^{-1})$	10
10	POP and PON transfer function	T_{part}	8100	$\#(\mu gChla^{-1})$	11
	Chemical reactions				
**	Biological oxygen demand of sub-euphotic sediments	k_{bio}	0.02	$mg\ m^{-2}\ d^{-1}$	12
**	Decomposition rate of BOD	k_{bod}	0.005	d^{-1}	12
**	Half saturation constant efficiency of DO on de-nitrification	k_{den}	0.01	$G\ m^{-3}$	13
11	PON ==> NH4	k_{n1}	0.01	d^{-1}	13
12	PON ==> DON	k_{n2}	0.02	d^{-1}	13
13	DON ==> NH4	k_{n3}	0.02	d^{-1}	13
14	NH4 ==> NO3	k_{n4}	0.15	d^{-1}	14
15	NO3 ==> N2	k_{n5}	0.10	d^{-1}	14
16	POP ==> SRP	k_{p1}	0.04	d^{-1}	14
17	POP ==> RP	k_{p2}	0.05	d^{-1}	14
18	RP ==> SRP	k_{p3}	0.02	d^{-1}	15
19	Half saturation constant for N nutrient limitation	$k_{(NO3+NH4)}$	3	$\mu g l^{-1}$	16
20	Half saturation constant for P nutrient limitation	k_{SRP}	1	$\mu g l^{-1}$	15

Table 7.2 Continued

21	Half saturation constant for Ammonia preferential uptake factor	k_{NH4}	25.0	$\mu g l^{-1}$	17
**	Half saturation constant for limitation of reactions by DO for nitrification	k_{nit}	2.0	$ml_{O2} l^{-1}$	12
**	Half saturation constant for limitation of reactions by DO for biochemical oxygen demand	k_{do}	0.5	$ml_{O2} l^{-1}$	12
**	Half saturation constant for limitation of reactions by DO for sediment processes	k_{sdo}	3.0	$ml_{O2} l^{-1}$	12
**	Density of BOD for settling	ρ_{BOD}	1040	Kgm^{-3}	12
	Nutrient temperature multipliers				
22	Nitrification	θ_{NO}	1.08	n. d.	18
23	Organic decomposition	θ_o	1.08	n. d.	18
24	Biological and chemical sediment oxygen demand	θ_{BOD}	1.08	n. d.	12
	Sediment Fluxes				
25	Release rate of phosphorus SRP	r_{SRP}	0.0001	$\mu g\ m^{-2}\ d^{-1}$	12
26	Release rate of nitrogen NH4	r_{NH4}	0.0001	$\mu g\ m^{-2}\ d^{-1}$	12
27	Temperature multiplier for sediment nutrient release	θ_S	1.08	n. d.	12
	Zooplankton parameters				
28	Zoo feeding rate on Chlorophyll	k_z	0.03	$\mu gChla\ l^{-1}$	11
	Particles				
29	Density of 7 particle size groups	ρ	1040	Kgm^{-3}	12

1) Bowie et al. (1985) Table 6-5, 2) Bowie et al. (1985) Table 6-18, 3) Bowie et al. (1985) Table 6-20, 4) Chapra (1997) Fig-2.11, 5) Chapra (1997), 6) Bowie et al. (1985) Table 6-4, 7) Marjanovic (1989) Table-16, pg. 326, 8) Jassby (per. com.), 9) Bowie et al. (1985) Table 6-19, 10) Hunter et al.(1990), 11) Hunter, per. Comm., 12) Schladow & Hamilton (1997), 13) Bowie et al. (1985) Table 5-3, 14) Bowie et al. (1985) Table 5-4, 15) Eppley et al. (1969), 16) Chapra (1997) Table 33.1, 17) Bowie et al. (1985) Table 5-5, 18) Chapra (1997) p 40.

175

Figure 7.5 A) Secchi depth, and B) Chla integrated over the Secchi depth for 1999.

Figure 7.5 B, for chlorophyll concentration shows an even greater improvement due to the GA calibration. Both the magnitude and the timing of changes in chlorophyll concentration are far better reproduced. Though differences exist, it must be borne in mind that Lake Tahoe is ultra-oligotrophic and that in absolute terms, the values predicted are approaching the detection limits of many laboratories. The error between simulated and measured concentration is generally less than 0.5 μgl^{-1}. In addition, the measured integrated chlorophyll concentrations above the Secchi depth are based on interpolating measurements at 0, 10, 20 and 100 m. By contrast the simulated values are based on model output that is at intervals of between 1 to 3 m.

Figure 7.6 A-H shows the simulated contour plots for 1999 together with the contour plots for those variables that are measured (Chla, NO3, NH4, SRP). The deep mixing that commences Day 30 dictates most of the consequent dynamics of the system. It is reasonably well reproduced by the model. The mixing pumps nutrients to the upper layers (mainly NO3), as well as dilutes chlorophyll concentration in the upper layers, as discussed above. These nutrients will boost the subsequent bloom of algae. It is not possible to meaningfully compare the two sets of plots. There are no chlorophyll measurements below 100 m, and nutrients are measured at 50 m intervals between the surface and 450 m (and at 10 m) at approximately monthly intervals. Thus sharp gradients would tend to be smoothed and possibly anomalous measurement values produce the appearance of vertical structure in the hypolimnion. However, despite this it can be seen that the most important nutrients, NO_3, NH_4 and SRP, all appear to be reproduced within a factor of 2. Note, that the simulated results produce a temporal gradient in the hypolimnetic values of nutrients, something that is not apparent in the measured data. This is discussed further in the following Section.
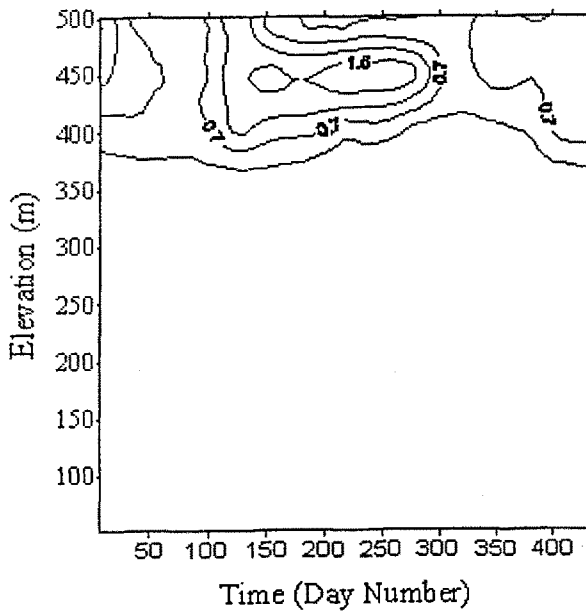
A) Chla field
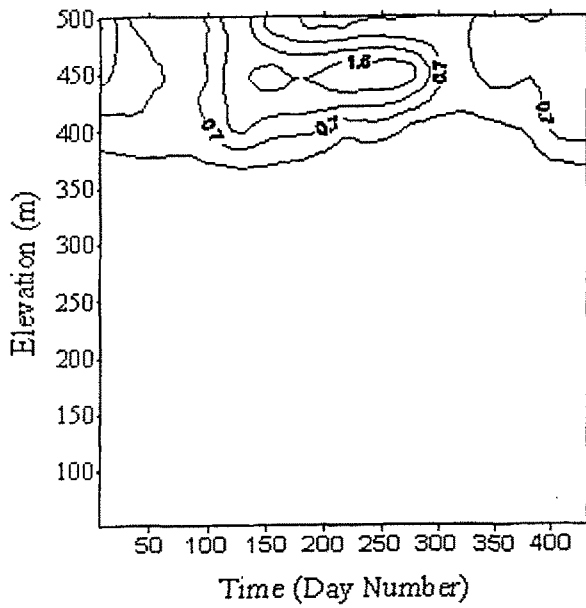
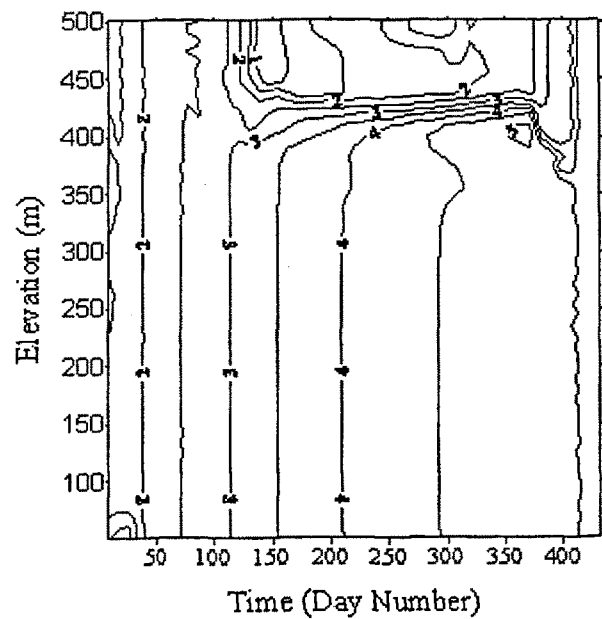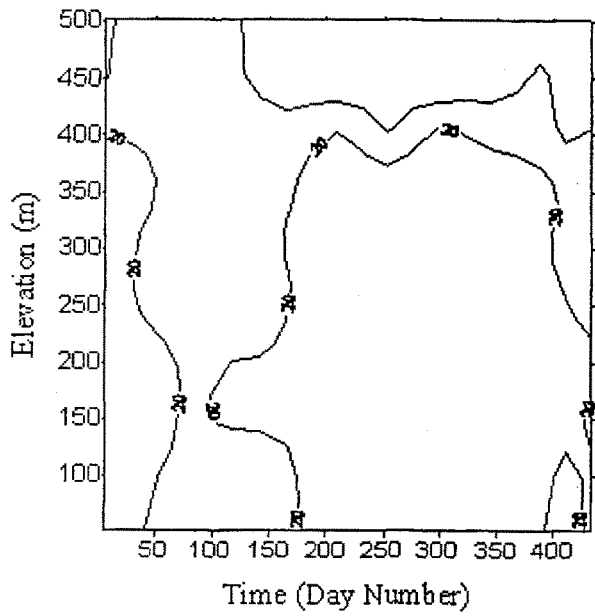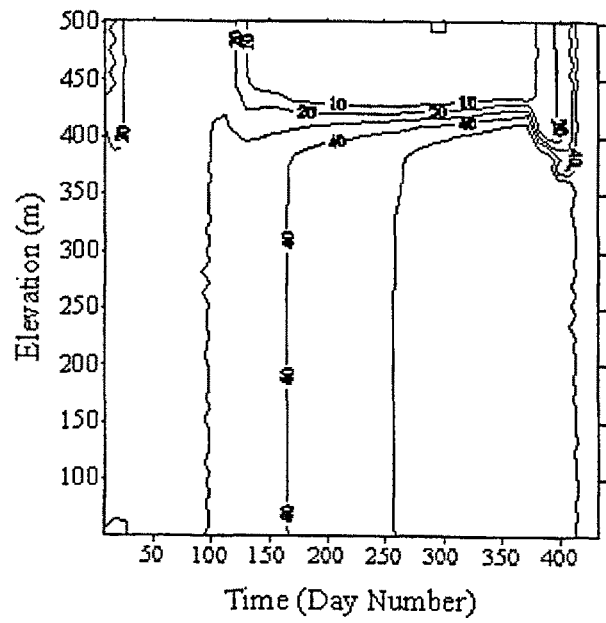B) Chla simulated
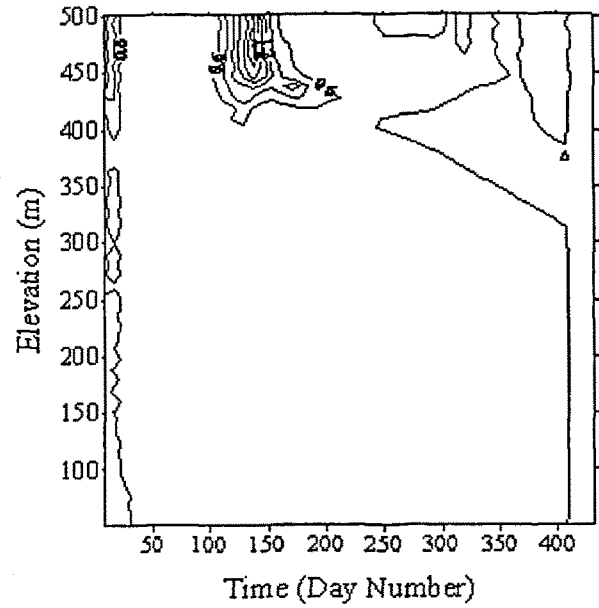
C) SRP field

D) SRP simulated

Figure 7.6 Measured and simulated contour plots for 1999: A) Chla measured, B) Chla simulated, C) SRP measured, D) SRP simulated, E) NO3 measured, F) NO3 simulated, G) NH4 measured, and H) NH4 simulated.
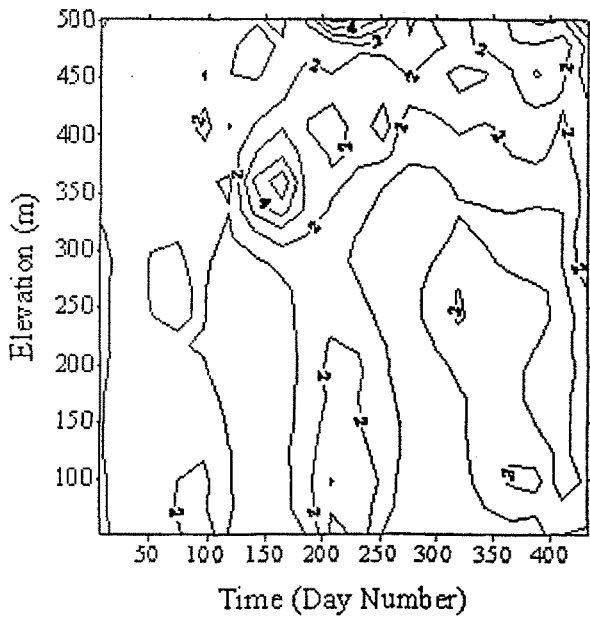
178

E) NO3 field
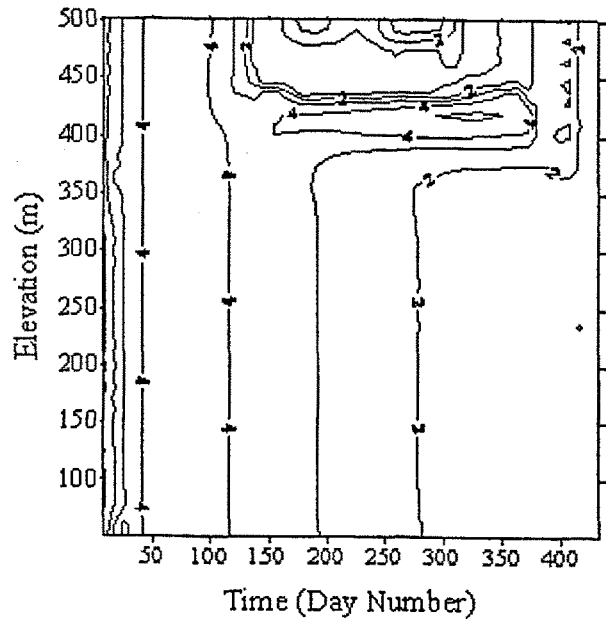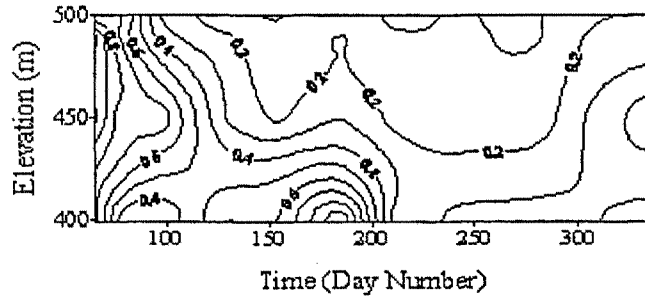

F) NO3 simulated

G) NH4 field

H) NH4 measured

Figure 7.6 Continued.

7.4 Validation

As a validation exercise, the calibration coefficients were used with the 1992 data. **Figure 7.7 A-H** shows the simulated contour plots for 1992 together with the contour plots for those variables that are measured (Chla, SRP, NO3, NH4). As with the previous calibration figures, it is difficult to compare contour plots based on high resolution simulation output with those from low resolution measurements. For example, vertical structure, such as the sharp nitricline that is clearly evident in **Fig. 7.7 F** (and known to exist (see for example Paerl et al., 1975), appears to be absent in the measurement contours of **Fig 7.7 E** due to smoothing by the contouring software. Nonetheless, most of the comparison figures seem to agree within a factor of two, as was the case for the calibration. The main exception to this is for chlorophyll concentration. Here, the field data does not give as clear an indication of the deep chlorophyll maximum, and its evolution in time. The predicted chlorophyll concentrations are also a factor of 3 higher than the measured. As was discussed in **Section 4.5** and illustrated in **Fig. 4.8**, the deep chlorophyll maximum could readily be missed with the sampling interval used.

Comparing **Figs 7.7 C** and **7.7 D** for SRP, it can be seen than the simulated values in the hypolimnion appear to increase over time, whereas in the field measurements there appears to be no such monotonic increase. The same difference was observed in the calibration output. This increase over time of the simulated values in the hypolimnion is due to the fact that SRP is produced from POP and RP, and consumed by algal uptake. In most of the hypolimnion, algal uptake is negligible due to light limitation, therefore there is a buildup in concentration. This suggests that the rate and coupling parameters are slightly out of balance, or the conceptual model of **Fig. 3.4** is too simplistic. The same types of patterns can be observed for the other nutrients plotted. It should be recalled, however, that the automated calibration exercise was focused on the mixed layer, so as to produce the best solution for Secchi depth prediction. There was no attempt to optimize the parameters that may control other parts of the system. Here is a clear example of the downside of this approach.
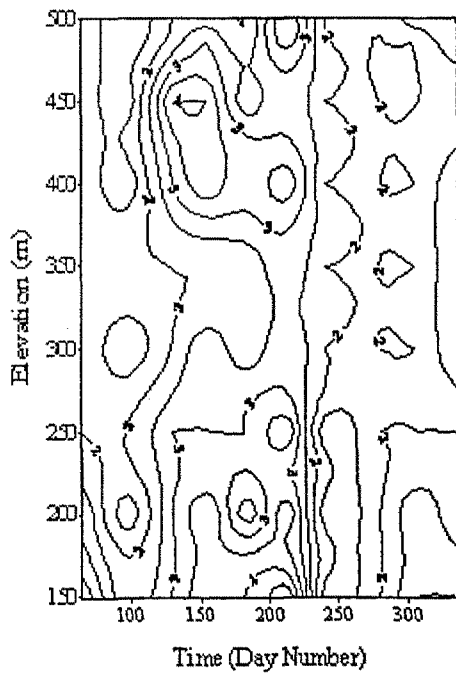
180

A) Chla field
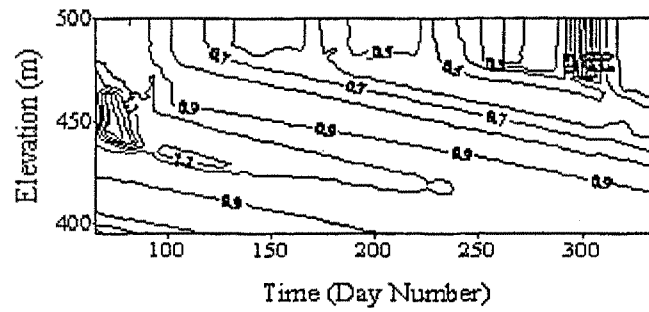
B) Chla simulated

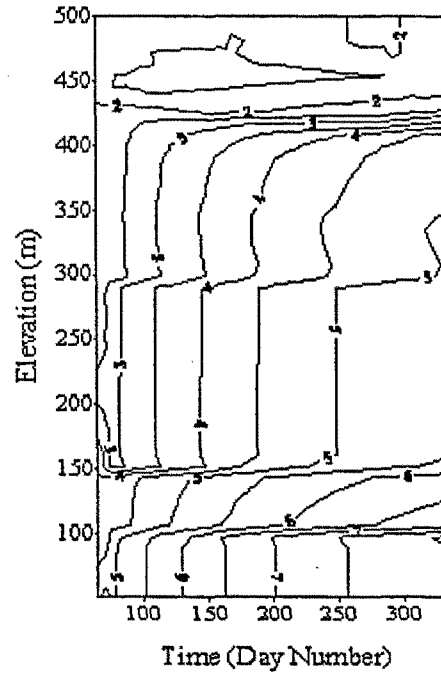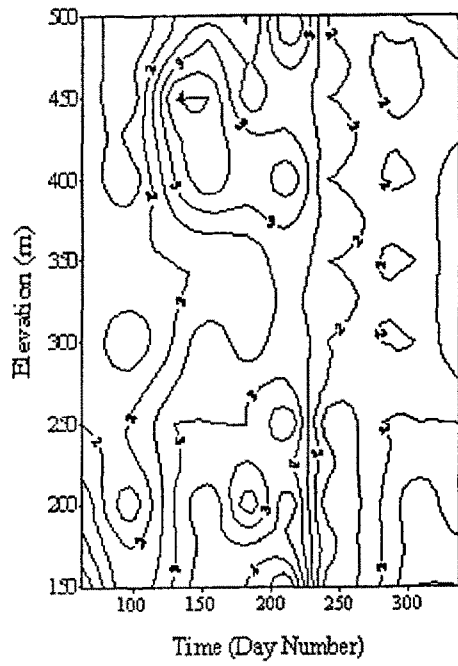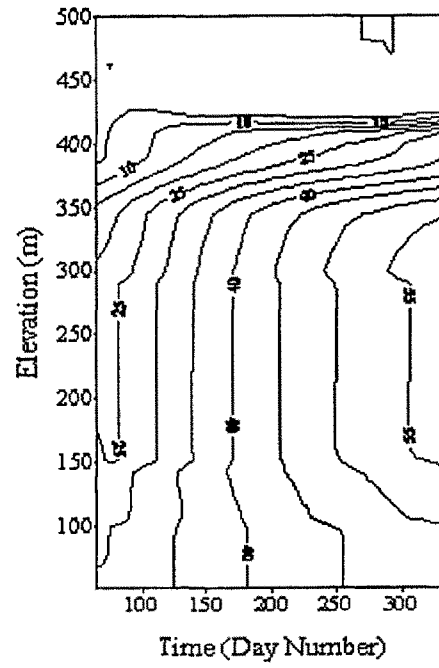C) SRP field

D) SRP simulated

Figure 7.7 Measured and simulated contour plots for 1992: A) Chla measured, B) Chla simulated, C) SRP measured, D) SRP simulated, E) NO3 measured, F) NO3 simulated, G) NH4 measured, and H) NH4 simulated.
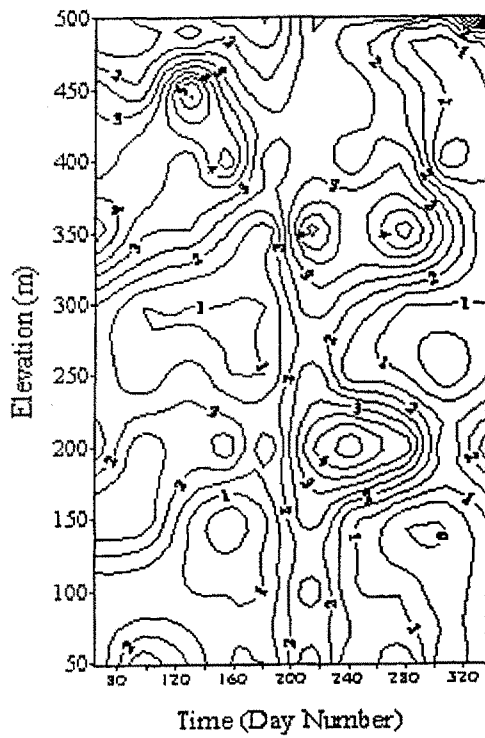
181

E) NO3 field

F) NO3 simulated

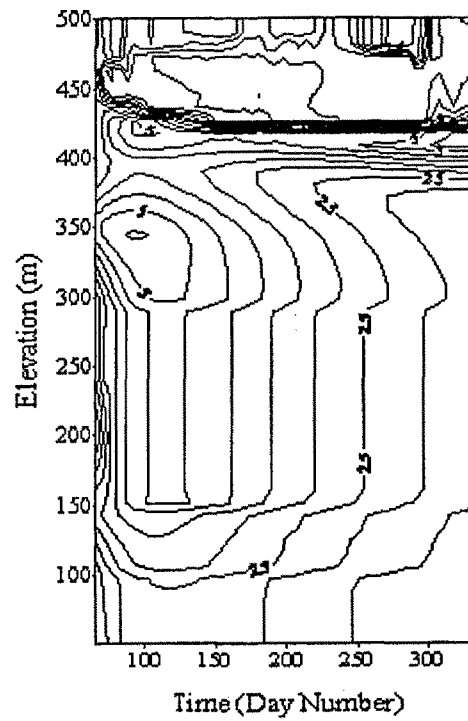

G) NH4 field

H) NH4 measured

Figure 7.7 Continued.

182

It should be noted that a plot of Secchi depth as a function of time was not plotted for the validation case. The reason for this omission is that the predicted Secchi depth is highly sensitive to the particle concentration and size distribution. For 1992 no particle size or concentration data were available. For the purposes of running the model, an initial particle distribution that was uniform in depth and conformed with the mean hyperbolic distribution found for Lake Tahoe in 1999 (Coker, 2000) was assumed. By contrast for the 1999 calibration, measured particle concentration distributions were available throughout the year. Consequently, the 1992 particle distribution is simply not correct and the resulting Secchi depth predictions are meaningless.

7.5 Conclusions

The results confirm that it is possible to successfully calibrate DLM for its intended use to predict changes in water clarity at Lake Tahoe. In some cases it is not possible to fully evaluate the performance of the calibrated model, due to the lack of measurements. However, it appears that the simulated results were sufficiently close to the few measured values and, more importantly, that the main features of the temporal and spatial dynamics were extremely well reproduced.

The results of the validation exercise, performed with a data set from a different year and for very different initial and forcing conditions, produced a match that was quantitatively similar to the calibration result.

In the work presented, a simple genetic algorithm with a relatively small population size was utilized. The GA provided results that were a significant improvement on those obtained by hundreds of manual simulations. The use of the GA was found well suited to the optimization of the system, proving to be, in conjunction with the best judgment of the modeler, a powerful tool for calibration.

Chapter 8: Application of the Model

In the preceding Chapter, it was shown that DLM-WQ could be calibrated and that the calibrated model could be validated with an independent data set. The intent of this Chapter is to now demonstrate some of the purposes to which this calibrated model may be applied. The examples given are by no means exhaustive; rather they are intended to just illustrate what may be achievable. It should also be recognized that the present calibration is to a degree tentative, in that many model assumptions may be improved upon as further research is conducted at Lake Tahoe. Therefore the results presented should also be considered as preliminary.

Two types of purposes are demonstrated. The first relates to some of the pressing management issues at Lake Tahoe. Three cases are considered. These are the effects of changing the stream water quality inputs, the effects of changing atmospheric water quality inputs, and finally a consideration of which potential end states may realize the desired level of water clarity. These cases were run for 1999 only. The changes imposed are purely hypothetical and do not necessarily represent what may be achievable in the Tahoe Basin. These results are all presented in terms of changes in the Secchi depth, as the issue of water clarity in Lake Tahoe is the focus of this research. Other measures that are not shown may display different degrees of change. Linked to this is the acknowledgement that the present simulations are for one year only, and that the results cannot be extrapolated in time. Thus a change that has no effect on Secchi depth in the first year may still alter lake conditions below the Secchi depth, so that in subsequent years the Secchi depth is indeed affected.

The second demonstration relates to some of the outstanding research issues that the model may be applied toward. The one example used is to contrast the limiting factors on algal growth for the two years modeled, 1992 and 1999. Again, the model results are not intended to explain what is necessarily occurring, but to help redefine the basic research questions that may still need to be addressed.

8.1 Changes in Nutrients and Particles in Stream Inflows

To examine the potential effect of changes in management in the Tahoe watershed, the nutrient and particle loads carried by the streams was altered in the stream input files. For Nitrogen all the N-species that were modeled (NO3, NH4, DON, and PON) were simultaneously reduced by the same fractions. For Phosphorous, all the P-species modeled (SRP, DOP, POP and RP) were likewise reduced. The same reduction factor was applied to all the 21 modeled inputs. For the reduction of particles in streams, only the inorganic particles (across the seven size classes) were considered. In all cases the flow of stream water was unchanged, and the assumed groundwater contribution to water quality was not changed. The hydrograph for the principal inflow, the Upper Truckee River is shown in **Fig. 4.4 B**. The baseline case represents the unaltered input files as used in the calibration exercise of **Chapter 7**. It should be noted in interpreting the following figures that the stream insertion depths vary with stream density (i.e. temperature) and the ambient lake density profile. Thus the insertion depth varies throughout the year and can frequently be below the Secchi depth.

Figure. 8.1 A-C shows the results for reductions in stream particles, nitrogen and phosphorus respectively. The number of particles was varied by a factor of 10 both above and below the baseline case. The assumed particle size concentration was held constant throughout the year, although stream flow rate varied daily. As described in Section 4.2, stream particle data were based on a small set of measurements (Coker, 2000) that varied from 7.3×10^3 to 1.2×10^6 particles ml^{-1}, with a mean of 1.8×10^5 particles ml^{-1}. For the baseline, the latter value was used. However, as the range of measurements is so large, and the effect of particles on clarity so pronounced it was considered prudent to explore a wide range of changes of particle concentration. For both nitrogen and phosphorus, a single reduction of 50% was considered.

Figure 8.1 A shows that an increase of particle numbers in the inflow by a factor of 10 has a dramatic impact on Secchi depth, decreasing it by up to 2 m during the summer and fall. A similar reduction in particle concentration yields almost no change from the baseline.
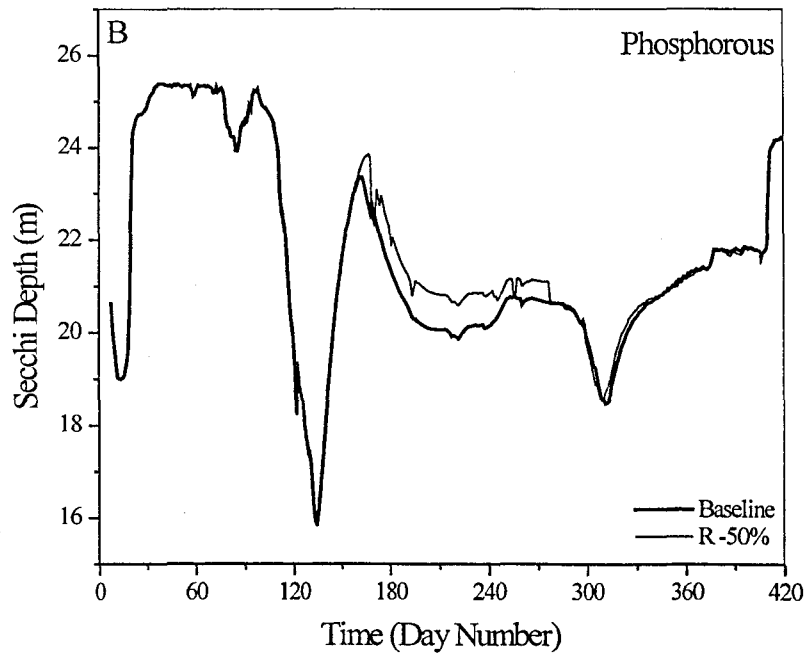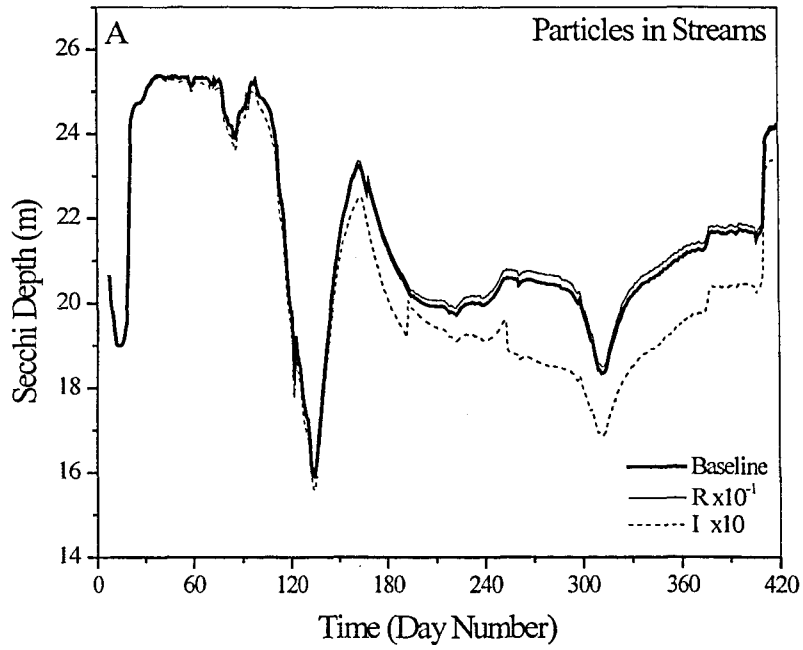
186

Figure 8.1 Streams scenarios for year 1999: A) particle reduction, B) Phosphorous reduction, and C) Nitrogen reduction.
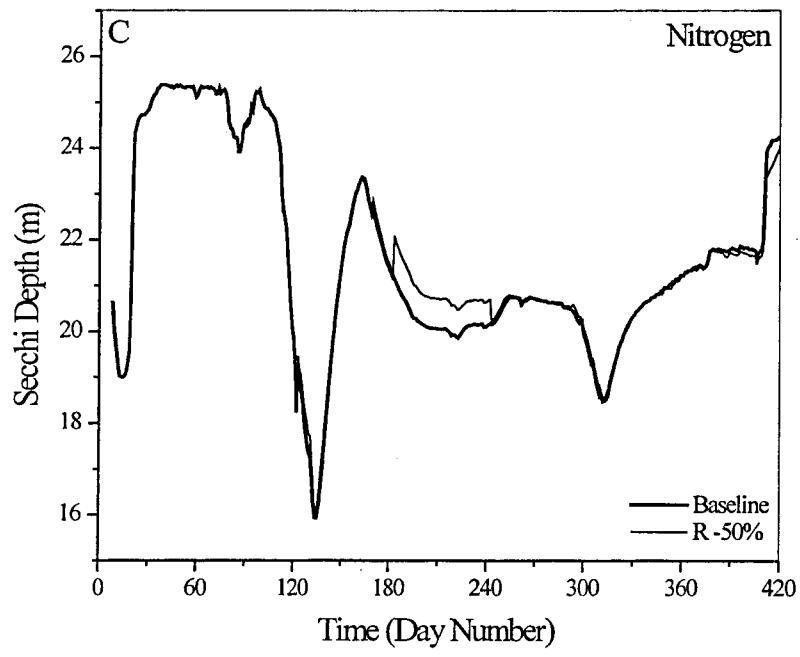
Figure 8.1 Continued.

While it is unknown what fraction of fine particle reduction can be attained in practice, what these results mainly show is that model output may change as more information on stream particle concentration and size distribution is collected.

Figure 8.1 B, C shows the effect of Phosphorus and Nitrogen reductions. Improvements in Secchi depth are on the order of 1 m. However, as both particulate and dissolved forms of these nutrients were reduced, it is the combined effect of both a reduction in scattering and absorption by Chla that have yielded this result.

8.2 Changes in Atmospheric Nutrient Deposition

Figure 8.2 A, B shows the effects of a 50% reduction of atmospheric deposition of Phosphorus and Nitrogen, respectively. Inorganic particle input by atmospheric loading is not considered in the model. As in **Section 8.1**, it is observed that the improvement in Secchi depth is of the order of 1 m for either nutrient. It is interesting to note that atmospheric deposition acts constantly during the year (although supplying nutrients at different rates depending on the succession of wet and dry days), whereas the distribution of nutrient supply by streams has a more seasonal behavior. Despite this it can be observed that the effect of both sources of nutrients is to alter Secchi depth during the summer and fall only. The reason for this is that in the spring, immediately after deep mixing, there is a large input of internal nutrients that drives the drop in Secchi depth observed to start around day 90. The improvement in clarity by a reduction in the external loads only occurs once these internal nutrients have been consumed.

8.3 Potential End States

The previous two sections have shown that changes in the input loadings of nutrients and particles can change the predicted Secchi disk. The amount of change in one year has been seen to be quite modest. This suggests that the store of nutrients and particles that are presently in the lake are much larger the relatively small amounts added externally in one year.
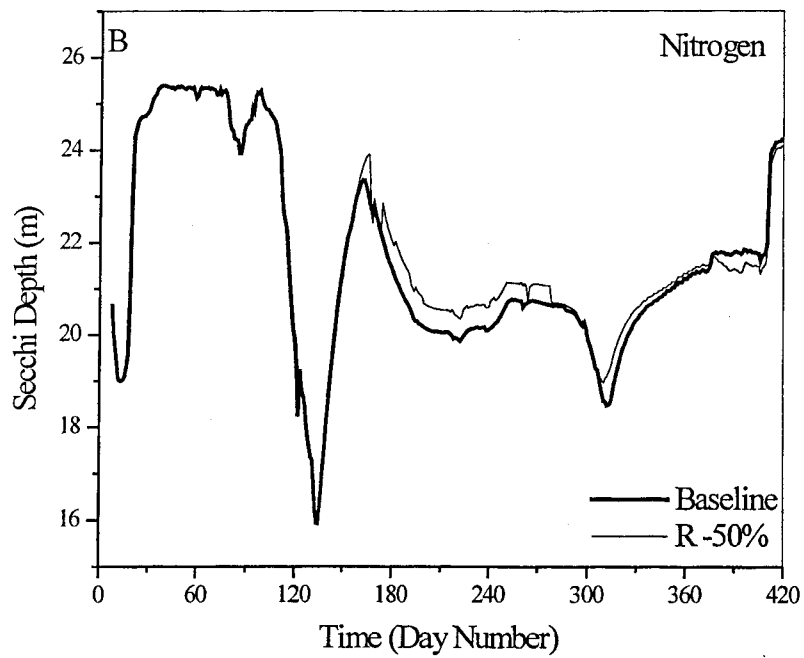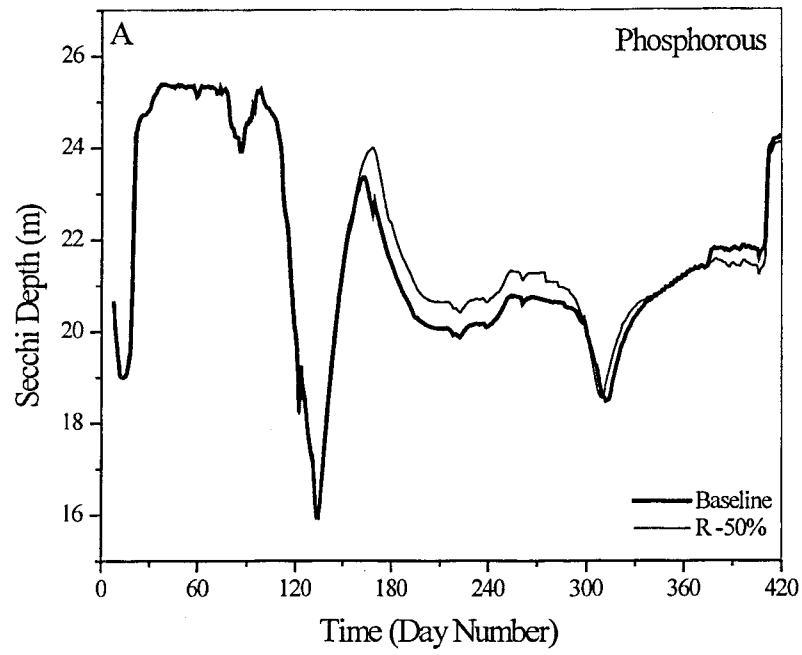
Figure 8.2 Atmospheric nutrient deposition for 1999: A) Nitrogen species reduction, and B) Phosphorous species reduction.

This is not surprising, given the lakes long hydraulic residence time. The cumulative effect over many years will in all likelihood be greater, however, it is beyond the scope of the present work to construct a synthetic long term data set to explore this issue further. Instead, a simpler approach is taken. The initial conditions that the model is give are altered by significant amounts to test the idea of what type of end state lake managers should be aiming for to yield particular water clarity improvements. Three cases were considered - increasing and reducing all inorganic particles, SRP, and NO3 respectively. In each case the initial profile supplied to the model for the test variable was changed by ±50%. All other inputs were as for the baseline case.

Figure 8.3 A shows the impact for changes in the initial concentration of all inorganic particles. The effect is dramatic. If the number of particles in Lake Tahoe were reduced by 50% (particularly in the finer class sizes) then the average Secchi depths through the year would be on the order of 30 m. A 50% increase would yield a further decline in clarity, although interestingly the change is not linear.

Similar concentration changes for the two nutrients (**Figs 8.3 B**, and **C**) produce changes in the predicted Secchi depth, but at a much reduced level. Note the different scale used in plotting these three figures compared with **Fig. 8.3 A.** In other words, if the nutrient concentration in the lake is reduced by 50%, then the improvement in clarity will be small. For SRP, in **Fig. 8.3 B**, a decrease in the initial profile produced a slight improvement in clarity. Surprisingly, an increase in concentration had either no effect or a slight improvement in clarity! Seemingly the dependence of lake clarity on phosphorus under present conditions is not very strong, although this does not mean that the addition of SRP does not increase total algal biomass. **Figure 8.3 C**, for NO3 shows a slightly greater effect than was evident for SRP. However, the change in Secchi depth is only of the order of 1 m with a 50% reduction in concentration.
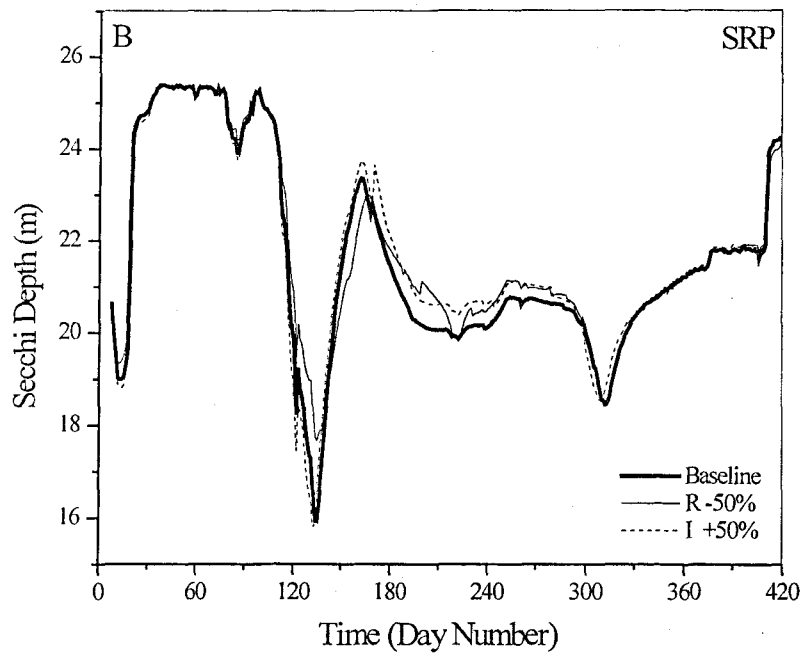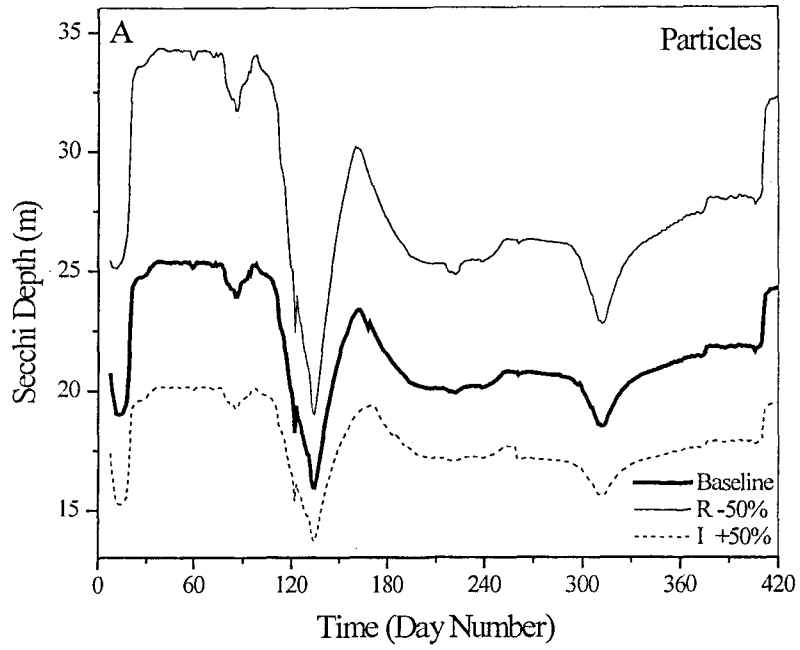
Figure 8.3 Effects on the predicted Secchi depth due by initial conditions: A) Particles, B) SRP, C) NO3, and D) NH4.
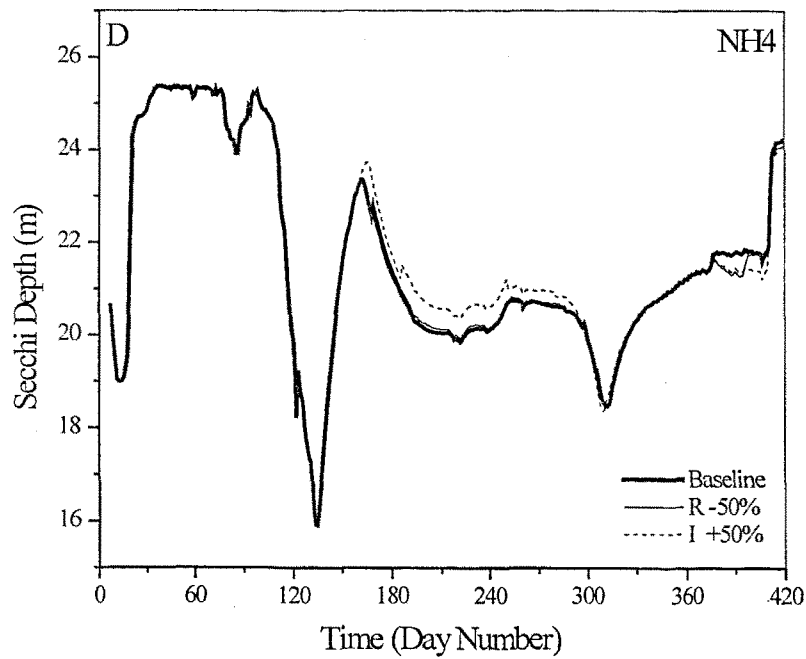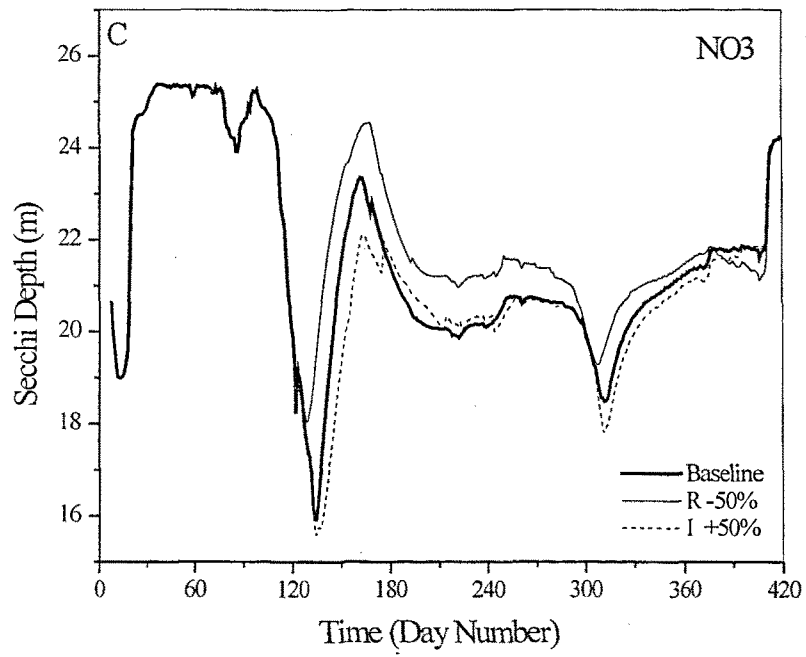
Figure 8.3 Continued.

8.4 Control of Algal Growth

As discussed in **Section 2.3**, the nutrient balance in Lake Tahoe has shifted in the last few decades from a classically N-limited alpine system, to a co-limited system between N and P. This interplay of nutrients can be examined using DLM-WQ. Recall that the model uses a minimum limiting nutrient formulation for algal growth. For each model layer, and at each sub-daily step, growth of phytoplankton is limited by a factor that is obtained from Eqn. (3.9), Eqn (3.10), and Eqn (3.11) as the minimum of the P, N and Light functions respectively. **Figure 8.4 A** maps the nature of growth limitation for the 1999 baseline case by plotting which resource limits. This is compiled at 12 noon, because limitation varies over the day, giving a totally light limited system at night. Only the upper 200 m have been plotted, as deeper water is always light limited. Each point is mapped according a code: 0 indicates P-limited, 1 indicates N-limited, and 2 indicates Light-limited. Each code is then assigned a gray scale value, such that P-limited is black, N-limited is gray, and Light-limited is white.

It can be seen that there is a variation of the limiting resource both in time and vertically through the water column. In the vertical, there exists a pronounced 3-layer structure. The top 10 to 20 m is limited by light inhibition, the precise depth varying throughout the year. There is a mid layer down to about 75 m depth where nutrients limit growth. Below this there is a layer that extends to the bottom where low levels of light limit growth.

Over time the middle layer is observed to shift between the P-limitation of winter, to a mainly N-limited structure from day 150 to 370. This is due to deep mixing in winter being responsible for adding large quantities of nitrate to the surface layers. 1999 was a year in which deep mixing was very pronounced. Once thermal stratification occurs and the available nitrogen is consumed, nitrogen takes over as the limiting nutrient. By day 370, layers of both N-limitation and P-limitation are seen. Also is noted a P limitation on the top layers by days 320 to 350. The nutrient limited layer experiences a vertical movement along the time, oscillating between surface to 75m of depth.
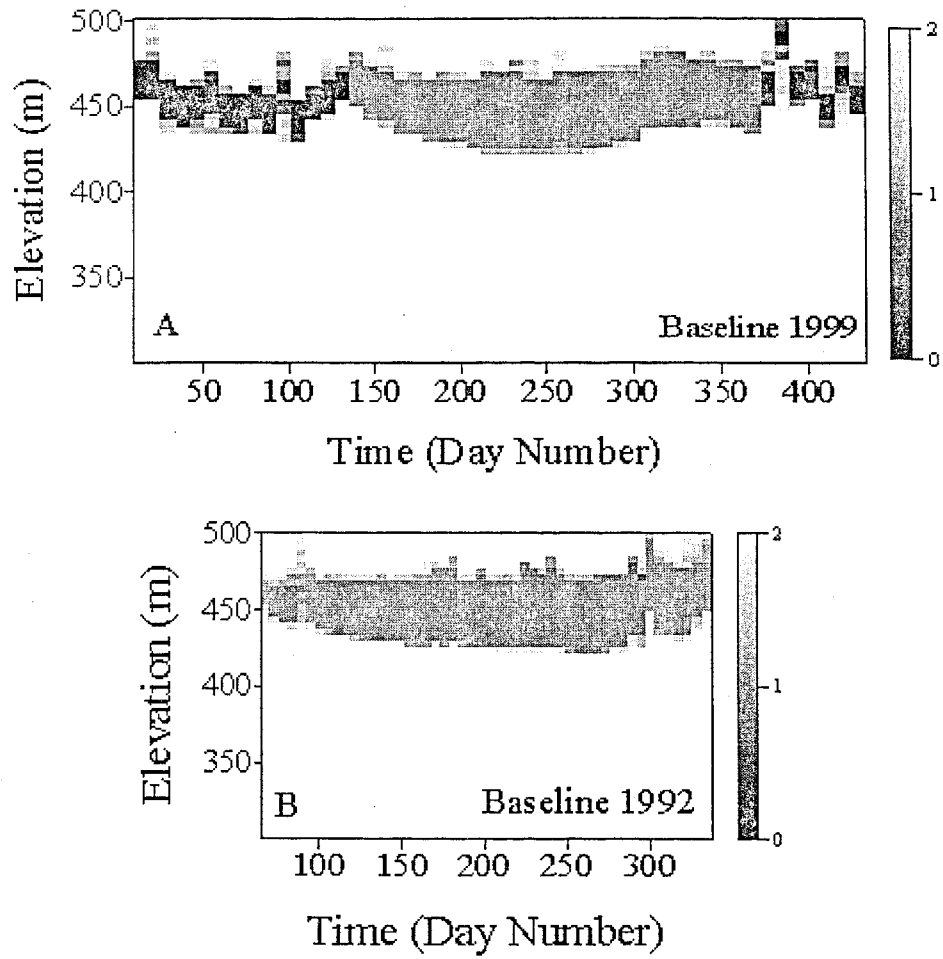
Figure 8.4 Growth limitation map: A) 1999 and B) 1992.

Part of the results of **Section 8.3** can now be better understood using these figures. Firstly, as the lake is light limited down to almost 20 m for much of the year, it is not surprising that changes in the nutrient levels do not have much effect on predicted Secchi depth. Chla concentration above the Secchi depth will only increase marginally and as Chla has only a relatively small effect of light transmission, the net change will be small. Similarly, the change in the middle of the year when phosphorus concentration is altered, is very slight. As the lake is nitrogen limited during that part of the year, phosphorus additions will have a small impact.

Fig 8.4 B shows the baseline case for 1992. Again, the 3-layer structure with vertical segmentation is repeated for 1992. Comparing the two baseline cases, it is evident that 1992 is N-limited through the year. 1992 and 1999 represent different states of the lake system: for 1992, the water column does not mix completely, while it does for 1999. This strong mixing event, supplies nutrients to the surface layers.

8.5 Conclusions

The four applications considered produced some interesting results and point to the utility of the model. Changing the water quality constituents of the streams and the atmospheric deposition, yielded changes in Secchi depth, but these were quite small. Improving water clarity at Lake Tahoe will clearly take many years of reduced loading. An estimate of how long this may take will require the development of a synthetic long-term data set. An indication of the type of change that will be required was obtained by altering the model's initial conditions. This suggested that the concentration of fine particles will need to be reduced by a factor of two before the lake reaches its pre-1970 clarity level. Reductions in nutrient concentrations appear to have a much smaller effect. Winter mixing is also seen to be remarkable as it determines to great extent the following year's nutrient limitation. It suggests that the lake is still primarily nitrogen limited, and phosphorus limitation occurs only after deep mixing, when there is a relative over-supply of nitrogen.

Chapter 9: Summary and Conclusions

This thesis had as its primary goal the development of a one-dimensional (preserving the vertical direction), coupled, hydrodynamic, ecological and optical model to predict water clarity in lakes and reservoirs as an aid to their management. In particular, the model was to be tested at Lake Tahoe, a lake that is clearly three dimensional in nature, and one that presently faces questions of how to best manage the watershed and the lake to restore lake clarity. To achieve this goal, there were four objectives:

- the implementation of new water quality and optical sub-models into DLM-WQ
- developing a calibration strategy based on a Genetic Algorithm technique.
- validating the model.
- describing the effects of different management and physical scenarios on lake water quality and on clarity.

The goal of the thesis has been met. Each of the stated objectives has been achieved, and in so doing a model that can address quantitatively the prediction of water clarity in Lake Tahoe has been developed. The adopted one-dimensional approach appears to adequately describe the changing conditions in the lake for two independent time periods of approximately one year's duration. Although a complete validation with for 1992 was not possible because of the total absence of particle data for that year (and the dominant role that fine particles have on lake clarity) the other measured lake parameters such as chlorophyll and nutrients compared well.

In a general sense the present model could be applied to any lake in which chlorophyll and particles are the primary determinant of water clarity, and in which a one-dimensional representation is appropriate. It is noteworthy that although Lake Tahoe is three-dimensional insofar as internal rotational effects are concerned, these did not appear to compromise the model's ability to match either the temperature profiles or

the water quality profiles. On the other hand, this model may not be appropriate (in its present form) for a lake that has a large contribution to light absorption by CDOM.

In a similar vein, the GA technique for model calibration has shown itself to be very effective at speeding and refining the process of model calibration, and could be implemented in any model where calibration is required. Although work still remains to be done on exploring how best to use the GA, it clearly was a successful approach.

For the particular case of Lake Tahoe, the model results suggest some interesting conclusions. These should, however, be taken as preliminary. For the present work only one-year simulations were conducted, and it is evident that the evolution of changes in water clarity will occur over many years. Firstly, it seems that the fine particles are exerting by far the largest influence on water clarity at Lake Tahoe. A reduction in the lake particle inventory by approximately 50% is required to return the lake to the clarity levels experienced 30 years ago. By contrast, removal of nutrients alone could not achieve this result. Of the principal sources of external nutrients, streamflow and atmospheric deposition, both appear on the basis of one-year simulations to have similarly small effects on clarity changes within a 12 month time frame. A comparison of their effects over the long term still remains to be considered. The effect of reducing stream-borne particles on water clarity appeared to be larger in magnitude than the effects of reducing stream-borne nutrients. However, this result must also be treated cautiously as the available data on stream-borne particles is sparse (compared with the nutrient data).

The model has shown its value as a tool to examine the driving forces of Lake Tahoe, both in a physical and ecological sense. The model structure allows for testing new hypothesis. For example, the role of Mysis and its interaction in the nutrient budget of the lake, acting as a biological pump of nutrients, has been treated quite simply in the present model. However, a number of different hypotheses could readily be tested. This would need to be done in close cooperation between modelers and field researchers.

Identification of data gaps has been highlighted as result of the modeling conducted to date. As has been demonstrated, the ability to calibrate and validate the model is

mainly limited by the poor spatial and temporal resolution of the data. In a broader context, it should be recognized that Lake Tahoe has a relatively high degree of monitoring, and that even greater data issues would exist for most other lakes. One of the most important findings of the model has been to identify the role of the inorganic and organic particles as a key factors in determining the clarity of Lake Tahoe, and the critical importance of determining the relative fraction of inorganic and organic sediments.

Once calibrated (for the intended use of the model), the test cases suggest that the model can be used to quantify magnitude and timing of responses to management changes. A better test of this will come once the model is run with multi-year data sets. Interestingly, even for one year simulations, the results of **Chapter 8** suggest that the lake (as modeled) does not respond linearly to changes in the inputs. This effect is likely to be more pronounced for multi-year simulations, thus pointing to the value of the model for management hypothesis testing.

Of future research that should be undertaken, then are a number of areas that stand out. The first is the construction of representative long-term synthetic data set. Long term simulations require to the definition and generation of sets of synthetic data of meteorological variables, stream inputs and outflows. Thus, it is needed an additional research to define adequate criteria that reflects the range of variability usually found in the lake and its watershed. A range of time scales will need to be captured in this data set, including El Nino effects, drought cycles, climate change and prely random variability.

Secondly, particles interactions are of key concern, because of the dominance that the particles appear to have on light attenuation. Areas that need further work include more data on the particle size distribution and its composition. An equally important area that has not been addressed in the present work are mechanisms of particle aggregation and removal from the water column. While this could be neglected for the one year simulations undertaken here, long term simulations are not possible without considering it fully.

For the purposes of producing an operating model in a reasonable time, relatively standard formulations were utilized for primary production and nutrient uptake. While these may indeed be satisfactory, it would be wise to consider some of the newer approaches that are now appearing in the literature. A related area to this is the better definition of the role of zooplankton and Mysis grazing on nutrient dynamics.

The temporal structure of the DCM is not completely reproduced by the model. This can be partially attributable to the calibration effort was focused on the top layers (relevant to determine the light distribution). However, further studies are required to explore the adequacy of the proposed relationships that describe the phytoplankton dynamics. Ratio constants and parameters of the microbial loop were assumed constants in time and space. The assumed constant ratio contents between Chla and nutrients may be changed with a formulation that takes into account the observed variability. The DCM is a very pronounced feature at Tahoe and in many oligotrophic systems, and it should be able to be adequately modeled.

The GA technique has been shown to be a useful for calibration purposes. The way in which it was implemented was complementary to the best judgment decisions by the modeler. Parallel implementation of the GA is the next natural step on the future development, as the CPU time required to achieve the convergence criteria for most of the simulations has been very long. The overall procedure is slowed by the time required to run DLM-WQ. The time spent manipulating the chromosomes during the selection or recombination phase is usually negligible. As the direct parallelization of the DLM-WQ code is not straightforward (it is indeed defined to run sequentially), it is believed that the time reduction may be attained by a class of parallel GAs in which sub-populations can be run independently on different processors.

References

Abbot, M.R., Denman, K.L., Powell, T.M., Richerson, P.J., Richards, R.C., and Goldman, C.R. (1984). "Mixing and the dynamics of the deep chlorophyll maximum in Lake Tahoe." *Limnol. Oceanogr.*, 29: 862-878.

Abbot, M.R., Powell, T.M. and Richerson, P.J. (1982). "The relationship of environmental variability to the spatial patterns of phytoplankton biomass in Lake Tahoe." *J. Plankton Res.*, 4(4): 927-941.

Ahlgren, I., Frisk, T., and Kamp-Nielsen, L. (1988). "Empirical and theoretical models of phosphorous loading, retention and concentration vs. trophic state." *Hydrobiologia*, 170: 285-303.

Beasley, D., Bull, D.R. and Martin, R.R. (1993a). "An overview of genetic algorithms: Part 1, Fundamentals." *University Computing*, 13(2): 58-69.

Beasley, D., Bull, D.R. and Martin, R.R. (1993b). "An overview of genetic algorithms: Part 2, Research Topics." *University Computing*, 15(4): 170-181.

Beck, M.B. (1983). "Sensitivity analysis, calibration and validation." In: G.T. Orlob and G.T. John (Editors), *Mathematical Modeling of Water Quality: Streams, Lakes and Reservoirs*. International Series on Applied Systems Analysis, Wiley and Sons, 425-467.

Beck, M.B. (1987). "Water quality modelling: a review of the analysis of uncertainty." *Water Res.*, 23(8): 1393-1442.

Bloss, S. and Harleman, D.R.F. (1980). "Effects of wind induced mixing on the seasonal thermocline in lakes and reservoirs." In: I.T. Carstens and T. McClimans (Ed.) *2nd International Symposium on Stratified Flows*, Vol. I, Trondheim, Norway.

Bohren, C.F. and Huffman, D.R. (1983). *Absorption and scattering of light by small particles*. Wiley, New York, 530 p.

Bowie, G.L., Mills, W.B., Porcella, D.B., Campbell, C.L., Pagenkopf, J.R., Rupp, G.L., Johnson, K.M., Chan, P.W.H., Gherini, S.A. and Chamberlain, C.E. (1985). *Rates, constants, and kinetics formulations in surface water quality modeling*, Tetra Tech, Incorporated. 2nd ed. Athens, U.S. Environmental Protection Agency, EPA 600/3-85/040, 455p.

Buiteveld, H., Hakvoort, J.H.M. and Donze, M. (1994). "The optical properties of pure water." *Ocean Optics XII*. SPIE vol. 2258:174-178.

Burgi, H.R., Elser, J.J., Richards, R.C. and Goldman, C.R. (1993). "Zooplankton patchiness in Lake Tahoe and Castel Lake USA." *Verh. Internat. Verein. Limnol.*, 25:378-382.

Byron, E.R. and Goldman, C.R. (1986). *Changing Water Quality at Lake Tahoe: The first five years of the Lake Tahoe.* Interagency Monitoring Program. Univ. California-Davis.

Byron, E.R., and Eloranta, P. (1984). "Recent historical changes in the diatom community of Lake Tahoe, California-Nevada, USA." *Verh. Internat. Verein. Limnol.,* 22: 1372-1376.

Byron, E.R., Folt, C.L. and Goldman, C.R. (1984). "Copepod and cladoceran success in an oligotrophic lake." *J. Plankton Res.,* 6: 45-65.

Carney, H.P. (1987). "Field tests of interspecific resource-based competition among phytoplankton." *Proc. Nation. Ac. Sci. (USA),* 84: 4148-4150.

Carney, H.P., Richerson, P.J., Goldman, C.R. and Richards, R.C. (1988). "Seasonal phytoplankton demographic processes and experiments on interspecific competition." *Ecology,* 69: 664-678.

Carroll, D.L. (1996a). "Chemical laser modeling with genetic algorithms." *AIAA J.,* 34(2): 338-346.

Carroll, D.L. (1996b) "Genetic Algorithms and Optimizing Chemical Oxygen-Iodine Lasers," In: H.B. Wilson, R.C. Batra, C.W. Bert, A.M.J. Davis, R.A. Schapery, D.S. Stewart, and F.F Swinson, (Editors), *Developments in Theoretical and Applied Mechanics,* Vol. XVIII. School of Engineering, The University of Alabama, 411-424.

Carstensen, J., Vanrolleghem, P., Rauch, W. and Reichert, P. (1997). "Terminology and methodology in modelling for water quality management- a discussion starter." *Water Sci. Technol.,* 36(5): 169-175.

Casamitjana, X. and Schladow, S.G. (1993). "Vertical distribution of particles in a stratified lake." *J. Eng. Eng.,* ASCE, 119(3): 443-462.

Chapra, S.C. (1997). *Surface Water-Quality Modeling.* McCraw-Hill, New York, 844p.

Chapra, S.C. and Reckhow, K.H. (1983). *Engineering approaches for lake management, Vol. 2.,* Ann Arbor Science, Boston, 492p.

Coker, J. (2000). *Optical water quality of Lake Tahoe,* Masters Thesis, University of California, Davis.

Cole, T.M. and Buchak, E.M. (1995). *CE-QUAL-W2: a two-dimensional, laterally averaged, hydrodynamic and water quality model, version 2.0.* Instruction Report EL-95- U.S. Army Corps of Engineers, Waterways Experiment Station. Vicksburg, MS.

Coon, T.G. (1978). *The deep chlorophyll maximum layer of Lake Tahoe, California-Nevada.* Masters Thesis, University of California, Davis.

202

Coon, T.G., Lopez, M., Richerson, P.J., Powell, T.M. and Goldman, C.R. (1987). "Summer dynamics of the deep chlorophyll maximum in Lake Tahoe." *J. Plankton Res.*, 9: 327-344.

Davies-Colley, R.J. (1988). "Measuring water clarity with a black disk." *Limnol. Oceanogr.*, 33(4, part 1): 616-623.

Davies-Colley, R.J. and Vant, W.N. (1988). "Estimation of optical properties of water from secchi disk depths." *Water Resour. Bull.* 24(6): 1329-1335.

Davies-Colley, R.J., Vant, W.N. and D.G. Smith. (1993). *Colour and clarity of natural waters: science and management of optical water quality.* Ellis Horwood, New York. 310p.

DiToro, D., O'Connor, S. and Thomann, R. (1971). "A dynamic model of the phytoplankton population in the Sacramento-San Joaquin Delta." *Nonequilibrium systems in water chemistry*, America Chemical Society, Washington, D.C., 1931-180.

Doney, C. S., Glover, D. M. and Najjar, R. G. (1996). "A new coupled, one-dimensional biological-physical model for the upper ocean: application to the JGOFS Bermuda Atlantic Time-series Study (BATS) site." *Deep-Sea Res. II*, 43(2-3): 591-624.

Duffie, J.A. and William A.B. (1991). *Solar engineering of thermal processes.* 2nd ed. Wiley, New York, 919p.

Effler S.W., and Perkins, M. (1996). "An optics model for Onondaga Lake." *Lake and Reserv. Manage.* 12(1): 115-125.

Effler S.W., Johnson, D.L., Jiao, J.F., and Perkins, M. (1992). "Optical impacts and sources of suspended solids in Onondaga Creek, USA." *Water Resour. Bull.* 28(2): 251-262.

Effler S.W., Perkins, M. and Johnson, D.L. (1998). "The optical water quality of Cannonsville Reservoir: Spatial and temporal patterns, and the relative roles of phytoplankton and inorganic tripton." *Lake and Reserv. Manage.* 14(2-3): 238-253.

Effler Steven W. (1988). "Secchi disc transparency and turbidity." *J. Environ. Eng.* ASCE 114(6): 1436-1447.

Elser, J.J. and Goldman, C.R. (1991). "Zooplankton effects on phytoplankton in lakes of contrasting trophic status." *Limnol. Oceanogr.* 36: 64-90.

Eppley, R.W., Rogers, N.J. and McCarthy J.J. (1969). "Half-Saturation Constants for Uptake of Nitrate and Ammonium by Marine Phytoplankton." *Limnol. Oceanogr.* 14(6): 912-920.

Ferris, J.M. and Christian, R. (1991). "Aquatic primary production in relation to microalgal responses to changing light: a review", *Aquat. Sci.*, 53(2-3): 1015-1621.

Fischer, H. B., List, E. J., Koh, R. C. Y., Imberger, J., and Brooks, N. H. (1979). *Mixing in Inland and Coastal Waters*. Academic Press, San Diego, 483p.

Gaillard, J. (1981). A predictive model for water quality in reservoirs and its application to selective withdrawal. Doctoral Dissertation. Colorado State University, Fort Colllins, 230 p.

Gardner, J.V., Larry, A.M. and Clarke, J.H. (1998). *The bathymetry of Lake Tahoe, California-Nevada*. US Geological Survey, Open-File Report 98-509.

Gardner, R.H., O'Neill, R.V., Mankin, J.B. and Carney, J. H. (1981). "A comparison of sensitivity analysis and error analysis based on a stream ecosystem model." *Ecol. Model.* 12: 173-190.

Gecek, S. and Legovc, T. (2001). "Nutrients and grazing in modeling the deep chlorophyll maximum." *Ecol. Model.*, 138: 143-152.

Goldberg, D.E. (1991) "A comparative analysis of selection schemes used in genetic algorithms." In: Gregory Rawlins (Editor), *Foundations of Genetic Algorithms*, Morgan Kaufmann Pub., San Mateo, CA, 69-93.

Goldberg, D.E. (1989). *Genetic Algorithms in search, optimization and machine learning*. Addison-Wesley, Reading, Mass., 412 p.

Goldberg. D.E., Deb, K. and Clark, J.H. (1992) "Genetic Algorithms, Noise, and the Sizing of Populations." In: *Complex Systems*, 6, Complex Systems Pub. Inc., 333-362.

Goldman, C.R. (1974). *Eutrophication of Lake Tahoe emphasizing water quality*. EPA-660/3-74-034, U.S. Gov. Printing Office. 408 p.

Goldman, C.R. (1981). "Lake Tahoe: Two decades of change in a nitrogen deficient oligotrophic lake." *Verh. Internat. Verein. Limnol.,* 21: 45-70.

Goldman, C.R., (1988). "Primary productivity, nutrients and transparency during the early onset of eutrophication in ultra-oligotrophic Lake Tahoe, California-Nevada." *Limnol. Oceanogr.,* 33(6): 1321-1333.

Goldman, C.R., and Jassby, A.D. (1990). "Spring mixing depth as a determinant of annual primary production in lakes." In: M.M. Tilzer and C. Serruya (Editors), *Large Lakes: ecological structure and function*. Springer-Verlag, 125-132p.

Goldman, C.R., Jassby, A.D. and Hackley, S.H. (1993). "Decadal, interannual, and seasonal variability in enrichment bioassays at Lake Tahoe, California-Nevada, USA." *Can. J. Fish. Aquat. Sci.,* 50 (7): 1489-1496.

Goldman, C.R., Jassby A.D., and Powell T. (1989). "Interannual fluctuations in primary production: meteorological forcing at two subalpine lakes." *Limnol. Oceanogr.,* 34(2): 310-323.

Goldman, C.R., Morgan M.D., Threlkeld, S.T., and Angeli, N. (1979). "A population analysis of the cladoceran disappearance from Lake Tahoe, California-Nevada." *Limnol. Oceanogr.*, 24: 289-297.

Hakanson, L., and Peters, R. H. (1995). *Predictive Limnology. Methods for predictive modeling.* SPB Academic Publishing, Amsterdam, 464 p.

Hamilton, D.P. and Schladow, S.G. (1997). "Prediction of water quality in lakes and reservoirs. Part I - Model description." *Ecol. Model.,* 96: 91-110.

Haney, J.D. and Jackson, G.A. (1996). "Modeling phytoplankton growth rates." *J. Plankton Res.,* 18(1): 63-85.

Hatch L.K. (1997). *The generation, transport, and fate of Phosphorous in the Lake Tahoe ecosystem.* Doctoral dissertation. University of California, Davis.

Hatch, L.K., Reuter, J.E. and Goldman C.R. (1999). "Relative importance of stream-borne particulate and dissolved phosphorus fractions to Lake Tahoe phytoplankton." *Can. J. Fish. Aquat. Sci.,* 56 (12): 2331-2339.

Hatch. L.K., Reuter, J.E. and Goldman, C.R. (2001). "Stream phosphorus transport in the Lake Tahoe Basin, 1989-1996." *Environ.l Monit. Assess.* 69: 63-83.

Henderson-Sellers, B. (1986). "Calculating the surface energy balance for lake and reservoir modeling: a review." *Reviews of Geophysics,* 24(3): 625-649.

Henderson-Sellers, B. (1988). "Sensitivity of thermal stratification models to changing boundary conditions." *Appl. Math. Model.* 12: 31-43.

Henderson-Sellers, B. (1989). "The sensitivity of thermocline models to parametrisations of the surface energy budget and of wind mixing." *Arch. Hydrobiol.,* 33: 113-122.

Henderson-Sellers, B. and Henderson-Sellers, A. (1996). "Sensitivity evaluation of environmental models using fractional factorial experimentation." *Ecol. Model.* 86: 291-295.

Heyvaert, A.C. (1998). *Biogeochemistry and paleolimnology of sediments from Lake Tahoe, California-Nevada.* Doctoral dissertation. University of California, Davis.

Hocking, G.C., Sherman, B.S. and Patterson, J.C. (1988). "An algorithm for selective withdrawal from a stratified reservoir." *J. Hydr. Div.,* ASCE, 114(7): 707-719.

Holland, J.H. (1975). Adaptation in Natural and Artificial Systems. MIT Press, 183p.

Holm-Hansen, O., Goldman, C.R. and Richards, R.C. (1976). "Chemical and biological characteristics of a water column in Lake Tahoe." *Limnol. Oceanogr.,* 21(4): 548-562.

Horne, A. J., and Goldman, C. R. (1994). *Limnology*. 2nd ed. McGraw-Hill, New York, 576 p.

Hüe, X., (1997). *Genetic Algorithms for Optimisation. Background and Applications*. Technology Watch Report. Edinburgh Parallel Computing Center. University of Edinburgh.

Hunter, D.A., Goldman, C.R. and Byron, E.R. (1990). "Changes in the phytoplankton community structure Lake Tahoe, California-Nevada." *Verh. Internat. Verein. Limnol.,* 24: 504-508.

Hutter, K. (1984). *Hydrodynamics of Lakes*. Springer-Verlag, New York, 341p.

Hutter, K. (1986). "Hydrodynamic modeling of lakes." In *Encyclopedia of Fluid Mechanics*. Gulf Publishing, Houston, 897-998.

Imberger, J. (1982). "Reservoir dynamic modeling." In: *Prediction of Water Quality*, E. M. O'Loughlin and P. Cullin (Eds.), Aust. Acad. Sci., Canberra, 223-248.

Imberger, J. and Parker, G. (1985). "Mixed layer dynamics in a lake exposed to a spatially variable wind field." *Limnol. Oceanogr.*, 39: 473-488.

Imberger, J. and Patterson, J. C. (1981). "A dynamic reservoir simulation model - DYRESM: 5", in *Transport Models for Inland and Coastal Waters*, edited by H. B. Fischer, Academic Press, New York, 310-361.

Imberger, J. and Patterson, J.C. (1990). "Physical Limnology." In: *Advances in Applied Mechanics*, 27: 303-475.

Imberger, J., Patterson, J.C., Hebbert, R.H.B. and Loh, I.C. (1978). "Dynamics of a reservoir of medium size." *J. Hydr. Div., ASCE*, 104(HY5): 725-743.

Imberger, J., Thompson, R.O.R.Y., and Fandry, C. (1976). "Selective withdrawal from a finite rectangular tank." *J. Fluid Mech.*, 78: 489-512.

Ivey, G. N. and Patterson, J.C. (1984). "A model of the vertical mixing in Lake Erie in summer." *Limnol. Oceanogr.*, 29: 553-563.

Janse, J.H., Vandonk, E. and Aldenberg, T. (1998). "A model study on the stability of the macrophyte-dominated state as affected by biological factors." *Wat. Res.* 32: 2696-2706.

Jassby, A.D. and Platt, T. (1976). "Mathematical formulation of the relationship between photosynthesis and light for phytoplankton." *Limnol. Oceanogr.*, 21: 540-547.

Jassby, A.D., Goldman, C.R. and Powell, T.M. (1992). "Trend, seasonality, and irregular fluctuations in primary productivity at Lake Tahoe, California-Nevada, USA).", *Hydrobiologia*, 246: 195-203.

206

Jassby, A.D., Goldman, C.R. and Reuter, J.E. (1995). "Long-term change in Lake Tahoe (California-Nevada, U.S.A.) and its relation to atmospheric deposition of algal nutrients.", *Arch. Hydrobiol.*, 135(1): 1-21.

Jassby, A.D., Goldman, C.E. and Richards, R.C. (1999). "Origins and scale dependence of temporal variability in the transparency of Lake Tahoe, California-Nevada." *Limnol. Oceanogr.*, 44(2): 282-294.

Jassby, A.D., Goldman, C.R., Reuter, J.E., Richards, R.C. and Heyvaert, A.C. (2001). "Lake Tahoe: Diagnosis and rehabilitation of a large mountain lake. The Great Lakes of the World (GLOW)" in *Food-web, health and integrity.* (ed.) M. Munawar and R.E. Hecky, Ecovision World Monograph Series, 431-454.

Jassby, A.D., Reuter, J.E., Axler, R.P., Goldman, C.R. and Hackley, S.H. (1994). "Atmospheric deposition of nitrogen and phosphorus in the annual nutrient load of Lake Tahoe (California-Nevada)." *Water Res.*, 30: 2207-2216.

Jorgensen, S.E. (1983). "Eutrophication models of lakes." In: S.E. Jorgensen (Editor), *Application of ecological modelling in environmental management,* part A., Amsterdam, Elsevier Sci. Publ., 227-282.

Jorgensen, S.E. (1993). "State of the art of ecological modeling." In: *International Congress on Modelling and Simulation*, Perth, Western Australia, proc. 2: 455-481.

Jorgensen, S.E. (1994). *Fundamentals of Ecological Modelling.* 2nd ed. Elsevier Scientific Publishing Co., Amsterdam, 628 p.

Jorgensen, S.E. and Gromiec, M. (1989). *Mathematical Submodels of Water Quality Systems.* Elsevier Scientific Publishing Co., Amsterdam.

Jorgensen, S.E., Halling-Sorensen, B. and Nielsen, S.N. (1996). *Handbook of Environmental and Ecological Modelling.* CRC, Lewis Publishers, Boca Raton.

Jorgensen, S.E., Kamp-Nielsen, L. and Jorgensen, L.A. (1981) "Parameter estimation in eutrophication modelling." *Ecol. Model.*, 13: 111-129.

Jorgensen, S.E., Kamp-Nielsen, L., and Jorgensen, L.A. (1986). "Examination of the generality of eutrophication models." *Ecol. Model.*, 32: 251-266.

Karagounis, I., Trösch, J., and Zamboni, F., (1993)."A coupled physical- biochemical lake model for forecasting water quality." *Aquat. Sci.*, 2: 87-102.

Karul, C., Soyupak, S. and Germen, E. (1998). "A new approach to mathematical water quality modeling in reservoirs: neural networks. " *Int. Rev. Hydrobiol.*, 83: 689-696.

Kiefer, D.A., Holm-Hansen, O., Goldman, C.R., Richards, R. and Berman, T. (1972). "Phytoplankton in Lake Tahoe: deep-living populations." *Limnol. Oceanogr.*, 17: 418-422.

Kirk, J. (1994). *Light and Photosynthesis in Aquatic Ecosystems.* Cambridge, Cambridge University Press.

Klepper, O. (1997). "Multivariate aspects of model uncertainty analysis: tools for sensitivity analysis and calibration." *Ecol. Model.*, 101: 1-13.

Klepper, O. and Hendrix, E.M.T. (1994). "A method for robust calibration of ecological models under different types of uncertainty." *Ecol. Model.*, 79: 161-182.

Kmet, T. and Straskraba, M. (1989). "Global behavior of a generalized aquatic ecosystem model." *Ecol. Model.*, 45: 95-110.

Lehman, T.D., Botkin, D.B. and Likens, G.E. (1975). "The assumptions and rationales of a computer model of phytoplankton population dynamics", *Limnol. Oceanogr.*, 20: 343-364.

Liu, M.S., Reuter, J.E. and Goldman, C.R. (2001). "Significance of atmospheric deposition of phosphorous for Lake Tahoe, California-Nevada, USA." ASLO poster session (in proc. in press). Loeb, S.L. and Eloranta, P.V (1984). "Near-shore littoral phytoplankton communities in Lake Tahoe, California-Nevada." *Verh. Internat. Verein Limnol.*, 22: 600-604.

Loehle, C. (1997). "A hypothesis testing framework for evaluating ecosystem model performance." *Ecol. Model.*, 97: 153-165.

Lopez, M. (1978). *Vertical and temporal distribution of phytoplankton populations of Lake Tahoe, California-Nevada, USA.* Masters Thesis, University of California, Davis.

Margalef, R. (1977). *Ecologia*, ed. Omega, Barcelona, 951p.

Marjanovic, P. (1989). Mathematical Modeling of Eutrophication Processes in Lake Tahoe: Water Budget, Nutrient Budget and Model Development. Doctoral dissertation. University of California , Davis.

Markofsky, M. and Harleman, D.R.F. (1973). "Prediction of water quality in stratified reservoirs." *J. Hydraul. Div. ASCE*, 99: 729-745.

Matsuoka, Y.T., Goga and Naito, M. (1986). "An eutrophication model of Lake Kasumigura." *Ecol. Model.*, 31: 201-219.

Mazumder, A. and Taylor, W. D. (1994). "Thermal Structure of lakes varying in size and water clarity." *Limnol. Oceanogr.* 39(4): 968-976.

McCord, S.A. and Schladow S.G. (1998) "Numerical simulations of degassing scenarios for CO_2-rich Lake Nyos, Cameroon. " *Journal of Geophysical Research B: Solid Earth*, 103(B6): 12355-12364.

Michalewicz, Z. (1992). Genetic Algorithms + Data Structures = Evolutionary Programs. Springer-Verlag, New York, 250 p.

208

Mitchell, B.G. (1990). "Algorithms for determining the absorption coefficient of aquatic particulates using the quantitative filter technique (QTF)." in *Ocean Optics X*. Orlando, FL: SPIE vol. 1302: 137-148.

Mobley, C.D. (1994). *Light and Water: Radiative Transfer in Natural Waters*. Academic Press, div. of Harcourt Brace & Co. San Diego, 592 p.

Morgan, M.D. (1979). *The dynamics of an introduced population of Mysis relicta (Loven) in Emerald Bay and Lake Tahoe, California-Nevada*. Doctoral dissertation, University of California, Davis.

Morgan, M.D. (1980)."Life history characteristics of two introduced populations of *Mysis relicta.*" *Ecology*, 61(3): 551-561.

Morgan, M.D., Threlkeld, S.T. and Goldman, C.R. (1978). "Impact of the introduction of kokanee (Oncorhynchus nerka) and opossum shrimp (Mysis relicta) on a subalpine lake." *J. Fish. Res. Board Can.* 35:1572-1579.

Mueller, D.K. (1982). "Mass balance model for estimation of phosphorous concentrations in reservoirs." *Water Resour. Bull.*, 18: 377-382.

Omlin, M. (2000). *Uncertainty analysis of model predictions for environmental systems: concepts and application to lake modelling*. Doctoral dissertation, University of Zurich, Switzerland.

Orlob, G.T. (1983). "One dimensional models for simulation of water quality in lakes and reservoirs," In *Mathematical Modeling of Water Quality: Streams Lakes, and Reservoirs*. G.T. Orlob and G.T. John (Eds.) International Series on Applied Systems Analysis, John Wiley and Sons, 227-273.

Orlob, G.T. and Selna, L.G. (1970). "Temperature variations in deep reservoirs." *J. Hydr. Div. ASCE*, 96: 391-410.

Pacala, S.W., Canham, C.D., Saponara, J., Silander, J.A. Jr, Kobe, R.K., Ribbens, E. (1996). "Forest models defined by field measurements: estimation, error analysis and dynamics." *Ecol. Monogr.*, 66(1): 1-44.

Paerl, H.W., Richards, R.C., Leonard, R.L. and Goldman, C.R. (1975). "Seasonal nitrate cycling as evidence for complete vertical mixing in Lake Tahoe, California-Nevada." *Limnol. Oceanogr.* 20(6): 1-8.

Palmarsson, S.O., Rueda, F.J., Hook, S.J., Prata, F.J., and Schladow, G. (2001). "Energetics of a Large Amplitude Upwelling Event." In: 6th International Workshop on *Physical Processes in Natural Waters*, Girona, Spain (in press).

Patterson, J.C., Hamblin, P.F. and Imberger, J. (1984). "Classification and dynamics simulation of the vertical density structure of lakes." *Limnol. Oceanogr.*, 29: 845-861.

Perkins MaryGail, and Steven W. Effler. (1996). "Optical Characteristics of Onondaga Lake: 1968-1990." Lake and Reserv. Manage. 12(1): 103-113.

209

Preisendorfer, R.W. (1961). "Application of radiative transfer theory to light measurements in the sea." In *IUGG Monograph*, 10: 11-29.

Preisendorfer, R.W. (1986). "Secchi disk science: Visual optics of natural waters." *Limnol. Oceanogr.* 31(5): 909-926.

Reckhow, K.H. and Chapra, S.C. (1983). *Engineering approaches for lake management, Vol. 1.* Ann Arbor Science, Boston, 340p.

Reichert, P. (1994). "AQUASIM - A tool for simulation and data analysis of aquatic systems." *Water Sci. Technol.*, 30(2): 21-30.

Reuter, J.E., Goldman, C.R., Jassby, A.D., Kavvas, L.M. and Schladow, G. 1998. *Annual Progress Report - 1998. Lake Clarity & Watershed Modeling - Presidential Deliverable.* John Muir Institute for the Environment, University of California, Davis, 28p.

Reuter, J.E., Jassby, A.D., Goldman, C.R. and Heyvaert, A.C. (2000). "Contribution of basin watersheds and atmospheric deposition to eutrophication at Lake Tahoe." *Watershed Management Council Networker*, 9(2).

Richards, R.C., Goldman, C.R., Byron, E. and Levitan, C. (1991). "The Mysids and Lake Trout of Lake Tahoe: A 25-year history of changes in the fertility, plankton and fishery of an alpine lake." *Amer. Fish. Soc. Sympos.* 9:30-38.

Richards, R.C., Goldman, C.R., Frantz, T.C. and Wickwire, R. (1975). "Where have all the Daphnia gone? The decline of a major cladocern population in Lake Tahoe, California-Nevada." *Verh. Internat. Verein. Limnol.* 19: 835-842.

Richerson, P.J. (1969). *Community ecology of the Lake Tahoe plankton.* Doctoral Dissertation, University of California, Davis.

Riley, M.J. and Stefan, H.G. (1988). "MINLAKE: A dynamic lake water quality simulation model." *Ecol. Model.*, 43: 155-182.

Rose, K.A. (1983). "A simulation comparison and evaluation of parameter sensitivity methods applicable to large models." In W. K. Lauenroth, G. V. Skogerboe and M. Flug, (Editors). *Analysis of Ecological Systems: State-of-the-Art in Ecological Modelling.* Elsevier, Amsterdam, 129-141.

Rybock, J.T. (1978). *Mysis relicta Loven in Lake Tahoe: vertical distribution and nocturnal predation.* Doctoral dissertation, University of California, Davis.

Rykiel, E.J. Jr. (1996). "Testing ecological models: the meaning of validation." *Ecol. Model.*, 90: 229-244.

Salençon, M.J. and Thébault, J.M. (1996). "Simulation model of a mesotrophic reservoir (lac de Pareloup, France): MELODIA, an ecosystem reservoir management model." *Ecol. Model.*, 84: 163-187.

Salençon, M.J. and Thébault, J.M. (1997). *Modélisation d'Écosystème Lacustre. Application à la Retenue de Pareloup.* 1st ed. Masson, Paris.

Sandgren, C.D. (1988). *Growth and Reproductive Strategies of Freshwater Phytoplankton,* Cambridge University Press, Cambridge.

Scardi, M. (1996). "Artificial neural networks as empirical models for estimating phytoplankton production." *Mar. Ecol. Ser.,* 139: 289-299.

Scavia, D. (1980). "An ecological model of lake Ontario." *Ecol. Model.,* 8: 49-78.

Schladow, S.G. and Hamilton, D.P. (1997). "Prediction of water quality in lakes and reservoirs. Part II - Model calibration, sensitivity analysis and application." *Ecol. Model.,* 96: 111-123.

Sherman, F.S., Imberger, J. and Corcos, G.M. (1978). "Turbulence and mixing in stably stratified waters." *Ann. Rev. Fluid. Mech.* 10: 267-288.

Smayda, T.J. (1974). "Some experiments on the sinking characteristics of two freshwater diatoms." *Limnol. Oceanogr.,* 19: 628-635.

Smith, D.G., Croker, G.F. and McFarlane, K. (1995a). "Human perception of water appearance. 1. Clarity and colour for bathing and aesthetics." *New Zeal. J. Mar. Fresh. Res.* 29(1): 29-43.

Smith, D.G., Croker, G.F. and McFarlane, K. (1995b). "Human perception of water appearance. 2. Colour judgment, and the influence of perceptual set on perceived water suitability for use." *New Zeal. J. Mar. Fresh. Res.* 29(1): 45-50.

Spear, R.C. and Hornberger, G.M. (1980). "Eutrophication in Peel Inlet- II. Identification of critical uncertainties via generalized sensitivity analysis." *Wat. Res.* 14: 43-49.

Spigel, R.H. and Imberger, J. (1980). "The classification of mixed layer dynamics in lakes of small to medium size." *J. Phys. Oceanogr.,* 19: 1104-1121.

Spigel, R.H., Imberger, J. and Rayner, K.N. (1986). "Modeling the diurnal mixed layer." *Limnol. Oceanogr.,* 31: 533-556.

Stefan, H. and Ford, D.E. (1975). "Temperature dynamics in dimictic lakes." *J. Hydr. Div., ASCE,* Paper 11058: 97-114.

Stocker, T. and Hutter, K. (1986). "One-dimensional models for topographic Rossby waves in elongated basins on the f-plane." *J. Fluid Mech.,* 170: 435-459.

Straskraba, M. (1994). "Ecothecnological models of reservoir water quality management." *Ecol. Model.* 74: 1-38.

Straskraba, M. and Gnauck, A. (1985). *Freshwater Ecosystems Modelling and Simulation*. Developments in Environmental Modelling, ed. Elsevier, Amsterdam, 310p.

Tarnay, L., Gertler, A.W., Blank, R.R. and Taylor Jr, G.E. (2001). "Preliminary measurements of summer nitric acid and ammonia concentrations in the Lake Tahoe Basin air-shed: implications for dry deposition of atmospheric nitrogen." *Environmental Pollution*, 113(2): 145-153.

Tennessee Valley Authority (1972). *Heat and Mass Transfer Between a Water Surface and the Atmosphere*. Water Resources Research Lab Rep. No. 14. TVA Div. Water Control Planning Engrg. Lab., Norris, TN.

Thébault, J.M. (1995). "Representation of phosphorus in lake ecosystem models." *Annal. Limnol.*, 31(2): 143-149.

Thodal, C.E. (1997). *Hydrogeology of Lake Tahoe Basin, California and Nevada, and Results of a ground-Water Quality Monitoring Network, Water Years 1990-92*. US Geological Survey, Water-Resources Investigations Report 97-4072.

Thompson, K.L. (2000). *Winter Mixing Dynamics and Deep Mixing in Lake Tahoe*. Masters Thesis, University of California, Davis.

TRPA (1982). *Environmental Thresholds Study*. Tahoe regional Planning Agency.

Tyler, J.E. (1968). "The Secchi Disk." *Limnol. Oceanogr.* 13:1-6.

USCE, (1986). *CEQUAL R1: A numerical one-dimensional model of reservoir water quality, user's manual*. Environmental and water quality operational studies instruction report E-82-1. Department of the army, U.S. Corps Engineers, Washington, DC, 427p.

van de Hulst, H.C. (1981). *Light Scattering by Small Particles*. Dover Publications, New York, 470p. (Originally published by John Wiley & Sons, New York , 1957).

Van Tassell, J.J., Beauchamp D.A., Thiede G.P., Gemperle, C.K., Richards, R.C. and Goldman, C.R. (2000). " Kokanee and Mysis influence on zooplankton dynamics and nutrients recycling in Lake Tahoe." in *Annual Progress Report 2000*, Tahoe Research Group, University of California, Davis.

Varela, R.A., Cruzado, A. and Tintore, J. (1994). "A simulation analysis of various biological and physical factors influencing the deep-chlorophyll maximum structure in oligotrophic areas." *J. Mar. Systems*, 5(2): 143-157.

Varela, R.A., Cruzado, A., Tintore, J. and Garcia Ladona, E. (1992). "Modelling the deep-chlorophyll maximum: a coupled physical- biological approach." *J. Mar Res.*, 50(3): 441-463.

Vincent, F.W. (1978). "Survival of aphotic phytoplankton in Lake Tahoe throughout prolonged stratification." *Verh. Internat. Verein. Limnol.* 20: 401-406.

212

Vollenweider, R.A. (1968). *The scientific basis of lake and stream eutrophication, with particular reference to phosphorous and nitrogen as eutrophication factors.* Technical Report DAS/DSI/68.27, Organization for Economic cooperation and Development, Paris, France.

Wallace, B.B., Hamilton, D.P. and Patterson, J.C. (1996). "Response of Photosynthesis Models to Light Limitation." *Int. Revue ges. Hydrobiol.*, 81: 315-324.

Yabunaka, K., Hosomi, M. and Murakami, A. (1997). "Novel application of a back-propagation artificial neural network model formulated to predict algal bloom." *Wat. Sci. Technol.*, 36: 89-97.

# Appendix A: Water Quality Sensitivity Analysis for 1999
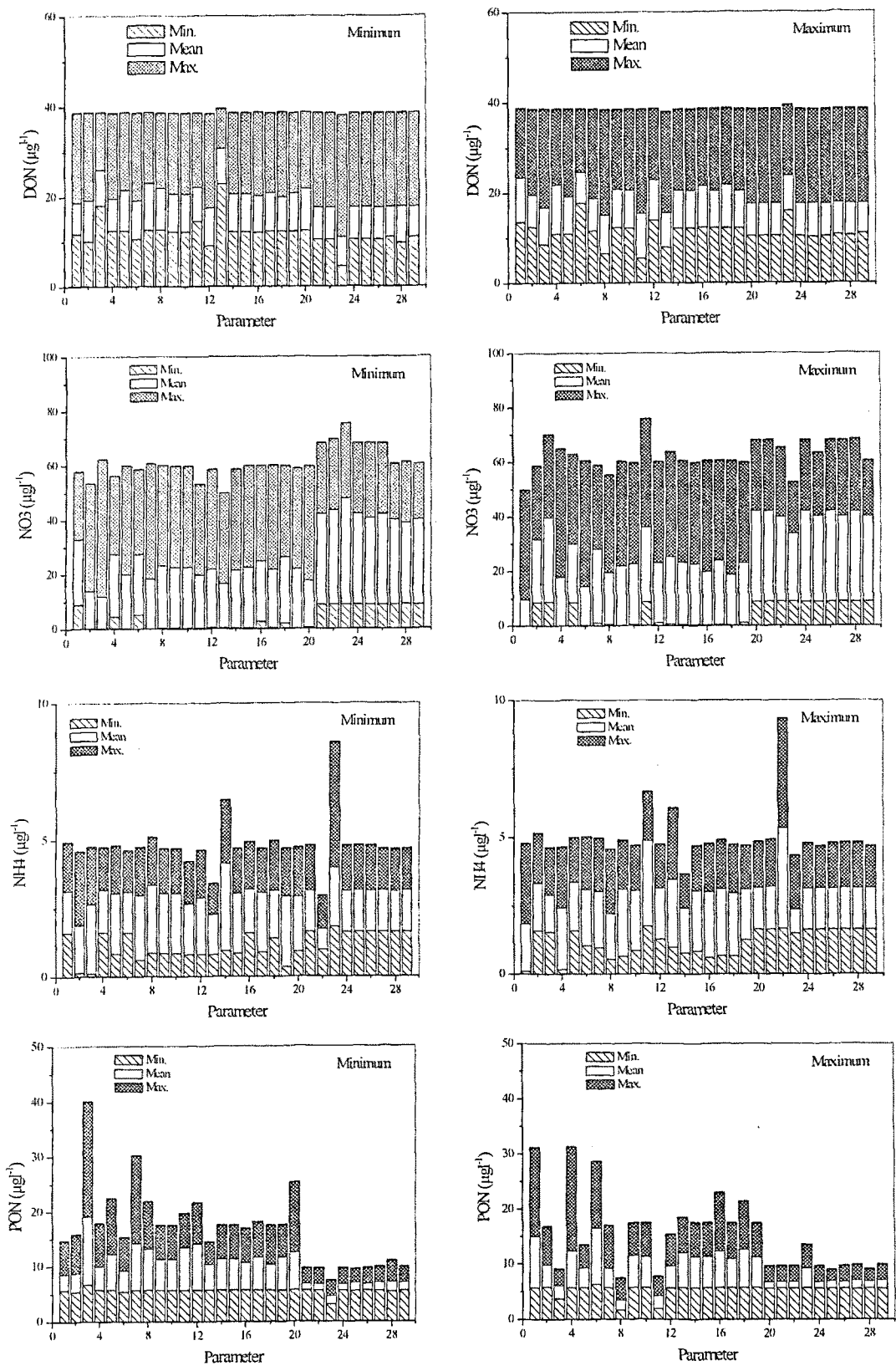
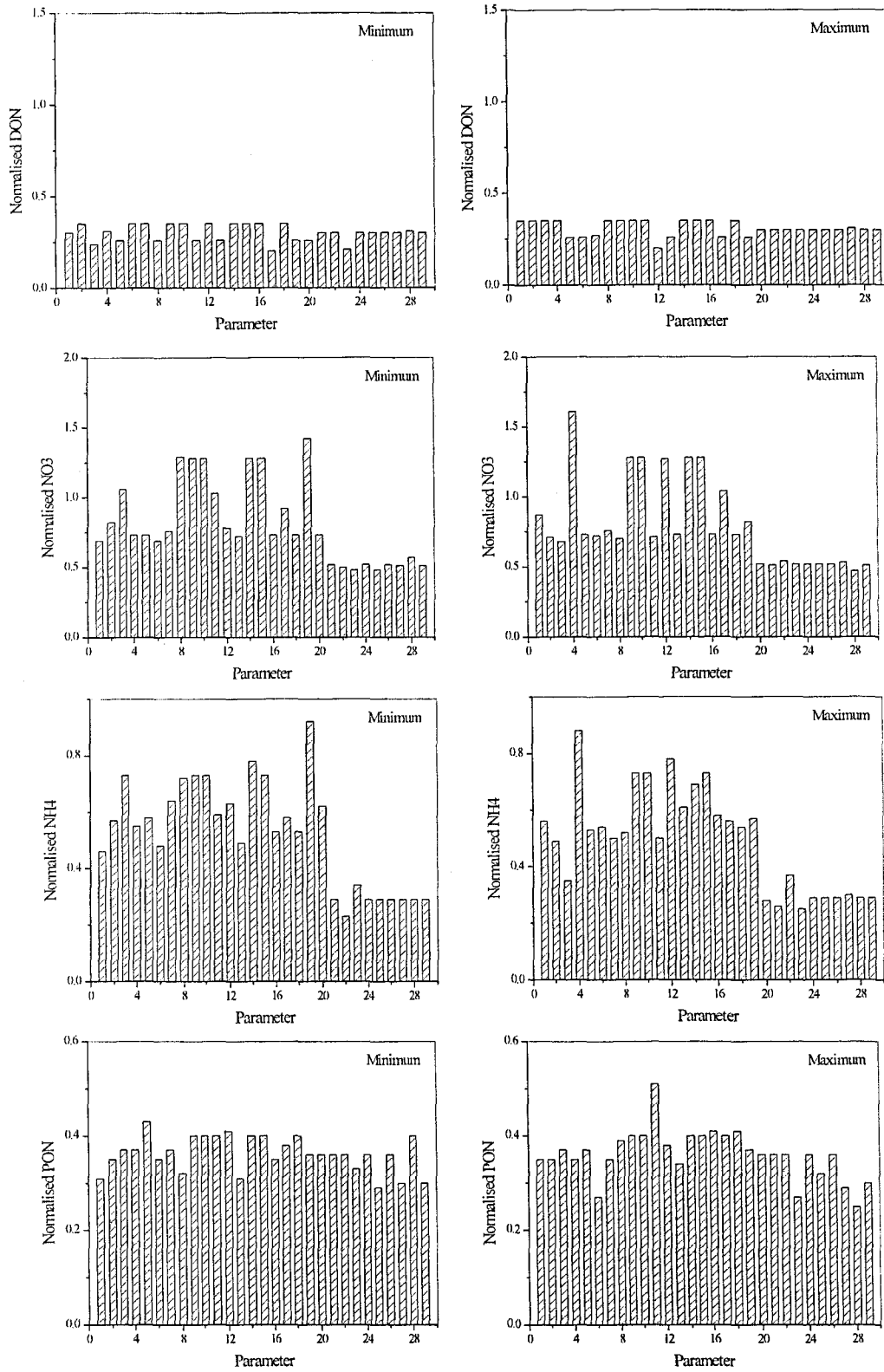**Figure A-1** Mean distribution DON, NO3,NH4 and PON for 1999.
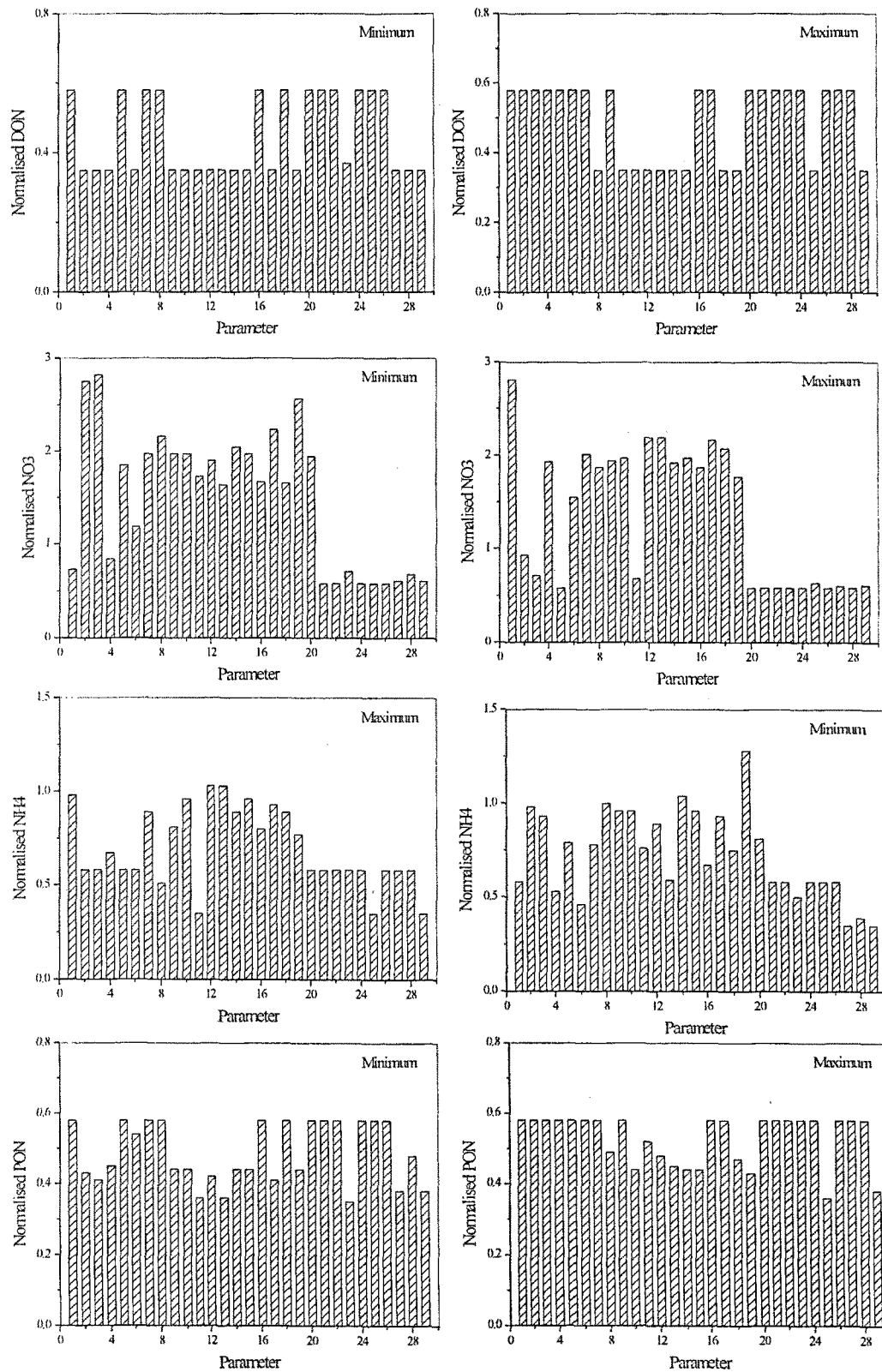
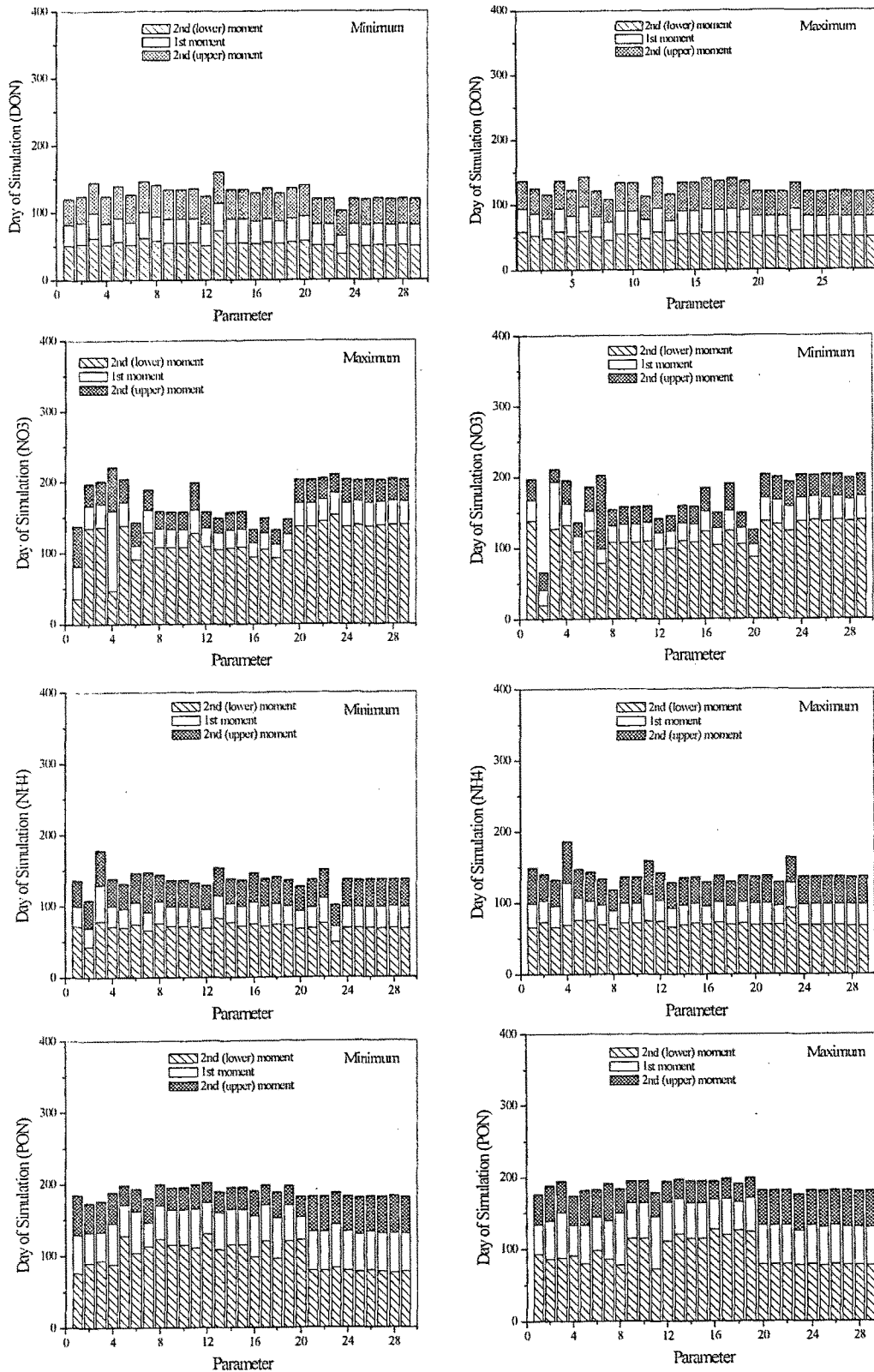**Figure A-2** Vertical distribution DON, NO3, NH4 and PON for 1999.
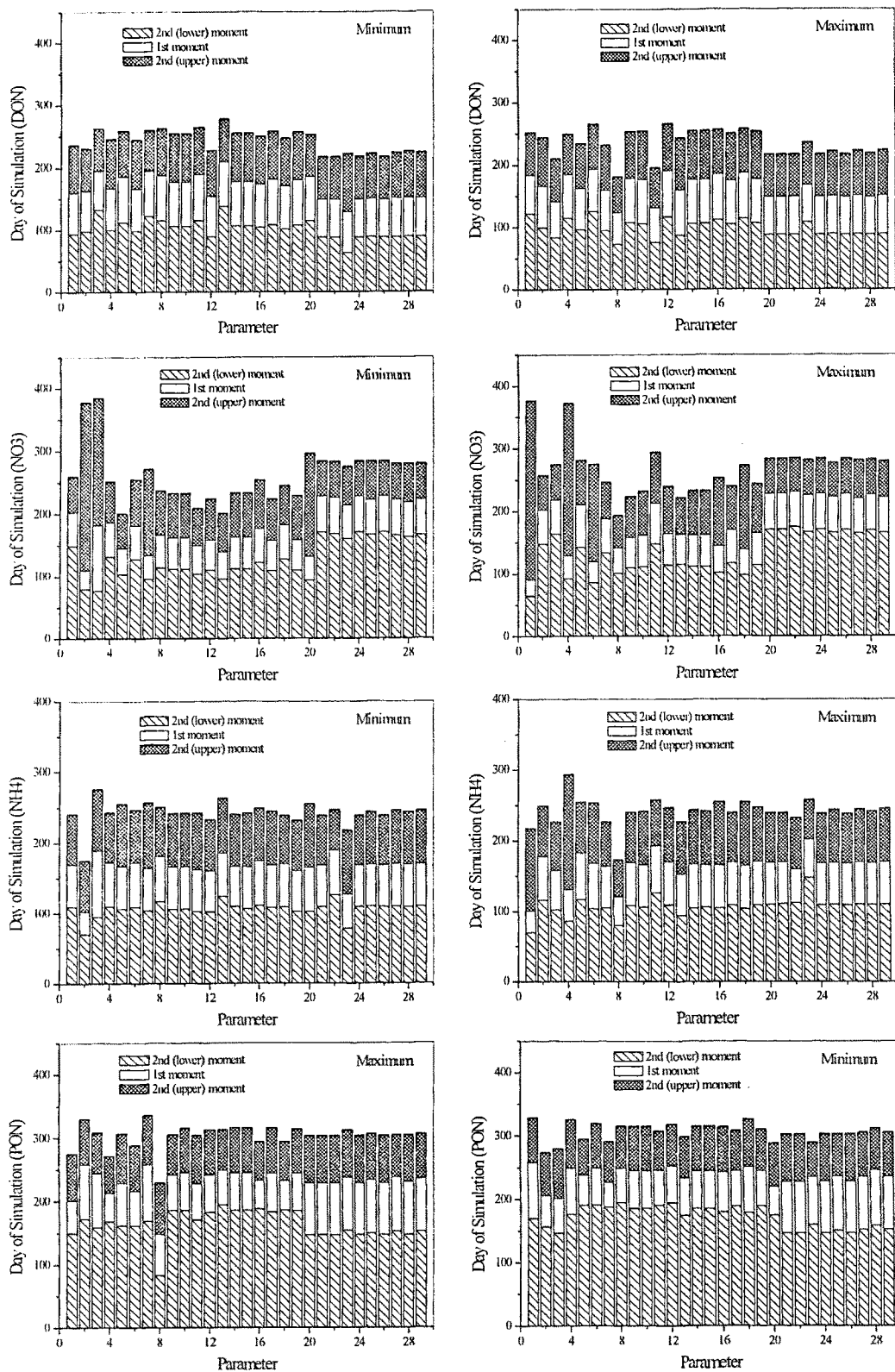
**Figure A-3** Time distribution DON, NO3, NH4 and PON for 1999.

218
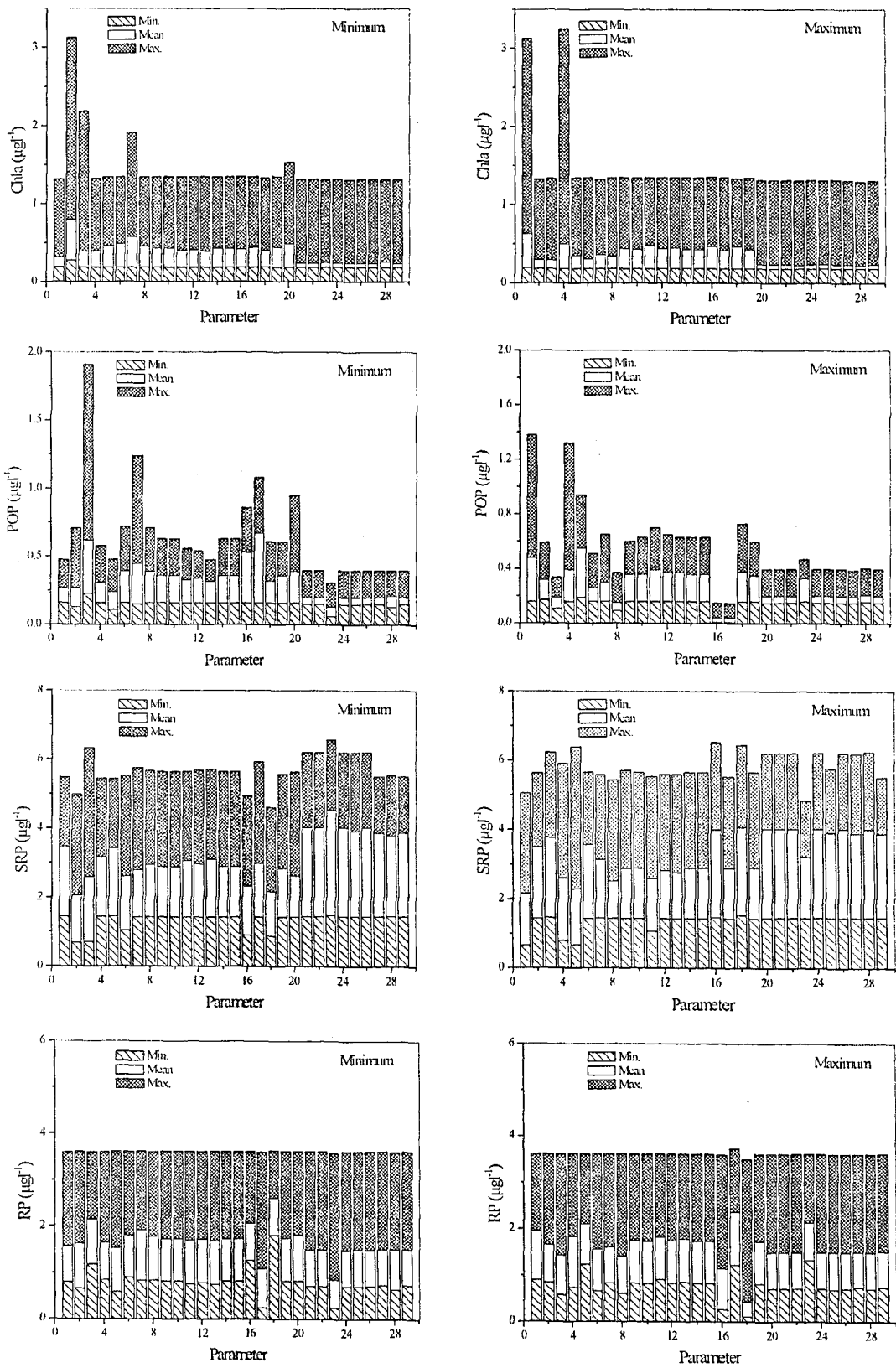
Figure A-4 Mean distribution Chla, POP, SRP, and RP for 1999.
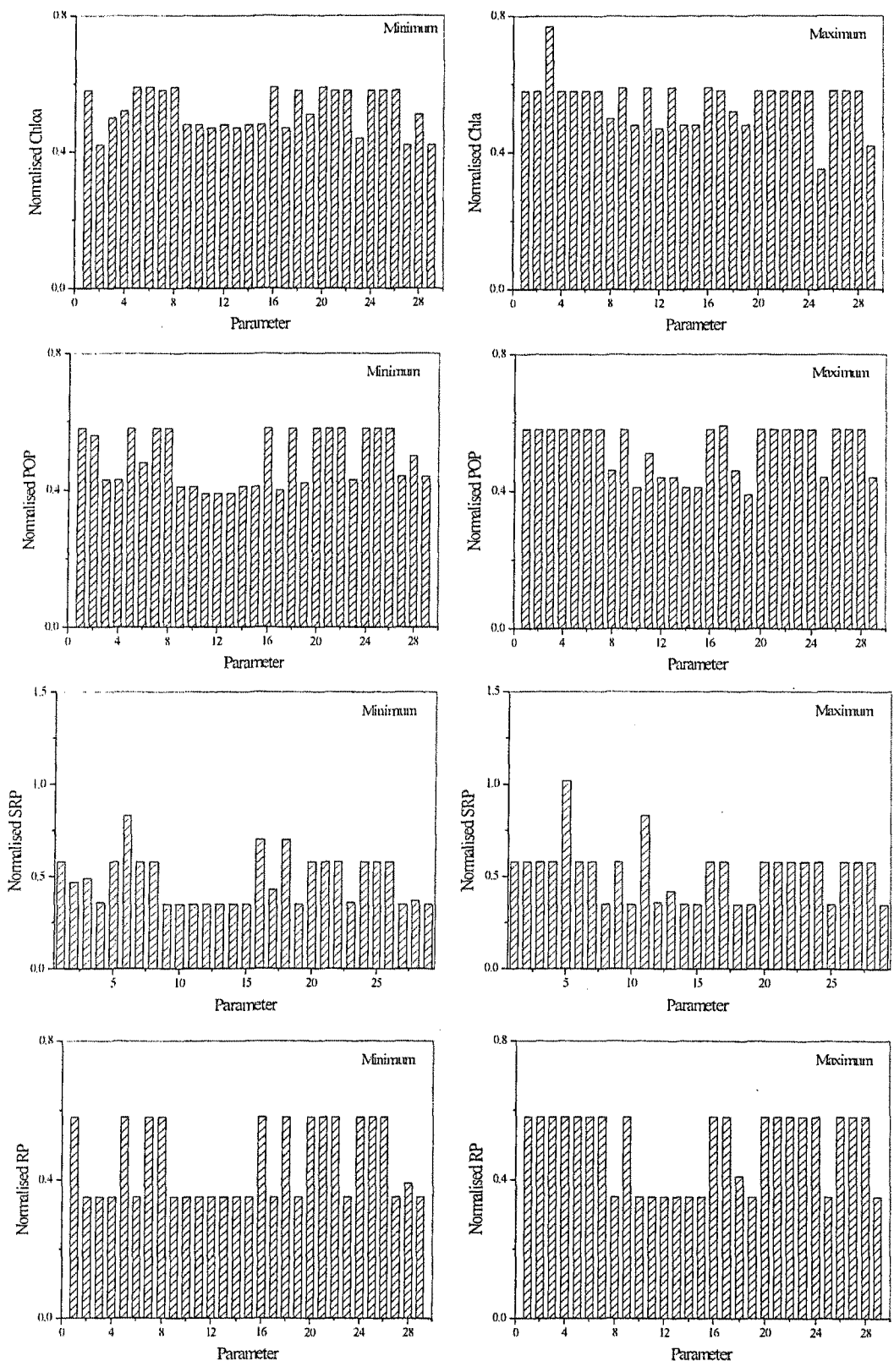
Figure A-5 Vertical distributions Chla, POP, SRP, and RP for 1999.
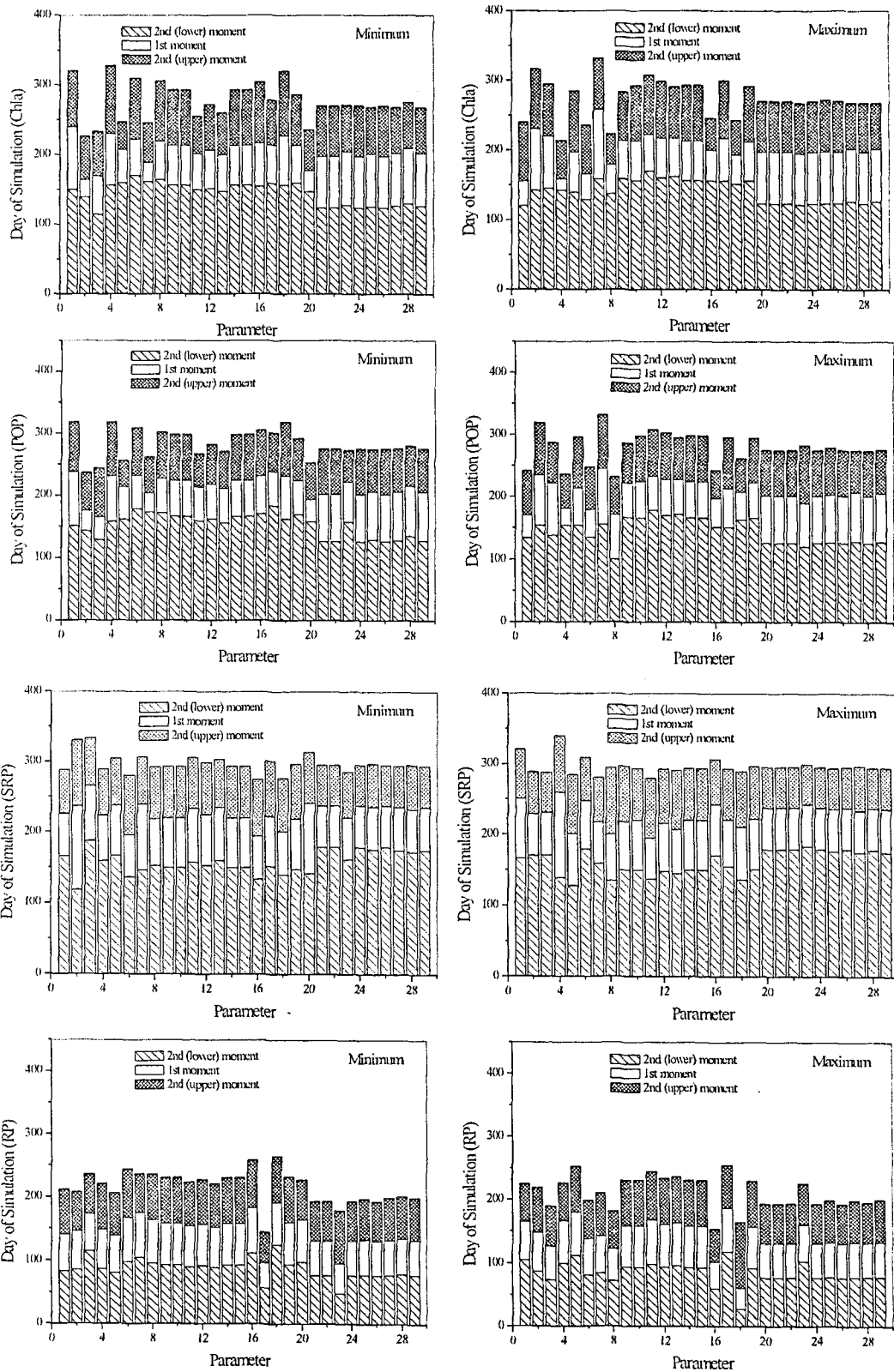
Figure A-6 Time distribution Chla, POP, SRP, and RP for 1999.

Appendix B: Water Quality Sensitivity Analysis for 1992
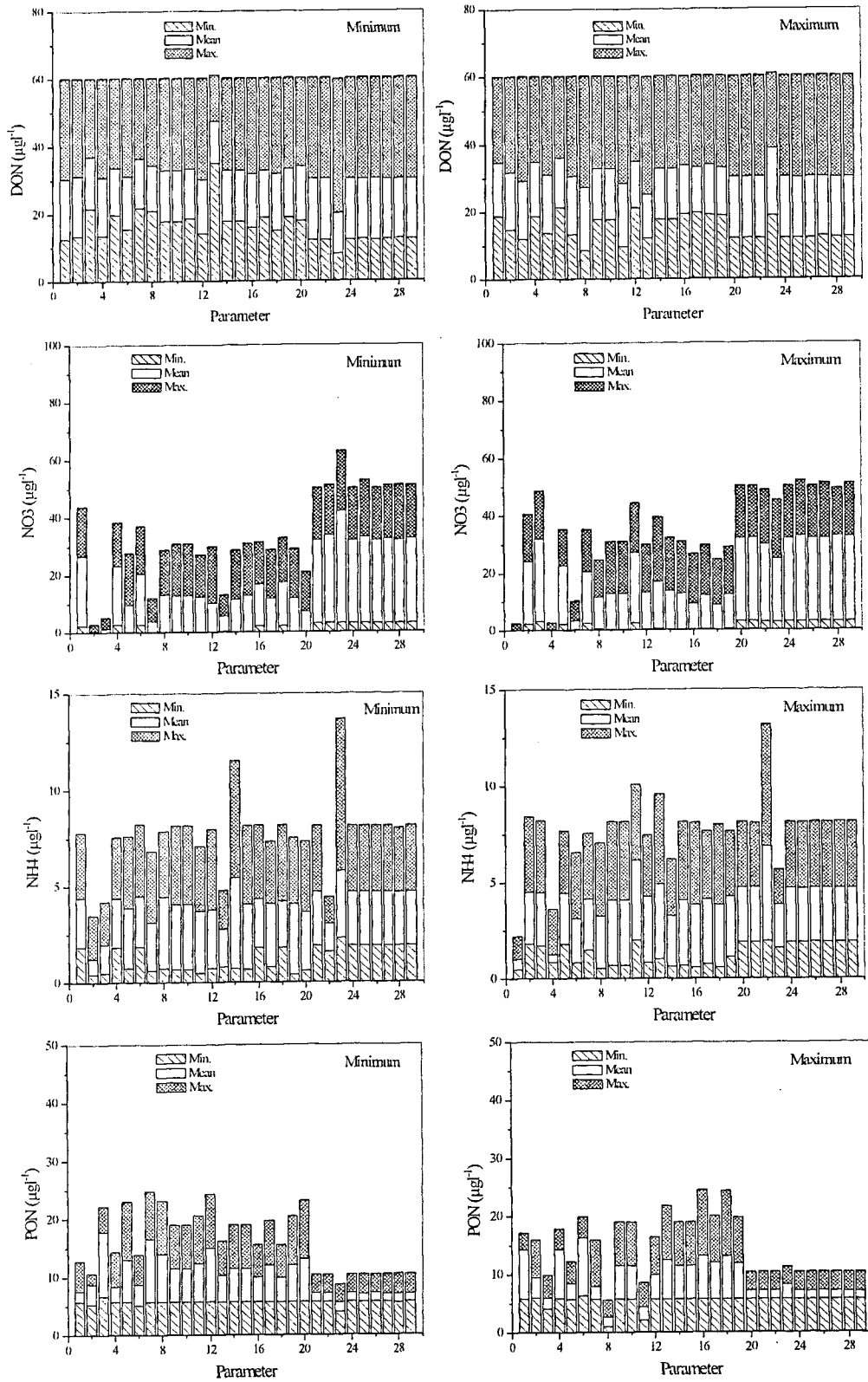
Figure B-1 Mean distribution DON, NO3, NH4 and PON for 1992.

Figure B-2 Vertical distribution DON, NO3, NH4 and PON for 1992.

Figure B-3 Time distribution DON, NO3, NH4 and PON for 1992.
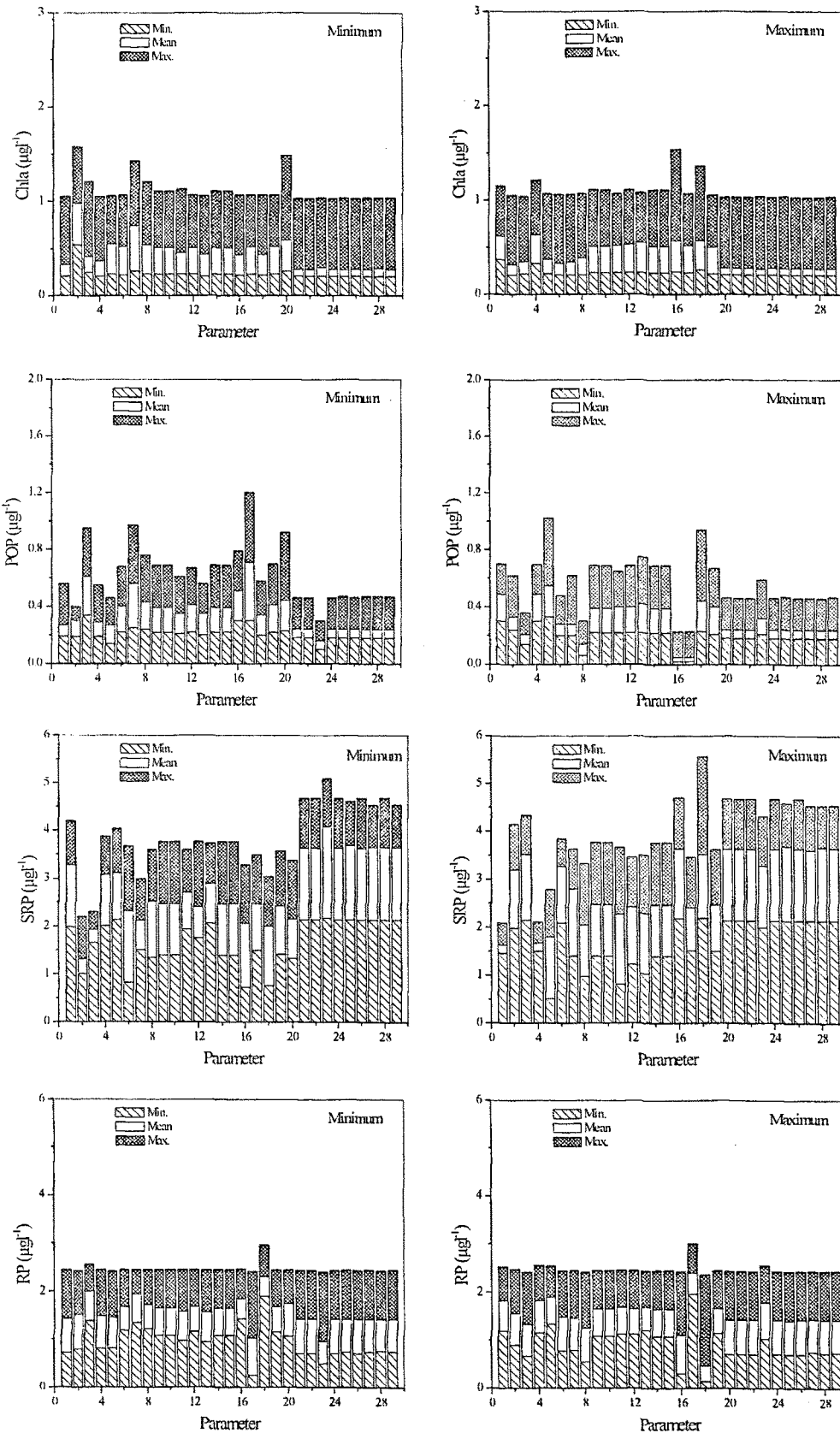
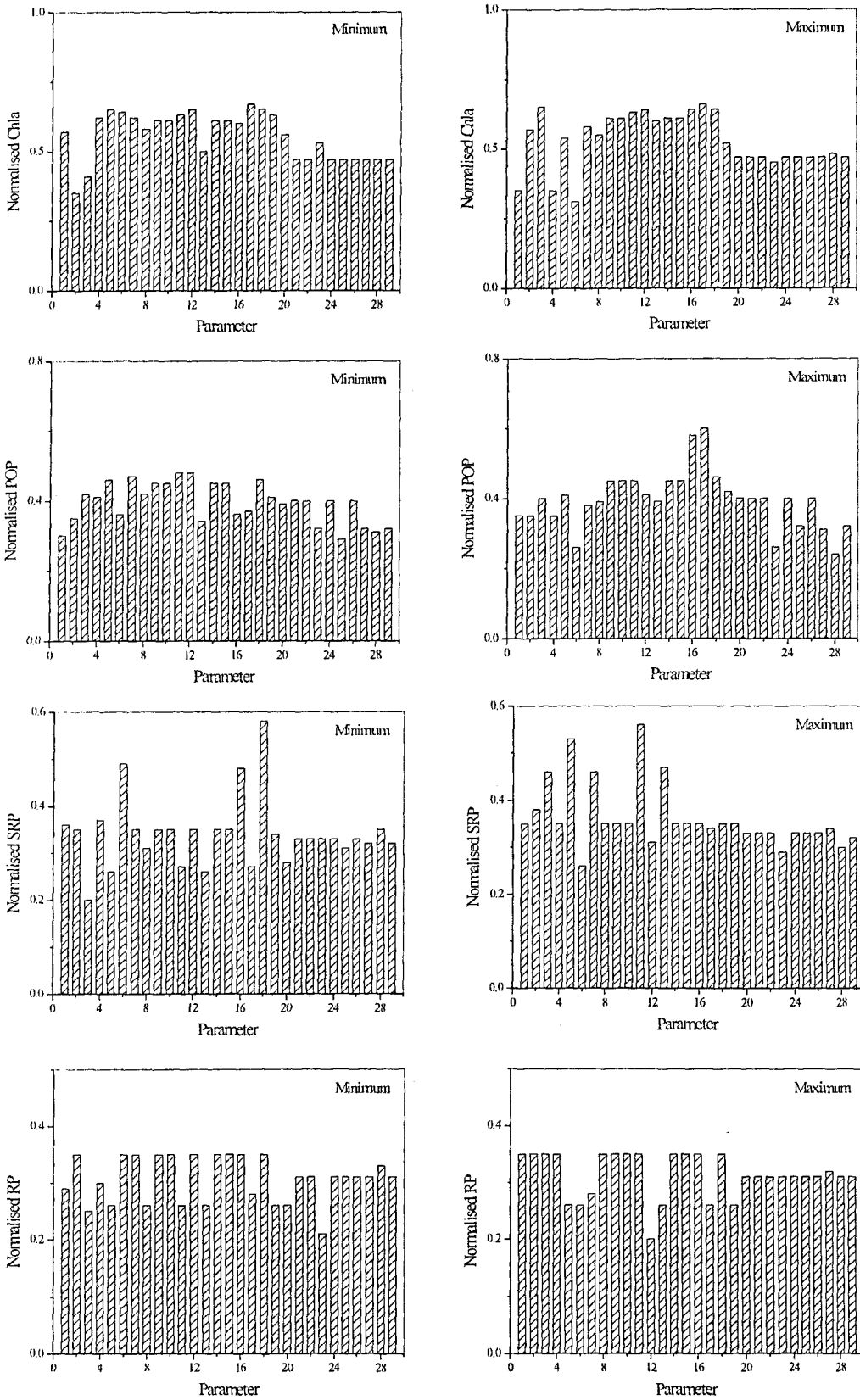**Figure B-4** Mean distribution Chla, POP, SRP, and RP for 1992.

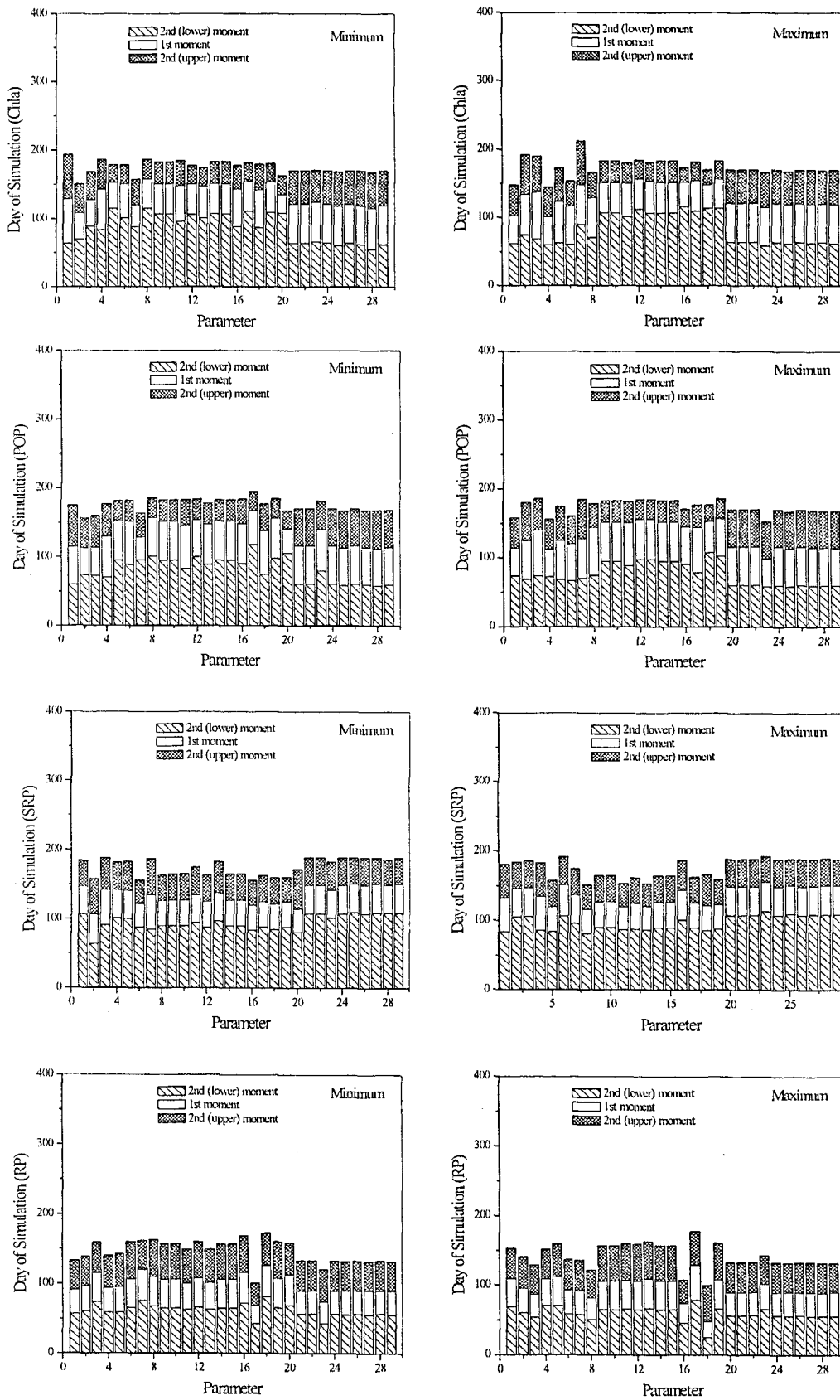**Figure B-5** Vertical distribution Chla, POP, SRP, and RP for 1992.

Figure B-6 Time distribution Chla, POP, SRP, and RP for 1992.